CENTRO DE INVESTIGACIÓN Y DE ESTUDIOS AVANZADOS DEL
INSTITUTO POLITÉCNICO NACIONAL

UNIDAD ZACATENCO

DEPARTAMENTO DE TOXICOLOGÍA

“PARTICIPACIÓN DE LOS TRANSPORTADORES DE GLUTAMATO EN LA NEUROTOXICIDAD DEL MANGANESO”

T E S I S

Que presenta

M. en C. MIGUEL ÁNGEL ESCALANTE LÓPEZ

Para obtener el grado de

DOCTOR EN CIENCIAS

EN LA ESPECIALIDAD DE

TOXICOLOGÍA

Directores de tesis:

Dr. Arturo Ortega Soto

Dra. Esther Ivonne López Bayghen Patiño

Ciudad de México Enero, 2020

AGRADECIMIENTOS

Gracias, de corazón, a mis tutores, el Dr. Arturo Ortega Soto y la Dra. Esther Ivonne López Bayghen Patiño. Gracias por su paciencia, dedicación, motivación, criterio y aliento. Ha sido un privilegio poder contar con su guía y ayuda.

De la misma forma, agradezco al Dr. Arnulfo Albores Medina, la Dra. María Isabel Hernández Ochoa, el Dr. José Antonio Arias Montaño y el Dr. Francisco Castelán por enriquecer mi formación profesional con sus observaciones y enseñanzas.

A la Dra. Babette Fuss, gracias por cobijarme como un miembro más de su laboratorio y por ser una excelente mentora.

Agradezco la asesoría técnica de Luisa Clara Regina Hernández Kelly, Blanca Roció Ibarra López y Luis Ángel Cid Cid, del Departamento de Toxicología, Cinvestav-IPN por el entrenamiento en las metodologías realizadas en este trabajo.

A mis abuelos, Oscar y Yolanda, gracias por enseñarme que una persona puede ser extraordinaria haciendo cosas ordinarias. No tengo palabras para agradecer todo lo que han hecho por mi.

A mi madre, Patricia, gracias por cada sacrificio y momento que hemos compartido juntos. Estoy seguro de que no podría estar escribiendo esto sin todo el apoyo y cariño que me has brindado.

A mi padre, José Antonio, agradezco sus consejos y enseñanzas. Gracias por creer en mi, y al mismo tiempo exigir más de mi.

A mi hermano, Toño, te agradezco haberme soportado durante toda nuestra infancia, se que fue un poco difícil. Gracias por tantos momentos de diversión y todo tu apoyo.

A mis amigos; siempre he tenido la firme convicción que ellos han moldeado mi vida de alguna u otra forma. Gracias Marc, Zila, Bruno, Edna, Orquidia, Donna, Sam, Nav y Elizabeth por hacer del laboratorio un segundo hogar para mi.

Y por ultimo, pero no menos importante, quiero agradecer especialmente a Carla. Gracias por ser mi mejor amiga, mi confidente, mi apoyo y mi motivo más hermoso para seguir adelante. En otras palabras, gracias por existir. ¡Te amo exagerada y desmesuradamente!

El presente trabajo fue realizado en el laboratorio de Neurotoxicología del Centro de Investigación y de Estudios Avanzados del I.P.N. bajo la dirección del Dr. Arturo Ortega Soto y la Dra. Esther Ivonne López Bayghen Patiño; y con la asesoría del Dr. Arnulfo Albores Medina, la Dra. María Isabel Hernández Ochoa, el Dr. José Antonio Arias Montaño y el Dr. Francisco Castelán.

Durante la realización del presente trabajo el autor contó con el apoyo de la beca 427091 del Consejo Nacional de Ciencia y Tecnología (CONACYT)

ÍNDICE DE CONTENIDOS

ÍNDICE DE FIGURAS

RESUMEN

El glutamato es el principal neurotransmisor excitador en el sistema nervioso central (SNC) de los vertebrados. Ejerce sus acciones a través de la activación de receptores específicos expresados tanto en neuronas como en células gliales. La sobreactivación de los receptores glutamatérgicos puede resultar en muerte neuronal, a este fenómeno se le conoce como excitotoxicidad. Los transportadores de aminoácidos excitadores enriquecidos en células gliales (GLAST y GLT-1) son los responsables de eliminar la gran mayoría de este aminoácido de la hendidura sináptica. Por lo tanto, la regulación precisa de estas proteínas es indispensable para una transmisión adecuada y también para prevenir lesiones excitotóxicas.

El manganeso (Mn) es un elemento esencial requerido en mínimas cantidades ya que es un cofactor para varios sistemas enzimáticos. Sin embargo, la acumulación excesiva de Mn en el cerebro altera la homeostasis del glutamato. Los mecanismos moleculares asociados a la neurotoxicidad del Mn se han centrado en la disfunción mitocondrial y la generación de especies reactivas de oxígeno (ROS), aún cuando es ampliamente conocido que la depleción energética compromete gravemente el proceso de remoción de glutamato. En este contexto, en esta contribución analizamos el efecto de la exposición a Mn en la función de los transportadores de glutamato, específicamente de GLAST.

Utilizando cultivos primarios de glía de Bergmann pudimos detectar un aumento en la actividad de GLAST después de una pre-incubación con Mn por 30 min, esto se explica por un cambio en la eficiencia catalítica (V_{max}/K_m) del transportador. Sin embargo, cuando se agrega Mn a la solución de captura (sin pre-incubación) hay una reducción significativa en la incorporación de [^{3}H]-D-Asp en función del tiempo. Por otro lado, la captura de glucosa se ve severamente afectada después de una pre-incubación con Mn por 30 min. Estos resultados sugieren que la exposición aguda a Mn tiene un efecto directo sobre funciones importantes de las células gliales, esto a su vez altera su acoplamiento con las neuronas y puede provocar cambios en la transmisión glutamatérgica.

ABSTRACT

Glutamate is the major excitatory amino acid neurotransmitter in the vertebrate brain. It exerts its actions through the activation of specific plasma membrane receptors expressed in neurons and glial cells. Overactivation of glutamate receptors results in neuronal death, known as excitotoxicity. A family of sodium-dependent glutamate transporters enriched in glial cells are responsible of the vast majority of the removal of this amino acid form the synaptic cleft. Therefore, a precise and exquisite regulation of these proteins is required not only for a proper glutamatergic transmission but also for the prevention of an excitotoxic insult.

Manganese is a trace element essential as a cofactor for several enzymatic systems, although in high concentrations is involved in the disruption of brain glutamate homeostasis. The molecular mechanisms associated to manganese neurotoxicity have been focused on mitochondrial function, although energy depletion severely compromises the glutamate uptake process.

Thus, in this contribution we analyzed the effect of manganese exposure on glial glutamate transporters function. To this end, we used the well-established model of chick cerebellar Bergmann glia cultures. A time and dose dependent modulation of [$_3$H]-D-aspartate uptake was found. An increase in the transporter catalytic efficiency, most probably linked to a discrete decrease in the K_m of the transporter was detected upon manganese exposure. Interestingly, glucose uptake was reduced by this metal. These results favor the notion of a direct effect of manganese on glial cells, this in turn alters their coupling with neurons and might lead to changes in glutamatergic transmission.

INTRODUCCIÓN

El glutamato como neurotransmisor

El aminoácido L-glutamato (Glu) es considerado el principal mediador de la neurotransmisión excitadora rápida en el Sistema Nervioso Central (SNC) de vertebrados, excitando virtualmente a cada neurona [1]. Aproximadamente, el 80-90% de las sinapsis establecidas en el cerebro son glutamatérgicas; y por lo tanto, el Glu participa en la mayoría de los aspectos relacionados con la función normal del cerebro, incluyendo la cognición, la memoria y el aprendizaje [2]. El Glu también desempeña un papel importante en el desarrollo del SNC, participando en la inducción y eliminación de sinapsis, migración, diferenciación y muerte celular.

El tejido cerebral contiene una concentración inusualmente alta de Glu, aproximadamente 5-15 mmol/kg [3, 4]. La mayor parte de este Glu se encuentra en las neuronas. La concentración de Glu en el interior de las neuronas glutamatérgicas es aproximadamente de 5 a 10 mM [3, 5–8]. Esto es varias veces más que cualquier otro aminoácido, y mucho más que en otros tipos de tejidos. La concentración de Glu en la hendidura sináptica después de la liberación mediada por un potencial de acción excede 1 mM durante <10 ms, y rápidamente vuelve a <20 nM entre los eventos de liberación [9]. La repolarización de las membranas, que son despolarizadas durante la actividad glutamatérgica, puede representar hasta el 80% del gasto de energía en el cerebro [10]. Por lo tanto, el alto consumo de glucosa y oxígeno en el cerebro provee en gran medida la energía necesaria para la actividad glutamatérgica.

El Glu participa en muchas reacciones llevadas a cabo en el cerebro (Fig. 1). Es sintetizado a partir del α-cetoglutarato, y es un precursor del ácido γ-aminobutírico (GABA) en las neuronas GABAérgicas, y de glutamina en las células gliales [11]. Además, es un constituyente de las proteínas y péptidos, por ejemplo: glutatión (GSH), el cual es una defensa importante contra el estrés oxidante en las células.

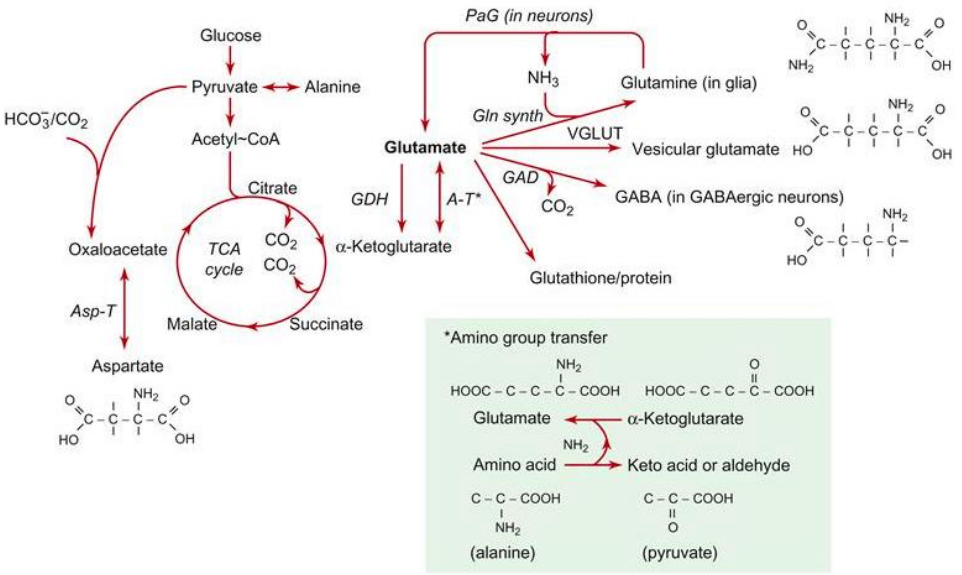

Figura 1. Síntesis, metabolismo y participación del Glu en diferentes reacciones llevadas a cabo en el cerebro [4]***.***

Tomó mucho tiempo aceptar al Glu como un neurotransmisor, en parte debido a su abundancia en el tejido cerebral y también porque está en la encrucijada de múltiples vías metabólicas [12, 13]. Aunque desde el principio se observó que el Glu desempeñaba un papel metabólico central en el cerebro [14], que las células cerebrales tienen una actividad de captura de Glu muy alta [15] y que el Glu tiene un efecto excitador [16], no fue sino hasta principios de la década de 1980 que el papel del Glu como neurotransmisor quedó establecido [17]. Con el tiempo, se identificaron varias familias de proteínas receptoras de Glu mediante clonación molecular. Los receptores se clasificaron como receptores de N-metil-D-aspartato (NMDA) [18–20], receptores del ácido α-amino-3-hidroxi-5-metil-4-isoxazol propiónico (AMPA) [21], receptores de kainato (KA) [22] y receptores metabotrópicos [23]. La mayoría de las células del sistema nervioso expresan al menos un tipo de receptor glutamatérgico [24–27].

Receptores glutamatérgicos

Los receptores glutamatérgicos han sido divididos en dos grandes grupos de acuerdo con su estructura y el sistema de traducción empleado. Los receptores

ionotrópicos están formados por 4-5 subunidades que constituyen un canal iónico, mientras que los receptores metabotrópicos forman dímeros que se encuentran acoplados a proteínas G triméricas [28].

Receptores ionotrópicos

Los receptores ionotrópicos han sido subdivididos según sus propiedades electrofisiológicas, farmacológicas y la homología entre sus secuencias en subfamilias. La primera subdivisión depende de un criterio farmacológico bien establecido, su activación por el NMDA. Este criterio, conformado a mediados de la década de los cincuenta del siglo pasado, concuerda perfectamente con el criterio molecular; sin embargo, la variedad molecular y el ensamblaje diferencial de las subunidades que componen estos receptores rebasa ampliamente la variedad farmacológica. Molecularmente se han descrito tres subfamilias de receptores NMDA y tres de receptores no NMDA [28].

Los receptores NMDA son canales iónicos abiertos por ligando y regulados por voltaje. En condiciones de reposo, el canal está bloqueado por Mg^{2+} de una manera dependiente de voltaje. Además, el receptor requiere de glicina para activarse eficientemente; asimismo es regulado por poliaminas y Zn^{2+}. Los receptores NMDA están formados por cuatro subunidades y por lo menos una de estas subunidades debe ser la subunidad GluN1 [28].

Los receptores no NMDA están formados por dos subgrupos, los receptores AMPA y los receptores KA [29]. La familia de los receptores AMPA está formada por cuatro subunidades denominadas: GluA1, GluA2, GluA3 y GluA4. Estas subunidades pueden ensamblarse entre sí y generar canales con diferentes propiedades electrofisiológicas. Además, cada subunidad presenta dos variantes de corte y empalme alternativo, las isoformas denominadas *flip/flop*. Por otra parte, el ARN mensajero (ARNm) de la subunidad GluA2 puede ser editado por la adenosina deaminasa tipo 2 (ADAR2), cuyo sustrato es una adenosina no apareada en una estructura del ARN que no presenta estructura de dúplex. La desaminación de la adenina la transforma en inosina, con la consecuente modificación del anticodón correspondiente, lo que durante el proceso de traducción origina el cambio de una

glutamina por una arginina en el segmento reentrante TMII y provoca un cambio en la selectividad del poro iónico, haciendo que el canal sea más permeable a sodio. Es de esta manera que los receptores que contienen al menos una subunidad GluA2 son preferentemente permeables a sodio [28].

Los receptores KA están constituidos por dos subfamilias, los receptores KA de baja afinidad y los receptores KA de alta afinidad. Las subunidades GluK1, GluK2 y GluK3 constituyen los receptores de baja afinidad, ya que en ensayos de unión de [^{3}H]-KA presentan una constante de afinidad de alrededor de 80 nM. Al co-ensamblarse, éstos forman canales iónicos funcionales. Dentro de esta familia génica se encuentra la denominada proteína de unión a KA (KBP), que no forma canales funcionales ni al co-ensamblarse con las otras subunidades. Los receptores de alta afinidad corresponden a las subunidades GluK4 y GluK5, que en ensayos de unión presentan una afinidad de 5 nM, pero que por sí solas no forman canales funcionales. Sin embargo, al co-expresarse con las subunidades GluK1, GluK2 o GluK3, cambian los parámetros cinéticos del canal iónico, por lo que se dice que son subunidades moduladoras [30].

Receptores metabotrópicos

Los receptores metabotrópicos son proteínas de siete segmentos transmembranales acoplados a proteínas G y presentan un extremo aminoterminal extenso. La homología con otros receptores acoplados a proteínas G (GPCR) es baja, de hecho, constituyen una familia génica diferente de la cual también es miembro el receptor de Ca^{2+}. De acuerdo con su secuencia, los receptores glutamatérgicos metabotrópicos han sido divididos en tres clases. La clase I está constituida por mGlu1 y mGlu5. Al expresarse en sistemas heterólogos, estos receptores se acoplan al metabolismo de los fosfoinosítidos. Presentan cuatro variantes de procesamiento (dos por cada subunidad) y son activados preferencialmente por el ácido quiscuálico y por otros agonistas tales como la 3,5-dihidroxifenilglicina (DHPG). Al parecer, es necesario que formen homodímeros para activarse [31]. La clase II está formada por las subunidades mGlu2 y mGlu3; estos receptores están acoplados a proteínas G_i; al parecer, no presentan isoformas

por corte y empalme alternativo y su principal agonista es el ácido 2R, 4R-4-amino pirrolidon-2,4-dicarboxílico (2R, 4R-4-ACPD). A la clase III pertenecen las subunidades mGlu4, mGlu6 y mGlu8, y aunque también están acoplados a la inhibición de la enzima adenilato ciclasa, su agonista principal es el ácido L-amino-4-fosfonobutírico (L-AP4).

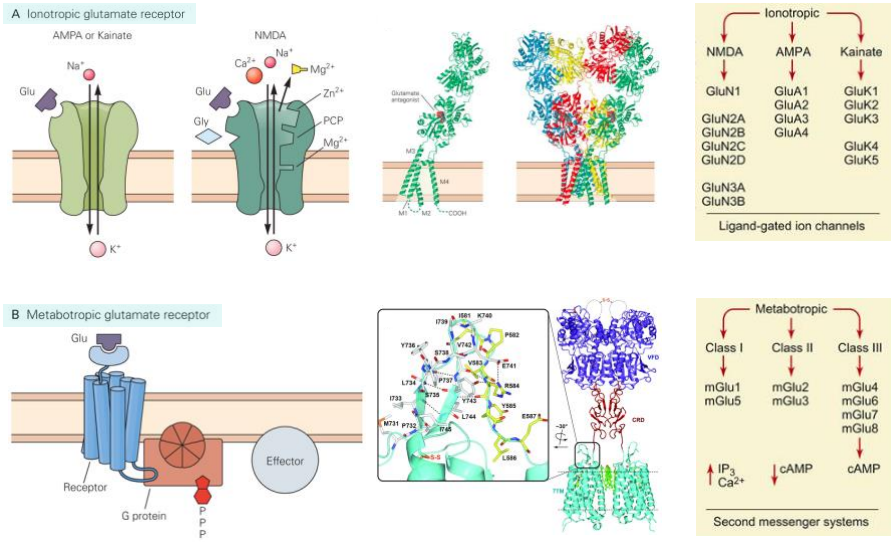

Figura 2. Receptores glutamatérgicos y sus familias moleculares.

Tanto los receptores ionotrópicos y metabotrópicos se subdividen en tres grupos. Estos grupos se componen de numerosas subunidades codificadas en genes diferentes. A. receptores ionotrópicos; B receptores metabotrópicos (Adaptado de [32]).

Remoción del glutamato extracelular

La activación excesiva de los receptores de Glu es dañina, puede matar neuronas [33] y oligodendrocitos [34]. Se ha demostrado que la activación de receptores glutamatérgicos ionotrópicos incrementa el consumo de energía [35, 36], lo que lleva a un influjo de Na_{+} y Ca_{+2} que tiene que ser contrarrestado con un proceso dependiente de energía, lo cual hace que las neuronas sean vulnerables al Glu después de periodos largos de privación de energía [37]. La activación de receptores de Glu genera especies reactivas de oxígeno [38], por lo que es de suma importancia mantener baja la concentración extracelular de este neurotransmisor. No existe evidencia de alguna enzima extracelular capaz de metabolizar significativamente el Glu; en consecuencia, la única manera rápida para retirarlo del

medio extracelular es por captura celular [39]. La captura de Glu es llevada a cabo por proteínas integrales de membrana, que utilizan los gradientes electroquímicos a través de las membranas plasmáticas como fuerza motriz para la internalización de este neurotransmisor.

Transportadores de membrana plasmática de aminoácidos excitadores

Concretamente, existen cinco transportadores de glutamato, denominados transportadores de aminoácidos excitadores (EAAT, por sus siglas en inglés) que difieren en su secuencia aminoacídica, capacidad de transporte para Glu, afinidad, velocidad de transporte, conductancia al cloruro y, sobre todo, localización celular. Todos los EAATs son dependientes de sodio en el ciclo de transporte, aparte de otros iones adicionales. Los genes que codifican los transportadores en los humanos son SLC1A3, SLC1A2, SLC1A1, SLC1A6 y SLC1A7, correspondientes a las proteínas EAAT1, EAAT2, EAAT3, EAAT4 y EAAT5 (las tres primeras también son conocidas como GLAST, GLT-1 y EAAC1 en roedores). Además, los transportadores EAAT1, 2 y 3 presentan variantes de corte y empalme alternativo en el procesamiento de sus ARNm que difieren en sus extremos amino o carboxilo. Esta característica confiere a cada variante posibilidades diferentes para interaccionar con otras proteínas, aunque no hay evidencias de diferencias funcionales entre ellas [40, 41]. Todas estas proteínas mantienen bajas concentraciones de Glu en la proximidad de sus receptores para evitar así un ciclo fútil de activación/desensibilización y procurar una relación señal-ruido apropiada que evite la activación excitotóxica. La concentración extracelular de Glu se mantiene en un rango de entre 10 y 100 nM [42, 43]. Los transportadores de glutamato, funcionando en situaciones fisiológicas, son capaces de mantener gradientes de concentración a través de la membrana plasmática de hasta un millón de veces. El mantenimiento de estos gradientes en condiciones celulares de reposo requiere un esfuerzo termodinámico de enormes proporciones llevado a cabo por el funcionamiento de los transportadores de glutamato que operan a través de ciclos de transporte con una estequiometria de una molécula de glutamato, tres de iones sodio y un protón, que se contraponen al movimiento de un ion potasio [44] (Fig. 3).

El funcionamiento de todos los transportadores de glutamato lleva aparejado un flujo termodinámico de iones cloruro no acoplado a través del transportador [44–46]. En este sentido, en los transportadores neuronales EAAT4 y EAAT5, este flujo de iones cloruro es muy robusto, y ambos funcionan como verdaderos canales de cloruro. El resto de los transportadores presentan un flujo desacoplado de cloruro mucho más limitado [47–50]. En muchos casos, el significado fisiológico de estas corrientes desacopladas de cloruro no está aún bien establecido.

La localización regional y celular de los trasportadores de glutamato es muy específica, lo que hace que su funcionamiento en condiciones fisiológicas no resulte redundante. EAAT1 (GLAST) y EAAT2 (GLT-1) se expresan de forma abundante y ubicua en el cerebro, aunque GLT-1 se encuentra principalmente en la neocorteza y el hipocampo, y GLAST en el cerebelo [3]. EAAT3, aunque ubicuo en el sistema nervioso central, se localiza principalmente en el soma y las dendritas de las neuronas del hipocampo, así como en el cerebelo y los ganglios basales. EAAT4 tiene una localización preferente en las dendritas de las células de Purkinje del cerebelo [51–54], y EAAT5 es una proteína confinada a terminales presinápticos de las células bipolares de la retina y fotorreceptores, con muy poca presencia en el resto del sistema nervioso [55, 56].

GLT-1 representa el 1% de todas las proteínas del cerebro, se expresa mayoritariamente en los astrocitos y es responsable de la mayor cantidad del transporte de glutamato al interior celular [57–59]. Por ello, la deleción genética de GLT-1 tiene como resultado la aparición de convulsiones en las primeras etapas del desarrollo y la muerte prematura de los animales [60]. Aunque en mucha menor proporción que en los astrocitos, se ha demostrado expresión presináptica de GLT-1 [61]. Este transportador localizado presinápticamente podría actuar reponiendo las reservas presinápticas de glutamato como vía alternativa al ciclo glutamato-glutamina. Tradicionalmente se ha postulado que el glutamato almacenado en las neuronas se recupera del entorno mediante los transportadores GLT-1 y GLAST localizados en los astrocitos; dentro de éstos es convertido en glutamina, la cual se transporta a las neuronas presinápticas, y de nuevo es transformado en glutamato, el cual se almacena en las vesículas sinápticas a la espera de ser liberado. GLAST

se expresa en los astrocitos y oligodendrocitos del sistema nervioso y, a diferencia de lo que ocurre con GLT-1, los animales con la deleción genética de esta proteína muestran pocas anormalidades funcionales [62].

Los transportadores de glutamato EAAT1 y EAAT2 forman complejos homotriméricos, mientras que algunos otros son heterotrímeros (EAAT3 y EAAT4) [63, 64]. Cada subunidad puede funcionar de forma independiente en cuanto al transporte, pero siempre en forma de trímeros. A lo largo del ciclo de transporte, cada subunidad sufre varios cambios conformacionales. En primer lugar, en el espacio extracelular se une una molécula de Glu, así como tres iones sodio y un protón. En ese momento, el transportador sufre un cambio conformacional adoptando una forma de "cara hacia adentro" que permite liberar estos sustratos hacia el citoplasma. Posteriormente, se une un ion potasio desde el interior, el cual es liberado al espacio extracelular mediante otro cambio conformacional de la proteína, volviendo al estado de "cara hacia fuera" [63, 65]. Cada protómero del complejo tiene una estructura peculiar formada por ocho regiones transmembranales orientadas no perpendicularmente [50, 66]. Mediante diferentes técnicas, principalmente mutagénesis dirigida, en los últimos años se ha podido determinar el sitio concreto de la proteína donde se unen tanto el sustrato como cada uno de los iones acoplantes [65].

La neurotransmisión glutamatérgica, tanto en su aspecto dinámico como de robustez, depende de la geometría de la sinapsis, así como del número de receptores y transportadores presentes en ella. En las sinapsis en las que hay un número importante de transportadores, el Glu se retira rápidamente del espacio extracelular; sin embargo, en las sinapsis con una baja densidad de transportadores, el Glu difunde hacia otras sinapsis cercanas, alterando su funcionamiento. Estos transportadores están sometidos a procesos de tráfico intracelular regulados por diversas vías de señalización. Desde hace tiempo se sabe que la proteincinasa C (PKC) tiene efectos diversos sobre los transportadores de glutamato, dependiendo del tipo celular en el que se expresen, lo que indica que la regulación del transporte de glutamato por PKC es compleja en muchos sentidos. Y no sólo depende del tipo celular, sino también del tipo de isoforma de PKC y de la

forma en que ésta se active [67, 68]. Hablando específicamente de GLT-1, procesos de fosforilación regulan la cantidad de ésta proteína presente en la superficie de la membrana plasmática [69]. Recientemente se ha demostrado que GLT-1 forma parte de agrupaciones dinámicas que cambian dependiendo de la actividad neuronal [70]. El número de transportadores en la membrana en un momento determinado refleja el equilibrio entre su inserción y su remoción. La endocitosis de GLT-1 depende de la ubiquitinación del transportador inducida por la activación de PKC y mediada por la ubiquitina ligasa Nedd4-2 [71, 72]. Otras cinasas, como la GSK3β, que desempeña un papel importante en múltiples procesos celulares, como el desarrollo neuronal o la plasticidad sináptica, también influyen en el tráfico intracelular de los transportadores de glutamato [73].

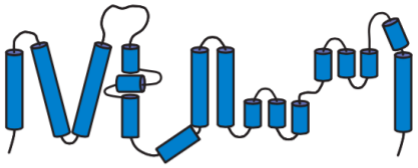

Transportadores de la familia SCL1

Transportadores:
Transportadores de Glu [EAAT1 (GLAST), EAAT2 (GLT-1), EAAT3 (EAAC1), EAAT4 y EAAT5]

Dependencia iónica:
Na^+, H^+ (simporte), K^+ (antiporte)

Estructura: seis segmentos TM y dos trímeros en el extremo C-terminal en forma de horquilla

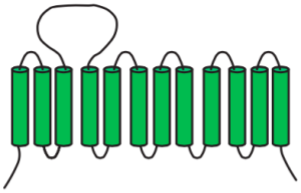

Transportadores de la familia SCL17

Transportadores: vGlut1–3

Dependencia iónica: H^+ (antiporte)

Estructura: de 6–12 segmentos TM predichos, se desconoce su estado de oligomerización

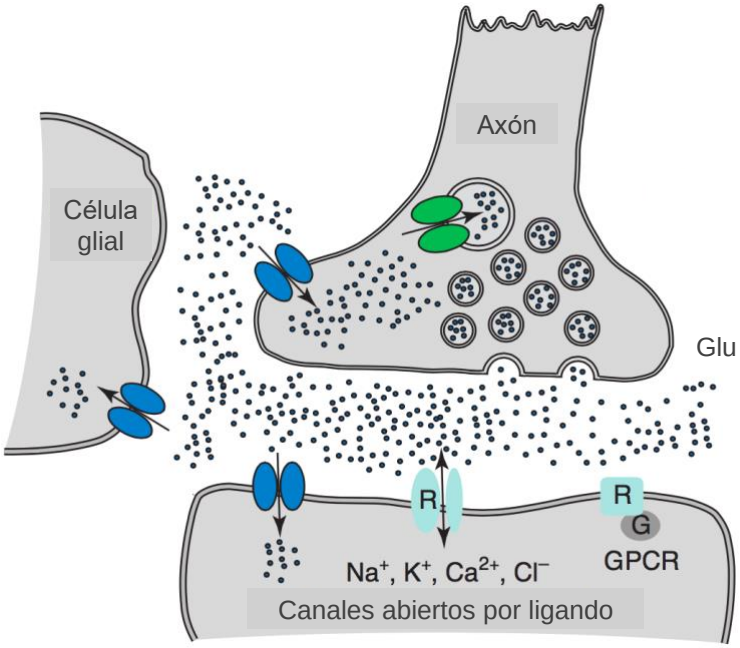

Figura 3. Familias de trasportadores glutamatérgicos.

En las terminales nerviosas presinápticas de sinapsis glutamatérgicas, los transportadores vesiculares de Glu (vGlut1-3; verde), pertenecientes a la familia de genes SLC17, acumulan el Glu en vesículas sinápticas para poder ser liberado posteriormente. El Glu ejerce sus funciones a través de los receptores ionotrópicos y metabotrópicos (cian). Los transportadores responsables de remover el Glu del medio extracelular pertenecen a la familia de genes SLC1 (EAATs1-5; azul), y están presentes en las membranas plasmáticas de neuronas presinápticas, células gliales adyacentes y neuronas postsinápticas. (Adaptado de [74]).

Células gliales

La glía es el grupo de células del sistema nervioso más abundante en el cerebro. Sin embargo, durante mucho tiempo se le consideró sólo como un elemento de soporte neuronal, que no cumplía ninguna función importante. Hoy se sabe que la glía participa en la formación, operación y modulación de los circuitos sinápticos. En consecuencia, los estudios recientes nos presentan a la glía como un elemento fundamental para investigar y conocer sobre la fisiología del SNC [75, 76]. Asimismo, la glía es un grupo heterogéneo de células nerviosas que cumplen funciones diversas en la fisiología del cerebro. Con base en su morfología, fisiología y localización, en el cerebro podemos identificar los siguientes principales tipos de glía: microglía, oligodendroglía, glía NG2, y astroglía. Las células gliales y las neuronas tienen un mismo origen embrionario pues derivan del neuroectodermo. La microglía es la excepción, pues tiene un origen mesodérmico.

Microglía

El cerebro cuenta con un sistema inmunitario, al igual que el resto del cuerpo. Los linfocitos presentes en el torrente sanguíneo alcanzan cualquier tejido en el cuerpo a través de los vasos sanguíneos. Sin embargo, el cerebro es la excepción, ya que la barrera hematoencefálica impide el paso de los linfocitos; su entrada al SNC puede resultar nociva para el cerebro. Por ello, se requieren células especiales que se ocupen de proporcionar inmunidad al cerebro, la microglía cubre esa función.

La microglía se encarga de vigilar que el cerebro conserve su integridad al reaccionar de manera inmediata ante cualquier daño que se produzca. En caso de infección, la microglía combate a los organismos nocivos, fagocitándolos y removiendo también las células muertas. La microglía, incluso, puede participar en la remodelación sináptica durante el desarrollo del SNC, al remover conexiones inapropiadas. Adicionalmente, la microglía se vuelve activa en enfermedades neurodegenerativas; si esto es benéfico o nocivo es todavía materia de debate y de investigación [77].

Oligodendroglía

El papel fundamental de este tipo de glía es facilitar la comunicación eléctrica entre las neuronas. La oligodendroglía comprende a los oligodendrocitos que se ubican en el SNC; las células de Schwann, que están presentes en el sistema nervioso periférico, son como los representantes de la oligodendroglía en los nervios periféricos. Ambos tipos gliales producen mielina, una lipoproteína que envuelve a los axones de las neuronas y hace más eficiente la comunicación neuronal, al acelerar la conducción eléctrica de los impulsos nerviosos.

Existen tres tipos de oligodendrocitos, de acuerdo con su ubicación entre los componentes del SNC: perineuronales, perivasculares e interfasciculares. Adicionalmente, la oligodendroglía contribuye al soporte metabólico necesario para el adecuado funcionamiento axonal [78]. Cuando los oligodendrocitos o las células de Schwann se afectan, se presenta un déficit metabólico y en la producción de mielina, lo que conlleva a una desmielinización de los axones. Las consecuencias de la desmielinización y el déficit metabólico de la oligodendroglía producen problemas cognitivos y motores, como los que se presentan en enfermedades neurodegenerativas como la esclerosis múltiple o las leucodistrofias.

Glía NG2

Anteriormente se pensaba que los contactos sinápticos se daban sólo entre neuronas. Sin embargo, la evidencia anatómico-funcional de que existían contactos sinápticos neurona-glía se consolidó en la década pasada.

Las células gliales identificadas como postsinápticas son las precursoras de los oligodendrocitos, que se distinguen de los otros tipos de células gliales porque producen la proteína de membrana NG2. La glía NG2 constituye del 5 al 8 por ciento del total de células del SNC y es probablemente el tipo glial del que menor información se dispone.

El papel que juega la glía NG2 en la fisiología del cerebro es controvertido, por lo que es campo fértil de estudio para la neurobiología [79]. Inicialmente, las células gliales NG2 fueron clasificadas como precursoras de los oligodendrocitos.

Sin embargo, estudios posteriores presentaron evidencia de que la glía NG2 podría participar en la formación de neuronas y astrocitos. Otro estudio reportó que sólo pueden generar oligodendrocitos. Para avivar aún más la controversia, un estudio reciente sugiere que la glía NG2 no sólo produce oligodendrocitos y astrocitos, sino también un tipo de glía radial exclusiva del cerebelo: la glía de Bergmann [80]. De esta manera, la controversia de la glía NG2 como precursora de distintos tipos de células nerviosas persiste, y el significado funcional de los contactos sinápticos que recibe sigue siendo intrigante.

Astroglía

La astroglía comprende a los astrocitos, las células ependimales y la glía radial. Una característica que tienen en común es la presencia de la proteína ácido gliofibrilar (GFAP), expresada en el citoesqueleto.

La palabra astrocito significa “célula en forma de estrella”. Este nombre, acuñado por Michael von Lenhossék en 1891, se basa en su morfología. Los astrocitos regulan la homeostasis del cerebro, al proveer energía y sustratos para la neurotransmisión, y participan activamente en la fisiología de la sinapsis tripartita. Los astrocitos fueron subclasificados en protoplasmáticos y fibrosos por Rudolf Albert von Kölliker y William Lloyd Andriezen en 1889 y 1893, respectivamente: los astrocitos fibrosos se ubican principalmente en la sustancia blanca, y están asociados a los axones; los astrocitos protoplasmáticos, asociados a los somas neuronales y las sinapsis, están presentes principalmente en la sustancia gris. En el pasado se pensaba que el papel de los astrocitos se restringía a la remoción de los neurotransmisores del espacio sináptico, lo que permitía una señalización precisa. Sin embargo, estudios recientes indican que los astrocitos tienen actividad neurogénica e incluso participan en la formación de las sinapsis y modulan la actividad sináptica gracias a una comunicación bidireccional con las neuronas [81, 82].

En las primeras etapas del desarrollo, la denominada glía radial es uno de los primeros tipos gliales en aparecer. Estas células presentan una morfología bipolar y expresan marcadores específicos como tenascina y vimentina,

fundamentales para determinar los patrones de migración neuronal [83]. A partir del nacimiento, estas células inician un proceso denominado “conversión astrocítica”, pierden su morfología bipolar, además de la expresión de vimentina, y aumenta la expresión de la proteína GFAP. Esta conversión es reversible y regulada por factores secretados por las neuronas [84].

Tanto en el cerebelo como en la retina hay poblaciones de glía radial que permanecen en el individuo adulto: las células de Müller en la retina, y las células de Bergmann en el cerebelo [85]. Ambos tipos celulares envuelven sinapsis glutamatérgicas; las células de Müller circundan dos sinapsis, las establecidas entre las células bipolares y el fotorreceptor, y las formadas por las células ganglionares y las mencionadas células bipolares [86]. Por otra parte, las células de Bergmann se ubican en la capa molecular de la corteza cerebelar, donde envuelven las sinapsis formadas por los axones de las células granulares (también llamadas fibras paralelas) y las dendritas de las células de Purkinje (Figs. 4 y 5) [87].

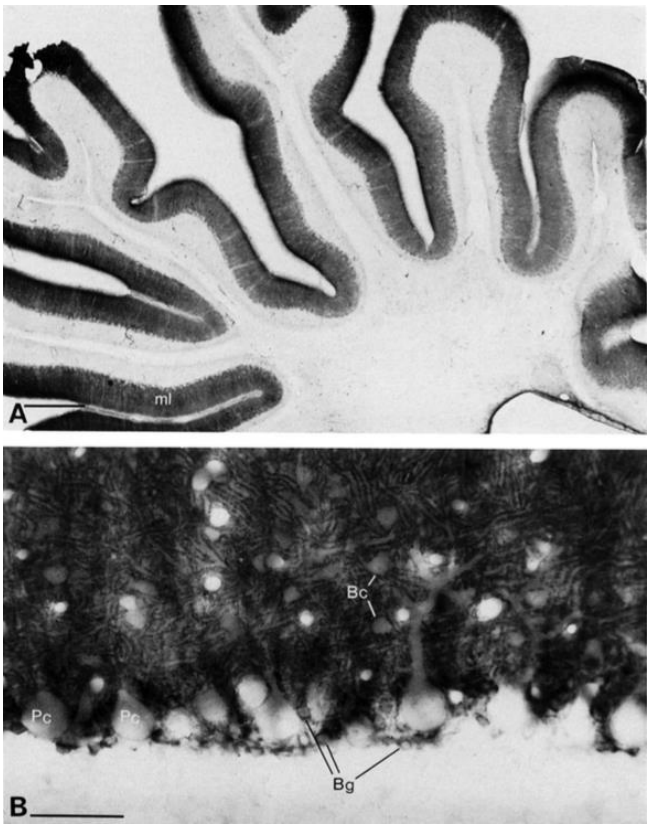

Figura 4. Rebanadas (50 µm de espesor) de cerebelo de pollo de 17 días de edad. A. La inmunorreactividad detectada por el anticuerpo IX-50 se localiza en las capas molecular (ml) y de Purkinje. Los puntos en la capa granular, en la sustancia blanca y en los núcleos profundos del cerebelo no son sitios inmunorreactivos. Representan glóbulos rojos, ya que presentan actividad de la enzima peroxidasa. (B) A una mayor magnificación, se puede observar como la inmunorreactividad esboza a las células de Purkinje (PC), sus dendritas, las células en canasta (Bc), y también parece estar asociada con las células gliales de Bergmann (Bg). Barras de escala: A = 500 µm; B = 50 µm [87].

Células gliales de Bergmann

Las células gliales de Bergmann (CGB) son el tipo de célula glial más abundante en la corteza del cerebelo de los vertebrados adultos y se les considera como un tipo de astrocito especializado. Durante el desarrollo, los procesos de las CGB proveen soporte estructural a la placa cerebelar, sus pies terminales se adhieren para formar una capa continua de glía limitando el cerebelo. Las fibras radiales de las CGB también actúan como una guía esencial para la migración de las células granulares [88]. Una vez terminada la morfogénesis cerebelar, las CGB permanecen como un soporte estructural importante, pero además tienen papeles adicionales en el mantenimiento, función y plasticidad de la sinapsis [89].

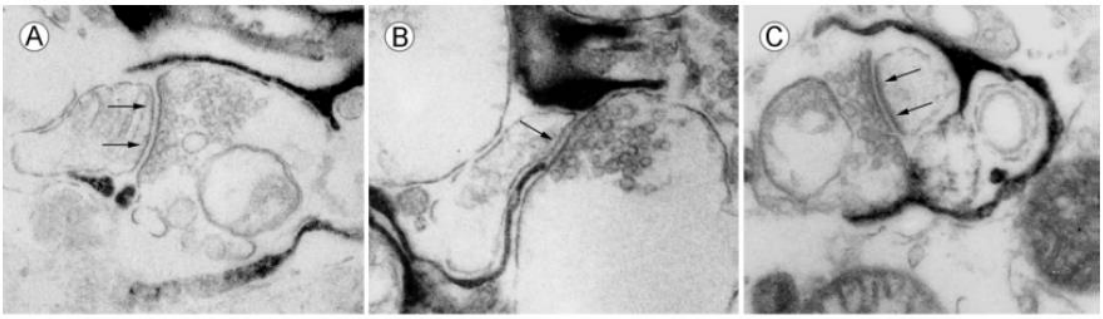

Figura 5. Imágenes de rebanadas de cerebelo de un ratón adulto (p30) obtenidas por MET. En los paneles A–C se observan sinapsis rodeadas por CGB (en negro). Las membranas post-sinápticas están marcadas por flechas [90].

El cerebelo es un sistema donde predominan las señales excitadoras, y las CGB participan en la regulación de estas señales al limitar la difusión del Glu liberado durante la actividad sináptica por medio de su captura, manteniendo así bajas las concentraciones extracelulares de dicho neurotransmisor. Diversos estudios han estimado que el 20% del Glu liberado durante una transmisión sináptica es removido por el compartimiento neuronal postsináptico, mientras que el 80% restante es capturado por las CGB [91]. Esto es importante debido a que las células de Purkinje son susceptibles a excitotoxicidad ocasionada por la excesiva estimulación de sus receptores glutamatérgicos [92].

Diversos estudios sugieren que las CGB también tienen papeles más activos

en la sinapsis. Ha sido demostrado que las células de Bergmann responden a la actividad neuronal glutamatérgica, por medio de la estimulación de los receptores glutamatérgicos que expresan, provocando un influjo de Ca^{2+}, seguido de la hidrólisis de fosfoinosítidos y la activación de PKC [93], MAPK [94], PI3K [95] y CaMKII [96]. La transducción de señales mediada por la activación de los receptores glutamatérgicos modifica la expresión de genes en múltiples modelos de aprendizaje, plasticidad sináptica e isquemia, durante el envejecimiento y en alteraciones neurológicas, tales como la epilepsia, la esquizofrenia y la enfermedad de Alzheimer. En CGB, el tratamiento con Glu induce cambios en el patrón de expresión de genes [97–104], que influye en la modulación de la transmisión y plasticidad sináptica.

Disfunciones de los transportadores de glutamato en enfermedades neurológicas

Dado el papel crítico de los transportadores de Glu en mantener los niveles de Glu por debajo del umbral tóxico, la alteración de la expresión y la función de estos transportadores conduce a lesiones neuronales excitotóxicas y está vinculado a numerosos trastornos neurológicos.

En algunos estudios se ha observado una disminución en la función y la expresión de GLT-1 y GLAST en astrocitos corticales derivados de pacientes con enfermedad de Alzheimer (EA) [105]. La expresión de GLT-1 también disminuye en modelos animales de EA [106]. La proteína β-amiloide (Aβ), cuya deposición excesiva como placas amiloides en el cerebro se considera que desempeña un papel clave en la etiología de la EA, ha sido relacionada con la reducción tanto en la expresión como en la función de GLT-1 y GLAST en astrocitos en cultivo [107, 108]. Además, en pacientes con esclerosis lateral amiotrófica (ELA) se ha observado una reducción en la expresión y función de GLT-1 [109, 110]. La alteración de la función de GLT-1 en la ELA es secundaria a la inflamación y el estrés oxidante [111]. La expresión y la función tanto de GLT-1 como de GLAST también disminuyen en modelos experimentales de epilepsia [112, 113].

En la enfermedad de Parkinson (EP), el deterioro de la función de los

transportadores de Glu está asociado con el daño a las neuronas dopaminérgicas nigroestriatales [114]. En un modelo experimental de EP, que emplea a la 6-hidroxidopamina para obtener una lesión unilateral del haz nigroestriado, se ha demostrado que GLT-1 y GLAST están significativamente reducidos en el estriado de las ratas lesionadas [115]. De forma similar, existe evidencia que el N-metil-4-fenilpiridinio (MPP+), un químico que simula síntomas similares a la EP en humanos y modelos animales, induce la desregulación de la captura de Glu tanto en modelos experimentales *in vitro* e *in vivo* [116, 117]. Clínicamente, el papel de los transportadores de Glu en la EP se apoya además en las observaciones sobre la disminución de la captura de Glu en plaquetas de pacientes con EP [118]. Sin embargo, el papel de los transportadores de Glu en los modelos animales de EP sigue siendo controvertido ya que algunos estudios no han observado cambios en los niveles de ARNm/proteína de estos transportadores en ratas lesionadas con 6-hidroxidopamina [119].

Efecto de los metales pesados sobre los transportadores de glutamato

Los transportadores astrocíticos de Glu son susceptibles a metales pesados, como el plomo (Pb), el metilmercurio (MeHg) y el manganeso (Mn). Se ha comprobado que el Pb disminuye la expresión y la función, tanto de GLAST como de GLT-1 [120]. Los efectos del Pb sobre los transportadores de Glu fueron específicos de la región, siendo el hipocampo el área más vulnerable, correlacionado con la preponderancia de los déficits cognitivos asociados con la exposición a Pb [121]. Otros estudios, también han observado que la exposición al MeHg desencadena un aumento de las especies reactivas de oxígeno, específicamente peróxido de hidrógeno (H_2O_2), que inhiben la función y la expresión de GLAST en cultivos primarios de astrocitos [122]. El MeHg también contribuye a la desregulación de la homeostasis del Glu al afectar la función GLAST y GLT-1 en células CHO transfectadas con estos transportadores [123]. Notablemente, estos efectos son atenuados por memantina, un antagonista de los receptores NMDA, consistente con la desregulación de la homeostasis del Glu inducida por MeHg [124].

Esencialidad y toxicidad del manganeso

El Mn es un elemento ubicuo presente de forma natural en el medio ambiente, incluyendo el agua y los alimentos. En el cuerpo humano el Mn se encuentra en todos los tejidos, donde se requiere para el metabolismo normal de aminoácidos, lípidos, proteínas y carbohidratos, y la generación de ATP. También participa en la coagulación de la sangre y la homeostasis de la glucosa, la respuesta inmune, la digestión, la reproducción y el crecimiento óseo [125–127]. Además, el Mn es un componente crítico de numerosas metaloenzimas, incluyendo la superóxido dismutasa (SOD), arginasa, fosfoenolpiruvato descarboxilasa y glutamina sintetasa (GS) [128–130].

A pesar de su requerimiento en múltiples procesos fisiológicos, la acumulación de Mn en el cerebro después de la exposición crónica a niveles excesivos de este metal, ya sea de fuentes ambientales u ocupacionales, ocasiona una serie de secuelas neurológicas conocidas como manganismo. Las características clínicas del manganismo son, en gran medida, análogas a las observadas en la EP, caracterizadas por disfunción cognitiva y motora [131, 132].

Fuentes de exposición

El Mn es naturalmente abundante en la corteza terrestre (0.1%) y el suelo (40-900 mg/kg) [133, 134]. El Mn se encuentra como óxidos, carbonatos y silicatos en minerales. La versatilidad de las propiedades químicas del Mn ha ampliado su uso industrial en las industrias del vidrio, cerámica, pintura, adhesivos y de soldadura. Este amplio uso del Mn ha dado lugar a preocupaciones de salud a nivel mundial. De hecho, la exposición ocupacional a Mn se ha documentado en múltiples industrias, incluyendo la industria de la fundición, la soldadura, la minería, la producción de baterías, vidrio y cerámica [135–139].

La principal fuente de exposición a Mn en la población humana es de la dieta, que se estima contiene 0.9-10 mg de Mn por día [140]. El arroz, los granos y las nueces son fuentes ricas de Mn con un exceso de 30 mg/kg, mientras que el contenido de Mn en el té es de 0.4-1.3 mg/taza. Los niveles de Mn en agua potable

están en el rango de 1-100 µg/L [14, 141]. Recientemente ha llamado la atención pública el alto contenido de Mn en las fórmulas infantiles en comparación con la leche humana [142], junto con el Mn en la nutrición parenteral. Este último es considerado un factor de riesgo para la toxicidad inducida por Mn ya que los mecanismos de regulación intestinal se pasan por alto, por lo que la administración intravenosa de Mn es 100% biodisponible [143, 144].

El Mn en vapores, aerosoles o material particulado en suspensión se deposita en el tracto respiratorio superior e inferior, y posteriormente entra en el torrente sanguíneo. En varios países, la introducción de un aditivo antidetonante en la gasolina que contiene Mn, metilciclopentadienil tricarbonilo de Mn (MMT), representa otra fuente de exposición a Mn por inhalación [145, 146].

Los consumidores de “drogas de diseño”, tales como la metcatinona, donde el permanganato de potasio se utiliza como un oxidante para su síntesis, también presentan secuelas neurodegenerativas que corresponden a una sintomatología parecida a la EP [147].

Absorción, transporte y excreción

La dieta representa la principal fuente de Mn en los seres humanos. El tracto gastrointestinal absorbe 1-5% del Mn ingerido; mientras que el 60-70% del Mn inhalado es exhalado por los pulmones [148, 149]. La absorción de Mn está estrechamente regulada y el exceso de Mn se excreta a través de la bilis [150]. Tanto el transporte activo y los mecanismos de difusión pasiva regulan la absorción oral del Mn y el proceso se rige por varios factores, incluyendo la edad y los niveles dietéticos de Mn y otros minerales [140, 150, 151]. Entre otros metales, las reservas de hierro (Fe) son particularmente importantes dada la relación inversa entre los niveles celulares de Fe y la captura de Mn [152, 153].

Debido a que la capa externa de electrones del Mn puede donar hasta 7 electrones, este elemento puede existir en 11 diferentes estados de oxidación, variando de –3 a +7 [154]. En tejidos vivos, el Mn ha sido encontrado como Mn^{+2} y Mn^{+3}. Mientras que los estados de oxidación Mn^{+5}, Mn^{+6}, Mn^{+7}, y los demás complejos de oxidación más bajos no están presentes en muestras biológicas [155].

En la sangre, el Mn está presente, predominantemente (> 90%), en el estado de oxidación +2 y se liga principalmente a β-globulina y albúmina. Una pequeña fracción de Mn^{+3} se acompleja con transferrina [156, 157]. El transporte del Mn^{+2} a través de la barrera hematoencefálica (BHE) y las membranas celulares es facilitado por el transportador de metales divalentes 1 (DMT1), el receptor NMDA, y los transportadores Zip8 y Zip14 [158–160], por nombrar algunos. La transferrina es el sistema de transporte más eficiente para Mn en el estado de oxidación +3 [161].

El Mn se distribuye por todo el cerebro y los niveles más altos de Mn se encuentran en el globo pálido y otros núcleos de los ganglios basales (estriado y sustancia negra) [162, 163]. El DMT1 y la transferrina también regulan la captura de Mn tanto en astrocitos como en neuronas [164, 165]. Generalmente, la concentración intracelular de Mn es mayor en tejidos ricos en mitocondrias y pigmentación.

El Mn en trastornos neurodegenerativos

Un número creciente de evidencias revela que la sobreexposición a Mn está implicada en múltiples enfermedades neurodegenerativas. La exposición crónica a un alto contenido de Mn puede precipitar la progresión de la EP por la disminución de recambio de dopamina estriatal y la promoción de un mal plegamiento y la agregación de α-sinucleína [166, 167]. También, diversos reportes sugieren que la exposición ocupacional a Mn está estrechamente relacionada con la ELA. Uno de estos trabajos reportó que trabajadores de la industria fundidora en Alemania han desarrollado manganismo y ELA [168]. Igualmente, se ha reportado que pacientes con ELA presentan un alto contenido de Mn en la médula espinal [169].

La sobreexposición a Mn también ha sido implicada en la enfermedad de Creutzfeldt-Jakob (ECJ), ya que el Mn provoca el plegamiento erróneo y la agregación de la proteína prión [170, 171]. Así mismo, la exposición a Mn puede desempeñar un papel en la EA, ya que muchos trabajos han mostrado que pacientes con niveles elevados de Mn presentan demencia y signos patológicos típicos de la EA [172].

Mecanismos de neurotoxicidad del Mn

Dado que la neurotoxicidad del Mn está asociada con múltiples enfermedades neurodegenerativas [173], se han llevado a cabo diversos estudios para comprender los mecanismos celulares y moleculares implicados en los efectos del Mn en el cerebro.

El estrés oxidante, la disfunción mitocondrial, la apoptosis, la inflamación y la excitotoxicidad han sido postulados como los principales mecanismos moleculares y celulares de la neurotoxicidad inducida por Mn. Debido a que el Mn se acumula en las regiones ricas en dopamina del cerebro, tales como el globo pálido, la sustancia negra y el estriado, la oxidación de dopamina inducida por Mn también se ha sugerido como mecanismo principal de su neurotoxicidad [174, 175]. El Mn induce directamente estrés oxidante, ya que tanto en ratas como en primates disminuye los niveles de GSH [176, 177], y el tratamiento con antioxidantes (N-acetilcisteína) revierte el fenotipo patológico inducido por Mn [178].

El secuestro preferencial de Mn en las mitocondrias hace que este organelo productor de energía sea vulnerable a la toxicidad de Mn. En las mitocondrias, el Mn interfiere con la fosforilación oxidativa al inhibir la F1-ATPasa a niveles bajos e inhibiendo el complejo I de la cadena de transporte de electrones a mayores concentraciones [179, 180]. La apoptosis y la inflamación también juegan un papel importante en la neurotoxicidad del Mn. Durante la apoptosis inducida por Mn, tanto las vías apoptóticas extrínsecas como las intrínsecas están activadas en astrocitos y neuronas [181, 182]. Por otra parte, el Mn potencía la liberación de varias moléculas inflamatorias, incluyendo citocinas, como TNF-α, IL-6 e IL-1β, prostaglandinas y óxido nítrico (NO) a partir de células gliales activadas [183–185]. La muerte neuronal excitotóxica también contribuye a la neurotoxicidad del Mn, ya que el Mn reduce la expresión y la función de los transportadores astrocíticos de Glu [186, 187]. La inhibición de receptores NMDA con MK-801, un antagonista de estos receptores, revierte las lesiones inducidas por Mn en el estriado de rata, confirmando la participación del daño neuronal excitotóxico en la neurotoxicidad inducida por Mn [188]. Estas observaciones fueron confirmadas por Xu y

colaboradores en un estudio posterior, que mostró que el MK-801 previene la neurotoxicidad inducida por Mn [189, 190]. El mismo grupo también mostró que el Mn causa neurotoxicidad en ratas al aumentar el Glu extracelular, secundario a la expresión alterada de los receptores NMDA [191]. De forma similar, Spadoni y colaboradores demostraron que existe una evidente correlación entre el aumento en la sensibilidad al Glu de los receptores glutamatérgicos postsinápticos y la pérdida neuronal causada por Mn en el globo pálido [192].

Sin embargo, los efectos más severos de la toxicidad de Mn pueden estar mediados por el deterioro funcional de los astrocitos causado por la reducción de la expresión y la función de los transportadores de Glu.

Efecto del Mn sobre los transportadores astrocíticos de glutamato

Los astrocitos acumulan preferentemente el Mn, concentrándolo de 50 a 60 veces más que las neuronas [193]. Por consiguiente, los astrocitos son considerados el sitio primario de daño temprano y disfunción ante niveles elevados de Mn en el cerebro.

La inflamación y el estrés oxidante están implicados en la desregulación de los transportadores astrocíticos de Glu inducida por Mn, ya que el estrés oxidante inhibe la función los transportadores de Glu [194]. En los astrocitos, estresores oxidantes como el peroxinitrito y el H_2O_2 inhiben la captura de Glu, mientras que el tratamiento con agentes reductores, como el ditiotreitol, restaura la captura de Glu [195]. Por otra parte, el papel de la neuroinflamación inducida por Mn se ha asociado con la disminución de la función y la expresión de los transportadores, ya que el tratamiento con Mn induce la liberación de la citoquina inflamatoria TNF-α [196], que reduce la expresión y la función de GLT-1 [197].

Por otro lado, la vía de señalización de PKC desempeña un papel crítico en la mediación de la disfunción de los transportadores astrocíticos de Glu inducida por Mn [198, 199]. El Mn aumenta la fosforilación de las isoformas PKC-α y δ en astrocitos [200], mientras que la inhibición de PKC revierte los efectos negativos sobre la función y los niveles de proteína de GLT-1 y GLAST, inducidos por Mn [198, 199].

La activación de la vía apoptótica inducida por Mn también desempeña un papel en la reducción de la expresión de los transportadores de Glu, ya que un inhibidor de las caspasas, Z-VAD-FMK, atenúa eficazmente la reducción inducida por Mn en la captura de Glu, así como en los niveles de GLT-1 y GLAST [201].

Así mismo, la activación de PKC inducida por Mn podría resultar en una reducción del tráfico de los transportadores de Glu hacia la membrana, ya que la activación de PKC inducida por ésteres de forbol reduce la expresión de GLT-1 en la superficie celular [69]. De igual forma, se ha descrito un papel similar para la fosforilación de PKC que conduce a la disminución de la actividad de GLAST [202]. Además de la activación de PKC, varios estudios *in vitro* e *in vivo* han demostrado que el Mn activa a otras cinasas, como las cinasas reguladas por señales extracelulares (ERK), las cinasas c-Jun N-terminal (JNK), las proteínas cinasas activadas por mitógenos (p38) y Akt, pero el papel definitivo de estas vías en la disminución de los transportadores de Glu inducida por Mn queda por esclarecer [203–206].

ANTECEDENTES

Recientemente, Karki y colaboradores investigaron los mecanismos de la regulación transcripcional de GLAST, y demostraron que NF-κB es un regulador positivo, y YY1 es un regulador negativo. Así mismo, demostraron que YY1 media la represión de los transportadores astrocíticos de Glu inducida por Mn [196, 207]. Este estudio estableció que el Mn activa a YY1 para inhibir la expresión y la función de GLAST (Fig. 6). Tanto GLAST como GLT-1 contienen sitios consenso para YY1, y el Mn aumenta la unión de YY1 a estos sitios en los promotores (Fig. 7). Estudios previos también han evaluado el papel de YY1 en la represión de los transportadores de Glu [208, 209].

Múltiples estudios han demostrado que diversos moduladores positivos de los transportadores de Glu, como los factores neuronales, la ceftriaxona, el factor de crecimiento epidérmico, los estrógenos y los moduladores selectivos de los receptores de estrógenos (SERM), activan al factor nuclear κB (NF-κB) para regular de manera positiva a los transportadores de Glu [207, 210–213]. Karki y colaboradores también demostraron que la activación de YY1 inducida por Mn puede suprimir completamente los efectos estimuladores mediados por NF-κB en los transportadores de Glu (Fig. 8), lo que indica que los efectos represivos de YY1 pueden superar con facilidad las vías reguladoras positivas [207].

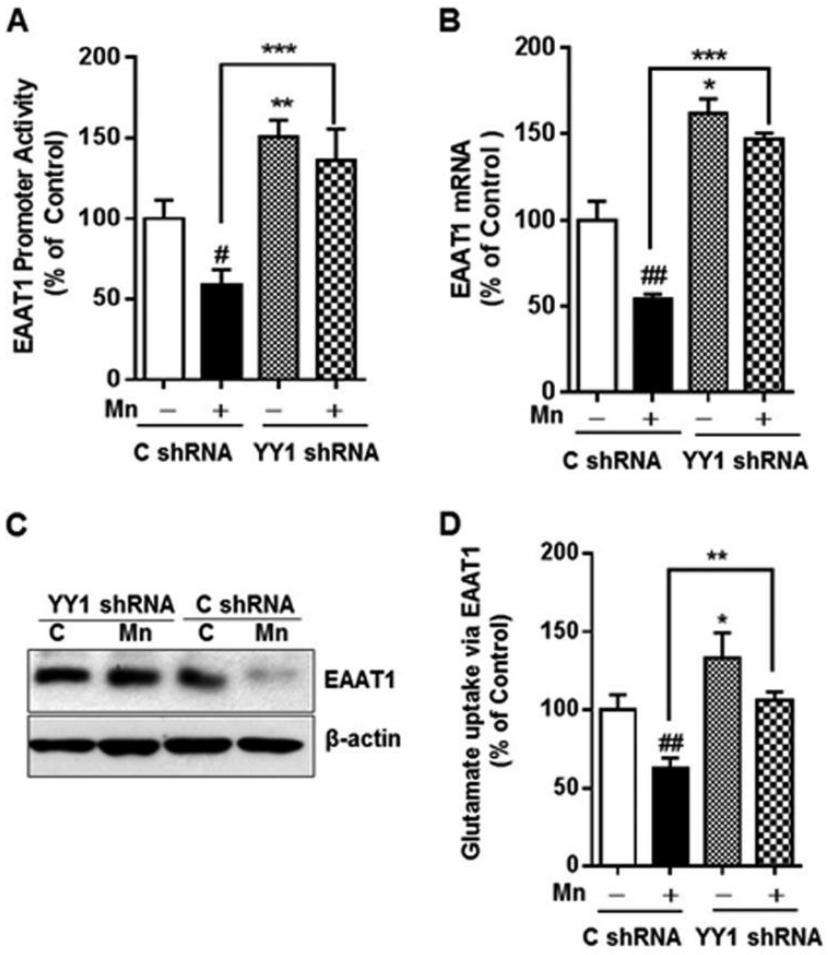

Figura 6. El silenciamiento de YY1 revierte la represión de la expresión y la función de EAAT1 inducida por Mn.

A, astrocitos humanos H4 fueron transducidos de forma estable con horquillas pequeñas de ARN (shRNAs por sus siglas en inglés; control o YY1) y posteriormente se transfectaron con 0.5 µg de una construcción conteniendo al gen luciferasa y al promotor de EAAT1, seguido del tratamiento con 250 µM de Mn durante 6 h. La actividad del promotor EAAT1 se determinó mediante el ensayo de luciferasa. B y C, las células que expresaron de forma estable los shRNAs control o de YY1 (C shRNA y YY1 shRNA, respectivamente) fueron tratadas con 250 µM de Mn durante 6 h, seguido por la determinación de los niveles de mensajero y proteína de EAAT1 por qPCR y Western blot, respectivamente. D las células que expresaron de forma estable C shRNA o de YY1 shRNA fueron tratadas con 250 µM de Mn durante 6 h, posteriormente se determinó la captura de Glu dependiente de EAAT1(las células fueron pretratadas con 100 µM de DHK durante 30 min.). *p<0.05, **p<0.01, ***p<0.001, #, p 0.05; ##, p 0.01; ANOVA seguido de la prueba post hoc de Tukey, n = 3-4 [207].

.

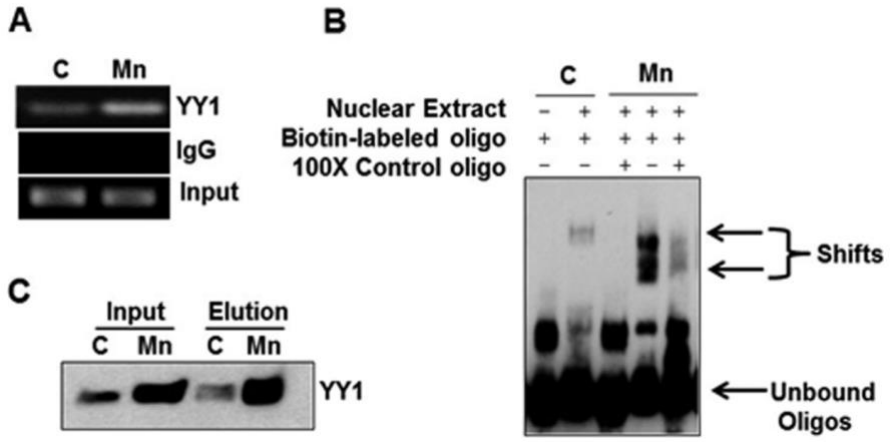

Figura 7. El Mn aumenta la unión de YY1 al promotor de EAAT1.

A, los astrocitos humanos H4 se trataron con Mn (250 µM, 6 h), seguido por el ensayo ChIP con un anticuerpo anti-YY1. La IgG de conejo fue utilizada como un control negativo, y los inputs para todas las muestras también se muestran. B, se utilizaron extractos nucleares preparados a partir de células tratadas con Mn (250 µM, 6 h) para realizar EMSAs con oligonucleótidos biotinilados que contenían los sitios de unión a YY1 del promotor de EAAT1. Los desplazamientos que contienen el complejo ADN-proteína se muestran con flechas. C, se realizó un DAPA con los oligonucleótidos biotinilados que contenían los sitios de unión a YY1 del promotor de EAAT1 y extractos nucleares de células tratadas y no tratadas (Mn y C, respectivamente) seguido por inumodetección en fase sólida contra YY1 [207].

Además, este grupo de investigación también proporcionó evidencia directa del papel de las histonas deacetilasas (HDACs) en la represión de los transportadores de Glu. La sobreexpresión de varias isoformas de HDACs resultó en la disminución de la actividad del promotor de GLAST [207] ya que las HDACs fueron reclutadas como correpresores por YY1 para inhibir la expresión de los transportadores de Glu (Fig. 9).

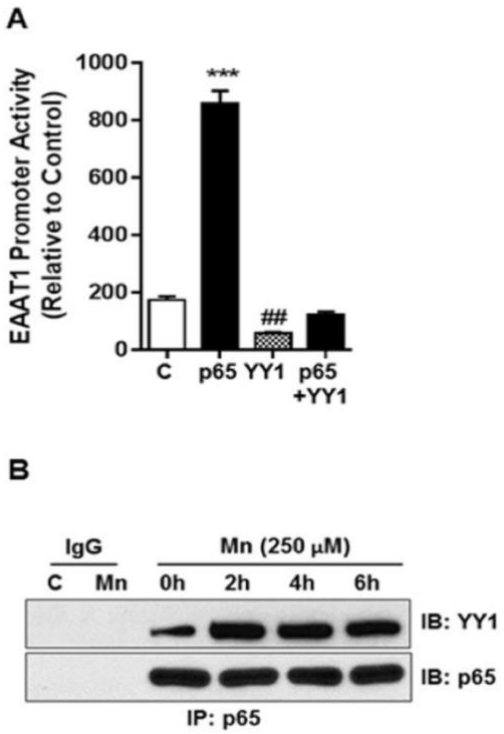

Figura 8. YY1 interactúa con p65, anulando los efectos estimulantes de este último sobre la actividad del promotor EAAT1.

A, los astrocitos humanos H4 fueron transfectados con YY1 o p65 (solos o en conjunto), y posteriormente se realizó el ensayo de luciferasa para determinar la actividad del promotor de EAAT1. B, las células fueron tratadas con Mn (250 μM) durante el periodo de tiempo indicado, y se usaron los extractos nucleares para realizar las Co-IPs para YY1 y p65. (***, p 0.001; ##, p 0.01; ANOVA seguido de la prueba post hoc de Tukey; n=3). Carril C, control; IB, inmunotransferencia; IP, inmunoprecipitación [207].

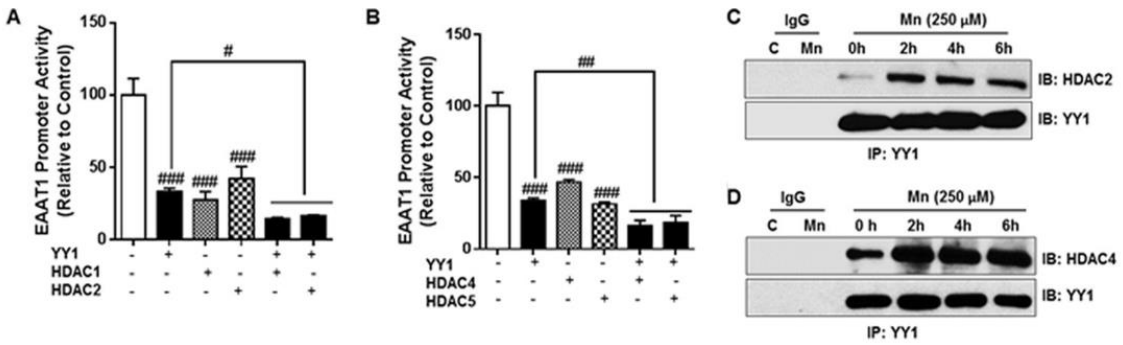

Figura 9. YY1 recluta a las HDACs como correpresores para inhibir EAAT1.

A y B, los astrocitos humanos H4 fueron transfectados con YY1 o con las isoformas designadas de HDACs (solos o en conjunto), y se midió la actividad del promotor de EAAT1. C y D, las células fueron tratadas con Mn (250 μM) durante los períodos de tiempo indicados, y los extractos nucleares fueron usados para determinar la interacción entre YY1 y HDAC2 o HDAC4 mediante Co-IPs. Se usó IgG de conejo como control negativo. (#, p 0.05; ##, p 0.01; ###, p 0.001; ANOVA seguido de la prueba post hoc de Tukey; n=3). Carril C, control; IB, inmunotransferencia; IP, inmunoprecipitación [207].

Por otro lado, aunque se conoce que el Mn se distribuye por todo el cerebro, ningún estudio se ha enfocado en analizar los efectos neurotóxicos de este elemento en otras regiones del cerebro distintas al globo pálido y el estriado. Sepúlveda y colaboradores observaron la deposición de Mn^{+2} en el bulbo olfatorio, la zona CA3 del hipocampo y en la materia gris del cerebelo de ratones infundidos con $MnCl_2$ continuamente durante 21 días (Fig. 10) [214].

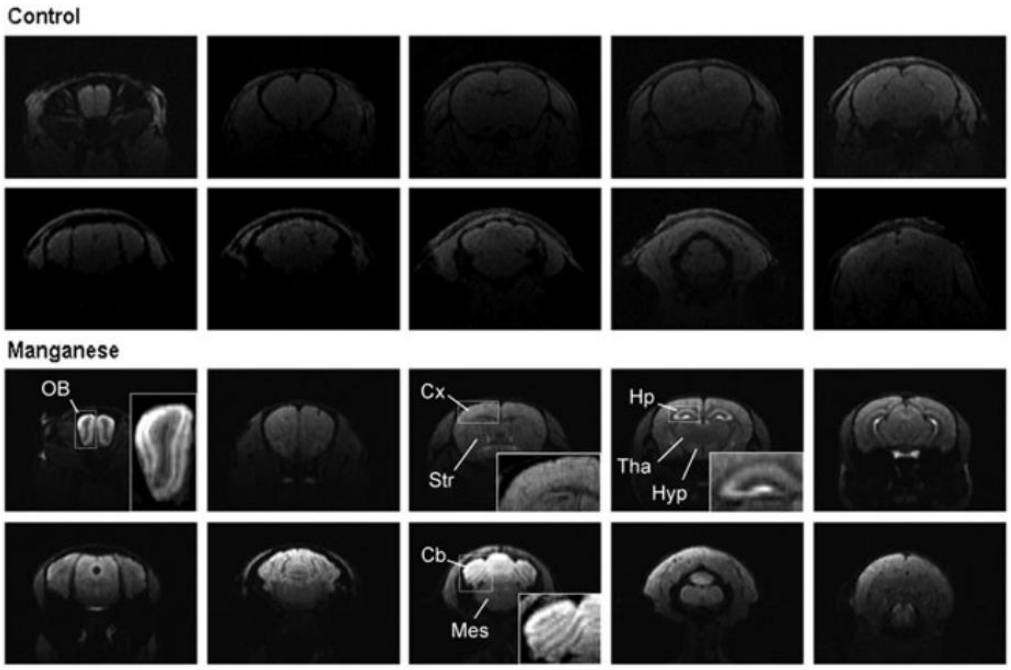

Figura 10. Imágenes de ratones infundidos con Mn^{+2} o solución salina obtenidas por RMI.
Imágenes representativas de cortes coronales que muestran el contraste típico obtenido 3 semanas después de la infusión con solución salina (control) o con 150 mg/mL de $MnCl_2$. Los recuadros muestran amplificaciones de las zonas destacadas. OB, bulbo olfatorio; Cx, Corteza; Str, estriado; Hp, hipocampo; Tha, tálamo; Hyp, hipotálamo; Cb, cerebelo; Mes, mesencéfalo [214].

Adicionalmente, Ye y Kim observaron un claro incremento en la acumulación de Mn en todas las regiones del cerebro que analizaron, siendo mayor la acumulación en el cerebelo (Fig. 11) [215].

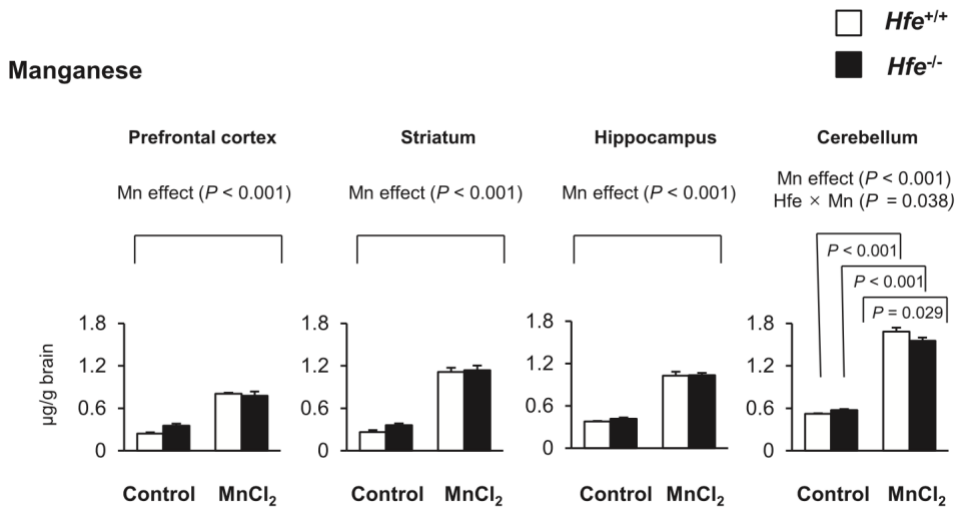

Figura 11. Efecto de la administración de Mn vía intranasal en los niveles de este elemento en diferentes regiones del cerebro de ratones silenciados para Hfe.

Se disectaron y recolectaron tejidos de la corteza prefrontal, el estriado, el hipocampo y el cerebelo, de ratones que fueron instilados intranasalmente con $MnCl_2$ (5 mg/kg) o agua. Las concentraciones de Mn en estado estacionario fueron cuantificadas por espectrometría de masas con plasma inductivamente acoplado (ICP-MS, n=7-8 por grupo). Las barras vacías y rellenadas representan a los ratones wild-type ($Hfe^{+/+}$) y los knockout para Hfe ($Hfe^{-/-}$), respectivamente. Los datos se presentan como el error estándar de la media (± SEM) y se analizaron mediante una ANOVA de dos vías, seguido de comparaciones post hoc [215].

Todas estas evidencias indican que la exposición crónica a Mn representa un problema de salud global, y sugieren que la acumulación de Mn en el cerebro puede ser un factor predisponente para varias enfermedades neurodegenerativas.

JUSTIFICACIÓN

Los hallazgos recientes sobre la distribución del Mn en el cerebro y la disfunción de los transportadores de glutamato en el manganismo indican la necesidad de investigaciones enfocadas en esclarecer los mecanismos implicados en la neurotoxicidad inducida por Mn.

Elucidar los mecanismos moleculares por los cuales el Mn afecta la expresión y/o función de los transportadores de glutamato es imprescindible para la identificación de blancos moleculares y el desarrollo de terapias potenciales contra enfermedades neurodegenerativas.

OBJETIVO GENERAL

Estudiar el efecto directo del Mn sobre funciones clave que desempeñan las células gliales de Bergmann (CGB) en el acoplamiento funcional entre neuronas y glía existente en sinapsis glutamatérgicas.

OBJETIVOS PARTICULARES

1) Evaluar la viabilidad celular después de la exposición a Mn en CGB.
2) Analizar el efecto del Mn sobre la captura de [^{3}H] D-Asp en CGB.
3) Determinar los efectos de la exposición a Mn sobre los parámetros cinéticos de GLAST en CGB.
4) Determinar los efectos de la exposición a Mn sobre los parámetros cinéticos del transporte de glucosa en CGB.

ESTRATEGIA EXPERIMENTAL

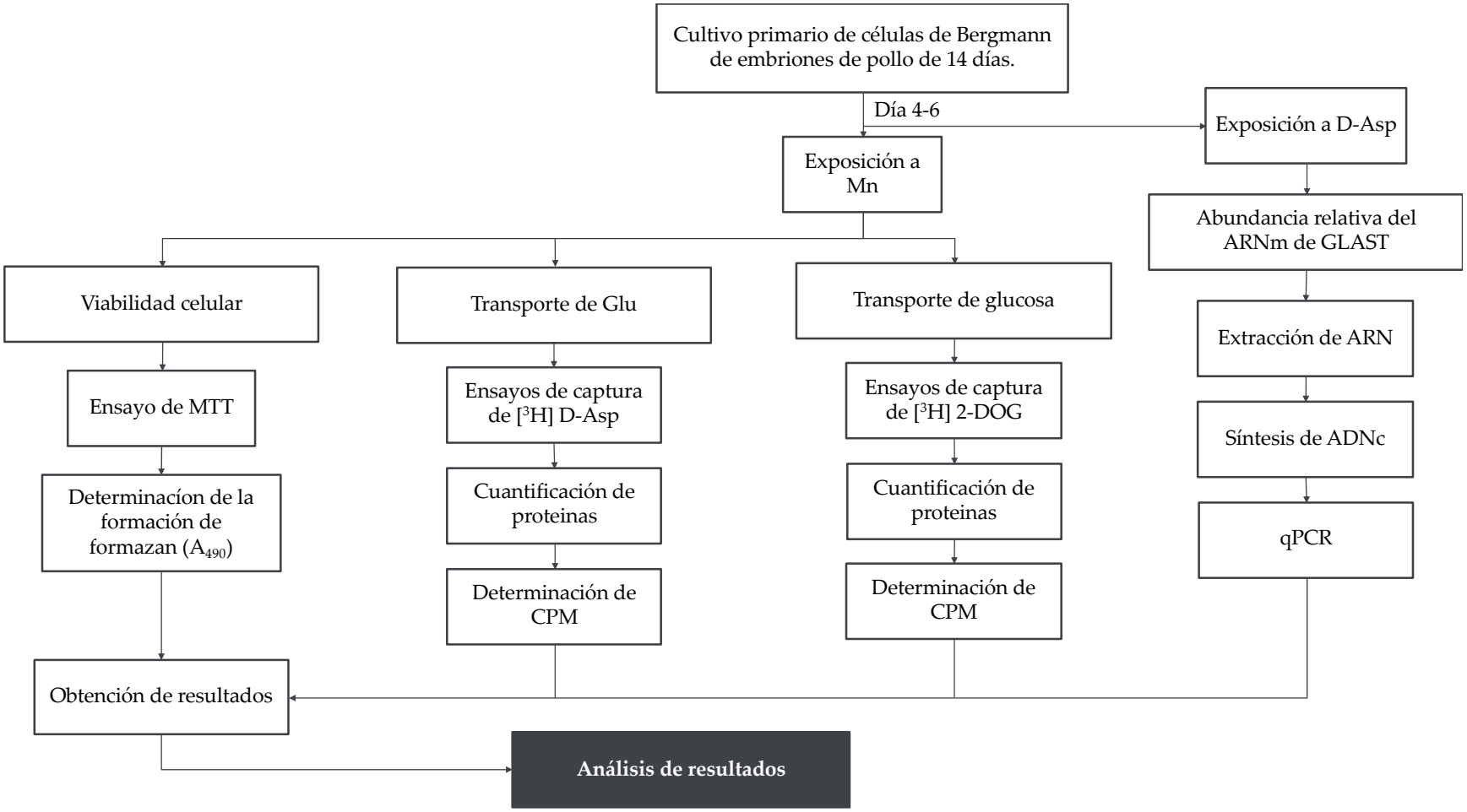

MATERIALES Y MÉTODOS

Animales

Los embriones de pollo (Avimex, Ciudad de México, México) se mantuvieron a 37 °C hasta su uso. Todos los experimentos se realizaron de acuerdo con las directrices internacionales sobre el uso ético de animales en investigación y fueron aprobados por el comité de ética animal del Cinvestav. Se hizo todo lo posible para reducir la cantidad de embriones utilizados y su sufrimiento.

Cultivos de células gliales de Bergmann

Los cultivos primarios de glía de Bergmann se prepararon conforme a un protocolo previamente establecido [216]. Las CGB fueron aisladas de cerebelos de embriones de pollo (14 días de edad). Los cerebelos fueron diseccionados, cortados en trozos pequeños e incubados durante 15 minutos a 37 °C en solución Puck que contenía tripsina (0.25 mg/mL) y desoxirribonucleasa (0.08 mg/mL) para disociar el tejido. Posteriormente, la solución fue eliminada y sustituida con Opti-MEM adicionado con suero fetal bovino (SFB) al 2.5%, glutamina 2 mM y gentamicina (50 µg/mL) para realizar la disociación mecánica. Las CGB fueron obtenidas mediante la eliminación repetida de las células disociadas y se diluyeron a una densidad de $1x10^6$ células/mL. Los cultivos se mantuvieron a 37 °C y en una atmosfera de 95% aire/5% CO_2 dentro de una incubadora humidificada. Todos los experimentos se realizaron de 4–7 días después del aislamiento.

Ensayo de viabilidad celular

La viabilidad celular se midió mediante el ensayo de bromuro de 3-(4,5-dimetiltiazol-2-il)-2,5-difeniltetrazolio (MTT) (Sigma-Aldrich, MO, EUA). Las CGB fueron sembradas en placas de 96 pozos ($1x10^5$ células/pozo) y mantenidas en cultivo como se mencionó anteriormente. Posteriormente, los cultivos fueron tratados con $MnCl_2$ o un vehículo en medio DMEM reducido en suero (0.5% de SFB) durante el tiempo indicado. Después del tratamiento, se añadieron 20 µL de solución de MTT (5 mg/mL) a cada pozo y las placas se incubaron durante 3 h a 37 °C.

Finalmente, el medio fue descartado e inmediatamente después se añadieron 50 µL de dimetilsulfóxido (DMSO) (Sigma-Aldrich, MO, EUA) a cada pozo para disolver los cristales de formazán formados. La absorbancia se midió con un lector de microplacas (BioTek Instruments, VT, EUA) a 570 nm. Los experimentos se realizaron por cuadruplicado en tres cultivos independientes.

Captura de [$_3$H]-D-aspartato

Los estudios de captura de [$_3$H]-D-aspartato se llevaron a cabo como se describió anteriormente [217]. Las CGB fueron sembradas en placas de 24 pozos (5x10$_5$ células/pozo) y mantenidas en cultivo como se mencionó anteriormente. El día del experimento, el medio de cultivo fue descartado y reemplazado con solución de captura a 37 ºC (solución amortiguadora con HEPES precalentada que contenía HEPES 25 mM, NaCl 130 mM, KCl 5.4 mM, $CaCl_2$ 1.8 mM, $MgCl_2$ 0.8 mM, glucosa 33.3 mM y NaH_2PO_4 1 mM a pH 7.4). Después, los cultivos fueron tratados con $MnCl_2$ (concentraciones indicadas) o un vehículo durante los períodos de tiempo indicados. Posterior al tratamiento, los cultivos fueron incubados con solución de captura precalentada adicionada con 0.4 µCi/mL de [$_3$H]-D-aspartato ([$_3$H]-D-Asp) (actividad específica: 16.5 Ci/mmol; Perkin Elmer, MA, EUA). La captura se terminó después de 12 minutos de incubación removiendo la solución de captura con el radioligando y lavando 3 veces con solución de captura enfriada con hielo. Finalmente, las células fueron lisadas por incubación con 0.25 mL/pozo de NaOH 0.1 N durante 2 h a temperatura ambiente. Del lisado obtenido, se transfirió una alícuota (0.24 mL) a un vial de centelleo conteniendo 2 mL de cóctel de centelleo líquido y 50 µL de ácido acético glacial (para disminuir la quimioluminiscencia) para medir la radiactividad en un analizador de centelleo líquido de sobremesa controlado por computadora (PerkinElmer, MA, EUA). El resto del lisado se usó para la determinación de proteínas mediante el método de Bradford (Bio-Rad, CA, EUA) [218]. Las cuentas obtenidas se corrigieron con los niveles de proteína y se calcularon como [$_3$H]-D-Asp pmol/(mg de proteína·min^{-1}). Los experimentos se realizaron por cuadruplicado en tres o cuatro cultivos independientes.

Para determinar los parámetros cinéticos K_m y V_{max}, los cultivos fueron tratados con $MnCl_2$ (200 µM) o un vehículo durante 30 min. Posterior al tratamiento, los cultivos fueron incubados con solución de captura precalentada adicionada con 0.4 µCi/mL de [^{3}H]-D-Asp (24.2 nM) + D-Asp (concentraciones de 0-250 µM de D-aspartato sin radiomarcaje) (Sigma-Aldrich, MO, EUA). La captura se terminó después de 12 minutos de incubación removiendo la solución de captura con el radioligando y lavando 3 veces con solución de captura enfriada con hielo. Finalmente, las células fueron lisadas por incubación con 0.25 mL/pozo de NaOH 0.1 N durante 2 h a temperatura ambiente. Las alícuotas obtenidas del lisado se usaron para determinar la radioactividad incorporada y el contenido de proteína como se describió anteriormente. Se utilizó una regresión no lineal robusta para ajustar un modelo a los datos experimentales y estimar los parámetros de la ecuación de Michaelis-Menten (GraphPad Prism Software; La Jolla, California, EUA). Los experimentos se realizaron por cuadruplicado en tres cultivos independientes.

Algunos experimentos se realizaron simplemente agregando $MnCl_2$ (concentración final de 200 µM) o un vehículo a la solución de captura adicionada con 0.4 µCi/mL [^{3}H]-D-Asp y se evaluó la radiactividad incorporada en función del tiempo. Posterior a los periodos de incubación indicados (1, 5, 10, 15, 30 y 60 min.) la captura se terminó removiendo la solución de captura con el radioligando y lavando 3 veces con solución de captura enfriada con hielo. Finalmente, las células fueron lisadas por incubación con 0.25 mL/pozo de NaOH 0.1 N durante 2 h a temperatura ambiente. Las alícuotas obtenidas del lisado se usaron para determinar la radioactividad incorporada y el contenido de proteína como se describió anteriormente. Se utilizó una regresión no lineal robusta para ajustar un modelo a los datos experimentales (GraphPad Prism Software; La Jolla, California, EUA). Los experimentos se realizaron por cuadruplicado en tres cultivos independientes.

Captura de [^{3}H]-2-desoxi-D-glucosa

Los estudios de captura de [^{3}H]-2-desoxi-D-glucosa se llevaron a cabo como se describió anteriormente [219]. Las CGB fueron sembradas en placas de 24 pozos

(5x10^5 células/pozo) y mantenidas en cultivo como se mencionó anteriormente. El día del experimento, el medio de cultivo fue descartado y reemplazado con solución de captura a 37 ºC (solución amortiguadora con HEPES precalentada que contenía HEPES 25 mM, NaCl 130 mM, KCl 5.4 mM, $CaCl_2$ 1.8 mM, $MgCl_2$ 0.8 mM, glucosa 5 mM y NaH_2PO_4 1 mM a pH 7.4). Después, los cultivos fueron tratados con $MnCl_2$ (200 µM) o un vehículo durante 30 min. Posterior al tratamiento, los cultivos fueron incubados con solución de captura precalentada adicionada con 0.8 µCi/mL de [^{3}H]-2-desoxi-D-glucosa ([^{3}H]-2-DG) (actividad específica: 32.5 Ci/mmol; Perkin Elmer, MA, EUA) + 2-DG (concentraciones de 0-5 mM de 2-desoxi-D-glucosa sin radiomarcaje) (Sigma-Aldrich, MO, EUA). La captura se terminó después de 30 minutos de incubación removiendo la solución de captura con el radioligando y lavando 3 veces con solución de captura (sin glucosa) enfriada con hielo. Finalmente, las células fueron lisadas por incubación con 0.25 mL/pozo de NaOH 0.1 N durante 2 h a temperatura ambiente. Del lisado obtenido, se transfirió una alícuota (0.24 mL) a un vial de centelleo conteniendo 2 mL de cóctel de centelleo líquido y 50 µL de ácido acético glacial (para disminuir la quimioluminiscencia) para medir la radiactividad en un analizador de centelleo líquido de sobremesa controlado por computadora (PerkinElmer, MA, EUA). El resto del lisado se usó para la determinación de proteínas mediante el método de Bradford (Bio-Rad, CA, EUA) [218]. Las cuentas obtenidas se corrigieron con los niveles de proteína y se calcularon como [^{3}H]-2-DG pmol/(mg de proteína·min^{-1}). Se utilizó una regresión no lineal robusta para ajustar un modelo a los datos experimentales y estimar los parámetros de la ecuación de Michaelis-Menten (GraphPad Prism Software; La Jolla, California, EUA). Los experimentos se realizaron por cuadruplicado en tres o cuatro cultivos independientes.

PCR en tiempo real

La determinación de los niveles relativos del ARN mensajero (ARNm) del transportador GLAST se obtuvieron mediante PCR en tiempo real. Las CGB fueron sembradas en placas de 12 pozos (1x10^6 células/pozo) y mantenidas en cultivo como se mencionó anteriormente. Posteriormente, los cultivos fueron tratados con

D-Asp (150 µM) en medio DMEM reducido en suero (0.5% de SFB) durante los períodos de tiempo indicados. Después del tratamiento, las células se cosecharon con TRIzol (Sigma-Aldrich, MO, EUA) y se aisló el ARN total utilizando el kit Direct-zol RNA MiniPrep (Zymo Research, CA, EUA). La reacción y detección se realizo utilizando un sistema de PCR en tiempo real (Applied Biosystem, CA, EUA). Las reacciones de PCR en tiempo real se llevaron a cabo en un volumen total de 10 µL, los cuales contenían: 20 ng del ARN molde de cada muestra, 200 nM de los cebadores apropiados (Tabla 1) y mastermix del kit KAPA SYBR® FAST One-Step qRT-PCR (Kapa Biosystems, MA, EUA). El protocolo de PCR se llevó a cabo de la siguiente manera: 5 minutos a 42 °C para la síntesis del ADN complementario (ADNc), seguido de 5 minutos a 95 °C para la inactivación. Después, 40 ciclos: 3 segundos a 95 °C para desnaturalizar y 30 segundos a la temperatura de hibridación (Ta) específica. Se detectó la fluorescencia al final de cada etapa de elongación. Las muestras se normalizaron con los niveles relativos del ARNm de la proteína ribosomal S17. La cuantificación relativa de ARNm en las muestras se calculó mediante el método 2-ΔΔCT. Los experimentos se realizaron por duplicado en cuatro cultivos independientes.

Tabla 1 Secuencias de cebadores para reacciones de PCR en tiempo real

ADNc	Cebador
GLAST	Sentido: GGCTGCGGGCATTCCTC
	Antisentido: CGGAGACGATCCAAGAACCA
S17	Sentido: CCGCTGGATGCGCTTCATCAG
	Antisentido: TACACCCGTCTGGGCAAC

GLAST: transportador de glutamato/aspartato, S17: proteína ribosómica S17

Análisis estadístico

Los resultados están expresados como la media ± SEM, de por lo menos tres cultivos independientes. El análisis estadístico se realizó con un análisis de varianza (ANOVA) de una vía, seguido de la prueba de comparación múltiple de Dunnett. Múltiples pruebas t de Student (una prueba por condición) se usaron para el análisis

estadístico de los experimentos cinéticos de transporte. Se consideró estadísticamente significativa a una probabilidad de 0.05 o menor. Todos los análisis se realizaron con el programa Prism 8 (GraphPad Prism Software; La Jolla, California, EUA).

RESULTADOS

Efecto de Mn sobre la viabilidad de las CGB

Numerosos estudios han establecido la susceptibilidad de varios tipos de células a la neurotoxicidad inducida por Mn, siendo los astrocitos más resistentes en comparación con las neuronas [220–223]. Aunque los ganglios basales representan el blanco principal para la neurotoxicidad de Mn, también se sabe que este metal se acumula en el cerebelo [224, 225], proporcionando así una razón para examinar las células derivadas de esta región. La viabilidad celular de las CGB se evaluó mediante el ensayo de MTT. Como se muestra en la Fig. 12, no hubo muerte celular aparente en los cultivos primarios de glía de Bergmann expuestos a varias concentraciones de Mn (100, 200, 300, 500 y 1000 μM) por diferentes períodos de tiempo (0.5, 12 y 24 h, panel A, B y C respectivamente).

Estos resultados nos permitieron avanzar y evaluar la actividad del transportador de glutamato/aspartato (GLAST) después de la exposición a Mn en ausencia de muerte celular.

La exposición a Mn modifica la captura de [^{3}H] D-Asp

Un creciente número de evidencias han demostrado que el Mn disminuye la expresión y función de GLAST/GLT-1 en cultivos de astrocitos, lo que posiblemente podría derivar en una lesión neuronal excitotóxica [196, 226]. Aunque estos estudios han avanzado nuestra comprensión sobre los mecanismos por los cuales el Mn reprime a estos transportadores, se desconocen las consecuencias de una exposición aguda a Mn sobre su función.

Con la finalidad de obtener información sobre un posible efecto sobre la actividad de GLAST como consecuencia a la exposición a Mn, realizamos ensayos de captura de [^{3}H]-D-Asp con una concentración fija del radioligando (24.2 nM). Se usó D-Asp, un análogo del glutamato, ya que tiene la ventaja de no ser metabolizado a glutamina por la enzima glutamina sintetasa (GS) y para descartar cualquier efecto sobre la captura mediado por la activación de los receptores glutamatérgicos. Las CGB expuestas a Mn por 30 minutos, a una concentración de 200 o 300 μM, mostraron un aumento significativo en la cantidad de [^{3}H]-D-Asp incorporado en las

células. Como se puede observar en la Fig. 13, este efecto es semejante, independientemente de si el Mn está o no está presente en la solución de captura. Cabe destacar que cuando el Mn está presente en la solución de captura, se observa una reducción marginal en el aumento de la actividad GLAST comparado con el aumento presentado en ausencia de Mn.

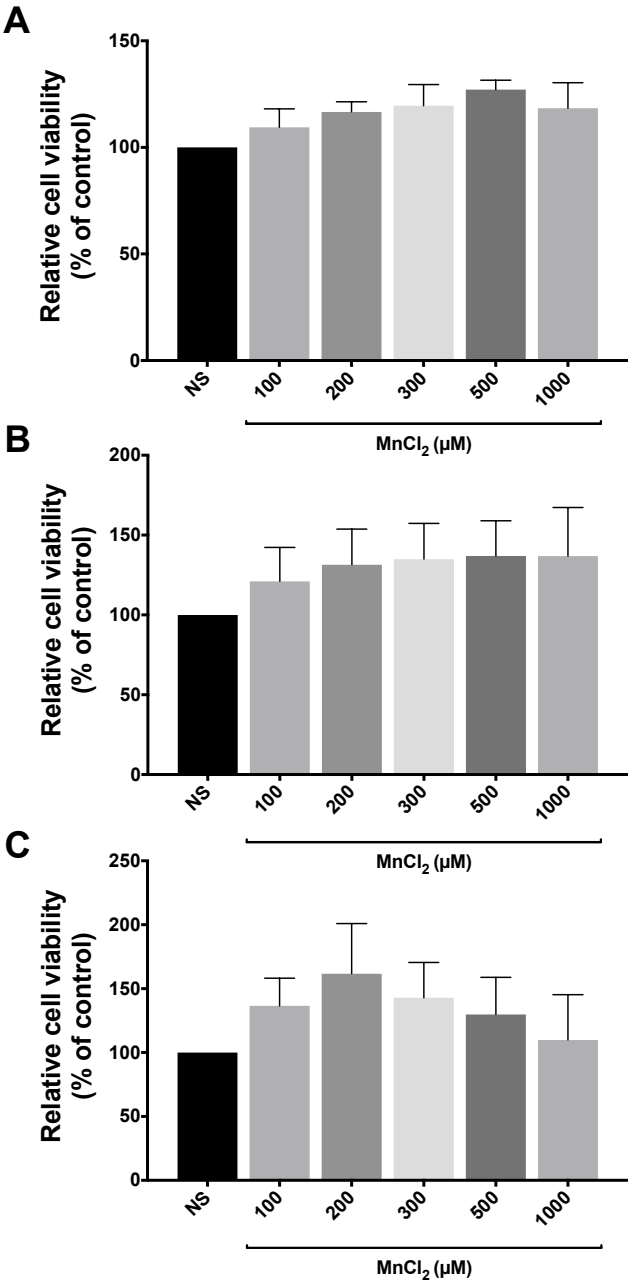

Figura 12. El Mn no afecta la viabilidad celular de las células gliales de Bergmann.

El formazán formado se cuantificó indirectamente en muestras obtenidas a partir de cultivos primarios de glía de Bergmann tratados con un vehículo (NS, no estimulado) o $MnCl_2$ (100, 200, 300, 500 o 1000 μM) durante 0.5 h (A), 12 h (B) o 24 h (C).

Estudios previos de nuestro grupo de investigación han demostrado que una exposición a D-Asp (1 mM) resulta en la reducción de la incorporación de [3H]-D-Asp en ensayos de captura y en la activación de diversas vías de transducción de señales en CGB [227, 228]. El hecho que el incremento de la actividad de GLAST inducida por Mn se anule mediante el tratamiento conjunto con D-Asp 1 mM sugiere que el D-Asp y el Mn desencadenan diferentes mecanismos que afectan la función GLAST.

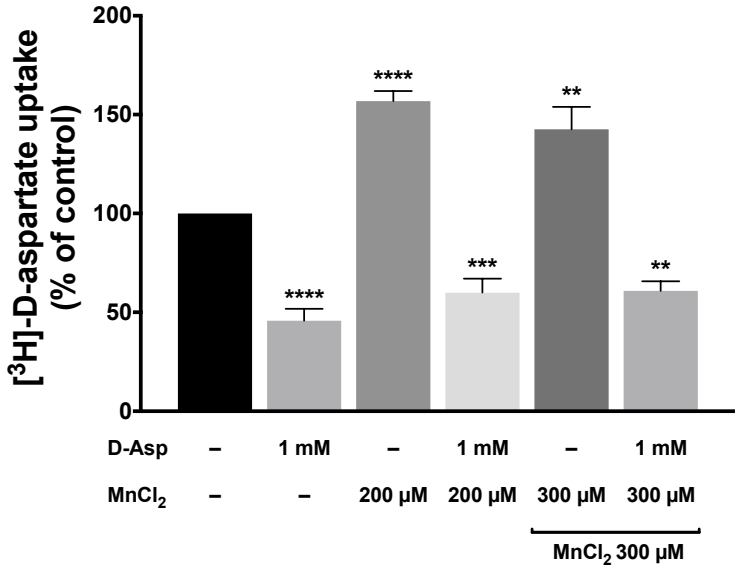

Figura 13. La exposición a Mn aumenta la actividad de GLAST.

La incorporación total de [3H]-D-Asp (0.4 µCi/mL, actividad específica: 16.5 Ci/mmol) se midió en cultivos primarios de glía de Bergmann tratados con un vehículo (NS, no estimulados) o $MnCl_2$ (200 o 300 µM) durante 0.5 h. Se añadió $MnCl_2$ (300 µM) a la solución de captura que contenía al radioligando, indicado por una barra con la leyenda "$MnCl_2$ 300 µM". Las diferencias estadísticamente significativas entre los controles y los grupos experimentales están indicadas por **p<0.01, ***p<0.001, ****p<0.0001 versus NS. Los datos se presentan como la media ± SEM de cuatro cultivos independientes, cada uno realizado por cuadruplicado (ANOVA de una vía seguido de la prueba de comparación múltiple de Dunnett).

Después de demostrar la existencia de un efecto sobre la actividad del transportador GLAST como consecuencia de una exposición a Mn, decidimos realizar estudios de tiempo y dosis respuesta para tratar de establecer una correlación directa entre el

efecto observado previamente y la exposición a Mn. Los resultados representados en la Fig. 14, corroboran así que el aumento de la actividad de GLAST inducida por Mn es dependiente de la dosis (A) y del tiempo (B). Además, también podemos observar que este efecto alcanza su máximo después de 5 minutos de incubación, sugiriendo que la temporalidad de causa-efecto es relativamente rápida.

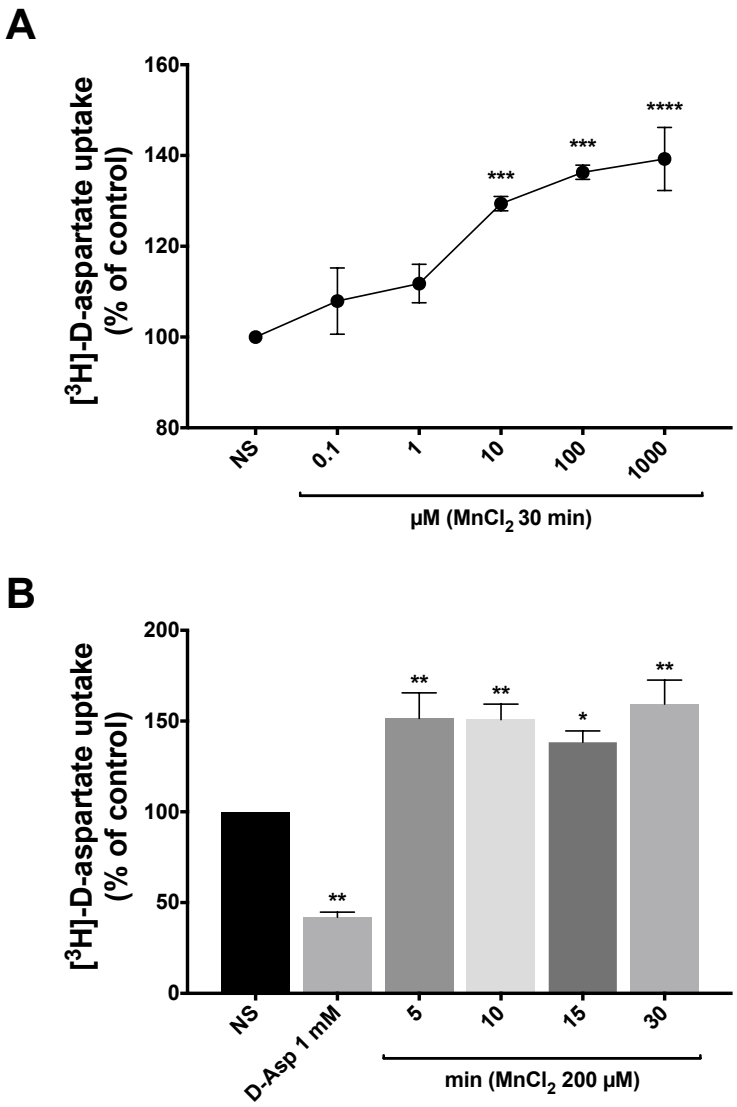

Figura 14. El aumento de la actividad de GLAST inducida por Mn depende de la dosis y del tiempo.

(A) La incorporación total de [3H]-D-Asp (0.4 µCi/mL, actividad específica: 16.5 Ci/mmol) se midió en cultivos primarios de glía de Bergmann tratados con un vehículo (NS, no estimulados) o $MnCl_2$ (0.1, 1, 10, 100 o 1000 µM) durante 0.5 h. **(B)** La incorporación total de [3H]-D-Asp (0.4 µCi/mL, actividad

específica: 16.5 Ci/mmol) se midió en cultivos primarios de glía de Bergmann tratados con un vehículo (NS, no estimulados) o $MnCl_2$ (200 µM) por los periodos de tiempo indicados (5, 10, 15 o 30 min). Las diferencias estadísticamente significativas entre los controles y los grupos experimentales están indicadas por *p<0.05, **p<0.01, ***p<0.001, ****p<0.0001 versus NS. Los datos se presentan como la media ± SEM de tres cultivos independientes, cada uno realizado por cuadruplicado. (ANOVA de una vía seguido de la prueba de comparación múltiple de Dunnett).

Los resultados obtenidos podrían explicarse de dos formas: 1) la exposición a Mn deriva en un aumento del número de transportadores (GLAST) en la membrana plasmática; o 2) la exposición a Mn, de alguna forma, afecta los parámetros cinéticos del transportador (GLAST).

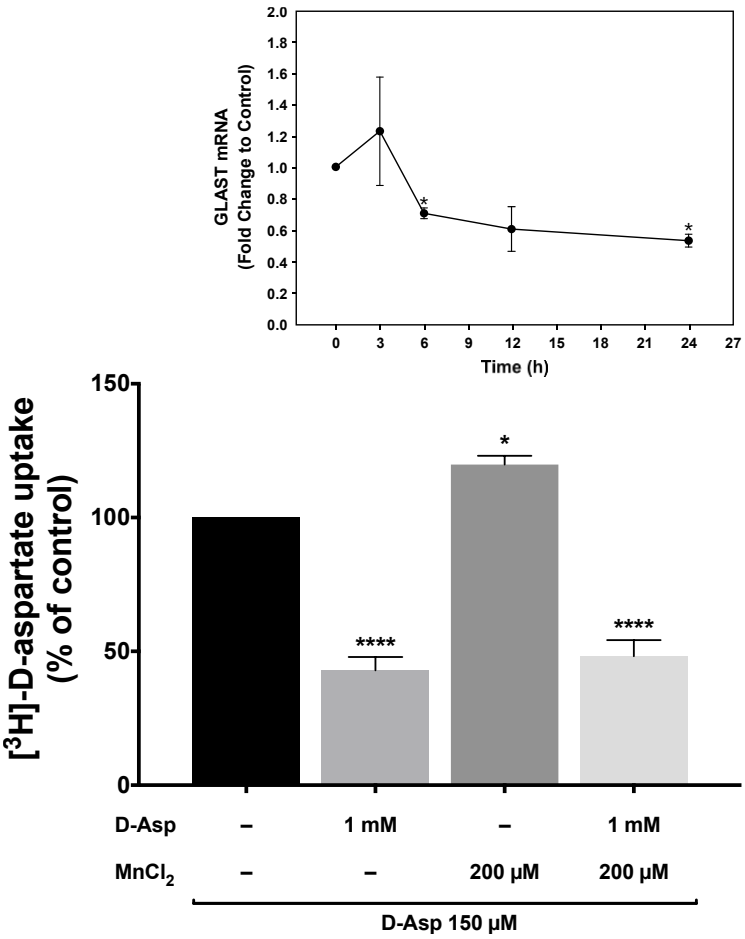

Figura 15. Efecto del Mn sobre la actividad de GLAST después de una disminución en los niveles relativos de ARNm de GLAST.

La incorporación total de [3H]-D-Asp (0.4 µCi/mL, actividad específica: 16.5 Ci/mmol) se midió en cultivos primarios de glía de Bergmann tratados con un vehículo (NS, no estimulados) o $MnCl_2$ (200

µM) durante 0.5 h, posterior a la pre-incubación con D-Asp (150 µM) por 24 h. Una incubación con D-Asp durante 24 h reduce la cantidad relativa de ARNm de GLAST en CGB (Recuadro: Se cuantificaron los niveles relativos de ARNm de GLAST en cultivos primarios de glía de Bergmann tratados con D-Asp 150 µM por 3, 6, 12 o 24 h). Las diferencias estadísticamente significativas entre los controles y los grupos experimentales están indicadas por *p<0.05, ****p<0.0001 versus NS. Los datos se presentan como la media ± SEM de tres cultivos independientes, cada uno realizado por cuadruplicado (ANOVA de una vía seguido de la prueba de comparación múltiple de Dunnett).

Para ayudar a esclarecer dicha disyuntiva, como primera aproximación diseñamos un paradigma experimental de ensayos de captura de [$_3$H]-D-Asp (similar al mencionado anteriormente) añadiendo una pre-incubación con D-Asp 150 µM por 24 h. Posterior a la pre-incubación, las CGB fueron expuestas a Mn (200 µM) o a un vehículo por 30 minutos. Sabemos, por trabajo inédito de nuestro laboratorio, que una incubación a largo plazo con D-Asp a una concentración (150 µM) a la cual la velocidad inicial (V_0) tiende a ser igual a la velocidad máxima (V_{max}) de transporte, disminuye significativamente la cantidad relativa de ARNm de GLAST (Fig. 15, recuadro) y consecuentemente reduce la captura de [$_3$H]-D-Asp en CGB (datos no mostrados). Bajo estas circunstancias, el efecto del Mn sobre la actividad de GLAST se mantiene como un aumento discreto pero significativo que también se anula mediante el tratamiento conjunto con D-Asp (Fig. 15). Este resultado sugiere fuertemente que la cantidad total de transportadores en la membrana plasmática no se ve afectada como consecuencia a la exposición a Mn.

Para corroborar este resultado y esclarecer la causa del aumento en la actividad del transportador, decidimos realizar estudios cinéticos para determinar si la exposición a Mn afectaba de alguna manera los parámetros cinéticos de GLAST y por consiguiente su función. Como se muestra en el panel A de la Fig. 16, no hay ninguna diferencia aparente entre la V_{max} de los cultivos tratados con Mn (200 µM) y aquellos tratados con un vehículo por 30 min. Este resultado confirma que el número de transportadores no se modifica después de una exposición aguda a Mn. Por otro lado, aunque observamos una reducción en la K_m, no hubo diferencia significativa al comparar los puntos evaluados entre cada condición. Esto nos llevó a realizar un análisis más detallado, en donde encontramos que los cultivos tratados con Mn por 30 minutos presentaban un aumento considerable en la eficiencia

catalítica (V_{max}/K_m) del transportador. V_{max}/K_m es la constante para la unión del sustrato y el producto en un complejo productivo, que a concentraciones mucho más pequeñas que K_m se convierte en el factor limitante de la reacción catalizada [229]. Este cambio en la eficiencia catalítica de GLAST podría explicar la mayor cantidad de [3H]-D-Asp incorporada por las CGB tratadas con Mn (panel A de la Fig. 16, recuadro rojo).

A

	Saturable Transport		
	V_{max} (pmol/mg·min)	K_m (µmol/L)	V_{max}/K_m (pmol/mg·min/(µmol/L))
NS	469.0	21.21	22.112
$MnCl_2$	437.0	16.46	26.549

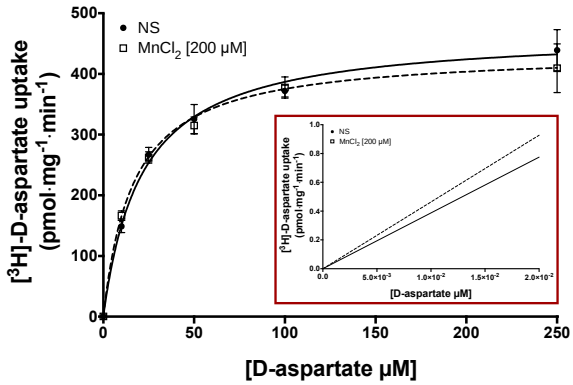

B

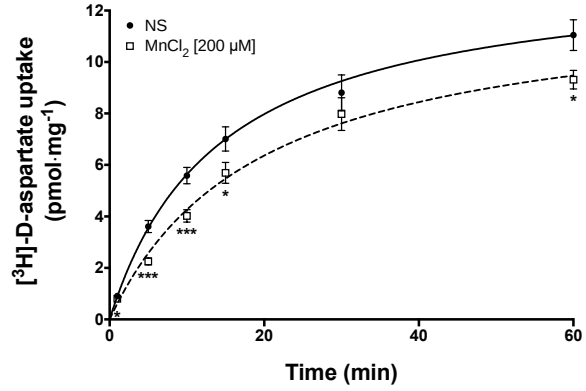

Figura 16. Impacto de la exposición a Mn en los parámetros cinéticos de GLAST.

(A) La incorporación total de [3H]-D-Asp (0.4 µCi/mL, actividad específica: 16.5 Ci/mmol) se midió en cultivos primarios de glía de Bergmann tratados con un vehículo (NS, no estimulados) o $MnCl_2$ (200 µM) durante 0.5 h. Se agregaron diversas concentraciones de D-Asp (en un rango de 0 a 250 µM) +

[^{3}H]-D-Asp (24.2 nM) a la solución de captura, y se midió la incorporación del radioligando después de 12 minutos para determinar los parámetros cinéticos del transportador. **(B)** La incorporación total de [^{3}H]-D-Asp (0.4 µCi/mL, actividad específica: 16.5 Ci/mmol) se midió en presencia ($MnCl_2$ 200 µM) o ausencia (NS) de Mn en la solución de captura (conteniendo al radioligando) por los periodos de tiempo indicados (1, 5, 10, 15, 30 o 60 min). Las diferencias estadísticamente significativas entre los controles y los grupos experimentales están indicadas por *p<0.05, ***p<0.001 versus NS. Los datos se presentan como la media ± SEM de tres cultivos independientes, cada uno realizado por cuadruplicado (múltiples pruebas t de Student). Se utilizó una regresión no lineal robusta para ajustar un modelo a nuestros datos y estimar los parámetros cinéticos.

En otro orden de ideas, decidimos examinar si la presencia *per se* de Mn (200 µM) en la solución de captura modificaba la función del transportador. El panel B de la Fig. 16 muestra que, efectivamente, hubo una reducción significativa en la incorporación de [^{3}H]-D-Asp en función del tiempo cuando el Mn estuvo presente durante el proceso de captura. Estos resultados apoyan la noción de una interacción directa, previamente no reportada, del Mn con GLAST.

El Mn afecta la actividad de transporte de glucosa

El acople metabólico entre astrocitos y neuronas es crítico para el metabolismo energético y la síntesis de neurotransmisores en el cerebro [230]. Las neuronas necesitan de los astrocitos, ya que carecen de la enzima piruvato carboxilasa (PC) y, por lo tanto, dependen de los astrocitos para la síntesis *de novo* de glutamato (Glu) y para la reposición de los intermediarios del ciclo de los ácidos tricarboxílicos [231–233]. Estudios previos han demostrado que el Mn provoca cambios en el metabolismo de la glucosa de astrocitos mediante la inhibición de la enzima GS [176, 234]. También se ha establecido que el Mn juega un papel importante en el metabolismo energético del cerebro al afectar a la enzima PC, especifica de astrocitos, y el transporte de glucosa tanto en astrocitos como en neuronas [235, 236].

Para obtener información sobre los mecanismos subyacentes a la alteración de la capacidad metabólica de los astrocitos después de una exposición aguda a Mn, realizamos estudios cinéticos con [^{3}H]-2-DG para determinar si el transporte de glucosa en CGB se veía afectado. Como se muestra en la Fig. 17, observamos una

clara reducción en la captura de glucosa en las células tratadas con Mn durante 30 min. Esta baja en la incorporación de [3H]-2-DG está relacionada con una disminución significativa de la V_{max} de transporte, lo que sugiere una reducción del número de transportadores de glucosa presentes en la membrana plasmática. Estos resultados añaden un orden de complejidad mayor a los efectos inducidos por Mn sobre la patología astrocítica, pudiendo causar una alteración en la homeostasis entre las neuronas y las CGB, y consecuentemente disfunción sináptica neuronal adicional y la activación de un estado excitotóxico.

	Saturable Transport		
	V_{max} (pmol/mg·min)	K_m (mmol/L)	V_{max}/K_m (pmol/mg·min/(mmol/L))
NS	2317	3.360	689.583
$MnCl_2$	1908	4.018	474.863

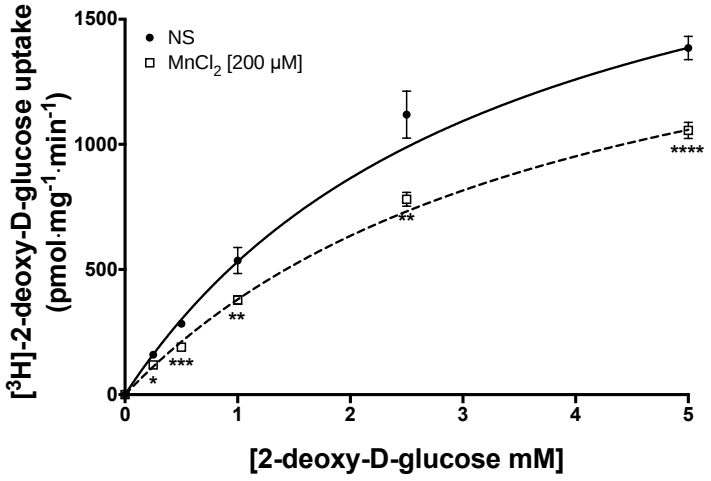

Figura 17. El Mn disminuye la capacidad de transporte de glucosa de las CGB.

La incorporación total de [3H]-2-DG (0.8 µCi/mL, actividad específica: 32.5 Ci/mmol) se midió en cultivos primarios de glía de Bergmann tratados con un vehículo (NS, no estimulados) o $MnCl_2$ (200 µM) durante 0.5 h. Se agregaron diversas concentraciones de 2-DG (en un rango de 0 a 5 mM) + [3H]-2-DG (24.6 nM) a la solución de captura, y se midió la incorporación del radioligando después de 30 minutos para determinar los parámetros cinéticos del transportador. Las diferencias estadísticamente significativas entre los controles y los grupos experimentales están indicadas por *p<0.05, **p<0.01, ***p<0.001, ****p<0.0001 versus NS. Los datos se presentan como la media ±

SEM de tres cultivos independientes, cada uno realizado por cuadruplicado (múltiples pruebas t de Student). Se utilizó una regresión no lineal robusta para ajustar un modelo a nuestros datos y estimar los parámetros cinéticos.

DISCUSIÓN

Los estudios realizados en las últimas décadas han proporcionado información invaluable sobre la causa, los efectos y los mecanismos de la neurotoxicidad inducida por Mn. Los hallazgos recientes sobre la participación de los transportadores de glutamato y las vías de señalización implicadas en la neurotoxicidad inducida por Mn proporcionan no solo nuevos conocimientos sobre los mecanismos moleculares, sino que también proporcionan nuevos blancos terapéuticos en el desarrollo de fármacos para atenuar los síntomas asociados con el manganismo, la EP y otros trastornos neurodegenerativos [187, 199, 200, 207, 237–240]. Las enfermedades neurodegenerativas son un grupo heterogéneo de enfermedades con fenotipos clínicos y etiologías genéticas distintas. Pese a que la mayoría de las enfermedades neurodegenerativas son esporádicas, es decir, no se conoce ningún vínculo genético, otras pueden atribuirse a mutaciones genéticas específicas. Si bien estas mutaciones afectan a una amplia variedad de proteínas, evidencias sustanciales apuntan a la excitotoxicidad como un mecanismo fundamental involucrado en la degeneración neuronal. La hiperactivación de los receptores de glutamato deteriora la homeostasis del calcio celular y activa la síntesis de óxido nítrico, la generación de radicales libres y la muerte celular programada [241].

EAAT1 (también conocido como GLAST) es uno de los dos principales transportadores de glutamato que elimina el exceso de Glu de las hendiduras sinápticas, evitando así la muerte neuronal excitotóxica. GLAST se concentra predominantemente en el cerebelo [242] y se expresa en astrocitos y CGB [58]. La relevancia funcional de este transportador se confirmó en estudios animales en los que la desactivación del gen SLC1A3 indujo un aumento del daño cerebelar y un tenue desorden motriz después de una lesión cerebral, lo que sugiere un papel activo de GLAST en la prevención del daño excitotóxico después de una lesión cerebral aguda [62]. Aunado a esto, diferentes investigaciones han demostrado que el cerebelo es una de las principales regiones del cerebro donde se acumula mayoritariamente el Mn [215, 224, 243], y que las neuronas granulares son significativamente más susceptibles a la toxicidad inducida por Mn en comparación

con neuronas neocorticales [244]. A pesar de la importancia de estos hallazgos, hasta la fecha no se conocen los efectos de la exposición aguda a Mn en glía radial, que por un lado envuelve completamente las sinapsis glutamatérgicas [245], y por otro lado no se somete a la llamada “conversión astrocítica” [246]. Potencialmente se podría argumentar que este no es un problema importante, pero está claro que la regulación de GLAST es diferente en glía radial en comparación con astrocitos corticales. Mientras que en la glía radial el Glu regula a la baja la expresión y función de GLAST, el efecto contrario tiene lugar en los astrocitos corticales [247–249]. Por lo tanto, en este trabajo decidimos estudiar el efecto de la exposición aguda (minutos) a Mn sobre los transportadores de glutamato que expresan las CGB en cultivo. Los cultivos primarios de glía de Bergmann aislados a partir de cerebelos de pollo son un modelo que ha demostrado ser sumamente útil en la caracterización de la participación de las células gliales en el acoplamiento funcional entre neuronas y glía existente en sinapsis glutamatérgicas [250].

Aunque es ampliamente aceptado que el Mn perjudica la expresión y la función de los dos principales transportadores de glutamato (GLAST y GLT-1), su mecanismo de acción sigue siendo estudiado. Se cree que el aumento de la producción de especies reactivas de oxígeno (ROS, por sus siglas en inglés) y TNF-α inducidos por Mn es la causa principal que conduce al deterioro de la función de los transportadores de glutamato. Las ROS inhiben la captura de Glu en astrocitos, y TNF-α disminuye los niveles de proteína y ARNm de GLAST y GLT-1 [197, 251, 252]. El estrés oxidativo también juega un papel importante en la regulación de la función de los transportadores de glutamato, ya que la actividad de estos está regulada por el estado redox de los residuos reactivos de cisteína, con una disminución dramática de la actividad una vez que la cisteína reducida se oxida [194]. Además, se ha descrito que la captura de los transportadores de aminoácidos excitadores 1, 2 y 3 es inhibida por peroxinitrito ($ONOO^-$) y peróxido de hidrógeno (H_2O_2), lo que sugiere un papel importante para el estrés oxidativo en la regulación de la actividad de los transportadores de glutamato [195]. Todos estos hallazgos apuntan a que la disfunción de los transportadores de glutamato en la neurotoxicidad inducida por Mn es un fenómeno secundario a la disfunción

mitocondrial y a la generación de citosinas proinflamatoras, entre otras cosas. Es por esta razón que nuestra investigación se enfocó en establecer una asociación directa entre la toxicidad del Mn y la función de los transportadores de glutamato. Nuestros resultados muestran un aumento de aproximadamente 1.5 veces en la actividad de GLAST (Fig. 13) debido al tratamiento de los cultivos primarios de glía de Bergmann con concentraciones fisiopatológicamente relevantes de $MnCl_2$ [253]. Dicho efecto resultó ser dependiente de la dosis y del tiempo, alcanzando su máximo después de 5 minutos (Fig. 14). Una vez establecida la causalidad y la dependencia del fenómeno observado, decidimos realizar curvas de saturación de Michaelis-Menten en cultivos control y en cultivos tratados con $MnCl_2$ para comprender cómo una exposición aguda a Mn resulta en una mayor eficiencia en el transporte de Glu (Fig.16). El aumento en la cantidad de radioligando incorporado después del tratamiento con Mn se puede atribuir a un cambio en la eficiencia catalítica (V_{max}/K_m) del transportador [254]. Estos resultados difieren a lo reportado anteriormente, donde la exposición a Mn disminuye la expresión tanto de GLAST y GLT-1 a nivel de ARNm y proteína, con una consecuente reducción de la captura de Glu en cultivos primarios de astrocitos de rata [207, 238, 255]. Esta diferencia puede deberse al paradigma experimental utilizado, ya que en los estudios donde se observa una disminución en la función de los transportadores de glutamato se emplearon tiempos de exposición más largos (horas). Sin embargo, no podemos descartar que esta diferencia sea intrínseca de los modelos utilizados. Se necesitan más trabajos para abordar y esclarecer esta aparente discrepancia.

Con base en nuestros resultados obtenidos, es tentador especular que el Mn interactúa con los transportadores de glutamato presentes en la membrana plasmática, lo que lleva a un cambio en su conformación que se refleja en una mayor eficiencia de captura a concentraciones bajas. Esto podría tener como consecuencia una disminución drástica de concentración basal de Glu extracelular. De ser así, aun cuando la concentración de Glu es demasiado baja para activar tónicamente a los receptores de glutamato, en ausencia de estimulación, la mayoría de los receptores glutamatérgicos estarían disponibles para activarse y habría perturbaciones en la señalización glutamatérgica [256].

Las células astrogliales son los elementos centrales de las unidades neurovasculares que integran los circuitos neuronales con el flujo sanguíneo local y el soporte metabólico. Con múltiples pies terminales que proporcionan una cobertura casi completa de la lámina basal de los vasos sanguíneos cerebrales [257], los astrocitos pueden actuar como un "puente", detectando la actividad sináptica y coordinando el suministro de oxígeno y glucosa con los requerimientos metabólicos del tejido nervioso [258, 259]. El aumento de la actividad de las neuronas desencadena señales de Ca^{2+} en los astrocitos, lo cual conduce a la liberación de agentes vasoactivos que regulan el flujo sanguíneo local [260–262]. Además, debido a su estrecha relación con la vasculatura, los astrocitos se han convertido en actores vitales en la producción, entrega, almacenamiento y utilización de la energía del cerebro, incluida la glucosa, así como sus intermediarios metabólicos, como el lactato, los cuerpos cetónicos, el glutamato y el piruvato [258, 263–268]. Dado que un gran número de estudios han demostrado que el Mn provoca cambios metabólicos en el metabolismo y transporte de la glucosa en astrocitos [176, 234–236], decidimos investigar si la exposición aguda a Mn afectaba el transporte de glucosa de los cultivos primarios de glía de Bergmann. Obtuvimos resultados que muestran una notable disminución de la captura de glucosa (Fig. 17) después del tratamiento con 200 µM $MnCl_2$ por 30 minutos, muy probablemente debida a una reducción del número de transportadores de glucosa presentes en la membrana plasmática. Estos resultados difieren de lo descrito anteriormente por Zwingmann y colaboradores. En cultivos primarios de astrocitos, ellos observaron una mayor captura y consumo de [1-^{13}C]glucosa, seguido de un aumento significativo en la liberación lactato marcado con ^{13}C como consecuencia a la exposición a manganeso [236]. Sin embargo, nuevamente, los esquemas experimentales y los modelos celulares empleados pueden explicar completamente esta discrepancia. Se necesitan más estudios para entender mejor las diversas formas en las que el Mn altera la función de los transportadores de glucosa y sus posibles consecuencias. Nuestros resultados demuestran que una exposición relativamente corta a Mn puede tener implicaciones severas sobre el transporte de glucosa de las CGB, poniendo en riesgo el adecuado suministro de intermediarios

metabólicos hacia las neuronas. Estos efectos inducidos por Mn pueden ocasionar una alteración en el acople metabólico entre neuronas y células gliales, lo que llevaría a una disfunción sináptica neuronal adicional y a la activación de un estado excitotóxico.

Los metales juegan papeles muy importantes en el cuerpo humano, manteniendo la estructura celular y regulando la expresión génica, la neurotransmisión y la respuesta antioxidante, por nombrar algunos. Sin embargo, la acumulación excesiva de metales en el sistema nervioso puede ser tóxica. En relación con otros órganos del cuerpo humano, la concentración de zinc (Zn) es más alta en el cerebro, donde se estima es de 150 µM, siendo hasta 10 veces mayor en comparación con los niveles de Zn sérico [269]. Aunque es bien sabido que el Zn está estrechamente unido a macromoléculas en el cerebro, existe un pequeño número de iones de Zn en forma libre (aproximadamente 10-15% del Zn total en el cerebro) [270] principalmente dentro de las vesículas sinápticas en sinapsis glutamatérgicas [271–273]. Durante la actividad neuronal, el Zn se libera hacia la hendidura sináptica junto con el Glu [274] donde interactúa con receptores, canales iónicos y transportadores para modular la actividad sináptica [275]. Estudios utilizando células de Müller aisladas de la retina de salamandra y ovocitos de *Xenopus laevis* como sistema de expresión heteróloga para EAAT1, han demostrado que el Zn^{2+} es un inhibidor no competitivo del transporte de glutamato mediado por GLAST/EAAT1. Además de inhibir el transporte de Glu, el Zn^{2+} potencia la activación de la conductancia aniónica de GLAST [47, 48]. Usando mutagénesis sitio-dirigida, Vandenberg y colaboradores demostraron que los residuos de histidina de EAAT1 en las posiciones 146 y 156 forman parte del sitio de unión a Zn^{2+} [48]. Una explicación, sugerida por Spiridon y colaboradores, para los diferentes efectos sobre el transporte versus la activación de la conductancia de cloruro, es que el Zn^{2+} puede estabilizar una conformación que ralentiza el paso del Glu a través del transportador. Con el Glu unido al transportador durante un período más largo, se puede lograr una activación más eficiente de la conductancia del cloruro [47]. Nuestros resultados revelaron una disminución significativa de la incorporación de [^{3}H]-D-Asp en función del tiempo cuando el Mn esta presente

durante el proceso de captura (Fig. 16, Panel B), algo muy similar al efecto reportado para el Zn sobre la actividad de GLAST. Tomando en cuenta los tamaños y cargas similares de manganeso y zinc divalentes [276], se podría esperar el Mn^{2+} interactúe con este transportar de una forma similar al Zn^{2+} para afectar su función.

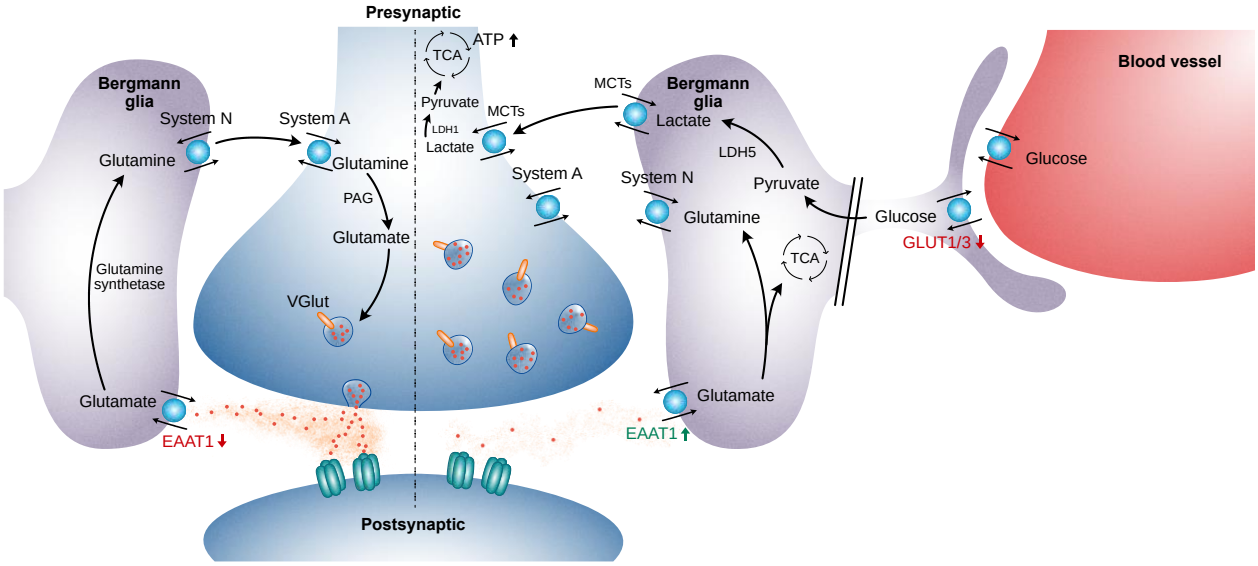

El Mn^{2+} como un posible modulador de la neurotransmisión glutamatérgica.

La exposición aguda a Mn^{2+} podría reducir la concentración de Glu basal en la hendidura sináptica e interrumpir el acoplamiento metabólico neurona-glía.

Figura 18. Modelo propuesto para los efectos de la exposición aguda a Mn sobre la actividad GLAST y el transporte de glucosa en CGB.

Con todo lo anteriormente mencionado, está claro que la exposición aguda de cultivos primarios de glía de Bergmann a Mn tiene un efecto directo sobre funciones primordiales de las células gliales. Esto, muy probablemente, podría comprometer la participación de las CGB en la sinapsis tripartita [277]. La Fig. 18 muestra un resumen gráfico de nuestros hallazgos y su posible impacto en la neurotransmisión glutamatérgica.

CONCLUSIONES

La exposición excesiva a Mn y su neurotoxicidad han llamado la atención recientemente. Identificar los objetivos celulares y moleculares del Mn es clave para comprender su toxicidad y desarrollar estrategias de prevención. Los astrocitos son las células gliales más abundantes en el SNC y desempeñan papeles esenciales en la homeostasis cerebral. Tras la exposición a niveles elevados de Mn, los astrocitos pueden fallar en el soporte de las neuronas, comprometiendo la suplementación de Gln, la regulación de la homeostasis de Glu/Gln y el mantenimiento de niveles adecuados de Glu extracelular.

Los estudios realizados en las últimas décadas han proporcionado información invaluable sobre la causa, los efectos y los mecanismos de la neurotoxicidad inducida por Mn. Sin embargo, las diferencias aparentes de nuestros resultados y lo previamente reportado, evidencia que aún queda mucho por comprender. Saber que los niveles excesivos de Mn extracelular en el SNC inhiben la captura de Glu mediante una interacción directa con los transportadores, abre un nuevo panorama en el entendimiento del papel que desempeña la excitotoxicidad en el manganismo y otras enfermedades neurodegenerativas.

Los eventos moleculares que subyacen a las alteraciones mediadas por Mn en la integridad glial-neuronal pueden tener implicaciones prometedoras para el desarrollo de futuras estrategias de tratamiento para la patología cerebral asociada con la toxicidad del Mn.

PERSPECTIVAS

1. Examinar si la conductancia de cloruro asociada al transporte Glu se ve afectada por la presencia de Mn^{2+}.

2. Determinar que aminoácidos forman parte del sitio de unión a Mn^{2+}.

3. Corroborar y caracterizar los mecanismos implicados en la remoción de los transportadores de glucosa después de una exposición aguda a Mn.

BIBLIOGRAFÍA

1. Watkins JC (1981) Pharmacology of excitatory amino acid transmitters. Adv Biochem Psychopharmacol 29:205–212
2. Headley PM, Grillner S (1990) Excitatory amino acids and synaptic transmission: the evidence for a physiological function. Trends Pharmacol Sci 11:205–211. https://doi.org/10.1016/0165-6147(90)90116-p
3. Danbolt NC (2001) Glutamate uptake. Prog Neurobiol 65:1–105
4. Scott T. Brady, George J. Siegel, R. Wayne Albers DLP (2012) Basic Neurochemistry: Principles of Molecular, Cellular, and Medical Neurobiology, 8th ed. Elsevier Academic Press
5. Ottersen OP, Zhang N, Walberg F (1992) Metabolic compartmentation of glutamate and glutamine: morphological evidence obtained by quantitative immunocytochemistry in rat cerebellum. Neuroscience 46:519–534. https://doi.org/10.1016/0306-4522(92)90141-n
6. Osen KK, Storm-Mathisen J, Ottersen OP, Dihle B (1995) Glutamate is concentrated in and released from parallel fiber terminals in the dorsal cochlear nucleus: a quantitative immunocytochemical analysis in guinea pig. J Comp Neurol 357:482–500. https://doi.org/10.1002/cne.903570311
7. Bramham CR, Torp R, Zhang N, et al (1990) Distribution of glutamate-like immunoreactivity in excitatory hippocampal pathways: a semiquantitative electron microscopic study in rats. Neuroscience 39:405–417. https://doi.org/10.1016/0306-4522(90)90277-b
8. Ottersen OP, Storm-Mathisen J, Bramham C, et al (1990) A quantitative electron microscopic immunocytochemical study of the distribution and synaptic handling of glutamate in rat hippocampus. Prog Brain Res 83:99–114. https://doi.org/10.1016/s0079-6123(08)61244-3
9. Dzubay JA, Jahr CE (1999) The concentration of synaptically released glutamate outside of the climbing fiber-Purkinje cell synaptic cleft. J Neurosci 19:5265–5274. https://doi.org/10.1523/JNEUROSCI.19-13-05265.1999
10. Attwell D, Laughlin SB (2001) An energy budget for signaling in the grey matter of the brain. J Cereb Blood Flow Metab 21:1133–1145. https://doi.org/10.1097/00004647-200110000-00001
11. Smith CUM (2002) Elements of Molecular Neurobiology, 3th ed. Wiley
12. Erecińska M, Silver IA (1990) Metabolism and role of glutamate in mammalian brain. Prog Neurobiol 35:245–296. https://doi.org/10.1016/0301-0082(90)90013-7
13. McKenna MC (2007) The glutamate-glutamine cycle is not stoichiometric: fates of glutamate in brain. J Neurosci Res 85:3347–3358. https://doi.org/10.1002/jnr.21444
14. Krebs HA (1935) Metabolism of amino-acids: The synthesis of glutamine from glutamic acid and ammonia, and the enzymic hydrolysis of glutamine in animal tissues. Biochem J 29:1951–1969. https://doi.org/10.1042/bj0291951
15. Stern JR, Eggleston L V, Hems R, Krebs HA (1949) Accumulation of glutamic acid in isolated brain tissue. Biochem J 44:410–418
16. CURTIS DR, PHILLIS JW, WATKINS JC (1960) The chemical excitation of spinal neurones by certain acidic amino acids. J Physiol 150:656–682. https://doi.org/10.1113/jphysiol.1960.sp006410
17. Fonnum F (1984) Glutamate: a neurotransmitter in mammalian brain. J Neurochem

42:1–11. https://doi.org/10.1111/j.1471-4159.1984.tb09689.x

18. Gonda X (2012) Basic pharmacology of NMDA receptors. Curr Pharm Des 18:1558–1567. https://doi.org/10.2174/138161212799958521
19. Bonaccorso C, Micale N, Ettari R, et al (2011) Glutamate binding-site ligands of NMDA receptors. Curr Med Chem 18:5483–5506. https://doi.org/10.2174/092986711798347225
20. Santangelo RM, Acker TM, Zimmerman SS, et al (2012) Novel NMDA receptor modulators: an update. Expert Opin Ther Pat 22:1337–1352. https://doi.org/10.1517/13543776.2012.728587
21. Rogawski MA (2013) AMPA receptors as a molecular target in epilepsy therapy. Acta Neurol Scand Suppl 9–18. https://doi.org/10.1111/ane.12099
22. Lerma J, Marques JM (2013) Kainate receptors in health and disease. Neuron 80:292–311. https://doi.org/10.1016/j.neuron.2013.09.045
23. Gregory KJ, Noetzel MJ, Niswender CM (2013) Pharmacology of metabotropic glutamate receptor allosteric modulators: structural basis and therapeutic potential for CNS disorders. Prog Mol Biol Transl Sci 115:61–121. https://doi.org/10.1016/B978-0-12-394587-7.00002-6
24. Steinhäuser C, Gallo V (1996) News on glutamate receptors in glial cells. Trends Neurosci 19:339–345. https://doi.org/10.1016/0166-2236(96)10043-6
25. Vernadakis A (1996) Glia-neuron intercommunications and synaptic plasticity. Prog Neurobiol 49:185–214. https://doi.org/10.1016/s0301-0082(96)00012-3
26. Forsythe ID, Barnes-Davies M (1997) Synaptic transmission: well-placed modulators. Curr Biol 7:R362–R365. https://doi.org/10.1016/s0960-9822(06)00175-8
27. Bergles DE, Roberts JD, Somogyi P, Jahr CE (2000) Glutamatergic synapses on oligodendrocyte precursor cells in the hippocampus. Nature 405:187–191. https://doi.org/10.1038/35012083
28. Watkins JC, Jane DE (2006) The glutamate story. Br J Pharmacol 147 Suppl 1:S100-8. https://doi.org/10.1038/sj.bjp.0706444
29. Pittenger C, Kandel E (1998) A genetic switch for long-term memory. C R Acad Sci III 321:91–96. https://doi.org/10.1016/s0764-4469(97)89807-1
30. Henley JM (1994) Kainate-binding proteins: phylogeny, structures and possible functions. Trends Pharmacol Sci 15:182–190. https://doi.org/10.1016/0165-6147(94)90146-5
31. Pin J-P, Kniazeff J, Goudet C, et al (2004) The activation mechanism of class-C G-protein coupled receptors. Biol cell 96:335–342. https://doi.org/10.1016/j.biolcel.2004.03.005
32. Kandel ER (2012) Principles of neural science, 5th ed. McGraw-Hill Education
33. Olney JW (1969) Brain lesions, obesity, and other disturbances in mice treated with monosodium glutamate. Science 164:719–721. https://doi.org/10.1126/science.164.3880.719
34. Werner P, Pitt D, Raine CS (2000) Glutamate excitotoxicity--a mechanism for axonal damage and oligodendrocyte death in Multiple Sclerosis? J Neural Transm Suppl 375–385. https://doi.org/10.1007/978-3-7091-6301-6_27
35. Pellerin L, Magistretti PJ (1994) Glutamate uptake into astrocytes stimulates aerobic glycolysis: a mechanism coupling neuronal activity to glucose utilization. Proc Natl Acad Sci U S A 91:10625–10629. https://doi.org/10.1073/pnas.91.22.10625

36. Pellerin L, Magistretti PJ (1997) Glutamate uptake stimulates Na+,K+-ATPase activity in astrocytes via activation of a distinct subunit highly sensitive to ouabain. J Neurochem 69:2132–2137. https://doi.org/10.1046/j.1471-4159.1997.69052132.x
37. Novelli A, Reilly JA, Lysko PG, Henneberry RC (1988) Glutamate becomes neurotoxic via the N-methyl-D-aspartate receptor when intracellular energy levels are reduced. Brain Res 451:205–212. https://doi.org/10.1016/0006-8993(88)90765-2
38. Bondy SC, Lee DK (1993) Oxidative stress induced by glutamate receptor agonists. Brain Res 610:229–233. https://doi.org/10.1016/0006-8993(93)91405-h
39. Balcar VJ, Johnston GA (1972) The structural specificity of the high affinity uptake of L-glutamate and L-aspartate by rat brain slices. J Neurochem 19:2657–2666. https://doi.org/10.1111/j.1471-4159.1972.tb01325.x
40. Utsunomiya-Tate N, Endou H, Kanai Y (1997) Tissue specific variants of glutamate transporter GLT-1. FEBS Lett 416:312–316. https://doi.org/10.1016/s0014-5793(97)01232-5
41. Peacey E, Miller CCJ, Dunlop J, Rattray M (2009) The four major N- and C-terminal splice variants of the excitatory amino acid transporter GLT-1 form cell surface homomeric and heteromeric assemblies. Mol Pharmacol 75:1062–1073. https://doi.org/10.1124/mol.108.052829
42. Cavelier P, Attwell D (2005) Tonic release of glutamate by a DIDS-sensitive mechanism in rat hippocampal slices. J Physiol 564:397–410. https://doi.org/10.1113/jphysiol.2004.082131
43. Herman MA, Jahr CE (2007) Extracellular glutamate concentration in hippocampal slice. J Neurosci 27:9736–9741. https://doi.org/10.1523/JNEUROSCI.3009-07.2007
44. Levy LM, Warr O, Attwell D (1998) Stoichiometry of the glial glutamate transporter GLT-1 expressed inducibly in a Chinese hamster ovary cell line selected for low endogenous Na+-dependent glutamate uptake. J Neurosci 18:9620–9628
45. Zerangue N, Kavanaugh MP (1996) Flux coupling in a neuronal glutamate transporter. Nature 383:634–637. https://doi.org/10.1038/383634a0
46. Owe SG, Marcaggi P, Attwell D (2006) The ionic stoichiometry of the GLAST glutamate transporter in salamander retinal glia. J Physiol 577:591–599. https://doi.org/10.1113/jphysiol.2006.116830
47. Spiridon M, Kamm D, Billups B, et al (1998) Modulation by zinc of the glutamate transporters in glial cells and cones isolated from the tiger salamander retina. J Physiol 506 (Pt 2):363–376. https://doi.org/10.1111/j.1469-7793.1998.363bw.x
48. Vandenberg RJ, Mitrovic AD, Johnston GA (1998) Molecular basis for differential inhibition of glutamate transporter subtypes by zinc ions. Mol Pharmacol 54:189–96
49. Machtens J-P, Kortzak D, Lansche C, et al (2015) Mechanisms of anion conduction by coupled glutamate transporters. Cell 160:542–553. https://doi.org/10.1016/j.cell.2014.12.035
50. Rose CR, Ziemens D, Untiet V, Fahlke C (2018) Molecular and cellular physiology of sodium-dependent glutamate transporters. Brain Res Bull 136:3–16. https://doi.org/10.1016/j.brainresbull.2016.12.013
51. Dehnes Y, Chaudhry FA, Ullensvang K, et al (1998) The glutamate transporter EAAT4 in rat cerebellar Purkinje cells: a glutamate-gated chloride channel concentrated near the synapse in parts of the dendritic membrane facing astroglia. J Neurosci 18:3606–3619

52. Furuta A, Martin LJ, Lin CL, et al (1997) Cellular and synaptic localization of the neuronal glutamate transporters excitatory amino acid transporter 3 and 4. Neuroscience 81:1031–1042. https://doi.org/10.1016/s0306-4522(97)00252-2
53. Tanaka J, Ichikawa R, Watanabe M, et al (1997) Extra-junctional localization of glutamate transporter EAAT4 at excitatory Purkinje cell synapses. Neuroreport 8:2461–2464. https://doi.org/10.1097/00001756-199707280-00010
54. Tanaka K (2000) Functions of glutamate transporters in the brain. Neurosci Res 37:15–19. https://doi.org/10.1016/s0168-0102(00)00104-8
55. Pow D V, Barnett NL (2000) Developmental expression of excitatory amino acid transporter 5: a photoreceptor and bipolar cell glutamate transporter in rat retina. Neurosci Lett 280:21–24. https://doi.org/10.1016/s0304-3940(99)00988-x
56. Schneider N, Cordeiro S, Machtens J-P, et al (2014) Functional properties of the retinal glutamate transporters GLT-1c and EAAT5. J Biol Chem 289:1815–1824. https://doi.org/10.1074/jbc.M113.517177
57. Danbolt NC, Storm-Mathisen J, Kanner BI (1992) An [Na+ + K+]coupled L-glutamate transporter purified from rat brain is located in glial cell processes. Neuroscience 51:295–310. https://doi.org/10.1016/0306-4522(92)90316-t
58. Rothstein JD, Martin L, Levey AI, et al (1994) Localization of neuronal and glial glutamate transporters. Neuron 13:713–725. https://doi.org/10.1016/0896-6273(94)90038-8
59. Lehre KP, Levy LM, Ottersen OP, et al (1995) Differential expression of two glial glutamate transporters in the rat brain: quantitative and immunocytochemical observations. J Neurosci 15:1835–1853
60. Tanaka K, Watase K, Manabe T, et al (1997) Epilepsy and exacerbation of brain injury in mice lacking the glutamate transporter GLT-1. Science 276:1699–1702. https://doi.org/10.1126/science.276.5319.1699
61. Petr GT, Sun Y, Frederick NM, et al (2015) Conditional deletion of the glutamate transporter GLT-1 reveals that astrocytic GLT-1 protects against fatal epilepsy while neuronal GLT-1 contributes significantly to glutamate uptake into synaptosomes. J Neurosci 35:5187–5201. https://doi.org/10.1523/JNEUROSCI.4255-14.2015
62. Watase K, Hashimoto K, Kano M, et al (1998) Motor discoordination and increased susceptibility to cerebellar injury in GLAST mutant mice. Eur J Neurosci 10:976–988. https://doi.org/10.1046/j.1460-9568.1998.00108.x
63. Yernool D, Boudker O, Jin Y, Gouaux E (2004) Structure of a glutamate transporter homologue from Pyrococcus horikoshii. Nature 431:811–818. https://doi.org/10.1038/nature03018
64. Nothmann D, Leinenweber A, Torres-Salazar D, et al (2011) Hetero-oligomerization of neuronal glutamate transporters. J Biol Chem 286:3935–3943. https://doi.org/10.1074/jbc.M110.187492
65. Ruan Y, Miyagi A, Wang X, et al (2017) Direct visualization of glutamate transporter elevator mechanism by high-speed AFM. Proc Natl Acad Sci U S A 114:1584–1588. https://doi.org/10.1073/pnas.1616413114
66. Slotboom DJ, Lolkema JS, Konings WN (1996) Membrane topology of the C-terminal half of the neuronal, glial, and bacterial glutamate transporter family. J Biol Chem 271:31317–31321. https://doi.org/10.1074/jbc.271.49.31317
67. Casado M, Bendahan A, Zafra F, et al (1993) Phosphorylation and modulation of brain glutamate transporters by protein kinase C. J Biol Chem 268:27313–27317

68. Ganel R, Crosson CE (1998) Modulation of human glutamate transporter activity by phorbol ester. J Neurochem 70:993–1000. https://doi.org/10.1046/j.1471-4159.1998.70030993.x
69. Kalandadze A, Wu Y, Robinson MB (2002) Protein kinase C activation decreases cell surface expression of the GLT-1 subtype of glutamate transporter. Requirement of a carboxyl-terminal domain and partial dependence on serine 486. J Biol Chem 277:45741–45750. https://doi.org/10.1074/jbc.M203771200
70. Murphy-Royal C, Dupuis JP, Varela JA, et al (2015) Surface diffusion of astrocytic glutamate transporters shapes synaptic transmission. Nat Neurosci 18:219–226. https://doi.org/10.1038/nn.3901
71. Garcia-Tardon N, Gonzalez-Gonzalez IM, Martinez-Villarreal J, et al (2012) Protein kinase C (PKC)-promoted endocytosis of glutamate transporter GLT-1 requires ubiquitin ligase Nedd4-2-dependent ubiquitination but not phosphorylation. J Biol Chem 287:19177–19187. https://doi.org/10.1074/jbc.M112.355909
72. Martinez-Villarreal J, Garcia Tardon N, Ibanez I, et al (2012) Cell surface turnover of the glutamate transporter GLT-1 is mediated by ubiquitination/deubiquitination. Glia 60:1356–1365. https://doi.org/10.1002/glia.22354
73. Zafra F, Ibáñez I, Giménez C (2017) Glutamate transporters: The arrestin connection. Oncotarget 8:5664–5665. https://doi.org/10.18632/oncotarget.13999
74. Gether U, Andersen PH, Larsson OM, Schousboe A (2006) Neurotransmitter transporters: molecular function of important drug targets. Trends Pharmacol Sci 27:375–383. https://doi.org/10.1016/j.tips.2006.05.003
75. Azevedo FAC, Carvalho LRB, Grinberg LT, et al (2009) Equal numbers of neuronal and nonneuronal cells make the human brain an isometrically scaled-up primate brain. J Comp Neurol 513:532–541. https://doi.org/10.1002/cne.21974
76. Herculano-Houzel S (2014) The glia/neuron ratio: how it varies uniformly across brain structures and species and what that means for brain physiology and evolution. Glia 62:1377–1391. https://doi.org/10.1002/glia.22683
77. Kettenmann H, Kirchhoff F, Verkhratsky A (2013) Microglia: new roles for the synaptic stripper. Neuron 77:10–18. https://doi.org/10.1016/j.neuron.2012.12.023
78. Lee Y, Morrison BM, Li Y, et al (2012) Oligodendroglia metabolically support axons and contribute to neurodegeneration. Nature 487:443–448. https://doi.org/10.1038/nature11314
79. Bergles DE, Jabs R, Steinhauser C (2010) Neuron-glia synapses in the brain. Brain Res Rev 63:130–137. https://doi.org/10.1016/j.brainresrev.2009.12.003
80. Chung S-H, Guo F, Jiang P, et al (2013) Olig2/Plp-positive progenitor cells give rise to Bergmann glia in the cerebellum. Cell Death Dis 4:e546. https://doi.org/10.1038/cddis.2013.74
81. Kriegstein A, Alvarez-Buylla A (2009) The glial nature of embryonic and adult neural stem cells. Annu Rev Neurosci 32:149–184. https://doi.org/10.1146/annurev.neuro.051508.135600
82. Perea G, Navarrete M, Araque A (2009) Tripartite synapses: astrocytes process and control synaptic information. Trends Neurosci 32:421–431. https://doi.org/10.1016/j.tins.2009.05.001
83. Yang HY, Lieska N, Shao D, et al (1994) Proteins of the intermediate filament cytoskeleton as markers for astrocytes and human astrocytomas. Mol Chem Neuropathol 21:155–176. https://doi.org/10.1007/BF02815349

84. Cameron RS, Rakic P (1991) Glial cell lineage in the cerebral cortex: a review and synthesis. Glia 4:124–137. https://doi.org/10.1002/glia.440040204
85. Morest DK, Silver J (2003) Precursors of neurons, neuroglia, and ependymal cells in the CNS: what are they? Where are they from? How do they get where they are going? Glia 43:6–18. https://doi.org/10.1002/glia.10238
86. Bringmann A, Pannicke T, Grosche J, et al (2006) Muller cells in the healthy and diseased retina. Prog Retin Eye Res 25:397–424. https://doi.org/10.1016/j.preteyeres.2006.05.003
87. Somogyi P, Eshhar N, Teichberg VI, Roberts JD (1990) Subcellular localization of a putative kainate receptor in Bergmann glial cells using a monoclonal antibody in the chick and fish cerebellar cortex. Neuroscience 35:9–30
88. Hatten ME (1999) Central nervous system neuronal migration. Annu Rev Neurosci 22:511–539. https://doi.org/10.1146/annurev.neuro.22.1.511
89. Koirala S, Corfas G (2010) Identification of novel glial genes by single-cell transcriptional profiling of Bergmann glial cells from mouse cerebellum. PLoS One 5:e9198. https://doi.org/10.1371/journal.pone.0009198
90. Grosche J, Kettenmann H, Reichenbach A (2002) Bergmann glial cells form distinct morphological structures to interact with cerebellar neurons. J Neurosci Res 68:138–149. https://doi.org/10.1002/jnr.10197
91. Kirischuk S, Kettenmann H, Verkhratsky A (2007) Membrane currents and cytoplasmic sodium transients generated by glutamate transport in Bergmann glial cells. Pflugers Arch 454:245–252. https://doi.org/10.1007/s00424-007-0207-5
92. Slemmer JE, De Zeeuw CI, Weber JT (2005) Don't get too excited: mechanisms of glutamate-mediated Purkinje cell death. Prog Brain Res 148:367–390. https://doi.org/10.1016/S0079-6123(04)48029-7
93. Cid ME, Ortega A (1993) Glutamate stimulates [3H]phorbol 12,13-dibutyrate binding in cultured Bergmann glia cells. Eur J Pharmacol 245:51–54. https://doi.org/10.1016/0922-4106(93)90168-9
94. Lopez-Colome AM, Ortega A (1997) Activation of p42 mitogen-activated protein kinase by glutamate in cultured radial glia. Neurochem Res 22:679–685. https://doi.org/10.1023/a:1027345808746
95. Millan A, Arias-Montano JA, Mendez JA, et al (2004) Alpha-amino-3-hydroxy-5-methyl-4-isoxazolepropionic acid receptors signaling complexes in Bergmann glia. J Neurosci Res 78:56–63. https://doi.org/10.1002/jnr.20237
96. Aguirre A, Lopez-Bayghen E, Ortega A (2002) Glutamate-dependent transcriptional regulation of the chkbp gene: signaling mechanisms. J Neurosci Res 70:117–127. https://doi.org/10.1002/jnr.10394
97. Sanchez G, Ortega A (1994) AMPA/KA receptor induced AP-1 DNA binding activity in cultured Bergmann glia cells. Neuroreport 5:2109–2112. https://doi.org/10.1097/00001756-199410270-00030
98. Lopez T, Lopez-Colome AM, Ortega A (1998) Changes in GluR4 expression induced by metabotropic receptor activation in radial glia cultures. Brain Res Mol Brain Res 58:40–46. https://doi.org/10.1016/s0169-328x(98)00094-1
99. Aguirre A, Lopez T, Lopez-Bayghen E, Ortega A (2000) Glutamate regulates kainate-binding protein expression in cultured chick Bergmann glia through an activator protein-1 binding site. J Biol Chem 275:39246–39253. https://doi.org/10.1074/jbc.M002847200

100. Gonzalez-Mejia ME, Morales M, Hernandez-Kelly LCR, et al (2006) Glutamate-dependent translational regulation in cultured Bergmann glia cells: involvement of p70S6K. Neuroscience 141:1389–1398. https://doi.org/10.1016/j.neuroscience.2006.04.076
101. Barrera I, Hernandez-Kelly LC, Castelan F, Ortega A (2008) Glutamate-dependent elongation factor-2 phosphorylation in Bergmann glial cells. Neurochem Int 52:1167–1175. https://doi.org/10.1016/j.neuint.2007.12.006
102. Zepeda RC, Barrera I, Castelan F, et al (2009) Glutamate-dependent phosphorylation of the mammalian target of rapamycin (mTOR) in Bergmann glial cells. Neurochem Int 55:282–287. https://doi.org/10.1016/j.neuint.2009.03.011
103. Barrera I, Flores-Mendez M, Hernandez-Kelly LC, et al (2010) Glutamate regulates eEF1A phosphorylation and ribosomal transit time in Bergmann glial cells. Neurochem Int 57:795–803. https://doi.org/10.1016/j.neuint.2010.08.017
104. Flores-Mendez MA, Martinez-Lozada Z, Monroy HC, et al (2013) Glutamate-dependent translational control in cultured Bergmann glia cells: eIF2alpha phosphorylation. Neurochem Res 38:1324–1332. https://doi.org/10.1007/s11064-013-1024-1
105. Liang Z, Valla J, Sefidvash-Hockley S, et al (2002) Effects of estrogen treatment on glutamate uptake in cultured human astrocytes derived from cortex of Alzheimer's disease patients. J Neurochem 80:807–814. https://doi.org/10.1046/j.0022-3042.2002.00779.x
106. Schallier A, Smolders I, Van Dam D, et al (2011) Region- and age-specific changes in glutamate transport in the AbetaPP23 mouse model for Alzheimer's disease. J Alzheimers Dis 24:287–300. https://doi.org/10.3233/JAD-2011-101005
107. Scimemi A, Meabon JS, Woltjer RL, et al (2013) Amyloid-beta1-42 slows clearance of synaptically released glutamate by mislocalizing astrocytic GLT-1. J Neurosci 33:5312–5318. https://doi.org/10.1523/JNEUROSCI.5274-12.2013
108. Matos M, Augusto E, Oliveira CR, Agostinho P (2008) Amyloid-beta peptide decreases glutamate uptake in cultured astrocytes: involvement of oxidative stress and mitogen-activated protein kinase cascades. Neuroscience 156:898–910. https://doi.org/10.1016/j.neuroscience.2008.08.022
109. Rothstein JD, Martin LJ, Kuncl RW (1992) Decreased glutamate transport by the brain and spinal cord in amyotrophic lateral sclerosis. N Engl J Med 326:1464–1468. https://doi.org/10.1056/NEJM199205283262204
110. Rothstein JD, Van Kammen M, Levey AI, et al (1995) Selective loss of glial glutamate transporter GLT-1 in amyotrophic lateral sclerosis. Ann Neurol 38:73–84. https://doi.org/10.1002/ana.410380114
111. Mhatre M, Floyd RA, Hensley K (2004) Oxidative stress and neuroinflammation in Alzheimer's disease and amyotrophic lateral sclerosis: common links and potential therapeutic targets. J Alzheimers Dis 6:147–157
112. Ueda Y, Doi T, Tokumaru J, et al (2001) Collapse of extracellular glutamate regulation during epileptogenesis: down-regulation and functional failure of glutamate transporter function in rats with chronic seizures induced by kainic acid. J Neurochem 76:892–900. https://doi.org/10.1046/j.1471-4159.2001.00087.x
113. Wong M, Ess KC, Uhlmann EJ, et al (2003) Impaired glial glutamate transport in a mouse tuberous sclerosis epilepsy model. Ann Neurol 54:251–256. https://doi.org/10.1002/ana.10648
114. Markiewicz I, Lukomska B (2006) The role of astrocytes in the physiology and

pathology of the central nervous system. Acta Neurobiol Exp (Wars) 66:343–358

115. Chung EKY, Chen LW, Chan YS, Yung KKL (2008) Downregulation of glial glutamate transporters after dopamine denervation in the striatum of 6-hydroxydopamine-lesioned rats. J Comp Neurol 511:421–437. https://doi.org/10.1002/cne.21852
116. Hazell AS, Itzhak Y, Liu H, Norenberg MD (1997) 1-Methyl-4-phenyl-1,2,3,6-tetrahydropyridine (MPTP) decreases glutamate uptake in cultured astrocytes. J Neurochem 68:2216–2219. https://doi.org/10.1046/j.1471-4159.1997.68052216.x
117. Yang Y-L, Meng C-H, Ding J-H, et al (2005) Iptakalim hydrochloride protects cells against neurotoxin-induced glutamate transporter dysfunction in in vitro and in vivo models. Brain Res 1049:80–88. https://doi.org/10.1016/j.brainres.2005.04.073
118. Ferrarese C, Zoia C, Pecora N, et al (1999) Reduced platelet glutamate uptake in Parkinson's disease. J Neural Transm 106:685–692. https://doi.org/10.1007/s007020050189
119. Robelet S, Melon C, Guillet B, et al (2004) Chronic L-DOPA treatment increases extracellular glutamate levels and GLT1 expression in the basal ganglia in a rat model of Parkinson's disease. Eur J Neurosci 20:1255–1266. https://doi.org/10.1111/j.1460-9568.2004.03591.x
120. Struzynska L, Chalimoniuk M, Sulkowski G (2005) Changes in expression of neuronal and glial glutamate transporters in lead-exposed adult rat brain. Neurochem Int 47:326–333. https://doi.org/10.1016/j.neuint.2005.05.005
121. Gilbert ME, Mack CM, Lasley SM (1999) The influence of developmental period of lead exposure on long-term potentiation in the adult rat dentate gyrus in vivo. Neurotoxicology 20:57–69
122. Allen JW, Mutkus LA, Aschner M (2001) Methylmercury-mediated inhibition of 3H-D-aspartate transport in cultured astrocytes is reversed by the antioxidant catalase. Brain Res 902:92–100. https://doi.org/10.1016/s0006-8993(01)02375-7
123. Mutkus L, Aschner JL, Syversen T, Aschner M (2005) Methylmercury alters the in vitro uptake of glutamate in GLAST- and GLT-1-transfected mutant CHO-K1 cells. Biol Trace Elem Res 107:231–245. https://doi.org/10.1385/BTER:107:3:231
124. Liu W, Xu Z, Deng Y, et al (2013) Protective effects of memantine against methylmercury-induced glutamate dyshomeostasis and oxidative stress in rat cerebral cortex. Neurotox Res 24:320–337. https://doi.org/10.1007/s12640-013-9386-3
125. Aschner JL, Aschner M (2005) Nutritional aspects of manganese homeostasis. Mol Aspects Med 26:353–362. https://doi.org/10.1016/j.mam.2005.07.003
126. Aschner M, Erikson KM, Dorman DC (2005) Manganese dosimetry: species differences and implications for neurotoxicity. Crit Rev Toxicol 35:1–32
127. Erikson KM, Thompson K, Aschner J, Aschner M (2007) Manganese neurotoxicity: a focus on the neonate. Pharmacol Ther 113:369–377. https://doi.org/10.1016/j.pharmthera.2006.09.002
128. Baly DL, Keen CL, Hurley LS (1985) Pyruvate carboxylase and phosphoenolpyruvate carboxykinase activity in developing rats: effect of manganese deficiency. J Nutr 115:872–879. https://doi.org/10.1093/jn/115.7.872
129. Bentle LA, Lardy HA (1976) Interaction of anions and divalent metal ions with phosphoenolpyruvate carboxykinase. J Biol Chem 251:2916–2921
130. Stallings WC, Metzger AL, Pattridge KA, et al (1991) Structure-function relationships

in iron and manganese superoxide dismutases. Free Radic Res Commun 12-13 Pt 1:259–268. https://doi.org/10.3109/10715769109145794

131. Huang CC, Chu NS, Lu CS, et al (1989) Chronic manganese intoxication. Arch Neurol 46:1104–1106. https://doi.org/10.1001/archneur.1989.00520460090018
132. Couper J (1837) On the effects of black oxide of manganese when inhaled into the lungs. Br Ann Med Pharmacy, Vital Stat Gen Sci 1:41–42
133. Burton NC, Guilarte TR (2009) Manganese neurotoxicity: lessons learned from longitudinal studies in nonhuman primates. Environ Health Perspect 117:325–332. https://doi.org/10.1289/ehp.0800035
134. Cooper WC (1984) The health implications of increased manganese in the environment resulting from the combustion of fuel additives: a review of the literature. J Toxicol Environ Health 14:23–46. https://doi.org/10.1080/15287398409530561
135. Bader M, Dietz MC, Ihrig A, Triebig G (1999) Biomonitoring of manganese in blood, urine and axillary hair following low-dose exposure during the manufacture of dry cell batteries. Int Arch Occup Environ Health 72:521–527. https://doi.org/10.1007/s004200050410
136. Bast-Pettersen R, Ellingsen DG, Hetland SM, Thomassen Y (2004) Neuropsychological function in manganese alloy plant workers. Int Arch Occup Environ Health 77:277–287. https://doi.org/10.1007/s00420-003-0491-0
137. Bowler RM, Nakagawa S, Drezgic M, et al (2007) Sequelae of fume exposure in confined space welding: a neurological and neuropsychological case series. Neurotoxicology 28:298–311. https://doi.org/10.1016/j.neuro.2006.11.001
138. Montes S, Riojas-Rodriguez H, Sabido-Pedraza E, Rios C (2008) Biomarkers of manganese exposure in a population living close to a mine and mineral processing plant in Mexico. Environ Res 106:89–95. https://doi.org/10.1016/j.envres.2007.08.008
139. Srivastava AK, Gupta BN, Mathur N, et al (1991) An investigation of metal concentrations in blood of industrial workers. Vet Hum Toxicol 33:280–282
140. Finley JW, Davis CD (1999) Manganese deficiency and toxicity: are high or low dietary amounts of manganese cause for concern? Biofactors 10:15–24. https://doi.org/10.1002/biof.5520100102
141. Williams M, Todd GD, Roney N, et al (2012) Toxicological Profile for Manganese. Atlanta (GA)
142. Krachler M, Rossipal E (2000) Concentrations of trace elements in extensively hydrolysed infant formulae and their estimated daily intakes. Ann Nutr Metab 44:68–74. https://doi.org/10.1159/000012823
143. Bertinet DB, Tinivella M, Balzola FA, et al (2000) Brain manganese deposition and blood levels in patients undergoing home parenteral nutrition. JPEN J Parenter Enteral Nutr 24:223–227. https://doi.org/10.1177/0148607100024004223
144. Hardy G (2009) Manganese in parenteral nutrition: who, when, and why should we supplement? Gastroenterology 137:S29-35. https://doi.org/10.1053/j.gastro.2009.08.011
145. Davis JM (1998) Methylcyclopentadienyl manganese tricarbonyl: health risk uncertainties and research directions. Environ Health Perspect 106 Suppl 1:191–201. https://doi.org/10.1289/ehp.98106s1191
146. Kaiser J (2003) Manganese: a high-octane dispute. Science 300:926–928

147. Sikk K, Taba P, Haldre S, et al (2010) Clinical, neuroimaging and neurophysiological features in addicts with manganese-ephedrone exposure. Acta Neurol Scand 121:237–243. https://doi.org/10.1111/j.1600-0404.2009.01189.x
148. Davidsson L, Cederblad A, Hagebo E, et al (1988) Intrinsic and extrinsic labeling for studies of manganese absorption in humans. J Nutr 118:1517–1521. https://doi.org/10.1093/jn/118.12.1517
149. Mena I (1974) The role of manganese in human disease. Ann Clin Lab Sci 4:487–491
150. Davis CD, Zech L, Greger JL (1993) Manganese metabolism in rats: an improved methodology for assessing gut endogenous losses. Proc Soc Exp Biol Med 202:103–108. https://doi.org/10.3181/00379727-202-43518
151. Dorman DC, Struve MF, James RA, et al (2001) Influence of dietary manganese on the pharmacokinetics of inhaled manganese sulfate in male CD rats. Toxicol Sci 60:242–251. https://doi.org/10.1093/toxsci/60.2.242
152. Davis CD, Malecki EA, Greger JL (1992) Interactions among dietary manganese, heme iron, and nonheme iron in women. Am J Clin Nutr 56:926–932. https://doi.org/10.1093/ajcn/56.5.926
153. Gunshin H, Mackenzie B, Berger U V, et al (1997) Cloning and characterization of a mammalian proton-coupled metal-ion transporter. Nature 388:482–488. https://doi.org/10.1038/41343
154. EPA (1984) Health Assessment Document for Manganese. Cincinnati OH US
155. Archibald FS, Tyree C (1987) Manganese poisoning and the attack of trivalent manganese upon catecholamines. Arch Biochem Biophys 256:638–650. https://doi.org/10.1016/0003-9861(87)90621-7
156. Aisen P, Aasa R, Redfield AG (1969) The chromium, manganese, and cobalt complexes of transferrin. J Biol Chem 244:4628–4633
157. Critchfield JW, Keen CL (1992) Manganese + 2 exhibits dynamic binding to multiple ligands in human plasma. Metabolism 41:1087–1092. https://doi.org/10.1016/0026-0495(92)90290-q
158. Aschner M, Gannon M (1994) Manganese (Mn) transport across the rat blood-brain barrier: saturable and transferrin-dependent transport mechanisms. Brain Res Bull 33:345–349. https://doi.org/10.1016/0361-9230(94)90204-6
159. Au C, Benedetto A, Aschner M (2008) Manganese transport in eukaryotes: the role of DMT1. Neurotoxicology 29:569–576. https://doi.org/10.1016/j.neuro.2008.04.022
160. Itoh K, Sakata M, Watanabe M, et al (2008) The entry of manganese ions into the brain is accelerated by the activation of N-methyl-D-aspartate receptors. Neuroscience 154:732–740. https://doi.org/10.1016/j.neuroscience.2008.03.080
161. Aschner M, Aschner JL (1990) Manganese transport across the blood-brain barrier: relationship to iron homeostasis. Brain Res Bull 24:857–860. https://doi.org/10.1016/0361-9230(90)90152-p
162. Dorman DC, Struve MF, Marshall MW, et al (2006) Tissue manganese concentrations in young male rhesus monkeys following subchronic manganese sulfate inhalation. Toxicol Sci 92:201–210. https://doi.org/10.1093/toxsci/kfj206
163. Guilarte TR, McGlothan JL, Degaonkar M, et al (2006) Evidence for cortical dysfunction and widespread manganese accumulation in the nonhuman primate brain following chronic manganese exposure: a 1H-MRS and MRI study. Toxicol Sci 94:351–358. https://doi.org/10.1093/toxsci/kfl106

164. Erikson KM, Aschner M (2006) Increased manganese uptake by primary astrocyte cultures with altered iron status is mediated primarily by divalent metal transporter. Neurotoxicology 27:125–130. https://doi.org/10.1016/j.neuro.2005.07.003
165. Suarez N, Eriksson H (1993) Receptor-mediated endocytosis of a manganese complex of transferrin into neuroblastoma (SHSY5Y) cells in culture. J Neurochem 61:127–131. https://doi.org/10.1111/j.1471-4159.1993.tb03546.x
166. Andre C, Truong TT, Robert JF, Guillaume YC (2005) Effect of metals on herbicides-alpha-synuclein association: a possible factor in neurodegenerative disease studied by capillary electrophoresis. Electrophoresis 26:3256–3264. https://doi.org/10.1002/elps.200500169
167. Peneder TM, Scholze P, Berger ML, et al (2011) Chronic exposure to manganese decreases striatal dopamine turnover in human alpha-synuclein transgenic mice. Neuroscience 180:280–292. https://doi.org/10.1016/j.neuroscience.2011.02.017
168. Voss H (1939) Progressive bulbar paralysis and amyotrophic lateral sclerosis from chronic manganese poisoning. Arch Gewerbepathol Gewerbehyg 9:464– 476
169. Miyata S, Nakamura S, Nagata H, Kameyama M (1983) Increased manganese level in spinal cords of amyotrophic lateral sclerosis determined by radiochemical neutron activation analysis. J Neurol Sci 61:283–293. https://doi.org/10.1016/0022-510x(83)90012-6
170. Hesketh S, Sassoon J, Knight R, Brown DR (2008) Elevated manganese levels in blood and CNS in human prion disease. Mol Cell Neurosci 37:590–598. https://doi.org/10.1016/j.mcn.2007.12.008
171. Levin J, Bertsch U, Kretzschmar H, Giese A (2005) Single particle analysis of manganese-induced prion protein aggregates. Biochem Biophys Res Commun 329:1200–1207. https://doi.org/10.1016/j.bbrc.2005.02.094
172. Banta RG, Markesbery WR (1977) Elevated manganese levels associated with dementia and extrapyramidal signs. Neurology 27:213–216. https://doi.org/10.1212/wnl.27.3.213
173. Bowman AB, Kwakye GF, Herrero Hernández E, Aschner M (2011) Role of manganese in neurodegenerative diseases. J. Trace Elem. Med. Biol. 25:191–203
174. Donaldson J, LaBella FS, Gesser D (1981) Enhanced autoxidation of dopamine as a possible basis of manganese neurotoxicity. Neurotoxicology 2:53–64
175. Oikawa S, Hirosawa I, Tada-Oikawa S, et al (2006) Mechanism for manganese enhancement of dopamine-induced oxidative DNA damage and neuronal cell death. Free Radic Biol Med 41:748–756. https://doi.org/10.1016/j.freeradbiomed.2006.05.018
176. Erikson KM, Dorman DC, Lash LH, Aschner M (2007) Manganese inhalation by rhesus monkeys is associated with brain regional changes in biomarkers of neurotoxicity. Toxicol Sci 97:459–466. https://doi.org/10.1093/toxsci/kfm044
177. Dobson AW, Weber S, Dorman DC, et al (2003) Oxidative stress is induced in the rat brain following repeated inhalation exposure to manganese sulfate. Biol Trace Elem Res 93:113–126. https://doi.org/10.1385/BTER:93:1-3:113
178. Hazell AS, Normandin L, Norenberg MD, et al (2006) Alzheimer type II astrocytic changes following sub-acute exposure to manganese and its prevention by antioxidant treatment. Neurosci Lett 396:167–171. https://doi.org/10.1016/j.neulet.2005.11.064
179. Chen JY, Tsao GC, Zhao Q, Zheng W (2001) Differential cytotoxicity of Mn(II) and

Mn(III): special reference to mitochondrial [Fe-S] containing enzymes. Toxicol Appl Pharmacol 175:160–168. https://doi.org/10.1006/taap.2001.9245

180. Gavin CE, Gunter KK, Gunter TE (1992) Mn2+ sequestration by mitochondria and inhibition of oxidative phosphorylation. Toxicol Appl Pharmacol 115:1–5. https://doi.org/10.1016/0041-008x(92)90360-5
181. Alaimo A, Gorojod RM, Kotler ML (2011) The extrinsic and intrinsic apoptotic pathways are involved in manganese toxicity in rat astrocytoma C6 cells. Neurochem Int 59:297–308. https://doi.org/10.1016/j.neuint.2011.06.001
182. Gonzalez LE, Juknat AA, Venosa AJ, et al (2008) Manganese activates the mitochondrial apoptotic pathway in rat astrocytes by modulating the expression of proteins of the Bcl-2 family. Neurochem Int 53:408–415. https://doi.org/10.1016/j.neuint.2008.09.008
183. Filipov NM, Dodd CA (2012) Role of glial cells in manganese neurotoxicity. J. Appl. Toxicol. 32:310–317
184. Filipov NM, Seegal RF, Lawrence DA (2005) Manganese potentiates in vitro production of proinflammatory cytokines and nitric oxide by microglia through a nuclear factor kappa B-dependent mechanism. Toxicol Sci 84:139–148. https://doi.org/10.1093/toxsci/kfi055
185. Liu M, Cai T, Zhao F, et al (2009) Effect of microglia activation on dopaminergic neuronal injury induced by manganese, and its possible mechanism. Neurotox Res 16:42–49. https://doi.org/10.1007/s12640-009-9045-x
186. Aschner M, Shanker G, Erikson K, et al (2002) The uptake of manganese in brain endothelial cultures. Neurotoxicology 23:165–168. https://doi.org/10.1016/s0161-813x(02)00056-6
187. Lee ESY, Sidoryk M, Jiang H, et al (2009) Estrogen and tamoxifen reverse manganese-induced glutamate transporter impairment in astrocytes. J Neurochem 110:530–544. https://doi.org/10.1111/j.1471-4159.2009.06105.x
188. Brouillet EP, Shinobu L, McGarvey U, et al (1993) Manganese injection into the rat striatum produces excitotoxic lesions by impairing energy metabolism. Exp Neurol 120:89–94. https://doi.org/10.1006/exnr.1993.1042
189. Xu B, Xu Z-F, Deng Y (2010) Protective effects of MK-801 on manganese-induced glutamate metabolism disorder in rat striatum. Exp Toxicol Pathol 62:381–390. https://doi.org/10.1016/j.etp.2009.05.007
190. Xu Z, Jia K, Xu B, et al (2010) Effects of MK-801, taurine and dextromethorphan on neurotoxicity caused by manganese in rats. Toxicol Ind Health 26:55–60. https://doi.org/10.1177/0748233709359275
191. Xu B, Xu Z-F, Deng Y (2010) Manganese exposure alters the expression of N-methyl-D-aspartate receptor subunit mRNAs and proteins in rat striatum. J Biochem Mol Toxicol 24:1–9. https://doi.org/10.1002/jbt.20306
192. Spadoni F, Stefani A, Morello M, et al (2000) Selective vulnerability of pallidal neurons in the early phases of manganese intoxication. Exp brain Res 135:544–551. https://doi.org/10.1007/s002210000554
193. Morello M, Canini A, Mattioli P, et al (2008) Sub-cellular localization of manganese in the basal ganglia of normal and manganese-treated rats An electron spectroscopy imaging and electron energy-loss spectroscopy study. Neurotoxicology 29:60–72. https://doi.org/10.1016/j.neuro.2007.09.001
194. Trotti D, Danbolt NC, Volterra A (1998) Glutamate transporters are oxidant-

vulnerable: a molecular link between oxidative and excitotoxic neurodegeneration? Trends Pharmacol Sci 19:328–334. https://doi.org/10.1016/s0165-6147(98)01230-9

195. Miralles VJ, Martinez-Lopez I, Zaragoza R, et al (2001) Na+ dependent glutamate transporters (EAAT1, EAAT2, and EAAT3) in primary astrocyte cultures: effect of oxidative stress. Brain Res 922:21–29. https://doi.org/10.1016/s0006-8993(01)03124-9
196. Karki P, Webb A, Smith K, et al (2014) Yin Yang 1 Is a Repressor of Glutamate Transporter EAAT2 , and It Mediates Manganese-Induced Decrease of EAAT2 Expression in. 34:1280–1289. https://doi.org/10.1128/MCB.01176-13
197. Sitcheran R, Gupta P, Fisher PB, Baldwin AS (2005) Positive and negative regulation of EAAT2 by NF-kappaB: a role for N-myc in TNFalpha-controlled repression. EMBO J 24:510–520. https://doi.org/10.1038/sj.emboj.7600555
198. Lee E, Sidoryk-Wegrzynowicz M, Yin Z, et al (2012) Transforming growth factor-alpha mediates estrogen-induced upregulation of glutamate transporter GLT-1 in rat primary astrocytes. Glia 60:1024–1036. https://doi.org/10.1002/glia.22329
199. Sidoryk-Wegrzynowicz M, Aschner M (2013) Role of astrocytes in manganese mediated neurotoxicity. BMC Pharmacol Toxicol 14:23. https://doi.org/10.1186/2050-6511-14-23
200. Sidoryk-Wegrzynowicz M, Lee E, Mingwei N, Aschner M (2011) Disruption of astrocytic glutamine turnover by manganese is mediated by the protein kinase C pathway. Glia 59:1732–1743. https://doi.org/10.1002/glia.21219
201. Sidoryk-Wegrzynowicz M, Lee E, Aschner M (2012) Mechanism of Mn(II)-mediated dysregulation of glutamine-glutamate cycle: focus on glutamate turnover. J Neurochem 122:856–867. https://doi.org/10.1111/j.1471-4159.2012.07835.x
202. Conradt M, Stoffel W (1997) Inhibition of the high-affinity brain glutamate transporter GLAST-1 via direct phosphorylation. J Neurochem 68:1244–1251. https://doi.org/10.1046/j.1471-4159.1997.68031244.x
203. Cordova FM, Aguiar ASJ, Peres T V, et al (2012) In vivo manganese exposure modulates Erk, Akt and Darpp-32 in the striatum of developing rats, and impairs their motor function. PLoS One 7:e33057. https://doi.org/10.1371/journal.pone.0033057
204. Ito Y, Oh-Hashi K, Kiuchi K, Hirata Y (2006) p44/42 MAP kinase and c-Jun N-terminal kinase contribute to the up-regulation of caspase-3 in manganese-induced apoptosis in PC12 cells. Brain Res 1099:1–7. https://doi.org/10.1016/j.brainres.2006.03.126
205. Peres TV, Pedro DZ, de Cordova FM, et al (2013) In vitro manganese exposure disrupts MAPK signaling pathways in striatal and hippocampal slices from immature rats. Biomed Res Int 2013:769295. https://doi.org/10.1155/2013/769295
206. Yin Z, Aschner JL, dos Santos AP, Aschner M (2008) Mitochondrial-dependent manganese neurotoxicity in rat primary astrocyte cultures. Brain Res 1203:1–11. https://doi.org/10.1016/j.brainres.2008.01.079
207. Karki P, Kim C, Smith K, et al (2015) Transcriptional Regulation of the Astrocytic Excitatory Amino Acid Transporter 1 (EAAT1) via NF-kappaB and Yin Yang 1 (YY1). J Biol Chem 290:23725–23737. https://doi.org/10.1074/jbc.M115.649327
208. Lee S-G, Kim K, Kegelman TP, et al (2011) Oncogene AEG-1 promotes glioma-induced neurodegeneration by increasing glutamate excitotoxicity. Cancer Res 71:6514–6523. https://doi.org/10.1158/0008-5472.CAN-11-0782

209. Rosas S, Vargas MA, Lopez-Bayghen E, Ortega A (2007) Glutamate-dependent transcriptional regulation of GLAST/EAAT1: a role for YY1. J Neurochem 101:1134–1144. https://doi.org/10.1111/j.1471-4159.2007.04517.x
210. Ghosh M, Yang Y, Rothstein JD, Robinson MB (2011) Nuclear factor-kappaB contributes to neuron-dependent induction of glutamate transporter-1 expression in astrocytes. J Neurosci 31:9159–9169. https://doi.org/10.1523/JNEUROSCI.0302-11.2011
211. Karki P, Webb A, Smith K, et al (2013) cAMP response element-binding protein (CREB) and nuclear factor kappaB mediate the tamoxifen-induced up-regulation of glutamate transporter 1 (GLT-1) in rat astrocytes. J Biol Chem 288:28975–28986. https://doi.org/10.1074/jbc.M113.483826
212. Karki P, Webb A, Zerguine A, et al (2014) Mechanism of raloxifene-induced upregulation of glutamate transporters in rat primary astrocytes. Glia 62:1270–1283. https://doi.org/10.1002/glia.22679
213. Lee S-G, Su Z-Z, Emdad L, et al (2008) Mechanism of ceftriaxone induction of excitatory amino acid transporter-2 expression and glutamate uptake in primary human astrocytes. J Biol Chem 283:13116–13123. https://doi.org/10.1074/jbc.M707697200
214. Sepulveda MR, Dresselaers T, Vangheluwe P, et al (2012) Evaluation of manganese uptake and toxicity in mouse brain during continuous MnCl2 administration using osmotic pumps. Contrast Media Mol Imaging 7:426–434. https://doi.org/10.1002/cmmi.1469
215. Ye Q, Kim J (2015) Effect of olfactory manganese exposure on anxiety-related behavior in a mouse model of iron overload hemochromatosis. Environ Toxicol Pharmacol 40:333–341. https://doi.org/10.1016/j.etap.2015.06.016
216. Ortega A, Eshhar N, Teichberg VI (1991) Properties of kainate receptor/channels on cultured Bergmann glia. Neuroscience 41:335–349
217. Ruiz M, Ortega A (1995) Characterization of an Na(+)-dependent glutamate/aspartate transporter from cultured Bergmann glia. Neuroreport 6:2041–2044
218. Bradford MM (1976) A rapid and sensitive method for the quantitation of microgram quantities of protein utilizing the principle of protein-dye binding. Anal Biochem 72:248–254. https://doi.org/10.1006/abio.1976.9999
219. Mendez-Flores OG, Hernández-Kelly LC, Suárez-Pozos E, et al (2016) Coupling of glutamate and glucose uptake in cultured Bergmann glial cells. Neurochem Int 98:72–81. https://doi.org/10.1016/j.neuint.2016.05.001
220. Lee E-SY, Yin Z, Milatovic D, et al (2009) Estrogen and tamoxifen protect against Mn-induced toxicity in rat cortical primary cultures of neurons and astrocytes. Toxicol Sci 110:156–167. https://doi.org/10.1093/toxsci/kfp081
221. Malthankar G V, White BK, Bhushan A, et al (2004) Differential lowering by manganese treatment of activities of glycolytic and tricarboxylic acid (TCA) cycle enzymes investigated in neuroblastoma and astrocytoma cells is associated with manganese-induced cell death. Neurochem Res 29:709–717
222. Kim J, Pajarillo E, Rizor A, et al (2019) LRRK2 kinase plays a critical role in manganese-induced inflammation and apoptosis in microglia. PLoS One 14:e0210248. https://doi.org/10.1371/journal.pone.0210248
223. Gandhi D, Sivanesan S, Kannan K (2018) Manganese-Induced Neurotoxicity and Alterations in Gene Expression in Human Neuroblastoma SH-SY5Y Cells. Biol

Trace Elem Res 183:245–253. https://doi.org/10.1007/s12011-017-1153-5

224. Sepúlveda MR, Dresselaers T, Vangheluwe P, Everaerts W (2012) Evaluation of manganese uptake and toxicity in mouse brain during continuous MnCl 2 administration using osmotic pumps. https://doi.org/10.1002/cmmi.1469
225. Ye Q, Kim J (2015) Effect of olfactory manganese exposure on anxiety-related behavior in a mouse model of iron overload hemochromatosis. Environ Toxicol Pharmacol 40:333–341. https://doi.org/10.1016/j.etap.2015.06.016
226. Karki P, Smith K, Johnson J, et al (2014) Role of transcription factor yin yang 1 in manganese-induced reduction of astrocytic glutamate transporters: Putative mechanism for manganese-induced neurotoxicity. Neurochem Int 88:53–59. https://doi.org/10.1016/j.neuint.2014.08.002
227. Martínez-Lozada Z, Hernández-Kelly LC, Aguilera J, et al (2011) Signaling through EAAT-1/GLAST in cultured Bergmann glia cells. Neurochem Int 59:871–879. https://doi.org/10.1016/j.neuint.2011.07.015
228. Martinez D, Garcia L, Aguilera J, Ortega A (2014) An acute glutamate exposure induces long-term down regulation of GLAST/EAAT1 uptake activity in cultured Bergmann glia cells. Neurochem Res 39:142–149. https://doi.org/10.1007/s11064-013-1198-6
229. Northrop DB (1998) On the Meaning of Km and V/K in Enzyme Kinetics. J Chem Educ 75:1153. https://doi.org/10.1021/ed075p1153
230. Bak LK, Schousboe A, Waagepetersen HS (2006) The glutamate/GABA-glutamine cycle: aspects of transport, neurotransmitter homeostasis and ammonia transfer. J Neurochem 98:641–653. https://doi.org/10.1111/j.1471-4159.2006.03913.x
231. Yu AC, Drejer J, Hertz L, Schousboe A (1983) Pyruvate carboxylase activity in primary cultures of astrocytes and neurons. J Neurochem 41:1484–1487. https://doi.org/10.1111/j.1471-4159.1983.tb00849.x
232. Danbolt NC (2001) Glutamate uptake. Prog Neurobiol 65:1–105
233. Hertz L, Zielke HR (2004) Astrocytic control of glutamatergic activity: astrocytes as stars of the show. Trends Neurosci 27:735–743. https://doi.org/10.1016/j.tins.2004.10.008
234. Erikson KM, Dorman DC, Fitsanakis V, et al (2006) Alterations of oxidative stress biomarkers due to in utero and neonatal exposures of airborne manganese. Biol Trace Elem Res 111:199–215. https://doi.org/10.1385/BTER:111:1:199
235. Shank RP, Bennett GS, Freytag SO, Campbell GL (1985) Pyruvate carboxylase: an astrocyte-specific enzyme implicated in the replenishment of amino acid neurotransmitter pools. Brain Res 329:364–367. https://doi.org/10.1016/0006-8993(85)90552-9
236. Zwingmann C, Leibfritz D, Hazell AS (2003) Energy metabolism in astrocytes and neurons treated with manganese: relation among cell-specific energy failure, glucose metabolism, and intercellular trafficking using multinuclear NMR-spectroscopic analysis. J Cereb Blood Flow Metab 23:756–771. https://doi.org/10.1097/01.WCB.0000056062.25434.4D
237. Johnson J, Pajarillo E, Karki P, et al (2018) Valproic acid attenuates manganese-induced reduction in expression of GLT-1 and GLAST with concomitant changes in murine dopaminergic neurotoxicity. Neurotoxicology 67:112–120. https://doi.org/10.1016/j.neuro.2018.05.001
238. Karki P, Webb A, Smith K, et al (2014) Yin Yang 1 is a repressor of glutamate

transporter EAAT2, and it mediates manganese-induced decrease of EAAT2 expression in astrocytes. Mol Cell Biol 34:1280–1289. https://doi.org/10.1128/MCB.01176-13

239. Karki P, Lee E, Aschner M (2013) Manganese Neurotoxicity: a Focus on Glutamate Transporters. Ann Occup Environ Med 25:4. https://doi.org/10.1186/2052-4374-25-4
240. Erikson K, Aschner M (2002) Manganese causes differential regulation of glutamate transporter (GLAST) taurine transporter and metallothionein in cultured rat astrocytes. In: NeuroToxicology. pp 595–602
241. Wong PC, Cai H, Borchelt DR, Price DL (2002) Genetically engineered mouse models of neurodegenerative diseases. Nat Neurosci 5:633–639. https://doi.org/10.1038/nn0702-633
242. Storck T, Schulte S, Hofmann K, Stoffel W (1992) Structure, expression, and functional analysis of a Na(+)-dependent glutamate/aspartate transporter from rat brain. Proc Natl Acad Sci U S A 89:10955–10959. https://doi.org/10.1073/pnas.89.22.10955
243. Jenkitkasemwong S, Akinyode A, Paulus E, et al (2018) SLC39A14 deficiency alters manganese homeostasis and excretion resulting in brain manganese accumulation and motor deficits in mice. Proc Natl Acad Sci U S A 115:E1769–E1778. https://doi.org/10.1073/pnas.1720739115
244. Hernández RB, Farina M, Espósito BP, et al (2011) Mechanisms of manganese-induced neurotoxicity in primary neuronal cultures: the role of manganese speciation and cell type. Toxicol Sci 124:414–423. https://doi.org/10.1093/toxsci/kfr234
245. Somogyi P, Tamás G, Lujan R, Buhl EH (1998) Salient features of synaptic organisation in the cerebral cortex. Brain Res Brain Res Rev 26:113–35
246. Buffo A, Rossi F (2013) Origin, lineage and function of cerebellar glia. Prog Neurobiol 109:42–63. https://doi.org/10.1016/j.pneurobio.2013.08.001
247. Gegelashvili G, Civenni G, Racagni G, et al (1996) Glutamate receptor agonists up-regulate glutamate transporter GLAST in astrocytes. Neuroreport 8:261–265
248. Bernabe A, Mendez JA, Hernandez-Kelly LCR, Ortega A (2003) Regulation of the Na+-dependent glutamate/aspartate transporter in rodent cerebellar astrocytes. Neurochem Res 28:1843–1849
249. Ramirez-Sotelo G, Lopez-Bayghen E, Hernandez-Kelly LCR, et al (2007) Regulation of the mouse Na+-dependent glutamate/aspartate transporter GLAST: putative role of an AP-1 DNA binding site. Neurochem Res 32:73–80. https://doi.org/10.1007/s11064-006-9227-3
250. Martinez-Lozada Z, Ortega A (2015) Glutamatergic Transmission: A Matter of Three. Neural Plast 2015:787396. https://doi.org/10.1155/2015/787396
251. Sorg O, Horn TF, Yu N, et al (1997) Inhibition of astrocyte glutamate uptake by reactive oxygen species: role of antioxidant enzymes. Mol Med 3:431–440
252. Su Z, Leszczyniecka M, Kang D, et al (2003) Insights into glutamate transport regulation in human astrocytes: cloning of the promoter for excitatory amino acid transporter 2 (EAAT2). Proc Natl Acad Sci U S A 100:1955–1960. https://doi.org/10.1073/pnas.0136555100
253. Bowman AB, Aschner M (2014) Considerations on manganese (Mn) treatments for in vitro studies. Neurotoxicology 41:141–142. https://doi.org/10.1016/j.neuro.2014.01.010

254. Northrop DB (1999) Rethinking fundamentals of enzyme action. Adv Enzymol Relat Areas Mol Biol 73:25–55, ix
255. Hazell AS, Norenberg MD (1997) Manganese decreases glutamate uptake in cultured astrocytes. Neurochem Res 22:1443–1447. https://doi.org/10.1023/A:1021994126329
256. Zorumski CF, Mennerick S, Que J (1996) Modulation of excitatory synaptic transmission by low concentrations of glutamate in cultured rat hippocampal neurons. J Physiol 494 (Pt 2):465–477. https://doi.org/10.1113/jphysiol.1996.sp021506
257. Mathiisen TM, Lehre KP, Danbolt NC, Ottersen OP (2010) The perivascular astroglial sheath provides a complete covering of the brain microvessels: an electron microscopic 3D reconstruction. Glia 58:1094–1103. https://doi.org/10.1002/glia.20990
258. Bélanger M, Allaman I, Magistretti PJ (2011) Brain energy metabolism: focus on astrocyte-neuron metabolic cooperation. Cell Metab 14:724–738. https://doi.org/10.1016/j.cmet.2011.08.016
259. Howarth C (2014) The contribution of astrocytes to the regulation of cerebral blood flow. Front Neurosci 8:103. https://doi.org/10.3389/fnins.2014.00103
260. Zonta M, Angulo MC, Gobbo S, et al (2003) Neuron-to-astrocyte signaling is central to the dynamic control of brain microcirculation. Nat Neurosci 6:43–50. https://doi.org/10.1038/nn980
261. Takano T, Tian G-F, Peng W, et al (2006) Astrocyte-mediated control of cerebral blood flow. Nat Neurosci 9:260–267. https://doi.org/10.1038/nn1623
262. Attwell D, Buchan AM, Charpak S, et al (2010) Glial and neuronal control of brain blood flow. Nature 468:232–243. https://doi.org/10.1038/nature09613
263. Zielke HR, Zielke CL, Baab PJ (2009) Direct measurement of oxidative metabolism in the living brain by microdialysis: a review. J Neurochem 109 Suppl 1:24–29. https://doi.org/10.1111/j.1471-4159.2009.05941.x
264. van Hall G, Strømstad M, Rasmussen P, et al (2009) Blood lactate is an important energy source for the human brain. J Cereb Blood Flow Metab 29:1121–1129. https://doi.org/10.1038/jcbfm.2009.35
265. Patel AB, Lai JCK, Chowdhury GMI, et al (2014) Direct evidence for activity-dependent glucose phosphorylation in neurons with implications for the astrocyte-to-neuron lactate shuttle. Proc Natl Acad Sci U S A 111:5385–5390. https://doi.org/10.1073/pnas.1403576111
266. Magistretti PJ, Allaman I (2015) A cellular perspective on brain energy metabolism and functional imaging. Neuron 86:883–901. https://doi.org/10.1016/j.neuron.2015.03.035
267. Camandola S, Mattson MP (2017) Brain metabolism in health, aging, and neurodegeneration. EMBO J 36:1474–1492. https://doi.org/10.15252/embj.201695810
268. Liu B, Teschemacher AG, Kasparov S (2017) Neuroprotective potential of astroglia. J Neurosci Res 95:2126–2139. https://doi.org/10.1002/jnr.24140
269. Mocchegiani E, Bertoni-Freddari C, Marcellini F, Malavolta M (2005) Brain, aging and neurodegeneration: role of zinc ion availability. Prog Neurobiol 75:367–390. https://doi.org/10.1016/j.pneurobio.2005.04.005
270. Levenson CW, Tassabehji NM (2007) Role and Regulation of Copper and Zinc

Transport Proteins in the Central Nervous System BT - Handbook of Neurochemistry and Molecular Neurobiology: Neural Membranes and Transport. In: Lajtha A, Reith MEA (eds). Springer US, Boston, MA, pp 257–284

271. Paoletti P, Vergnano AM, Barbour B, Casado M (2009) Zinc at glutamatergic synapses. Neuroscience 158:126–136. https://doi.org/10.1016/j.neuroscience.2008.01.061
272. Sensi SL, Paoletti P, Bush AI, Sekler I (2009) Zinc in the physiology and pathology of the CNS. Nat Rev Neurosci 10:780–791. https://doi.org/10.1038/nrn2734
273. Karol N, Brodski C, Bibi Y, et al (2010) Zinc homeostatic proteins in the CNS are regulated by crosstalk between extracellular and intracellular zinc. J Cell Physiol 224:567–574. https://doi.org/10.1002/jcp.22168
274. Lee J-Y, Cho E, Seo J-W, et al (2012) Alteration of the cerebral zinc pool in a mouse model of Alzheimer disease. J Neuropathol Exp Neurol 71:211–222. https://doi.org/10.1097/NEN.0b013e3182417387
275. Takeda A, Tamano H (2012) Proposed glucocorticoid-mediated zinc signaling in the hippocampus. Metallomics 4:614–618. https://doi.org/10.1039/c2mt20018j
276. Bock CW, Katz AK, Markham GD, Glusker JP (1999) Manganese as a Replacement for Magnesium and Zinc: Functional Comparison of the Divalent Ions. J Am Chem Soc 121:7360–7372. https://doi.org/10.1021/ja9906960
277. Miyazaki T, Yamasaki M, Hashimoto K, et al (2017) Glutamate transporter GLAST controls synaptic wrapping by Bergmann glia and ensures proper wiring of Purkinje cells. Proc Natl Acad Sci 114:7438–7443. https://doi.org/10.1073/pnas.1617330114

ANEXOS

1. Samantha A. Spencer, Edna Suárez-Pozos, **Miguel Escalante**, Yu Par Myo and Babette Fuss. 2020. “Sodium–Calcium Exchangers of the SLC8 Family in Oligodendrocytes: Functional Properties in Health and Disease”. Neurochemical Research, doi:10.1007/s11064-019-02949-4.

2. Elizabeth J. Thomason, **Miguel Escalante**, Donna J. Osterhout, and Babette Fuss. 2019. “The Oligodendrocyte Growth Cone and Its Actin Cytoskeleton: A Fundamental Element for Progenitor Cell Migration and CNS Myelination”. Glia, doi:10.1002/glia.23735.

3. **Miguel Escalante**, Jazmín Soto-Verdugo, Luisa C. Hernández-Kelly, Dinorah Hernández-Melchor, Esther López-Bayghen, Tatiana N. Olivares-Bañuelos, and Arturo Ortega. 2019. “GLAST Activity Is Modified by Acute Manganese Exposure in Bergmann Glial Cells”. Neurochemical Research, doi:10.1007/s11064-019-02848-8.

4. Reynaldo Tiburcio-Félix, **Miguel Escalante-López**, Bruno López-Bayghen, Daniel Martínez, Luisa C. Hernández-Kelly, Samuel Zinker, Dinorah Hernández-Melchor, Esther López-Bayghen, Tatiana N. Olivares-Bañuelos, and Arturo Ortega. 2018. “Glutamate-Dependent Translational Control of Glutamine Synthetase in Bergmann Glia Cells”. Molecular Neurobiology 55 (6): 5202–9. doi:10.1007/s12035-017-0756-3.

Neurochemical Research
https://doi.org/10.1007/s11064-019-02949-4

ORIGINAL PAPER

Sodium–Calcium Exchangers of the SLC8 Family in Oligodendrocytes: Functional Properties in Health and Disease

Samantha A. Spencer[1] · Edna Suárez-Pozos[1] · Miguel Escalante[1,2] · Yu Par Myo[1] · Babette Fuss[1]

Received: 2 November 2019 / Revised: 20 December 2019 / Accepted: 23 December 2019

Abstract

The solute carrier 8 (SLC8) family of sodium–calcium exchangers (NCXs) functions as an essential regulatory system that couples opposite fluxes of sodium and calcium ions across plasmalemmal membranes. NCXs, thereby, play key roles in maintaining an ion homeostasis that preserves cellular integrity. Hence, alterations in NCX expression and regulation have been found to lead to ionic imbalances that are often associated with intracellular calcium overload and cell death. On the other hand, intracellular calcium has been identified as a key driver for a multitude of downstream signaling events that are crucial for proper functioning of biological systems, thus highlighting the need for a tightly controlled balance. In the CNS, NCXs have been primarily characterized in the context of synaptic transmission and ischemic brain damage. However, a much broader picture is emerging. NCXs are expressed by virtually all cells of the CNS including oligodendrocytes (OLGs), the cells that generate the myelin sheath. With a growing appreciation of dynamic calcium signals in OLGs, NCXs are becoming increasingly recognized for their crucial roles in shaping OLG function under both physiological and pathophysiological conditions. In order to provide a current update, this review focuses on the importance of NCXs in cells of the OLG lineage. More specifically, it provides a brief introduction into plasmalemmal NCXs and their modes of activity, and it discusses the roles of OLG expressed NCXs in regulating CNS myelination and in contributing to CNS pathologies associated with detrimental effects on OLG lineage cells.

Keywords Oligodendrocyte · Myelin · Sodium–calcium exchangers · Ion homeostasis · Signaling

Introduction

Signaling mediated by the divalent cation calcium is of critical importance for proper functioning of the central nervous system (CNS) [1]. More precisely, spatially and temporally well-coordinated dynamics of intracellular calcium signals act on diverse downstream targets. They, thereby, engage in a multitude of functions ranging from cellular metabolism and gene expression to cell migration and differentiation in both CNS neurons [2–4] and CNS glial cells, i.e. astrocytes [5, 6], microglia [7, 8], and oligodendrocytes (OLGs) [9–13]. On the other hand, abnormalities in calcium signaling are thought to underlie many different neurological and neurodegenerative diseases [14–19]. Thus, there is a critical need for maintaining a well-balanced calcium homeostasis to ensure faultless CNS function. This need is addressed by molecular players that control the movement of calcium ions across membranes and are represented by numerous types of calcium channels and transporters, including the solute carrier 8 (SLC8) family of sodium–calcium exchangers (NCXs).

Historically, the phenomenon of sodium–calcium exchange across the plasma membrane was first described to occur in squid axons and the mammalian heart but it has since been recognized to apply to most mammalian cell types [20–24]. In the CNS, the activity of NCXs has probably been best characterized as a counter transport system

Special Issue: In honor of Professor Michael Robinson.

Samantha A. Spencer and Edna Suárez-Pozos have contributed equally to this manuscript.

✉ Babette Fuss
Babette.Fuss@vcuhealth.org

[1] Department of Anatomy and Neurobiology, Virginia Commonwealth University School of Medicine, Box 980709, Richmond, VA 23298, USA

[2] Departamento de Toxicología, Centro de Investigación y de Estudios Avanzados del Instituto Politécnico Nacional, Ciudad de México, Mexico

Published online: 11 January 2020

that is present in astrocytes and neurons, where it plays important physiological roles by regulating synaptic transmission and plasticity [6, 25–29]. Under pathophysiological conditions, changes in the expression and function of NCXs in astrocytes, neurons and microglia have been associated with neurodegeneration and neuroinflammation [30–36]. Thus, NCXs are increasingly recognized as a critical regulatory system controlling CNS function. Despite a growing knowledge base, however, the roles of NCXs in glial cells belonging to the oligodendrocyte (OLG) lineage are only starting to emerge.

This review is focused on providing an update on the current knowledge on plasmalemmal NCXs in OLGs, the myelinating cells of the CNS. In more detail, it presents a brief overview on the role of plasmalemmal NCXs in maintaining calcium and sodium homeostasis. In addition, it provides a detailed discussion on the functional involvement of OLG expressed NCXs in regulating OLG differentiation and myelination, and in contributing to the pathophysiology in a variety of CNS diseases affecting cells of the OLG lineage.

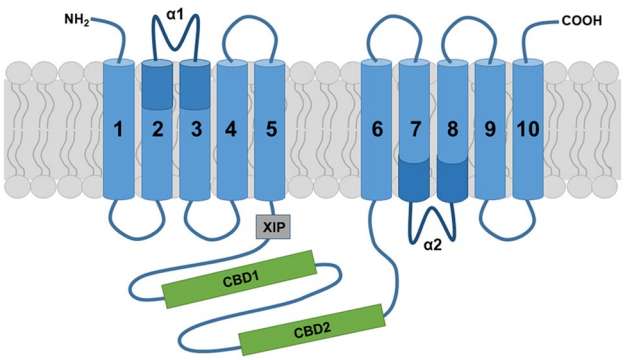

Fig. 1 Topology model for sodium calcium exchangers of the SLCA8 family. The current model for NCX topology proposes five transmembrane helices in both the first and second hydrophobic cluster. The two conserved α-repeats (α1 and α2) contain ion-coordinating amino acid residues that are involved in ion transport activities. The cytosolic f-loop encompasses the two calcium binding domains CBD1 and CBD2, and the eXchanger Inhibitory Peptide (XIP) site, which is present in NCX1 and NCX3 and has been implicated in sodium-dependent inactivation

Sodium–Calcium Exchangers of the SLC8 Family: A Brief Overview

The SLC8 family of NCXs represents one branch of the much larger calcium-cation antiporter (CaCA) superfamily. Collectively, CaCA family members play critical roles in regulating cellular calcium homeostasis by facilitating the efflux of calcium against its electrochemical gradient and in counter exchange for other cations. In the case of NCXs, one calcium ion is counter exchanged by three sodium ions [37–40]. In mammals, NCXs are encoded by three *SLC8* genes: *SLC8A1* (NCX1) [41], *SLC8A2* (NCX2) [42], and *SLC8A3* (NCX3) [43]. Interestingly, a fourth family member, NCX4 encoded by *SLC8A4,* has been found present in teleost, amphibian, and reptilian species; in mammals and birds, however, it has secondarily and independently been lost [44–46]. Recent evidence further suggests that the long-wanted mitochondrial sodium–calcium exchanger is encoded by the *SLC8B1* gene giving rise to the protein product NCLX [47–49]. This review is focused on the three mammalian *SLC8A*-derived NCXs, for which in the following the NCX nomenclature will be used for both genes and proteins, and uppercase letters will be used independent of the referenced species.

The three distinct mammalian NCXs share a highly conserved overall structure and characteristic transport functions [50]. More specifically, current structural models predict that mammalian NCXs are composed of ten transmembrane helices (TM1-10) and a long cytosolic f-loop positioned between TM5 and TM6 (Fig. 1) [51]. The transmembrane helices are arranged in two pseudo-symmetrical halves (TM1-5 and TM6-10), which form a tightly packed core domain. Notably, TM2-3 and TM7-8 contain two highly conserved homologous sequence motifs, the α1 and α2-repeat; these α repeats form a pocket, including twelve ion-coordinating residues (four in TM2 and TM7, and two in TM3 and TM8) and four ion binding sites, that is responsible for ion recognition and translocation [51–54]. This structure and the presence of two distinct passageways for separate access of sodium and calcium ions to their respective central binding sites [51–54] allows an alternating-access model of secondary active transport; in other words, they allow consecutive exposure of ligand binding domains at opposite sides of the membrane and, upon each ion-binding event, a conversion between two major conformational states, an inward-facing and an outward-facing state [55, 56]. The directionality of NCX-mediated ion exchange is reversible and depends on the relative concentrations of calcium and sodium ions as well as the membrane potential. Thus, NCXs can operate in a forward (calcium efflux) and reverse (calcium influx) mode both of which are thought to exert important physiological functions [20, 57]. NCX activity is regulated through a tandem of calcium-binding domains, CBD1 and CBD2, which are located within the cytosolic f-loop [58–62]. The CBD1 domain functions as the primary high-affinity allosteric calcium sensor [63, 64], while the CBD2 domain of NCX1 and NCX3 (but not NCX2) is subject to alternative splicing, thereby conferring different kinetic properties to individual NCX splice variants [61, 65–69]. Based on these features, increased intracellular calcium levels activate the forward mode, while the reverse mode is favored in the presence of increased intracellular sodium concentrations and a positive membrane potential [20]. In addition, increased

cytosolic sodium levels have been shown to transiently inactivate NCX1 and NCX3 (but not NCX2) via interaction of sodium with a site that is located outside of the CBD domains and has been referred to as the eXchanger Inhibitory Peptide (XIP) autoinhibitory region [47, 63, 66, 70, 71]. Such inactivation can prevent entry of a toxic amount of calcium through reverse mode operation. Interestingly, sodium-mediated inactivation can be relieved by calcium-binding to CBD2 splice variants containing one of the mutually exclusive alternatively spliced exons, namely exon A in NCX1 and exon B in NCX3; these splice variants are expressed preferentially in excitable cells [44, 61, 66, 70, 72–74]. From a functional point of view, it is notable that isoforms and splice variants such as NCX2 and NCX3-AC, which exhibit low sensitivity to sodium-dependent inactivation, are capable to retain forward mode activity even during high amplitude and prolonged sodium transients [75, 76]. Apart from calcium and sodium, NCX activity has been found to be regulated allosterically by non-transported ion species (protons and other monovalent cations), phosphatidylinositol bisphosphate and other acidic phospholipids, and an interacting fatty-acid binding protein referred to as soluble cytosolic regulatory protein (SCRP) or regulatory protein of the squid nerve sodium calcium exchanger (ReP1-NCXSQ) [77–79].

Due to their different regulatory properties, one mechanism of tissue- and/or cell type-specific calcium homeostasis can be achieved by the differential expression of specific *NCX* genes and, in the case of *NCX1* and *NCX3*, their individual splice variants [57, 75, 80–82]. In this context, NCX2 and NCX3 are present primarily in brain and skeletal muscle, whereas NCX1 is found more universally distributed [41–43, 83, 84]. Cardiac and skeletal muscle cells express predominantly one *NCX* isoform/splice variant while several isoform/splice variants coexist in neurons and glial cells, possibly allowing, especially in the latter, a parallel increase in both calcium and sodium ions [75, 83]. Hence, calcium and sodium signaling can be tightly linked through the activities of NCXs, a phenomenon that has been best characterized for astrocytes and their regulatory roles in synaptic transmission [6, 26, 75, 85]. Furthermore, different tissues, i.e. heart, kidney and brain, have been found to express *NCX1* via three alternate promoters, resulting in independent transcriptional regulation in the absence of changes in protein structure or function [86–89]. In this context, the brain *NCX1* promoter represents a ubiquitous GC-rich TATA-less promoter that gives rise to the majority of the *NCX1* transcripts found in the brain, possibly through binding at its AP-2 binding site, but it is also active elsewhere [86].

Taken together, plasmalemmal NCXs function as unique transporter systems that control intracellular calcium homeostasis and that can directly couple the transfer of calcium and sodium ions across membranes. Cell- and tissue-specific characteristics of calcium–sodium exchange are achieved through the different regulatory properties of the individual NCXs and their alternatively spliced variants as well as through specific *NCX1* promoter use. Hence, NCXs critically contribute to the tight control of calcium and sodium signaling events that is necessary to maintain physiological conditions within the CNS [6, 75, 90].

Sodium–Calcium Exchangers in Oligodendrocytes

Oligodendrocytes (OLGs) are specialized cells of the CNS that generate the axon enwrapping myelin sheath, which enables rapid and efficient saltatory conduction and provides metabolic axonal support [91]. During development, cells of the OLG lineage originate as bipolar and migratory OLG progenitor cells (OPCs), which undergo a stepwise lineage progression by maturing first into premyelinating immature OLGs that extend a complex process network and then into mature OLGs that produce and maintain the myelin sheath [92, 93]. Next to extensive alterations in morphology, precisely regulated changes in gene expression patterns mark each of the individual stages of the OLG lineage [94–97].

The first characterization of NCXs in cells of the OLG lineage dates back to a study published by Quednau et al. [83], which revealed, using reverse transcriptase-polymerase chain reaction (RT-PCR), that all three mammalian genes are expressed in primary cultures of differentiating OLGs. Regarding the presence of alternatively spliced variants, both exon A and B containing mRNA transcripts were detected for *NCX1* but only exon B containing ones were found for *NCX3*. Subsequent investigations confirmed these results but they also suggested that while *NCX2* is the most highly expressed *NCX* gene in the brain (except the brain stem), its levels may be relatively low in OLGs [98, 99]. When assessing the distribution of NCX1 on myelinated axons in vivo in the adult rodent CNS, positive results were obtained for the optic nerve and spinal cord but not the corpus callosum, hence indicating regional heterogeneity pertaining the expression of the different *NCX* genes in mature OLGs [100]. Markedly, a developmental switch in *NCX* gene expression was observed in primary cultures of cortical OLG lineage cells in which *NCX1* was found to be expressed predominantly at the progenitor stage while *NCX3* expression was seen upregulated once cells started to differentiate [101, 102]. Consistent with the view that NCX3 represents the main contributor to sodium–calcium exchange in cortical OLGs, *NCX3*-targeted gene silencing was found to reduce overall NCX activity (forward and reverse mode) by about 80% [101]. Given the expression of *NCX1* in the adult optic nerve and spinal cord, it appears, however, that the developmental downregulation of *NCX1* may be specific to cortical

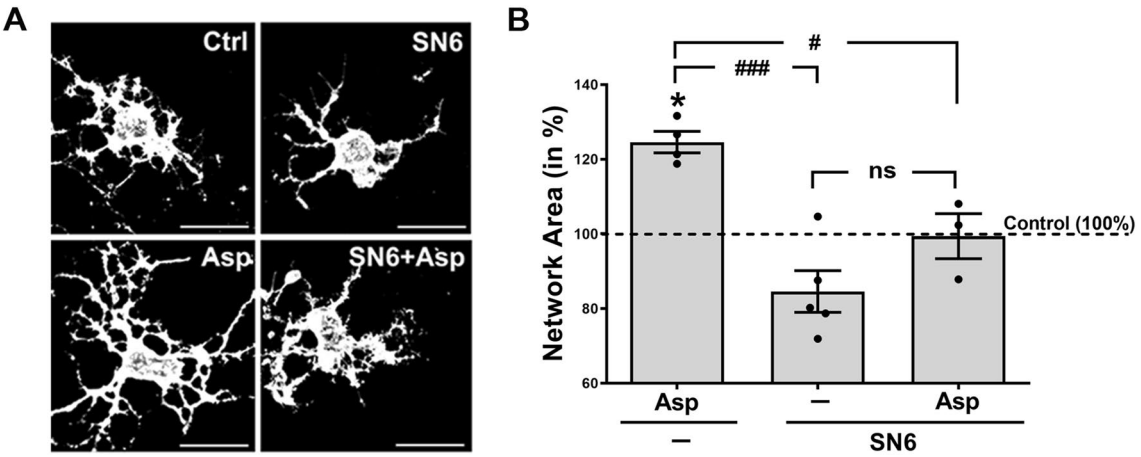

Fig. 2 Inhibition of the reverse mode of Na^+/Ca^{2+} exchange attenuates glutamate transporter stimulated morphological maturation of oligodendrocytes. Cells were treated for 6 h as indicated. Asp (D-Asp, 100 µM), SN6 (a selective inhibitor of Na^+/Ca^{2+} exchange (reverse mode), 10 µM). **a** Representative images of differentiating oligodendrocytes after immunostaining with O4 hybridoma supernatants. Scale bars: 20 µm. **b** Graph depicting network areas. The mean values for control (non-treated) cells were set to 100% (dotted horizonal line) and experimental values were calculated accordingly. Dots represent individual experiments, horizontal lines indicate means, error bars are depicted as SEM. $^{*}p \leq 0.05$ (compared to control; one sample *t* test); $^{\#}p \leq 0.05$, $^{\#\#\#}p \leq 0.001$, ^{ns}not significant (ANOVA, Tukey's multiple comparison test)

OLG lineage cells and aimed at generating regional differences in the characteristics of sodium–calcium exchange within differentiating and mature OLGs.

Functionally, it has been proposed that NCX1 activity in OPCs contributes to the regulation of OPC migration, possibly via a mechanism that is induced by signaling through gamma-aminobutyric acid (GABA) receptors and subsequent elevation in intracellular sodium levels triggering calcium influx (and compensatory sodium efflux) through reverse operation of the exchanger (Fig. 3a) [99]. This pathway has been characterized in OPCs using hippocampal slices [99], and calcium signaling has been shown to contribute to the regulation of OPC migration [9, 11, 103, 104]. However, GABA-stimulated OPC migration events have not yet been assessed in detail in vivo [105], and they may be specific to OPCs leaving the postnatal subventricular zone (SVZ) [99].

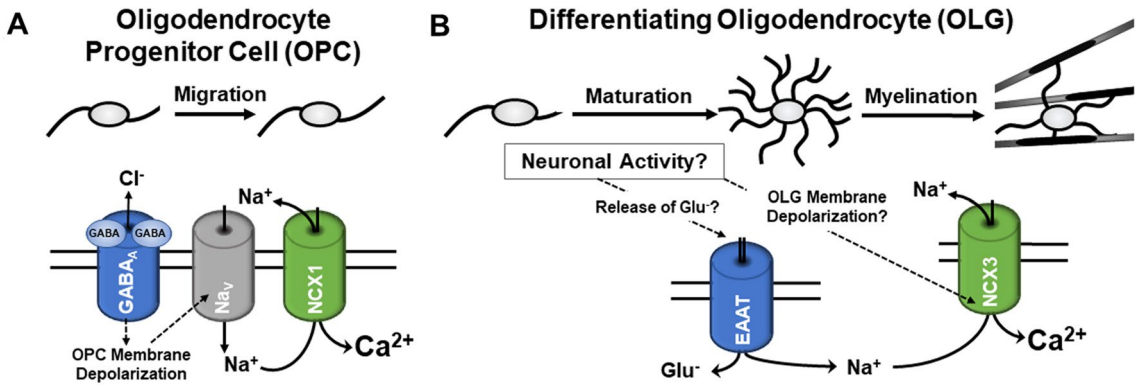

Fig. 3 Proposed physiological roles of NCX activities in cells of the OLG lineage. **a** For OPCs located in the postnatal subventricular zone (SVZ), activation of $GABA_A$ receptors has been reported to induce a chemotactic migration response that is mediated by calcium influx via reverse mode NCX1 activity triggered by sodium influx through non-inactivating sodium channels (Na_v) after GABA-induced membrane depolarization [99]. **b** For differentiating and myelinating OLGs, a differentiation promoting role emerges for NCX3 [101, 102]. Thus far, two neuronal activity-induced pathways have been proposed. First, OLG membrane depolarization-induced reverse mode NCX activity has been implicated in promoting the syntheses of the myelin protein myelin basic protein (MBP) and the process of active myelination [106, 107]. Second, activation of sodium-dependent glutamate transporters (EAAT), presumably through glutamate release from electrically active axons, was found to promote the morphological maturation of differentiating OLGs by a molecular mechanism involving reverse mode NCX activity and an increase in intracellular calcium concentration (Fig. 2) [109, 110]

In differentiating and myelinating OLGs, NCX3 activity has been implicated in promoting OLG maturation [101, 102] and the onset of local synthesis of *myelin basic protein* (*MBP*) [106]. As an underlying mechanism for the latter, it has been proposed that neuronal activity, presumably through an increase in extracellular potassium concentration, leads to local increases in intracellular sodium levels and changes in membrane potential; these changes drive an influx of calcium via reverse mode NCX3 activity, thereby triggering the onset local *MBP* translation in the vicinity of electrically active axons [106, 107]. Consistent with a prominent role of NCX3 in regulating the appearance of myelin proteins, protein levels for MBP and 2′,3′-cyclic-nucleotide 3′-phosphodiesterase (CNP) were found to be reduced in the spinal cords of *NCX3* knockout mice [101]. It is of note that the CNS myelin mRNA pool has recently been found to be much larger than previously recognized [108]. Specifically, it was found to include mRNAs, such as *PLP1* and *CNP,* which have traditionally been associated with a localization solely to the OLG soma. These findings suggest that locally regulated translation may affect a broader range of myelin-related transcripts, thus providing a new level of complexity to the regulation of myelination in general and via the activity of NCXs.

In our own studies, we identified a signaling mechanism that promotes the morphological maturation of OLGs, i.e. process outgrowth and branching, via activation of OLG expressed sodium-dependent glutamate transporters and subsequent increase in intracellular calcium concentrations [109, 110]. Based on studies done in astrocytes, the observed influx in calcium was proposed to be mediated by reverse mode NCX activity [109, 111]. To address this hypothesis experimentally, primary cultures of differentiating OLGs were treated, prior to stimulating sodium-dependent glutamate transporters via application of D-aspartate (D-Asp), with the selective NCX inhibitor SN6 that blocks preferentially reverse mode operation [112, 113]. D-Asp was used in these experiments as glutamate-equivalent transporter substrate since it has been described to not stimulate non-NMDA ionotropic and metabotropic glutamate receptors [114, 115] and to not be metabolized by glutamine synthetase [116]. As shown in Fig. 2, D-Asp treatment increased process outgrowth and the OLG's process network area to an extent similar to the one reported previously [109]. Importantly, this effect could be effectively blocked by pre-incubation with SN6, thus demonstrating an activation of NCX reverse mode activity downstream of glutamate transporter activation. In support of in vivo relevance of this pathway, recent studies demonstrated that D-Asp treatment can stimulate in vivo remyelination by promoting OLG maturation via a pathway that involves, among others, the activation of glutamate transporters and the sodium–calcium exchanger NCX3 [117]. Considering that glutamate is released along at least a subset of unmyelinated and electrically active axons [118–120], the glutamate transporter–NCX pathway may, similar to the extracellular potassium-OLG membrane depolarization pathway [106, 107], contribute to the adaptive program of electrical activity-dependent myelination (Fig. 3b) [121–124]. Future studies are, however, needed to determine the in vivo contribution of either pathway to developmental myelination and myelin repair and to establish the extent of crosstalk and interaction, beyond an involvement of NCX reverse mode activity, between these two pathways.

Collectively, it becomes apparent that sodium–calcium exchange is critically involved in the regulation of various physiological processes related to CNS myelination. In OPCs, it is primarily NCX1 that is involved in controlling cell migration in vitro and possibly from the postnatal SVZ into the brain parenchyma. At more mature stages of the OLG lineage, NCX3 emerges as the primary *NCX* gene in OLGs in which sodium–calcium exchange has been implicated in signaling pathways promoting maturation. Remarkably, all these physiological roles have been shown mediated by well-controlled reverse mode NCX activities leading to calcium influx.

Potential Contributions of Oligodendrocyte-Expressed Sodium–Calcium Exchangers to CNS Disease

Premyelinating OLGs have been shown to be particularly vulnerable to hypoxic-ischemic injury, a process that has been implicated in brain injury in premature infants [125]. Interestingly, oxygen–glucose deprivation (OGD) as a model of ischemic damage was found to lead to a downregulation of *NCX3* expression in premyelinating OLGs; attenuation of this downregulation was shown to prevent calcium overload, an effect that was attributed to NCX3 forward mode operation (Fig. 4b), thereby improving OLG viability and maturation [126]. Similar observations were made under conditions of lead (Pb) poisoning, whereby Pb is thought to enhance the generation of reactive oxygen species, to reduce the antioxidant defense system of cells and to decrease the expression of calcium extrusion proteins [127, 128]. Thus, under conditions of hypoxic-ischemic injury and oxidative stress, NCX3 activity appears to exert protective functions by ameliorating injury to premyelinating OLGs. Such a beneficial role for NCX3 is supported by studies investigating ischemic preconditioning as a mechanism by which a brief non-injurious episode of ischemia protects the brain from a subsequent lethal insult. This protective effect has, at least in part, been attributed to an upregulation of NCX1 and NCX3 [30, 129, 130]. Interestingly, in addition to beneficial forward mode NCX activity, reverse mode operation

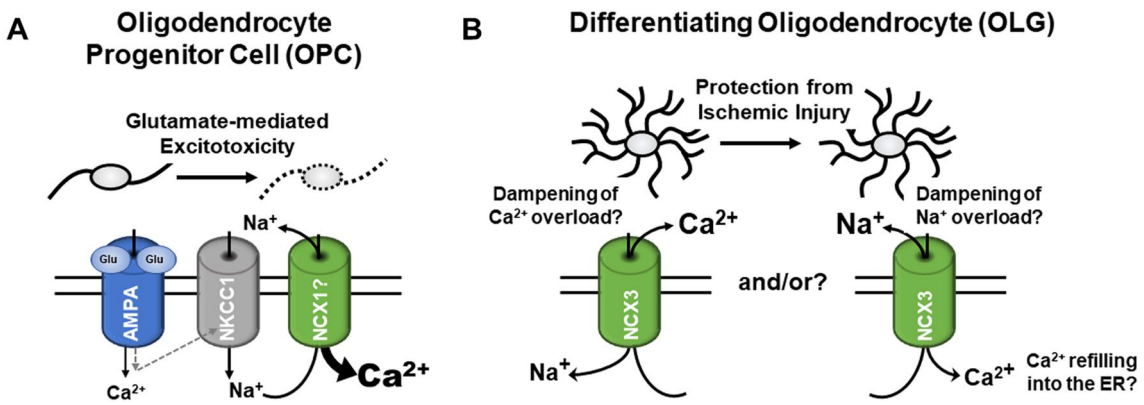

Fig. 4 Proposed pathophysiological roles of NCX activities in cells of the OLG lineage. **a** For OPCs, overactivation of AMPA receptors has been associated with glutamate-mediated excitotoxic injury; more specifically, a pathway involving the sodium–potassium-chloride co-transporter 1 (NKCC1) and the reverse mode of NCX activity has recently been described to lead to calcium overload and OPC injury upon prolonged AMPA receptor activation [132]. **b** For differentiating OLGs a protective role of NCX3 activity is emerging in the context of ischemic-hypoxic injury and oxidative stress; possible beneficial effects of both forward (left) [126] and reverse mode activity have been proposed [129, 131]

has been implicated in counteracting ischemia-induced injury processes by dampening intracellular sodium overload and promoting calcium refilling into the endoplasmic reticulum (Fig. 4b) [129, 131]. Undoubtedly, further research will be necessary to more precisely define the contributions of NCX activities to the pathology seen upon hypoxic-ischemic injury to the brain.

Somewhat different from the above proposed protective roles, reverse mode NCX activity has, during glutamate-mediated excitotoxicity, been proposed to trigger calcium overload and to thereby compromise mitochondrial function and OLG viability [132]. In OPCs, such pathological reverse mode NCX activity has been shown to be triggered by activation of AMPA (alpha-amino-3-hydroxy-5-methyl-4-isoxazolepropionic acid) receptors and subsequent sodium influx via the sodium–potassium-chloride co-transporter 1 (NKCC1) (Fig. 4a) [132]. Increased levels of glutamate, possibly triggering pathways of glutamate-mediated excitotoxicity, have been associated with OLG and myelin damage in a number of human CNS pathologies and their rodent animal models; these include the major demyelinating disease in human, Multiple Sclerosis (MS) [133–135], hypoxia/ischemia-mediated neonatal and adult white matter damage [136, 137], and spinal cord injury [75, 138, 139]. For human adult OLGs, however, it has been reported that the expression of AMPA receptor subunits is low and that they are resistant to excitotoxic injury [140]. On the other hand, AMPA receptor-mediated calcium signaling in rodents has been described to be transiently enhanced in perinatally-derived OPCs and immature OLGs [141, 142], thus pointing toward a developmental window of vulnerability in both rodents and humans that may be altered under inflammatory conditions associated with CNS injury.

The origin of cells for glioblastoma multiforme (GBM), the most lethal primary neoplasm in the CNS, has been proposed to be represented, next to neural stem cells, by OPCs [143]. Given the vulnerability of OPCs to reverse mode NCX activity-induced cell death (see above) and evidence for NCX expression by glioma cells [144, 145], selective blockade of the forward mode of NCX activity has, in analogy to studies done in other cancer cell types [146], been explored as a strategy to suppress GBM growth [147]. Remarkably, inhibition of forward mode NCX activity was found to suppress tumor growth of established glioma cell lines both in vitro and in vivo. Treatment of astrocytes under the same conditions was found to not affect cell viability, possibly due to differences in *NCX* gene expression patterns. Effects on other CNS cells, importantly neurons and cells of the OLG lineage, however, were not assessed in these studies.

In summary, alterations in NCX expression and/or activity in both the forward and reverse mode have been implicated in contributing to a variety of CNS pathologies. Currently, however, knowledge about the exact contributions of either mode of activity, individual NCX genes or alternatively spliced variants is limited, thus complicating the design of well-targeted therapeutic approaches.

Conclusions

Cells of the OLG lineage have been reported to express all three of the mammalian NCX genes. However, *NCX3* is beginning to emerge as the most prominent *NCX* gene in differentiating and mature OLGs, where it has been identified to play crucial roles in regulating OLG maturation

and myelin sheath formation [101, 102, 106, 107]. NCX1, on the other hand, appears to be primarily operative during OPC migration [99]. Despite an increasing awareness of NCX function in OLGs, knowledge still remains limited. For example, increasing evidence has revealed diversity and potential heterogeneity within the OLG lineage [148–151]. In this regard, NCX2 may be enriched in a subtype of mature OLGs possibly involved in synaptic activity [148]. Such potential regional differences, however, have not been investigated in detail. In addition, potential diversity in sodium–calcium exchanger kinetics, due to the expression of different *NCX* genes and/or splice variants, has not been fully explored. Notably, most of the functional roles of NCXs in OLGs have been associated with changes in intracellular calcium concentrations. In contrast, little is known about potential roles of intracellular sodium transients in OLGs, despite the known coupling of calcium and sodium ion fluxes and crosslinking between calcium and sodium signaling [75].

In addition, to their involvement in developmental processes, NCXs expressed by OLG lineage cells have been implicated in contributing to pathophysiological mechanisms under a number of neurological disorder conditions. Thus, characterizing NCX activity may provide insight into novel therapeutic approaches. Thus far, therapeutically targeting NCX activity has shown promise in patients with coronary heart disease [152]. In addition, NCXs have been proposed as druggable targets for the treatment of cerebral ischemia [31, 153] and brain tumors [147]. However, it is becoming increasingly clear that NCXs play diverse roles under various pathological conditions and compared to physiological processes. Thus, a deeper understanding of the functional roles of NCXs under both physiological and pathophysiological conditions as well as within the diverse cell types of the CNS, including OLGs, is needed to be able to specifically target individual CNS disease promoting processes involving NCXs.

Acknowledgements The authors are supported by Grants from the National Institute of Health (Grant No.: R01NS045883; BF), the National Multiple Sclerosis Society (Grant No.: RG-1506-04546; BF) and the Commonwealth Health Research Board (Grant No.: 236-04-17 BF).

Compliance with Ethical Standards

Conflict of interest The authors declare that they have no potential conflicts.

References

1. Kawamoto EM, Vivar C, Camandola S (2012) Physiology and pathology of calcium signaling in the brain. Front Pharmacol 3:61. https://doi.org/10.3389/fphar.2012.00061
2. Brini M, Calì T, Ottolini D, Carafoli E (2014) Neuronal calcium signaling: function and dysfunction. Cell Mol Life Sci 71:2787–2814. https://doi.org/10.1007/s00018-013-1550-7
3. Horigane S-I, Ozawa Y, Yamada H, Takemoto-Kimura S (2019) Calcium signalling: a key regulator of neuronal migration. J Biochem 165:401–409. https://doi.org/10.1093/jb/mvz012
4. Toth AB, Shum AK, Prakriya M (2016) Regulation of neurogenesis by calcium signaling. Cell Calcium 59:124–134. https://doi.org/10.1016/j.ceca.2016.02.011
5. Shigetomi E, Patel S, Khakh BS (2016) Probing the complexities of astrocyte calcium signaling. Trends Cell Biol 26:300–312. https://doi.org/10.1016/j.tcb.2016.01.003
6. Verkhratsky A, Untiet V, Rose CR (2019) Ionic signalling in astroglia beyond calcium. J Physiol. https://doi.org/10.1113/JP277478
7. Färber K, Kettenmann H (2006) Functional role of calcium signals for microglial function. Glia 54:656–665. https://doi.org/10.1002/glia.20412
8. Brawek B, Garaschuk O (2013) Microglial calcium signaling in the adult, aged and diseased brain. Cell Calcium 53:159–169. https://doi.org/10.1016/j.ceca.2012.12.003
9. Zhang M, Liu Y, Wu S, Zhao X (2019) Ca^{2+} Signaling in oligodendrocyte development. Cell Mol Neurobiol 39:1071–1080. https://doi.org/10.1007/s10571-019-00705-4
10. Pitman KA, Young KM (2016) Activity-dependent calcium signalling in oligodendrocyte generation. Int J Biochem Cell Biol 77:30–34. https://doi.org/10.1016/j.biocel.2016.05.018
11. Butt AM (2006) Neurotransmitter-mediated calcium signalling in oligodendrocyte physiology and pathology. Glia 54:666–675. https://doi.org/10.1002/glia.20424
12. Soliven B (2001) Calcium signalling in cells of oligodendroglial lineage. Microsc Res Tech 15:672–679
13. Cheli VT, Santiago González DA, Spreuer V, Paez PM (2015) Voltage-gated Ca++ entry promotes oligodendrocyte progenitor cell maturation and myelination in vitro. Exp Neurol 265:69–83. https://doi.org/10.1016/j.expneurol.2014.12.012
14. Burgoyne RD, Helassa N, McCue HV, Haynes LP (2019) Calcium sensors in neuronal function and dysfunction. Cold Spring Harb Perspect Biol. https://doi.org/10.1101/cshperspect.a035154
15. Schrank S, Barrington N, Stutzmann GE (2019) Calcium-handling defects and neurodegenerative disease. Cold Spring Harb Perspect Biol. https://doi.org/10.1101/cshperspect.a035212
16. Berridge MJ (2014) Calcium signalling and psychiatric disease: bipolar disorder and schizophrenia. Cell Tissue Res 357:477–492. https://doi.org/10.1007/s00441-014-1806-z
17. Shigetomi E, Saito K, Sano F, Koizumi S (2019) Aberrant CalciuASN Neuro m signals in reactive astrocytes: a key process in neurological disorders. Int J Mol Sci. https://doi.org/10.3390/ijms20040996
18. Verkhratsky A, Rodríguez-Arellano JJ, Parpura V, Zorec R (2017) Astroglial calcium signalling in Alzheimer's disease. Biochem Biophys Res Commun 483:1005–1012. https://doi.org/10.1016/j.bbrc.2016.08.088
19. Nedergaard M, Rodríguez JJ, Verkhratsky A (2010) Glial calcium and diseases of the nervous system. Cell Calcium 47:140–149. https://doi.org/10.1016/j.ceca.2009.11.010
20. Blaustein MP, Lederer WJ (1999) Sodium/calcium exchange: its physiological implications. Physiol Rev 79:763–854
21. DiPolo Reinaldo, Beauge L (1987) Plasma membrane mechanisms for intracellular calcium regulation in squid axons. Acta Physiol Pharmacol Latinoam 37:437–444
22. Khananshvili D (1990) Distinction between the two basic mechanisms of cation transport in the cardiac $Na(+)$-Ca^{2+} exchange system. Biochemistry 29:2437–2442. https://doi.org/10.1021/bi00462a001

23. Reeves JP, Condrescu M, Chernaya G, Gardner JP (1994) Na^+/Ca^{2+} antiport in the mammalian heart. J Exp Biol 196:375–388
24. Baker PF, Blaustein MP, Hodgkin AL, Steinhardt RA (1969) The influence of calcium on sodium efflux in squid axons. J Physiol 200:431–458. https://doi.org/10.1113/jphysiol.1969.sp008702
25. Reyes RC, Verkhratsky A, Parpura V (2012) Plasmalemmal Na^+/Ca^{2+} exchanger modulates Ca^{2+}-dependent exocytotic release of glutamate from rat cortical astrocytes. ASN Neuro. https://doi.org/10.1042/AN20110059
26. Parpura V, Sekler I, Fern R (2016) Plasmalemmal and mitochondrial Na(+) -Ca(2 +) exchange in neuroglia. Glia 64:1646–1654. https://doi.org/10.1002/glia.22975
27. Roome CJ, Power EM, Empson RM (2013) Transient reversal of the sodium/calcium exchanger boosts presynaptic calcium and synaptic transmission at a cerebellar synapse. J Neurophysiol 109:1669–1680. https://doi.org/10.1152/jn.00854.2012
28. Jeon D, Yang Y-M, Jeong M-J et al (2003) Enhanced learning and memory in mice lacking Na^+/Ca^{2+} exchanger 2. Neuron 38:965–976. https://doi.org/10.1016/s0896-6273(03)00334-9
29. Molinaro P, Viggiano D, Nisticò R et al (2011) Na^+–Ca^{2+} exchanger (NCX3) knock-out mice display an impairment in hippocampal long-term potentiation and spatial learning and memory. J Neurosci 31:7312–7321. https://doi.org/10.1523/JNEUROSCI.6296-10.2011
30. Molinaro P, Cuomo O, Pignataro G et al (2008) Targeted disruption of Na^+/Ca^{2+} exchanger 3 (NCX3) gene leads to a worsening of ischemic brain damage. J Neurosci 28:1179–1184. https://doi.org/10.1523/JNEUROSCI.4671-07.2008
31. Pignataro G, Sirabella R, Anzilotti S et al (2014) Does Na^+/Ca^{2+} exchanger, NCX, represent a new druggable target in stroke intervention? Transl Stroke Res 5:145–155. https://doi.org/10.1007/s12975-013-0308-8
32. Jeffs GJ, Meloni BP, Sokolow S et al (2008) NCX3 knockout mice exhibit increased hippocampal CA1 and CA2 neuronal damage compared to wild-type mice following global cerebral ischemia. Exp Neurol 210:268–273. https://doi.org/10.1016/j.expneurol.2007.10.013
33. Sirabella R, Sisalli MJ, Costa G et al (2018) NCX1 and NCX3 as potential factors contributing to neurodegeneration and neuroinflammation in the A53T transgenic mouse model of Parkinson's Disease. Cell Death Dis 9:725. https://doi.org/10.1038/s41419-018-0775-7
34. Takuma K, Ago Y, Matsuda T (2013) The glial sodium-calcium exchanger: a new target for nitric oxide-mediated cellular toxicity. Curr Protein Pept Sci 14:43–50
35. Noda M, Ifuku M, Mori Y, Verkhratsky A (2013) Calcium influx through reversed NCX controls migration of microglia. Advances in experimental medicine and biology. Springer, Boston, pp 289–294
36. Boscia F, Gala R, Pannaccione A et al (2009) NCX1 expression and functional activity increase in microglia invading the infarct core. Stroke 40:3608–3617. https://doi.org/10.1161/STROKEAHA.109.557439
37. Khananshvili D (2013) The SLC8 gene family of sodium-calcium exchangers (NCX)—structure, function, and regulation in health and disease. Mol Aspects Med 34:220–235. https://doi.org/10.1016/j.mam.2012.07.003
38. Lytton J (2007) Na^+/Ca^{2+} exchangers: three mammalian gene families control Ca^{2+} transport. Biochem J 406:365–382. https://doi.org/10.1042/BJ20070619
39. Carafoli E (1987) Intracellular calcium homeostasis. Annu Rev Biochem 56:395–433. https://doi.org/10.1146/annurev.bi.56.070187.002143
40. Philipson KD, Nicoll DA (2000) Sodium–calcium exchanger: a molecular perspective. Annu Rev Physiol 62:111–133. https://doi.org/10.1146/annurev.physiol.62.1.111
41. Nicoll D, Longoni S, Philipson K (1990) Molecular cloning and functional expression of the cardiac sarcolemmal Na(+)-Ca2 + exchanger. Science 250:562–565. https://doi.org/10.1126/science.1700476
42. Li Z, Matsuokas S, Hryshkob LV et al (1994) Cloning of the NCX2 isoform of the plasma membrane Na^+–Ca^{2+} exchanger. J Biol Chem 269:17434–17439
43. Nicoll DA, Quednau BD, Qui Z et al (1996) Cloning of a third mammalian Na^+–Ca^{2+} exchanger, NCX3. J Biol Chem 271:24914–24921. https://doi.org/10.1074/jbc.271.40.24914
44. On C, Marshall CR, Perry SF et al (2009) Characterization of zebrafish (Danio rerio) NCX4: a novel NCX with distinct electrophysiological properties. Am J Physiol Physiol 296:C173–C181. https://doi.org/10.1152/ajpcell.00455.2008
45. On C, Marshall CR, Chen N et al (2008) Gene structure evolution of the Na^+–Ca^{2+} exchanger (NCX) family. BMC Evol Biol 8:127. https://doi.org/10.1186/1471-2148-8-127
46. Marshall CR, Fox JA, Butland SL et al (2005) Phylogeny of Na +/Ca2 + exchanger (NCX) genes from genomic data identifies new gene duplications and a new family member in fish species. Physiol Genomics 21:161–173. https://doi.org/10.1152/physiolgenomics.00286.2004
47. Boyman L, Williams GSB, Khananshvili D et al (2013) NCLX: the mitochondrial sodium calcium exchanger. J Mol Cell Cardiol 59:205–213
48. Palty R, Silverman WF, Hershfinkel M et al (2010) NCLX is an essential component of mitochondrial Na^+/Ca^{2+} exchange. Proc Natl Acad Sci USA 107:436–441. https://doi.org/10.1073/pnas.0908099107
49. Palty R, Sekler I (2012) The mitochondrial Na^+/Ca^{2+} exchanger. Cell Calcium 52:9–15
50. Linck B, Qiu Z, He Z et al (1998) Functional comparison of the three isoforms of the Na^+/Ca^{2+} exchanger (NCX1, NCX2, NCX3). Am J Physiol 274:C415–C423. https://doi.org/10.1152/ajpcell.1998.274.2.C415
51. Ren X, Philipson KD (2013) The topology of the cardiac Na^+/Ca^{2+} exchanger, NCX1. J Mol Cell Cardiol 57:68–71. https://doi.org/10.1016/j.yjmcc.2013.01.010
52. Liao J, Li H, Zeng W et al (2012) Structural insight into the ion-exchange mechanism of the sodium/calcium exchanger. Science 335:686–690. https://doi.org/10.1126/science.1215759
53. Liao J, Marinelli F, Lee C et al (2016) Mechanism of extracellular ion exchange and binding-site occlusion in a sodium/calcium exchanger. Nat Struct Mol Biol 23:590–599. https://doi.org/10.1038/nsmb.3230
54. Giladi M, Shor R, Lisnyansky M, Khananshvili D (2016) Structure-functional basis of ion transport in sodium–calcium exchanger (NCX) proteins. Int J Mol Sci 17:1949. https://doi.org/10.3390/ijms17111949
55. Jardetzky O (1966) Simple allosteric model for membrane pumps. Nature 211:969–970. https://doi.org/10.1038/211969a0
56. Forrest LR, Krämer R, Ziegler C (2011) The structural basis of secondary active transport mechanisms. Biochim Biophys Acta 1807:167–188. https://doi.org/10.1016/j.bbabio.2010.10.014
57. Khananshvili D (2014) Sodium-calcium exchangers (NCX): molecular hallmarks underlying the tissue-specific and systemic functions. Pflugers Arch 466:43–60. https://doi.org/10.1007/s00424-013-1405-y
58. Giladi M, Hiller R, Hirsch JA, Khananshvili D (2013) Population shift underlies Ca^{2+}-induced regulatory transitions in the sodium-calcium exchanger (NCX). J Biol Chem 288:23141–23149. https://doi.org/10.1074/jbc.M113.471698
59. Ottolia M, Nicoll DA, John S, Philipson KD (2010) Interactions between Ca^{2+} binding domains of the Na^+–Ca^{2+} exchanger and secondary regulation. Channels 4:159–162. https://doi.org/10.4161/chan.4.3.11386

60. Giladi M, Lee SY, Ariely Y et al (2017) Structure-based dynamic arrays in regulatory domains of sodium-calcium exchanger (NCX) isoforms. Sci Rep 7:993. https://doi.org/10.1038/s41598-017-01102-x
61. Hilge M, Aelen J, Vuister GW (2006) Ca^{2+} regulation in the Na^{+}/Ca^{2+} exchanger involves two markedly different Ca^{2+} sensors. Mol Cell 22:15–25. https://doi.org/10.1016/j.molcel.2006.03.008
62. Besserer GM, Ottolia M, Nicoll DA et al (2007) The second Ca2 + -binding domain of the Na + -Ca 2 + exchanger is essential for regulation: crystal structures and mutational analysis. Proc Natl Acad Sci U S A 104:18467–18472. https://doi.org/10.1073/pnas.0707417104
63. Hilgemann DW, Matsuoka S, Nagel GA, Collins A (1992) Steady-state and dynamic properties of cardiac sodium-calcium exchange. Sodium-dependent inactivation. J Gen Physiol 100:905–932. https://doi.org/10.1085/jgp.100.6.905
64. Hilge M (2013) Ca(2 +) regulation in the Na(+)/Ca (2 +) exchanger features a dual electrostatic switch mechanism. Adv Exp Med Biol 961:27–33. https://doi.org/10.1007/978-1-4614-4756-6_3
65. Hilge M (2012) Ca^{2+} regulation of ion transport in the Na^{+}/Ca^{2+} exchanger. J Biol Chem 287:31641–31649. https://doi.org/10.1074/jbc.R112.353573
66. Tal I, Kozlovsky T, Brisker D et al (2016) Kinetic and equilibrium properties of regulatory Ca2 + -binding domains in sodium–calcium exchangers 2 and 3. Cell Calcium 59:181–188. https://doi.org/10.1016/J.CECA.2016.01.008
67. Steinman L, Altmann D, Sansom D et al (1996) Multiple sclerosis: a coordinated immunological attack against myelin in the central nervous system. Cell 85:299–302. https://doi.org/10.1016/S0092-8674(00)81107-1
68. Lee SY, Giladi M, Bohbot H et al (2016) Structure-dynamic basis of splicing-dependent regulation in tissue-specific variants of the sodium-calcium exchanger. FASEB J 30:1356–1366. https://doi.org/10.1096/fj.15-282251
69. Giladi M, Bohbot H, Buki T et al (2012) Dynamic features of allosteric Ca^{2+} sensor in tissue-specific NCX variants. Cell Calcium 51:478–485. https://doi.org/10.1016/j.ceca.2012.04.007
70. Matsuoka S, Nicoll DA, He Z, Philipson KD (1997) Regulation of cardiac Na(+)-Ca^{2+} exchanger by the endogenous XIP region. J Gen Physiol 109:273–286. https://doi.org/10.1085/jgp.109.2.273
71. Li Z, Nicoll DA, Collins A et al (1991) Identification of a peptide inhibitor of the cardiac sarcolemmal Na(+)-Ca^{2+} exchanger. J Biol Chem 266:1014–1020
72. Giladi M, Tal I, Khananshvili D (2016) Structural Features of Ion Transport and Allosteric Regulation in Sodium-Calcium Exchanger (NCX) Proteins. Front Physiol 7:30. https://doi.org/10.3389/fphys.2016.00030
73. Hilgemann DW, Collins A, Matsuoka S (1992) Steady-state and dynamic properties of cardiac sodium-calcium exchange. Secondary modulation by cytoplasmic calcium and ATP. J Gen Physiol 100:933–961. https://doi.org/10.1085/jgp.100.6.933
74. Chernysh O, Condrescu M, Reeves JP (2008) Sodium-dependent inactivation of sodium/calcium exchange in transfected Chinese hamster ovary cells. Am J Physiol Cell Physiol 295:C872–C882. https://doi.org/10.1152/ajpcell.00221.2008
75. Verkhratsky A, Trebak M, Perocchi F et al (2018) Crosslink between calcium and sodium signalling. Exp Physiol 103:157–169. https://doi.org/10.1113/EP086534
76. Michel LYM, Verkaart S, Koopman WJH et al (2014) Function and regulation of the Na^{+}–Ca^{2+} exchanger NCX3 splice variants in brain and skeletal muscle. J Biol Chem 289:11293–11303. https://doi.org/10.1074/jbc.M113.529388
77. DiPolo R, Beaugé L (2006) Sodium/calcium exchanger: influence of metabolic regulation on ion carrier interactions. Physiol Rev 86:155–203
78. Berberián G, Bollo M, Montich G et al (2009) A novel lipid binding protein is a factor required for MgATP stimulation of the squid nerve Na^{+}/Ca^{2+} exchanger. Biochim Biophys Acta 1788:1255–1262. https://doi.org/10.1016/j.bbamem.2008.12.016
79. Cousido-Siah A, Ayoub D, Berberián G et al (2012) Structural and functional studies of RePl-NCXSQ, a protein regulating the squid nerve Na^{+}/Ca^{2+} exchanger. Acta Crystallogr D 68:1098–1107. https://doi.org/10.1107/S090744491202094X
80. Lariccia V, Amoroso S (2018) Calcium- and ATP-dependent regulation of Na/Ca exchange function in BHK cells: comparison of NCX1 and NCX3 exchangers. Cell Calcium 73:95–103. https://doi.org/10.1016/j.ceca.2018.04.007
81. Dyck C, Omelchenko A, Elias CL et al (1999) Ionic regulatory properties of brain and kidney splice variants of the NCX1 Na-Ca 2 exchanger. J Gen Physiol 114:701–711. https://doi.org/10.1085/jgp.114.5.701
82. Matsuoka S (2004) Forefront of Na^{+}/Ca^{2+} exchanger studies: regulation kinetics of Na^{+}/Ca^{2+} exchangers. J Pharmacol Sci 96:12–14. https://doi.org/10.1254/jphs.fmj04002x2
83. Quednau BD, Nicoll D, Philipson KD (1997) Tissue specificity and alternative splicing of the Na^{+}/Ca^{2+} exchanger isoforms NCXl, NCX2, and NCX3 in rat. Am J Physiol 272:C1250–C1261. https://doi.org/10.1152/ajpcell.1997.272.4.C1250
84. Nakasaki Y, Iwamoto T, Hanada H et al (1993) Cloning of the rat aortic smooth muscle Na +/Ca2 + exchanger and tissue-specific expression of isoforms1. J Biochem 114:528–534. https://doi.org/10.1093/oxfordjournals.jbchem.a124211
85. Rose CR, Ransom BR (1996) Mechanisms of H+ and Na+ changes induced by glutamate, kainate, and D-aspartate in rat hippocampal astrocytes. J Neurosci 16:5393–5404
86. Nicholas SB, Yang W, Lee SL et al (1998) Alternative promoters and cardiac muscle cell-specific expression of the Na^{+}/Ca^{2+} exchanger gene. Am J Physiol 274:H217–H232. https://doi.org/10.1152/ajpheart.1998.274.1.H217
87. Barnes KV, Cheng G, Dawson MM, Menick DR (1997) Cloning of cardiac, kidney, and brain promoters of the feline ncx1 gene. J Biol Chem 272:11510–11517
88. Koban MU, Brugh SA, Riordon DR et al (2001) A distant upstream region of the rat multipartite Na(+)-Ca(2+) exchanger NCX1 gene promoter is sufficient to confer cardiac-specific expression. Mech Dev 109:267–279. https://doi.org/10.1016/s0925-4773(01)00548-2
89. Lee S-L, Yu ASL, Lytton J (1994) Tissue-specific Expression of Na + -Ca2 + exchanger Isoforms. J Biol Chem 269:14849–14852
90. Yu X-M, Groveman BR, Fang X-Q, Lin S-X (2010) The role of intracellular sodium (Na+) in the regulation of calcium (Ca2+)-mediated signaling and toxicity. Health (Irvine Calif) 02:8–15. https://doi.org/10.4236/health.2010.21002
91. Stadelmann C, Timmler S, Barrantes-Freer A, Simons M (2019) Myelin in the Central Nervous System: structure, Function, and Pathology. Physiol Rev 99:1381–1431. https://doi.org/10.1152/physrev.00031.2018
92. Pfeiffer S, Warrington AE, Bansal R (1993) The oligodendrocyte and its many cellular processes. Trends Cell Biol 3:191–197. https://doi.org/10.1016/0962-8924(93)90213-K
93. Michalski JP, Kothary R (2015) Oligodendrocytes in a nutshell. Front Cell Neurosci 9:340. https://doi.org/10.3389/fncel.2015.00340
94. Elbaz B, Popko B (2019) Molecular control of oligodendrocyte development. Trends Neurosci 42:263–277. https://doi.org/10.1016/j.tins.2019.01.002

95. Tiane A, Schepers M, Rombaut B et al (2019) From OPC to oligodendrocyte: an epigenetic journey. Cells. https://doi.org/10.3390/cells8101236
96. Sock E, Wegner M (2019) Transcriptional control of myelination and remyelination. Glia 67:2153–2165. https://doi.org/10.1002/glia.23636
97. Wheeler NA, Fuss B (2016) Extracellular cues influencing oligodendrocyte differentiation and (re)myelination. Exp Neurol 283:512–530. https://doi.org/10.1016/j.expneurol.2016.03.019
98. Yu L, Colvin RA (1997) Regional differences in expression of transcripts for Na^+/Ca^{2+} exchanger isoforms in rat brain. Mol Brain Res 50:285–292. https://doi.org/10.1016/S0169-328X(97)00202-7
99. Tong XP, Li XY, Zhou B et al (2009) Ca2 + signaling evoked by activation of Na + channels and Na +/Ca2 + exchangers is required for GABA-induced NG2 cell migration. J Cell Biol 186:113–128. https://doi.org/10.1083/jcb.200811071
100. Steffensen I, Waxman SG, Mills L, Stys PK (1997) Immunolocalization of the Na^+-Ca^{2+} exchanger in mammalian myelinated axons. Brain Res 776:1–9. https://doi.org/10.1016/S0006-8993(97)00868-8
101. Boscia F, D'avanzo C, Pannaccione A et al (2012) Silencing or knocking out the Na +/Ca2 + exchanger-3 (NCX3) impairs oligodendrocyte differentiation. Cell Death Differ 19:562–572. https://doi.org/10.1038/cdd.2011.125
102. Boscia F, D'Avanzo C, Pannaccione A et al (2013) New roles of NCX in glial cells: activation of microglia in ischemia and differentiation of oligodendrocytes. Adv Exp Med Biol 961:307–316. https://doi.org/10.1007/978-1-4614-4756-6_26
103. Simpson PB, Armstrong RC (1999) Intracellular signals and cytoskeletal elements involved in oligodendrocyte progenitor migration. Glia 26:22–35
104. Paez PM, Fulton D, Colwell CS, Campagnoni AT (2009) Voltage-operated Ca^{2+} and Na^+ channels in the oligodendrocyte lineage. J Neurosci Res 87:3259–3266. https://doi.org/10.1002/jnr.21938
105. Habermacher C, Angulo MC, Benamer N (2019) Glutamate versus GABA in neuron-oligodendroglia communication. Glia 67:2092–2106. https://doi.org/10.1002/glia.23618
106. Friess M, Hammann J, Unichenko P et al (2016) Intracellular ion signaling influences myelin basic protein synthesis in oligodendrocyte precursor cells. Cell Calcium 60:322–330. https://doi.org/10.1016/j.ceca.2016.06.009
107. Hammann J, Bassetti D, White R et al (2018) α2 isoform of Na+, K+-ATPase via Na^+, Ca^{2+} exchanger modulates myelin basic protein synthesis in oligodendrocyte lineage cells in vitro. Cell Calcium 73:1–10. https://doi.org/10.1016/j.ceca.2018.03.003
108. Thakurela S, Garding A, Jung RB et al (2016) The transcriptome of mouse central nervous system myelin. Sci Rep 6:25828. https://doi.org/10.1038/srep25828
109. Martinez-Lozada Z, Waggener CT, Kim K et al (2014) Activation of sodium-dependent glutamate transporters regulates the morphological aspects of oligodendrocyte maturation via signaling through calcium/calmodulin-dependent kinase IIβ's actin-binding/-stabilizing domain. Glia 62:1543–1558. https://doi.org/10.1002/glia.22699
110. Suárez-Pozos E, Thomason EJ, Fuss B (2019) Glutamate transporters: expression and function in oligodendrocytes. Neurochem Res. https://doi.org/10.1007/s11064-018-02708-x
111. Martínez-Lozada Z, Hernández-Kelly LC, Aguilera J et al (2011) Signaling through EAAT-1/GLAST in cultured Bergmann glia cells. Neurochem Int 59:871–879. https://doi.org/10.1016/j.neuint.2011.07.015
112. Iwamoto T, Kita S, Shigekawa M (2002) Functional analysis of Na^+/Ca^{2+} exchanger using novel drugs and genetically engineered mice. Nihon Yakurigaku Zasshi 120:91P–93P
113. Iwamoto T, Inoue Y, Ito K et al (2004) The exchanger inhibitory peptide region-dependent inhibition of Na^+/Ca^{2+} exchange by SN-6 [2-[4-(4-nitrobenzyloxy)benzyl]- thiazolidine-4-carboxylic acid ethyl ester], a novel benzyloxyphenyl derivative. Mol Pharmacol 66:45–55. https://doi.org/10.1124/mol.66.1.45
114. Gong XQ, Frandsen A, Lu WY et al (2005) D-aspartate and NMDA, but not L-aspartate, block AMPA receptors in rat hippocampal neurons. Br J Pharmacol 145:449–459. https://doi.org/10.1038/sj.bjp.0706199
115. Sugiyama H, Ito I, Watanabe M (1989) Glutamate receptor subtypes may be classified into two major categories: a study on Xenopus oocytes injected with rat brain mRNA. Neuron 3:129–132. https://doi.org/10.1016/0896-6273(89)90121-9
116. Bender AS, Woodbury DM, White HS (1997) The rapid L- and D-aspartate uptake in cultured astrocytes. Neurochem Res 22:721–726. https://doi.org/10.1023/a:1027358211472
117. de Rosa V, Secondo A, Pannaccione A et al (2019) d-Aspartate treatment attenuates myelin damage and stimulates myelin repair. EMBO Mol Med 11:e9278. https://doi.org/10.15252/emmm.201809278
118. Kukley M, Capetillo-Zarate E, Dietrich D (2007) Vesicular glutamate release from axons in white matter. Nat Neurosci 10:311–320. https://doi.org/10.1038/nn1850
119. Ziskin JL, Nishiyama A, Rubio M et al (2007) Vesicular release of glutamate from unmyelinated axons in white matter. Nat Neurosci 10:321–330. https://doi.org/10.1038/nn1854
120. Wake H, Lee PR, Fields RD (2011) Control of local protein synthesis…background. Science 333:1647–1652. https://doi.org/10.1126/science.1206998
121. Foster AY, Bujalka H, Emery B (2019) Axoglial interactions in myelin plasticity: evaluating the relationship between neuronal activity and oligodendrocyte dynamics. Glia 67:2038–2049. https://doi.org/10.1002/glia.23629
122. Monje M (2018) Myelin plasticity and nervous system function. Annu Rev Neurosci 41:61–76. https://doi.org/10.1146/annurev-neuro-080317-061853
123. Chorghay Z, Káradóttir RT, Ruthazer ES (2018) White matter plasticity keeps the brain in tune: axons conduct while glia wrap. Front Cell Neurosci 12:428. https://doi.org/10.3389/fncel.2018.00428
124. Bechler ME, Swire M, Ffrench-Constant C (2018) Intrinsic and adaptive myelination-A sequential mechanism for smart wiring in the brain. Dev Neurobiol 78:68–79. https://doi.org/10.1002/dneu.22518
125. Back SA, Luo NL, Borenstein NS et al (2001) Late oligodendrocyte progenitors coincide with the developmental window of vulnerability for human perinatal white matter injury. J Neurosci 21:1302–1312. https://doi.org/10.1523/jneurosci.21-04-01302.2001
126. Cai Q, Ma T, Tian Y et al (2018) Catalpol inhibits ischemia-induced premyelinating oligodendrocyte damage through regulation of intercellular calcium homeostasis via Na^+/Ca^{2+} exchanger 3. Int J Mol Sci. https://doi.org/10.3390/ijms19071925
127. Ma T, Wu X, Cai Q et al (2015) Lead poisoning disturbs oligodendrocytes differentiation involved in decreased expression of NCX3 inducing intracellular calcium overload. Int J Mol Sci 16:19096–19110. https://doi.org/10.3390/ijms160819096
128. Deng W, McKinnon RD, Poretz RD (2001) Lead exposure delays the differentiation of oligodendroglial progenitors in vitro. Toxicol Appl Pharmacol 174:235–244. https://doi.org/10.1006/TAAP.2001.9219
129. Pignataro G, Cuomo O, Vinciguerra A et al (2013) NCX as a key player in the neuroprotection exerted by ischemic preconditioning and postconditioning. Adv Exp Med Miol 961:223–240. https://doi.org/10.1007/978-1-4614-4756-6_19

130. Pignataro G, Gala R, Cuomo O et al (2004) Two sodium/calcium exchanger gene products, NCX1 and NCX3, play a major role in the development of permanent focal cerebral ischemia. Stroke 35:2566–2570. https://doi.org/10.1161/01.STR.0000143730.29964.93
131. Gerkau NJ, Rakers C, Durry S et al (2018) Reverse NCX attenuates cellular sodium loading in metabolically compromised cortex. Cereb Cortex 28:4264–4280. https://doi.org/10.1093/cercor/bhx280
132. Chen H, Kintner DB, Jones M et al (2007) AMPA-mediated excitotoxicity in oligodendrocytes: role for Na^+-K^+-Cl—co-transport and reversal of Na^+/Ca^{2+} exchanger. J Neurochem 102:1783–1795. https://doi.org/10.1111/j.1471-4159.2007.04638.x
133. Stover JF, Pleines UE, Morganti-Kossmann MC et al (1997) Neurotransmitters in cerebrospinal fluid reflect pathological activity. Eur J Clin Invest 27:1038–1043. https://doi.org/10.1046/j.1365-2362.1997.2250774.x
134. Macrez R, Stys PK, Vivien D et al (2016) Mechanisms of glutamate toxicity in multiple sclerosis: biomarker and therapeutic opportunities. Lancet Neurol 15:1089–1102. https://doi.org/10.1016/S1474-4422(16)30165-X
135. Newcombe J, Uddin A, Dove R et al (2008) Glutamate receptor expression in multiple sclerosis lesions. Brain Pathol 18:52–61. https://doi.org/10.1111/j.1750-3639.2007.00101.x
136. Follett PL, Deng W, Dai W et al (2004) Glutamate receptor-mediated oligodendrocyte toxicity in periventricular leukomalacia: a protective role for topiramate. J Neurosci 24:4412–4420. https://doi.org/10.1523/JNEUROSCI.0477-04.2004
137. McCracken E, Fowler JH, Dewar D et al (2002) Grey matter and white matter ischemic damage is reduced by the competitive AMPA receptor antagonist, SPD 502. J Cereb Blood Flow Metab 22:1090–1097. https://doi.org/10.1097/00004647-200209000-00006
138. Park E, Velumian AA, Fehlings MG (2004) The role of excitotoxicity in secondary mechanisms of spinal cord injury: a review with an emphasis on the implications for white matter degeneration. J Neurotrauma 21:754–774. https://doi.org/10.1089/0897715041269641
139. Rosenberg LJ, Teng YD, Wrathall JR (1999) 2,3-Dihydroxy-6-nitro-7-sulfamoyl-benzo(f)quinoxaline reduces glial loss and acute white matter pathology after experimental spinal cord contusion. J Neurosci 19:464–475
140. Wosik K, Ruffini F, Almazan G et al (2004) Resistance of human adult oligodendrocytes to AMPA/kainate receptor-mediated glutamate injury. Brain 127:2636–2648. https://doi.org/10.1093/brain/awh302
141. Itoh T, Beesley J, Itoh A et al (2002) AMPA glutamate receptor-mediated calcium signaling is transiently enhanced during development of oligodendrocytes. J Neurochem 81:390–402. https://doi.org/10.1046/j.1471-4159.2002.00866.x
142. Ceprian M, Fulton D (2019) Glial cell AMPA receptors in nervous system health, injury and disease. Int J Mol Sci. https://doi.org/10.3390/ijms20102450
143. Fan X, Xiong Y, Wang Y (2019) A reignited debate over the cell(s) of origin for glioblastoma and its clinical implications. Front Med 13:531–539. https://doi.org/10.1007/s11684-019-0700-1
144. Hsu LS, Chou WY, Chueh SH (1995) Evidence for a Na^+/Ca^{2+} exchanger in neuroblastoma x glioma hybrid NG108-15 cells. Biochem J 309:445–452. https://doi.org/10.1042/bj3090445
145. Amoroso S, De Maio M, Russo GM et al (1997) Pharmacological evidence that the activation of the Na(+)-Ca^{2+} exchanger protects C6 glioma cells during chemical hypoxia. Br J Pharmacol 121:303–309. https://doi.org/10.1038/sj.bjp.0701092
146. Rodrigues T, Estevez GNN, Tersariol ILDS (2019) Na +/Ca2 + exchangers: unexploited opportunities for cancer therapy? Biochem Pharmacol 163:357–361. https://doi.org/10.1016/j.bcp.2019.02.032
147. Hu H-J, Wang S-S, Wang Y-X et al (2019) Blockade of the forward Na^+/Ca^{2+} exchanger suppresses the growth of glioblastoma cells through Ca^{2+}-mediated cell death. Br J Pharmacol 176:2691–2707. https://doi.org/10.1111/bph.14692
148. Marques S, Zeisel A, Codeluppi S et al (2016) Oligodendrocyte heterogeneity in the mouse juvenile and adult central nervous system. Science 352:1326–1329. https://doi.org/10.1126/science.aaf6463
149. Foerster S, Hill MFE, Franklin RJM (2019) Diversity in the oligodendrocyte lineage: plasticity or heterogeneity? Glia 67:1797–1805. https://doi.org/10.1002/glia.23607
150. Spitzer SO, Sitnikov S, Kamen Y et al (2019) Oligodendrocyte Progenitor Cells Become Regionally Diverse and Heterogeneous with Age. Neuron 101:459.e5–471.e5. https://doi.org/10.1016/j.neuron.2018.12.020
151. Jäkel S, Agirre E, Mendanha Falcão A et al (2019) Altered human oligodendrocyte heterogeneity in multiple sclerosis. Nature 566:543–547. https://doi.org/10.1038/s41586-019-0903-2
152. Watanabe Y (2019) Cardiac Na^+/Ca^{2+} exchange stimulators among cardioprotective drugs. J Physiol Sci. https://doi.org/10.1007/s12576-019-00721-5
153. Song S, Luo L, Sun B, Sun D (2019) Roles of glial ion transporters in brain diseases. Glia. https://doi.org/10.1002/glia.23699

Received: 31 May 2019 | Revised: 26 September 2019 | Accepted: 1 October 2019

DOI: 10.1002/glia.23735

GLIA

WILEY

REVIEW ARTICLE

The oligodendrocyte growth cone and its actin cytoskeleton: A fundamental element for progenitor cell migration and CNS myelination

Elizabeth J. Thomason[1] | Miguel Escalante[1,2] | Donna J. Osterhout[3] | Babette Fuss[1]

[1]Department of Anatomy and Neurobiology, Virginia Commonwealth University School of Medicine, Richmond, Virginia

[2]Departamento de Toxicología, Centro de Investigación y de Estudios Avanzados del Instituto Politécnico Nacional, Ciudad de México, Mexico

[3]Department of Cell and Developmental Biology, State University of New York Upstate Medical University, Syracuse, New York

Correspondence
Babette Fuss, Department of Anatomy and Neurobiology, Virginia Commonwealth University School of Medicine, Richmond, VA 23298.
Email: babette.fuss@vcuhealth.org

Funding information
Commonwealth Health Research Board; National Institute of Neurological Disorders and Stroke; National Multiple Sclerosis Society; Upstate Foundation

Abstract

Cells of the oligodendrocyte (OLG) lineage engage in highly motile behaviors that are crucial for effective central nervous system (CNS) myelination. These behaviors include the guided migration of OLG progenitor cells (OPCs), the surveying of local environments by cellular processes extending from differentiating and pre-myelinating OLGs, and during the process of active myelin wrapping, the forward movement of the leading edge of the myelin sheath's inner tongue along the axon. Almost all of these motile behaviors are driven by actin cytoskeletal dynamics initiated within a lamellipodial structure that is located at the tip of cellular OLG/OPC processes and is structurally as well as functionally similar to the neuronal growth cone. Accordingly, coordinated stoichiometries of actin filament (F-actin) assembly and disassembly at these OLG/OPC growth cones have been implicated in directing process outgrowth and guidance, and the initiation of myelination. Nonetheless, the functional importance of the OLG/OPC growth cone still remains to be fully understood, and, as a unique aspect of actin cytoskeletal dynamics, F-actin depolymerization and disassembly start to predominate at the transition from myelination initiation to myelin wrapping. This review provides an overview of the current knowledge about OLG/OPC growth cones, and it proposes a model in which actin cytoskeletal dynamics in OLG/OPC growth cones are a main driver for morphological transformations and motile behaviors. Remarkably, these activities, at least at the later stages of OLG maturation, may be regulated independently from the transcriptional gene expression changes typically associated with CNS myelination.

KEYWORDS
actin cytoskeleton, growth cone, migration, myelination, oligodendrocyte

1 | INTRODUCTION

Oligodendrocytes (OLGs) are specialized cells of the central nervous system (CNS) that generate the axon enwrapping myelin sheath, which enables rapid and efficient saltatory conduction and provides metabolic axonal support (Stadelmann, Timmler, Barrantes-Freer, & Simons, 2019). During development, cells of the OLG lineage originate as bipolar and migratory OLG progenitor cells (OPCs) within distinct regions of the CNS (Miller, 2005; Naruse, Ishizaki, Ikenaka, Tanaka, & Hitoshi, 2017; Ono et al., 2018; Richardson, Kessaris, & Pringle, 2006). From their points of origin, OPCs migrate throughout the CNS along pathways that are guided by various extracellular cues including the endothelial surface of blood vessels (Jarjour & Kennedy, 2004; Miller, Payne, Milner, Zhang, & Orentas, 1997; Small, Riddle, & Noble, 1987; Tsai et al., 2016). Once OPCs reach their final destination they differentiate and ultimately myelinate axonal segments. This process

of OLG differentiation occurs in a stepwise progression that is characterized by gene expression patterns, which are controlled by both intrinsic and extrinsic signals, and ultimately include typical myelin genes such as proteolipid protein (*Plp1*) and myelin basic protein (*Mbp*; Elbaz & Popko, 2019; Emery & Lu, 2015; Gregath & Lu, 2018; Liu, Moyon, Hernandez, & Casaccia, 2016; Pol et al., 2017; Wheeler & Fuss, 2016). In addition, OLG differentiation features extensive changes in morphology as OPCs mature first into differentiating, premyelinating OLGs, which extend a complex and expanded process network, and then into mature OLGs generating a fully functional myelin sheath (Bauer, Richter-Landsberg, & Ffrench-Constant, 2009; Michalski & Kothary, 2015; Pfeiffer, Warrington, & Bansal, 1993).

Within the past few years, it has been recognized that myelination likely follows a basic intrinsic program that functions in the absence of extrinsic molecular instruction. This intrinsic program is thought to be modulated by a so-called "adaptive program" initiated by extrinsic molecular signals and/or axonal electrical activity (Bechler, Byrne, & Ffrench-Constant, 2015; Bechler, Swire, & Ffrench-Constant, 2018; de Faria Jr., Pama, Evans, Luzhynskaya, & Karadottir, 2018; Foster, Bujalka, & Emery, 2019; Gibson, Geraghty, & Monje, 2018). Thus, the regulation of myelination via the action of extracellular factors, here referred to as "extrinsically modulated myelination," could be considered a form of "adaptive" myelination. Remarkably, such extrinsically modulated myelination has been reported to operate on a neuron/axon individual basis (Hines, Ravanelli, Schwindt, Scott, & Appel, 2015; Koudelka et al., 2016; Lundgaard et al., 2013; Mitew et al., 2018), hence requiring each of the multiple processes of differentiating OLGs to respond to a signal in an independent fashion. This idea is further supported by histological studies describing the presence of "transitional" OLGs, which retain most of their radial processes but have few single processes leading each to a newly forming myelin sheath (Butt, Ibrahim, & Berry, 1997; Hardy & Friedrich Jr., 1996). Such individualized responses require specialized sensing features at the tips of outgrowing processes. In this regard, the tips of the leading processes of migratory OPCs have been shown to feature structural and functional similarities to neuronal growth cones (Jarjour & Kennedy, 2004; Schmidt et al., 1997; Simpson & Armstrong, 1999), and similar observations have been made for the tips of processes extending from differentiating OLGs (Asou, Hamada, & Sakota, 1995; Fox, Afshari, Alexander, Colello, & Fuss, 2006; Hardy & Friedrich Jr., 1996; Kachar, Behar, & Dubois-Dalcq, 1986; Michalski, Cummings, O'Meara, & Kothary, 2016; Rumsby, Afsari, Stark, & Hughson, 2003; Song, Goetz, Baas, & Duncan, 2001; Zuchero et al., 2015). Thus, OLG/OPC growth cones emerge as a characteristic feature of OLG lineage cells.

In neurons, growth cone behavior has been well-established to be driven to a large extent by the dynamic features of the actin cytoskeleton (Dent, Gupton, & Gertler, 2011; Gomez & Letourneau, 2014; Vitriol & Zheng, 2012). Likewise, OLG/OPC growth cones and their actin cytoskeletal dynamics are thought to play a key role in guiding the morphological changes associated with each of the stages of the OLG lineage. This idea is consistent with the critical functions ascribed to the actin cytoskeleton in controlling overall OLG morphology (Brown & Macklin, 2019; Domingues et al., 2018; Seixas et al., 2019). Notably, actin cytoskeletal mechanisms do not function in isolation and there is often crosstalk between actin- and microtubule-based cytoskeletal activities. With regard to the OLG/OPC growth cone, however, the microtubule-rich central region has up to now received extremely little attention. The reader is referred to previously published review articles that discuss the increasingly recognized relevance of the microtubule-rich central region to motile growth cone behaviors in neurons (Cammarata, Bearce, & Lowery, 2016; Kahn & Baas, 2016), as well as to those that address more general roles of the microtubule cytoskeleton in OLG lineage cells (Bauer et al., 2009; Richter-Landsberg, 2001, 2008, 2016). This review focuses on the actin cytoskeletal aspects of the OLG/OPC growth cone by providing an overview of its role in driving dynamic morphological changes at the different stages of the OLG lineage. More specifically, this review presents an introduction into the molecular basis of how actin cytoskeletal dynamics drive growth cone behaviors as they have been revealed from studies done in neurons and are emerging as critical effector mechanisms in shaping the morphologies and motile activities of OLGs and OPCs. Furthermore, evidence is discussed in support of a model in which the regulation of cytoskeletal changes, at least at the later stages of OLG maturation, is uncoupled from the transcriptional control of gene expression traditionally associated with CNS myelination.

2 | THE CRITICAL ROLE OF THE GROWTH CONE'S ACTIN CYTOSKELETON IN DRIVING DYNAMIC CHANGES IN MORPHOLOGY: A BRIEF INTRODUCTION ON THE NEURONAL GROWTH CONE

The unique structural feature termed the growth cone was first described by Santiago Ramón y Cajal as a "cone-like lump with a peripheral base" decorated by triangular or short thorny processes and located at the distal tip of advancing axons (Ramón & Cajal, 1890a, 1890b; Tamariz & Varela-Echavarria, 2015). This structure is now known to function as a highly motile signaling center that surveys and integrates information from the extracellular environment to guide neuronal migration as well as axon outgrowth and pathfinding (Goodman, 1996; Marin, Valiente, Ge, & Tsai, 2010; Tessier-Lavigne & Goodman, 1996; Vitriol & Zheng, 2012). Notably, it is becoming increasingly apparent that growth cones are also present at the distal tips of OPCs and OLGs, where they function according to principles similar to those described for neuronal growth cones. Thus, for a better understanding, a brief introduction into the basic mechanisms of actin cytoskeletal dynamics with a focus on their specific roles in neuronal growth cones is presented prior to discussing their emerging functions in driving the behaviors of growth cones and associated changes in OPC motility and OLG morphology.

In general, dynamic actin cytoskeletal changes are defined by a precisely controlled interplay between the assembly of double-helical actin filaments (F-actin), through polymerization of globular actin

(G-actin), and their disassembly, mediated by F-actin severing and depolymerizing factors. Within this framework, well-organized F-actin growth is enabled by the highly polarized structure of F-actin, which is characterized by a "barbed" or "plus" end and a "pointed" or "minus" end (Holmes, Popp, Gebhard, & Kabsch, 1990). Due to the kinetics for actin polymerization, G-actin monomer addition occurs predominantly at barbed ends, while disassembly takes place mainly at pointed ends (Fujiwara et al., 2018; Shekhar, Pernier, & Carlier, 2016). Based on this feature, a fundamental concept of actin cytoskeletal dynamics and F-actin turnover lies in a process referred to as treadmilling (Figure 1; Pantaloni, Le Clainche, & Carlier, 2001; Wegner, 1976). During treadmilling, filament disassembly by net loss of ADP-bound actin monomers at the pointed end is balanced by net barbed end growth through polymerization of ATP-bound actin monomers and subsequent hydrolysis of ATP. As a result, F-actin filaments coexist with actin monomers at a "steady-state" but seemingly move in one direction, leading to, for example, outward expansion of the cell membrane and forward movement of cellular protrusions (Carlier & Shekhar, 2017; Narita, 2011; Neuhaus, Wanger, Keiser, & Wegner, 1983).

In all cells, the assembly and disassembly of actin filaments, and their organization into higher-order actin networks, is regulated by a plethora of actin-binding proteins, the activities and binding of which are controlled by various signaling pathways (Pollard & Cooper, 2009; Winder & Ayscough, 2005), and actin posttranslational modifications (Varland, Vandekerckhove, & Drazic, 2019). In this context, actin polymerization is energetically unfavorable until there is a nucleus of three associating monomers. Thus, de novo actin polymerization is initiated by actin nucleators such as the Arp2/3 complex, which is best known for its function in driving the formation of branched actin networks within sheet-like lamellipodial protrusions located at the leading edge of cells or the advancing growth cone (Bailly et al., 2001; Korobova & Svitkina, 2008; Mullins, Bieling, & Fletcher, 2018; Pollard, 2007). The nucleating function of Arp2/3 is further enhanced or activated by nucleation promoting factors such as Wiskott–Aldrich syndrome protein (WASP), Neural WASP (N-WASP), and members of the WASP-family verprolin-homologous protein (WAVE) family (Kurisu & Takenawa, 2009; Machesky & Insall, 1998; Takenawa & Suetsugu, 2007). The actin nucleating formins, on the other hand, have been primarily implicated in driving the formation of parallel-bundled actin filaments found in slender rod-like protrusions known as filopodia (Breitsprecher & Goode, 2013; Courtemanche, 2018; Pollard, 2007). Upon nucleation, F-actin filament growth is mediated by the actin polymerization machinery, which includes profilin, an actin-binding protein initially proposed to sequester G-actin monomers but now thought to promote the assembly of G-actin into F-actin (Alkam, Feldman, Singh, & Kiaei, 2017; Kang, Purich, & Southwick, 1999). Counterbalancing of actin polymerization is achieved by the actin disassembly machinery, the best-characterized components of which are the actin-depolymerizing factor (ADF) and members of the cofilin family (Van Troys et al., 2008). These proteins enable actin turnover by binding to ADP-F-actin and promoting the dissociation of ADP-actin from the pointed ends of F-actin filaments (Kanellos & Frame, 2016). Higher-order F-actin structures, which are responsible for the overall appearance of cells or particular subcellular structures such as dendritic spines, are generally shaped through F-actin bundling and F-actin crosslinking mechanisms, involving proteins such as α-actinin or calcium/calmodulin-dependent protein kinase IIβ (CaMKIIβ; Lin & Redmond, 2009; Okamoto, Bosch, & Hayashi, 2009; Winder & Ayscough, 2005).

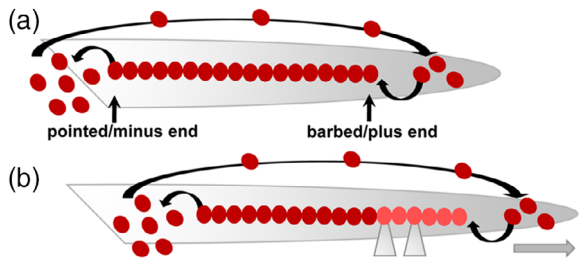

FIGURE 1 Diagram illustrating actin dynamics during treadmilling and forward protrusion of cellular processes. (a) F-actin filament growth occurs at the barbed/plus end and is balanced by net filament disassembly at the pointed/minus end and by recycling of G-actin subunits back to the barbed/plus end (large arrow at the top). Thus, F-actin filaments coexist with G-actin monomers at a "steady state." (b) When the actin filament is anchored to a growth promoting (permissive) substrate via the action of adhesion complexes (grey triangles), actin retrograde flow (from the barbed/plus end to the pointed/minus end; not shown) is reduced, and the F-actin filament seemingly moves in one direction, leading to forward movement of cellular protrusions (grey arrow). Actin monomers are depicted as filled circles; newly polymerized F-actin is represented by lighter color filled circles

For growth cones of migratory neurons and outgrowing axons, it has been well-established that sensing and responding to extracellular cues is enabled by filopodia and lamellipodia, respectively, that is, two key structural features located within the F-actin rich peripheral region (Figure 2). In a simplified model, forward movement of the growth cone is driven by Arp2/3-dependent F-actin polymerization (Korobova & Svitkina, 2008) alongside an attenuation of myosin-based F-actin retrograde flow. The latter process is enabled by selective engagement of the so-called "clutch", a multimolecular point contact complex that, similar to focal adhesions, anchors F-actin with respect to an extracellular substrate (Gomez & Letourneau, 2014; Letourneau, 1981; Lowery & Van Vactor, 2009). Through the engagement of the clutch, actin polymerization exceeds retrograde flow during protrusion. In contrast, during growth cone retraction, retrograde flow and/or F-actin breakdown exceed actin polymerization. An intermediate scenario occurs during growth cone turning, which is thought to be initiated by spatial alterations in growth cone calcium concentrations (Gasperini et al., 2017; Zheng, 2000) followed by asymmetrical polymerization and disruption of the growth cone's F-actin cytoskeleton (Gallo & Letourneau, 2004; Gomez & Letourneau, 2014).

Changes in actin cytoskeletal organization and dynamics, such as those described above, are regulated by upstream signaling cascades initiated by extracellular factors which can function as either attractive/permissive or repulsive/non-permissive cues. In this context, Rho family GTPases have emerged as key intracellular mediators governing

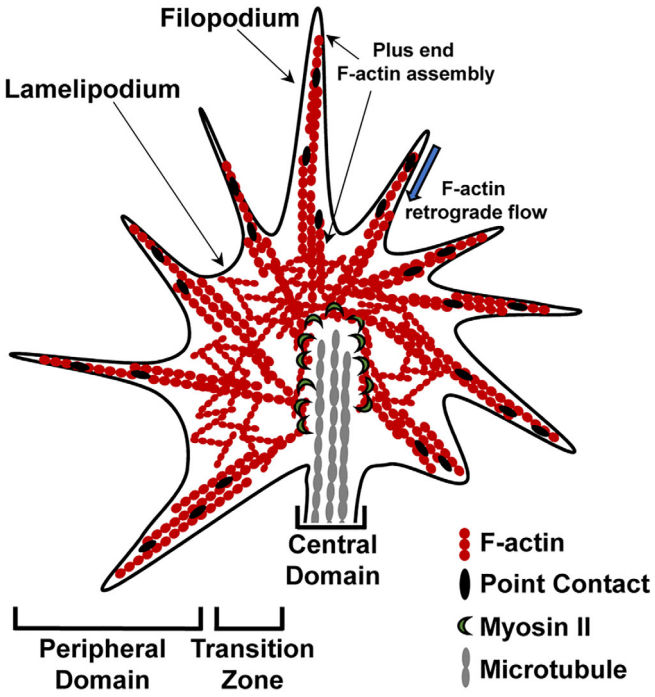

FIGURE 2 Schematic of the growth cone, the main driver of process outgrowth, branching, and guidance. The growth cone is divided into three distinct compartments: The actin-rich peripheral region containing filopodia and lamellipodia, the central region enriched in dense microtubule arrays, and the transition zone characterized by the presence of actomyosin contractile structures. Forward movement of the growth cone, ultimately leading to process outgrowth, is initiated by actin polymerization within the peripheral domain of the growth cone, attenuation of F-actin retrograde flow, and engagement of focal contact points, also referred to as the "clutch." Polymerization of microtubules is then necessary to complete process outgrowth. Process branching can be achieved through growth cone splitting, while growth cone turning in response to guidance cues involves an asymmetric regulation of F-actin cytoskeletal structures and F-actin polymerization/depolymerization

cell morphogenesis and movement, whereby most studies have focused on the classic Rho family GTPases RhoA, Rac1, and Cdc42, which are regulated by the opposing actions of Rho-specific guanine nucleotide exchange factors (GEFs) and GTPase-activating proteins (GAPs; Lawson & Ridley, 2018; Narumiya & Thumkeo, 2018). In neuronal growth cones, activation of RhoA is most commonly associated with growth cone collapse in response to repulsive cues (Borisoff et al., 2003; Kopp et al., 2012), while Rac1 and Cdc42 are generally implicated in the regulation of lamellipodial dynamics and actin polymerization/filopodia formation, respectively (Kuhn et al., 2000). Seemingly paradoxically though, RhoA-mediated contractile forces were found in neurons to lead to both the retraction/collapse of growth cones and the extension of axons (Hall & Lalli, 2010; Jalink et al., 1994). This phenomenon may be explained by the concept that contractile forces during growth cone retraction/collapse are generated at F-actin bundles located within the growth cones' central domain and transition zone (Zhang, Schaefer, Burnette, Schoonderwoert, & Forscher, 2003) rather than intra-axonally as described for axon extension (Gallo, 2006) or at the cell periphery as established for stress fiber formation in fibroblasts (Ridley & Hall, 1992). Interestingly, growth cone collapse induced by the repulsive cue semaphorin 3A (Sema3A, originally called collapsin-1) was found to occur by a RhoA-independent mechanism requiring the signal transducer collapsin response mediator protein 2 (CRMP2; Goshima, Nakamura, Strittmatter, & Strittmatter, 1995). Since CRMP2 has also been identified as a downstream target in RhoA-dependent growth cone collapse, CRMP2 may serve as a critical cytoskeleton regulatory convergent point in the process of growth cone collapse (Tan et al., 2015). The above provides a glimpse into the intricacy of growth cone regulation through the activities of actin regulatory proteins and upstream signaling pathways. Further complexity may be added by cell type-specific and/or context-dependent modulation of the growth cone's actin-based dynamics and motile functions (Dent et al., 2011; Korobova & Svitkina, 2008; Lowery & Van Vactor, 2009; Strasser, Rahim, VanderWaal, Gertler, & Lanier, 2004). Thus, it is not surprising that the functional roles of these proteins and pathways in shaping growth cone behaviors are currently not fully understood.

Taken together, it is evident that dynamic rearrangements of the actin cytoskeleton are a driving force for motile growth cone behaviors and subsequent changes in morphology. As discussed below, this fundamental concept also applies to cells of the OLG lineage, in particular bipolar and migratory progenitor cells, and differentiating OLGs that extend initially a simple and then increasingly complex process network.

3 | THE GROWTH CONE AND ITS ACTIN CYTOSKELETON AS A DRIVER OF DYNAMIC MORPHOLOGICAL CHANGES IN OLG LINEAGE CELLS

3.1 | Growth cone-driven OPC migration

OPCs can be characterized as migratory cells with highly motile protrusions (Hughes, Kang, Fukaya, & Bergles, 2013; Kirby et al., 2006) of which the leading process extends an OPC growth cone at its distal tip (Jarjour & Kennedy, 2004; Schmidt et al., 1997; Simpson & Armstrong, 1999). Next to a cytoskeletal framework in common with neuronal growth cones (Figure 2), OPC growth cones also hold components of the actin nucleating Arp2/3 complex (Bacon, Lakics, Machesky, & Rumsby, 2007). In addition, Arp2/3 complex activities have been assigned an important role in establishing a lamellipodium-rich OPC growth cone and to, thereby, enable guided migratory responses (Li, Wang, Lucas, Li, & Yao, 2015). The nucleation-promoting factor N-WASP, on the other hand, has functionally been associated primarily with the extension and stabilization of filopodia rather than the formation of the OPC growth cone lamellipodium (Bacon et al., 2007). It is of note here, that the role of the Arp2/3 complex in filopodia extension still remains to some extent controversial and may apply to only certain cell types, possibly including OPCs (Korobova & Svitkina, 2008; Steffen et al., 2006; Yang & Svitkina,

2011; Young, Heimsath, & Higgs, 2015). Nevertheless, the above data support the idea that in OPCs the migratory guiding function of the growth cone located at the tip of the leading process is dependent on Arp2/3-mediated F-actin polymerization.

Overall, guided migratory responses can be either toward an attractive cue or away from a repulsive cue. In the context of OPC migration, PDGF-AA and FGF have been identified as attractive cues, and consistent with a critical role of actin-based motility driven by the OPC growth cone, migratory responses to these cues were found to be dependent on intracellular calcium signals, F-actin polymerization, and myosin-based contractile forces (Simpson & Armstrong, 1999). More precisely, in vitro cell culture studies imply that PDGF-AA-guided OPC migration is mediated by a signaling pathway that involves activation of Fyn tyrosine kinase, followed by sequential activation of the actin cytoskeleton regulators cyclin-dependent kinase 5 (Cdk5) and WAVE2 (Miyamoto, Yamauchi, & Tanoue, 2008). However, no OPC migration deficits were seen in conditional *Cdk5* knockout mice (He et al., 2011; Luo et al., 2018), indicating that Cdk5 involvement may not represent an essential component of a molecular pathway instructing OPC migration in vivo.

Semaphorins and netrins have also been implicated in guiding the migratory trajectories of OPCs (Cohen, 2005; Jarjour et al., 2003; Ortega et al., 2012; Sugimoto et al., 2001; Tsai & Miller, 2002). In particular, in vitro assays revealed that netrin-1 can trigger a rapid and persistent decrease in OPC surface area, process length, and process number (Jarjour et al., 2003). This finding is consistent with the concept that repellent cues can, in vitro, induce process retraction through a mechanism that is initiated by growth cone collapse. Consistently, activation of the Rho GTPase RhoA and its effector Rho kinase (ROCK) were found to be required for the OPC's chemorepellent response to netrin-1 (Rajasekharan, Bin, Antel, & Kennedy, 2010). The in vivo role of netrin-1-mediated repulsion has been associated with a dispersal of OPCs from the restricted domain of their origin in the developing spinal cord, the ventral ventricular zone (Tsai, Macklin, & Miller, 2006; Tsai, Tessier-Lavigne, & Miller, 2003). In agreement with such a functional role in dispersal, over-expression of netrin-1 during early phases of myelin repair was found to impair OPC recruitment and remyelination (Tepavcevic et al., 2014). Similar to netrin-1, members of the semaphorin family have been reported to function as repellent cues for OPCs by inducing growth cone collapse and altered migratory patterns (Cohen, Rottkamp, Maric, Barker, & Hudson, 2003; Okada, Tominaga, Horiuchi, & Tomooka, 2007; Spassky et al., 2002). However, currently available data are variable, in particular for Sema3F for which both repulsive and attractive OPC responses have been reported (Boyd, Zhang, & Williams, 2013; Cohen et al., 2003; Piaton et al., 2011; Spassky et al., 2002; Sugimoto et al., 2001; Xiang, Zhang, & Huang, 2012). Nevertheless, an in vivo role in guiding OPC migration is indicated for Sema3A and Sema6A, which are both ligands of Plexin-A4, by the observed differences in OPC and Sema3A/6A distribution patterns when comparing the developing cortex in Plexin-A4 deficient mice with the one in wild-type mice (Okada & Tomooka, 2012). It is worth mentioning that CRMP2 has been found present in Sema3A-responsive differentiating OLGs (Ricard et al., 2001) and, it has been implicated in a RhoA-dependent pathway of process retraction in these cells (Fernandez-Gamba et al., 2012). Whether similar roles may apply for OPCs, however, still needs to be investigated.

More recently, the nervous system vasculature has been identified as a critical substrate for guiding OPC migration via a molecular interaction that is dependent on Wnt pathway activated expression of *Cxcr4* (*chemokine receptor 4*) in OPCs and that, on the endothelial site, likely involves the presence of the Cxcr4 ligand Sdf1/Cxcl12 (stromal cell-derived factor 1/C-X-C motif chemokine 12; Banisadr et al., 2011; Dziembowska et al., 2005; Tian et al., 2018; Tsai et al., 2016). Interestingly, tightly regulated interactions between Cxcr4 and the actin cytoskeleton have been assigned crucial functions during leucocytes migration and the reorganization of the actin cytoskeleton at the protrusive leading edge (Martinez-Munoz et al., 2018; Okabe, Fukuda, & Broxmeyer, 2002). However, the precise roles of the actin cytoskeleton and the OPC growth cone in Cxcr4-mediated OPC migration still need to be determined.

From the findings described above, it becomes evident that actin cytoskeletal dynamics within the growth cone of the leading process of an OPC play a critical role in guiding OPC migration. Apart from the long-range cues discussed here, short-range cues, often represented by components of the extracellular matrix such as fibronectin (OPC migration promoting; Frost, Kiernan, Faissner, & ffrench-Constant, 1996) or tenascin-C (OPC migration inhibiting; Garcion, Faissner, & ffrench-Constant, 2001; Kiernan, Gotz, Faissner, & ffrench-Constant, 1996), have also been reported to regulate OPC motility (Jarjour & Kennedy, 2004). Moreover, there is evidence that expression of OPC guidance cues within demyelinated lesions may play critical roles in influencing OPC recruitment and myelin repair under pathological conditions (Boyd et al., 2013; Piaton et al., 2011; Tepavcevic et al., 2014; Williams et al., 2007). Despite the critical role of OPC guidance cues present during development and myelin repair, surprisingly little is currently known about the regulatory mechanisms directing actin cytoskeletal changes in the OPC growth cone, the main driver of OPC migratory behaviors.

3.2 | Growth cone-driven process dynamics in differentiating and premyelinating OLGs

Similar to OPCs, differentiating OLGs have been found to extend OLG growth cones at the distal tips of their multiple processes (Asou et al., 1995; Fox et al., 2006; Kachar et al., 1986; Michalski et al., 2016; Rumsby et al., 2003; Song et al., 2001; Zuchero et al., 2015). Given the postmigratory and premyelinating characteristics of these cells, the functional importance of their growth cones lies in surveying the local environment in search of axonal segments to be myelinated and/or inappropriate targets to be avoided. As a first step toward surveillance of the surrounding area, differentiating OLGs develop a highly branched, complex process network. This process is driven by the nucleating functions of the Arp2/3 complex in combination with WASP/WAVE family members, all of which have been found present in differentiating OLGs and their growth cones (Bacon et al., 2007).

The idea that actin assembly by the Arp2/3 complex drives the extension of complex process networks at premyelinating stages of the OLG lineage is corroborated by the observation that inhibition of Arp2/3 in vitro in cultures of differentiating OLGs impairs F-actin assembly, the establishment of lamellipodium-rich growth cones, and process outgrowth and branching (Zuchero et al., 2015). These deficits in actin-driven morphological maturation of OLGs were found to be associated with a significant reduction in myelination initiation, that is, axon ensheathment, in vitro in a co-culture system and in vivo in conditional *ArpC3* knockout mice. Similarly, loss of WAVE1 function via over-expression of dominant-negative WAVE1 or *WAVE1* knockout was seen to impair growth cone formation and process outgrowth in differentiating OLGs (Kim et al., 2006). Furthermore, a critical role of Arp2/3 complex function in initial myelin ensheathment has been identified by pharmacological inhibition of N-WASP in explant cultures (Bacon et al., 2007). Interestingly though, in *WAVE1* knockout mice, hypomyelination, ultimately a consequence of decreased numbers of OLG processes and myelination initiation, was observed in the corpus callosum and optic nerve but not the spinal cord (Kim et al., 2006). This finding may indicate that the regulation of actin cytoskeletal dynamics in growth cones of differentiating OLGs may follow regionally heterogeneous mechanisms due to differences in the importance of Arp2/3 in general, variances in Arp2/3 complex subunit composition or the variable nature of the functionally predominant Arp2/3 nucleation promoting factor (Pizarro-Cerda, Chorev, Geiger, & Cossart, 2017). It is of note that in the case of conditional *ArpC3* knockout mice and pharmacological inhibition of N-WASP, available published data are currently restricted to the optic nerve (Zuchero et al., 2015).

In light of the proposed intrinsic program of myelination, the ability of OLG growth cones to recognize nonpermissive targets becomes evident (Almeida, 2018). Indeed, neuronal junction adhesion molecule 2 (JAM2) has been identified as a nonpermissive somatodendritic cue necessary for preventing non-axonal myelination of neurons (Redmond et al., 2016). Similarly, galectin-4 has been recently proposed to function as a repulsive cue for the initiation of myelination and to thereby define nonmyelinated axonal segments (Diez-Revuelta et al., 2017). Members of the IgLON family, which represent GPI anchored adhesion molecules expressed by both OLGs and neurons, have also been identified as repulsive cues with functional importance in preventing precocious developmental myelination of specific fiber tracts (Sharma et al., 2015). Specific axon selection for myelination has additionally been reported to involve bidirectional Eph-ephrin signaling, whereby OLG process retraction in response to ephrin A1-EphA4 forward signaling was found to be mediated by a signaling cascade involving RhoA, the RhoA downstream target Rho kinase (ROCK) and the motor protein myosin II (Cohen, 2005; Harboe, Torvund-Jensen, Kjaer-Sorensen, & Laursen, 2018; Linneberg, Harboe, & Laursen, 2015). This finding provides evidence for a critical role of RhoA in driving the actin cytoskeletal changes that ultimately lead to process retraction when differentiating OLGs respond to nonpermissive cues. Interestingly, in studies on OLG growth cone turning and retraction behavior, collagen IV, a component of the capillary basement membrane, was identified as a nonpermissive substrate for growth cones of differentiating OLGs (Fox et al., 2006). This observation indicates that repulsive cues may also be involved in preventing interactions with blood vessels at the later stages of the OLG lineage.

In addition to repulsion, attraction and permissive cues have also been found to play a critical role in guiding OLG processes, in particular in the context of extrinsically modulated promotion of myelination (Almeida, 2018). Such permissive cues include extracellular matrix molecules, the best characterized of which is laminin-2/merosin (Bechler et al., 2015). First, a number of in vitro studies identified laminin-2/merosin as a permissive substrate for OLG growth cones on which filopodia formation, and process outgrowth and branching are augmented (Eyermann, Czaplinski, & Colognato, 2012; Fox et al., 2006; Lafrenaye & Fuss, 2011; Michalski et al., 2016). Collectively, these studies point toward a signaling pathway that is initiated by an interaction of laminin-2/merosin with the nonintegrin extracellular matrix receptor dystroglycan, which is associated with point contact complexes of OLG filopodia and process branch points. This interaction then leads to the sequential activation of Fyn tyrosine kinase, focal adhesion kinase (FAK) and the Rho GTPases Rac1 and Cdc42 (Eyermann et al., 2012; Hoshina et al., 2007; Lafrenaye & Fuss, 2011; Liang, Draghi, & Resh, 2004; Osterhout, Wolven, Wolf, Resh, & Chao, 1999; Schafer, Muller, Luhmann, & White, 2016). Consistent with an in vivo relevance of this pathway, reduced numbers of myelinated axons of particularly smaller diameter have been reported for the CNS of mice carrying a spontaneous mutation at the laminin $\alpha 2$ chain gene locus (Chun, Rasband, Sidman, Habib, & Vartanian, 2003), and of knockout mice for Fyn (constitutive; Sperber et al., 2001; Umemori, Sato, Yagi, Aizawa, & Yamamoto, 1994) and FAK (conditional; Camara et al., 2009; Forrest et al., 2009). An important role of Fyn and FAK activation in promoting OLG process outgrowth is further supported by the finding that the process outgrowth promoting effect of netrin-1 is also mediated by the activation of these two kinases (Rajasekharan et al., 2009; Rajasekharan et al., 2010). Moreover, Fyn activation was found to deactivate RhoA via p190 RhoGAP, a step thought to be critical for the morphological differentiation of OLGs (Liang et al., 2004; Rajasekharan et al., 2009; Rajasekharan et al., 2010; Wolf, Wilkes, Chao, & Resh, 2001). As a step further downstream, this pathway has been implicated in mediating a downregulation of the motor protein non-muscle myosin II, which has been shown to function as an inhibitor of OLG process outgrowth and branching (Wang et al., 2012; Wang, Tewari, Einheber, Salzer, & Melendez-Vasquez, 2008). Thus, activation of Fyn and FAK, associated with a deactivation of RhoA, emerges as a crucial component of the actin cytoskeletal regulatory machinery that promotes growth cone-driven process outgrowth and branching in differentiating OLGs and, thereby, the initiation of CNS myelination.

In contrast to the above described pathway involving an inactivation of RhoA, complementary roles for the Rho GTPases Rac1 and Cdc42 in regulating process outgrowth and branching in differentiating OLGs are questioned by the in vivo observation that their conditional knockout in cells of the OLG lineage does not lead to reduced numbers of myelinated fibers (Thurnherr et al., 2006). Interestingly,

potential alternate molecular players have been identified. First, Ermin, which shares structural and functional characteristics with ERM proteins known to act in concert with Rho family GTPases, has been identified in differentiating OLGs and found to function as an actin-binding protein that induces process outgrowth and branching (Brockschnieder, Sabanay, Riethmacher, & Peles, 2006). Second, junction-mediating and -regulatory protein (Jmy), a multifunctional actin cytoskeleton regulator that can act as a nucleation promoting factor for the Arp2/3 complex or nucleate unbranched filaments by itself (Zuchero, Coutts, Quinlan, Thangue, & Mullins, 2009), has recently been characterized as a novel player in driving F-actin polymerization, and process outgrowth and branching in differentiating OLGs (Azevedo et al., 2018).

Next to the extracellular matrix proteins such as laminin-2/merosin, adhesion molecules have been proposed to function as permissive signals for the initiation of myelination; these include the neural cell adhesion molecules L1 (Laursen, Chan, & ffrench-Constant, 2009), N-cadherin (Chen et al., 2017; Schnadelbach, Ozen, Blaschuk, Meyer, & Fawcett, 2001), and Necl-1 (Park et al., 2008). The implicated diversity of permissive cues suggests that extrinsically modulated myelination of axons may be regulated by local molecular signatures that identify individual subpopulations of axons to be myelinated. In support of this idea, it has been shown that laminin-2/merosin is present on only a subset of axons in the CNS (Colognato et al., 2002) and that just some subtypes of neurons modulate myelination by signals that are released along their axons (Koudelka et al., 2016). In light of the increasing recognition of OLG heterogeneity (Dimou & Simons, 2017; Foerster, Hill, & Franklin, 2019; Marques et al., 2016; Ornelas et al., 2016; Spitzer et al., 2019; Trotter & Mittmann, 2019; van Bruggen, Agirre, & Castelo-Branco, 2017), one might postulate that different OLG subtypes may respond in an individual fashion to the various cues provided by subpopulations of axons. It should be noted here that current knowledge related to the role of the OLG growth cone and its actin cytoskeleton during OLG differentiation and the initiation of myelination is still rather limited. This gap in knowledge is nicely illustrated by a recently published study in which myelination was characterized in mice over-expressing the extracellular domain of the cell adhesion molecule Cadm4 in OLGs (Elazar et al., 2019). This strategy is thought to interfere with cell–cell interactions involving OLG expressed Cadm4. In these mice, the formation of tight, and thus nondynamic, OLG cell contacts was found to cause a number of phenotypic changes in myelination that reflect the inability of OLG processes to respond to positive as well as negative cues. There are, however, other myelin aberrations, such as a mixed hypo- and hypermyelination phenotype in the corpus callosum, that is, with the current knowledge available, difficult to explain.

Additional complexity comes into view when considering that extrinsically modulated myelination can also be mediated by electrical activity and vesicular release of neurotransmitters, in particular glutamate, along unmyelinated axons (Bechler et al., 2018; de Faria Jr., Pama, Evans, Luzhynskaya, & Karadottir, 2018; Gibson et al., 2018). In this context, our data revealed that glutamate-mediated activation of sodium-dependent glutamate transporters, which are expressed by differentiating OLGs, initiates a signaling cascade that drives actin cytoskeletal changes leading to an increase in process outgrowth and branching (Martinez-Lozada et al., 2014; Suarez-Pozos, Thomason, & Fuss, 2019; Waggener, Dupree, Elgersma, & Fuss, 2013). In this pathway, activation of glutamate transport is thought to activate the reverse mode of sodium-calcium exchange, resulting in a transient increase in intracellular calcium concentration and subsequent inactivation of the actin-binding/bundling activity of calcium/calmodulin-dependent protein kinase IIβ (CaMKIIβ). A critical in vivo role for neuronal activity-induced calcium transients within processes of differentiating OLGs and elongating myelin sheaths has been recently demonstrated in studies using the developing zebrafish as a model system (Baraban, Koudelka, & Lyons, 2018; Krasnow, Ford, Valdivia, Wilson, & Attwell, 2018). Thus, analogous to the involvement of CaMKIIβ during dendritic spine remodeling in response to neuronal activity (Lin & Redmond, 2009; Okamoto et al., 2009), initiation of the glutamate transporter-CaMKIIβ pathway in OLGs may lead to a transient increase in actin cytoskeleton flexibility that enables remodeling and outgrowth of OLG processes. Details to the physical and functional interactions with other actin cytoskeleton regulators involved in this OLG process outgrowth promoting pathway have, however, not yet been investigated.

Taken together, it becomes clear that dynamic actin-cytoskeletal mechanisms initiated at the tips of outgrowing OLG processes represent key players in driving the morphological aspects of OLG differentiation, that is, process outgrowth and branching, and the initiation of myelination. Changes in overall morphology occurring at the transition from OPC to differentiating OLG are likely regulated to a large extent by an intrinsic program. In contrast, there is increasing evidence that at later stages, especially during the initiation of myelination, both permissive and nonpermissive extracellular cues regulate actin cytoskeletal dynamics at individual OLG processes that ultimately determine their decision on whether to modulate myelination or to withdraw.

3.3 | Leading edge-driven myelin wrapping by myelinating OLGs

Once myelination is initiated, it is completed by the concentric wrapping of the myelin sheath around the axonal segment. This spiral growth is driven by the leading edge of the inner tongue, located adjacent to the axon, and it occurs simultaneously with compaction, that is, exclusion of cytoplasm and adhesion of the different layers of myelin membrane (Snaidero et al., 2014; Snaidero & Simons, 2014). In contrast to myelin wrapping, compaction starts at the outermost layers and is thought to be mediated by myelin basic protein (MBP), one of the few proteins present within compacted myelin (Aggarwal et al., 2013; Nawaz et al., 2015; Snaidero & Simons, 2017; Zuchero et al., 2015). Somewhat unexpectedly, a peak in F-actin levels was seen in white matter at the time point when myelination starts to occur (Zuchero et al., 2015) while continuing myelin sheath wrapping was found associated with a decline in F-actin levels (Nawaz et al., 2015; Zuchero et al., 2015). Similarly, in differentiating OLG cultures,

extension of membranous sheets was found associated with reduced levels of F-actin and could be induced experimentally by triggering F-actin disassembly (Nawaz et al., 2015; Wilson & Brophy, 1989; Zuchero et al., 2015). Consistent with the observed decrease in F-actin, myelin wrapping appeared unaffected when *ArpC3* was deleted after initiation of myelination (Zuchero et al., 2015). Collectively, these data put forward the idea that myelin sheath wrapping is driven by F-actin disassembly. This notion is reinforced by the observation that actin assembly promoting proteins such as Arp2/3 complex components are statistically enriched in differentiating and premyelinating OLGs, while actin disassembly promoting proteins, particularly gelsolin and members of the ADF/cofilin family, are prevalent in actively myelinating OLGs (Cahoy et al., 2008; Lena et al., 1994; Zhang et al., 2014). Indeed, inducing F-actin disassembly by surgically implanting latrunculin A loaded gelfoam on the dorsal spinal cord surface during the time-window of active CNS myelination caused a robust increase in myelin sheath wrapping (Zuchero et al., 2015). Conversely, myelin thickness was found slightly reduced in *gelsolin* knockout mice (Zuchero et al., 2015). Similar to the above, myelin sheaths in mice with constitutive and conditional deletion of *ADF* and *cofilin1*, respectively, were characterized by increased F-actin levels and reduced thickness when compared to the ones in control animals; in contrast, initiation of myelination appeared unaffected in these mice (Nawaz et al., 2015). Taken together, these data demonstrate that actual wrapping of the myelin sheath is a process that can mechanistically be distinguished from OLG process outgrowth and the initiation of myelination as it is driven by a robust increase in F-actin depolymerization that ultimately leads to the elimination of F-actin within myelin sheaths.

The importance of F-actin depolymerization in myelin sheath wrapping raises the intriguing question of which forces drive the leading edge of the inner tongue to achieve multiple layers of ensheathment. Based on the measurement of tension, Nawaz et al. (2015) proposed a model in which movement of the membranous sheath occurs independently of stable adhesions with the extracellular matrix and is powered by cycles of F-actin based inflation and deflation at the leading edge of the advancing inner tongue. The idea of adhesion-independent motion is supported by the in vitro finding that OLGs are capable of concentrically wrapping their membranes around inert fibers (Bechler et al., 2015; Espinosa-Hoyos et al., 2018; Lee et al., 2012). The model proposed by Zuchero et al. (2015) is similarly based on adhesion-independent forward movement of the inner tongue but builds on the assumption of a lack of F-actin at the leading edge. In this case, movement is proposed to be driven by myosin II-independent blebbing, that is, hydrostatic pressure generated in the cytoplasm (Paluch & Raz, 2013), whereby membrane compaction by MBP is hypothesized to sufficiently increase intracellular pressure. Notably, structure–function studies related to the maintenance of cytoplasmic channels within myelin sheaths provide evidence for a critical role of F-actin in stabilizing cytoplasm-rich areas by mechanisms that involve the myelin protein 2′/3′-cyclic nucleotide 3′phosphodiesterase (CNP) and antagonize MBP-mediated compaction (Snaidero et al., 2017). These findings highlight the complexity of actin cytoskeletal dynamics during myelination, and they uncover regional cytoskeletal heterogeneity within the myelin sheath, which may favor the presence of F-actin at the leading edge of the advancing inner tongue. Despite the still ongoing discussion about the fine details of the mechanism driving the movement of the advancing inner tongue during myelin sheath wrapping, the present data support a model in which this process is based on some form of adhesion-independent migratory movement that is associated with an overall increase in F-actin disassembly.

Most of the extracellular cues modulating myelination have thus far been associated with OLG process outgrowth and the initiation of myelination. In the case of laminin2/merosin, however, it has additionally been proposed that for late-stage differentiating OLGs, initial spreading is promoted at the OLG growth cone contact site with laminin2/merosin-positive axons. The signaling pathway that has been implicated in this process involves the integrin receptor α6β1 and downstream activation of integrin-linked kinase (ILK; Buttery & ffrench-Constant, 1999; Chun et al., 2003; Colognato et al., 2002; Michalski et al., 2016). In vivo, reduced numbers of particularly smaller diameter myelinated axons have been reported during the developmental window of active myelination for mice in which a dominant-negative form of integrin β1 is expressed in OLGs (Camara et al., 2009). OLG process outgrowth is apparently not affected in cells derived from these mice, reinforcing the idea that laminin2/merosin-integrin β1 signaling affects primarily initial membrane spreading and not, as shown for laminin2/merosin-dystroglycan signaling, process outgrowth and branching. In further support of a role of the above pathway in specifically membrane spreading, OLGs deficient in ILK show a reduced capacity to enwrap neurites in a coculture system (Camara et al., 2009; O'Meara et al., 2013), and there is a developmentally transient reduction in the number of myelinated axons, again with a preferential effect on smaller diameter axons, in conditional *Ilk* knockout mice (Camara et al., 2009; O'Meara et al., 2013). Importantly, and consistent with a critical role of F-actin disassembly during membrane spreading, aberrant F-actin accumulation was seen when ILK-deficient OLGs were differentiated on laminin2/merosin as a substrate (Michalski et al., 2016; O'Meara et al., 2013). It should be noted here, however, that ILK has additionally been shown to regulate OLG growth cones and their cytoskeleton by laminin2/merosin-independent mechanisms (Elazar et al., 2019; Michalski et al., 2016).

Overall, it is becoming increasingly apparent that myelin sheath spreading and myelin wrapping requires an increase in F-actin disassembly. Thus, there is a critical shift in the role of the OLG protrusion located actin cytoskeleton during the transition from differentiating OLGs characterized by process outgrowth to mature OLGs actively involved in myelin wrapping.

4 | REGULATORY PROGRAMS FOR THE OLG GROWTH CONE AND ITS ACTIN CYTOSKELETON

4.1 | Regulation of OLG morphology in coordination with the transcriptional expression of OLG differentiation genes

During CNS development, the extensive changes in cellular morphology that occur at the transition from OPC to differentiating OLG are

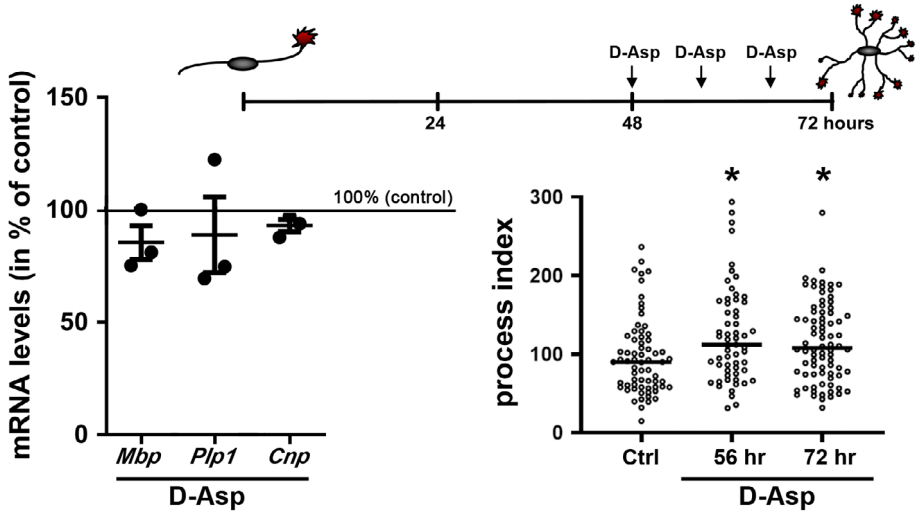

FIGURE 3 Stimulation of process outgrowth via activation of sodium-dependent glutamate transport does not affect myelin gene expression. Differentiating OLGs were isolated and cultured as previously described (Martinez-Lozada et al., 2014). Cells were treated with D-Asp as indicated in the scheme shown in upper right. mRNA levels for the myelin genes myelin basic protein (*Mbp*), proteolipid protein (*Plp1*) and cyclic nucleotide phosphodiesterase (*Cnp*) were determined by real-time RT qPCR analysis at 72 hr (24 hr post-initial D-Asp treatment) and relative expression levels were determined using the ΔΔCT method (bottom left graph). Statistical significance was assessed by ANOVA, and revealed no statistically significant changes in myelin gene mRNA levels. OLG morphology was assessed as previously described (Martinez-Lozada et al., 2014) revealing a significant increase in process index under both conditions, that is, when analyzed at 8 hr post one-time D-Asp application (56 hr) and at 24 hr post D-Asp application at 8-hr intervals (72 hr; bottom right graph; horizontal lines indicate medians). Statistical significance was assessed by ANOVA (nonparametric Kruskal–Wallis and Dunn's post hoc test). $*p \geq .05$ (compared to nonstimulated control [Ctrl])

well-coordinated with gene expression patterns that have been associated with the progression along the OLG lineage (Elbaz & Popko, 2019; Emery & Lu, 2015; Pol et al., 2017). In order to achieve synchronization, changes in morphology and gene expression may be regulated by actin cytoskeletal dynamics in both the cytoplasm and the nucleus, and they could, thereby, be directly coupled. In this context, and in general, actin cytoskeletal dynamics have been implicated in chromatin remodeling and the control of transcriptional gene expression profiles (Klages-Mundt, Kumar, Zhang, Kapoor, & Shen, 2018; Sinha, Biswas, & Soni, 2018; Viita & Vartiainen, 2017; Virtanen & Vartiainen, 2017). In addition, contractile forces associated with the activities of non-muscle myosin II (NMII) are thought to control nuclear morphology and function (Kanellos et al., 2015; Wiggan, Schroder, Krapf, Bamburg, & DeLuca, 2017). Thus, it is not surprising that NMII, shown to function as an inhibitor of process outgrowth at the transition from OPC to differentiating OLG, has also been found to affect the OLG's transcriptional gene expression program (Rusielewicz et al., 2014; Wang et al., 2008; Wang et al., 2012). Consistent with the idea that nuclear actin cytoskeletal dynamics regulate transcriptional gene expression during these earlier stages of the OLG lineage, nuclear actin has been implicated in regulating the repressive histone marks that are necessary for heterochromatin formation and for the transition from OPC to differentiating OLG (Hernandez et al., 2016; Liu et al., 2015; Tsai & Casaccia, 2019). Interestingly, this epigenetic regulation has been found to be associated with a decrease in the levels of microtubule (i.e., stathmin) and F-actin (i.e., gelsolin) severing proteins, suggesting that the highly dynamic behavior of OPCs is supported by relatively high levels of cytoskeleton severing proteins; reducing their levels upon initiation of OPC differentiations is then thought to allow a shift toward cytoskeleton polymerization and process outgrowth (Hernandez et al., 2016; Liu et al., 2015; Liu, Muggironi, Marin-Husstege, & Casaccia-Bonnefil, 2003).

Collectively, the above-described observations suggest that, at the early stages of the OLG lineage and especially at the transition from OPC to differentiating OLG, actin cytoskeletal dynamics, OLG morphology, and transcriptional changes in OLG differentiation genes may be regulated by mechanisms that are directly coupled to each other.

4.2 | Evidence for a regulation of OLG morphology and transcriptional myelin gene expression by mechanisms that function independently from each other

In contrast to the tightly coupled mechanisms discussed above, there is increasing evidence that, once OLGs reach premyelinating stages, cytoskeletal dynamics may be regulated independently from the transcriptional gene expression changes typically associated with myelination. For example, conditional knockout of *ArpC3*, shown to greatly affect OLG process outgrowth and the initiation of CNS myelination, was not seen associated with significant changes in MBP protein levels in this in vivo model (Zuchero et al., 2015). In cell culture studies, inactivation of the Fyn tyrosine kinase, via treatment of differentiating OLGs with the tyrosine kinase inhibitors PP1 and PP2 over a period of 4 days, has been described to lead to a robust inhibition of process outgrowth; at the same time, this treatment was not

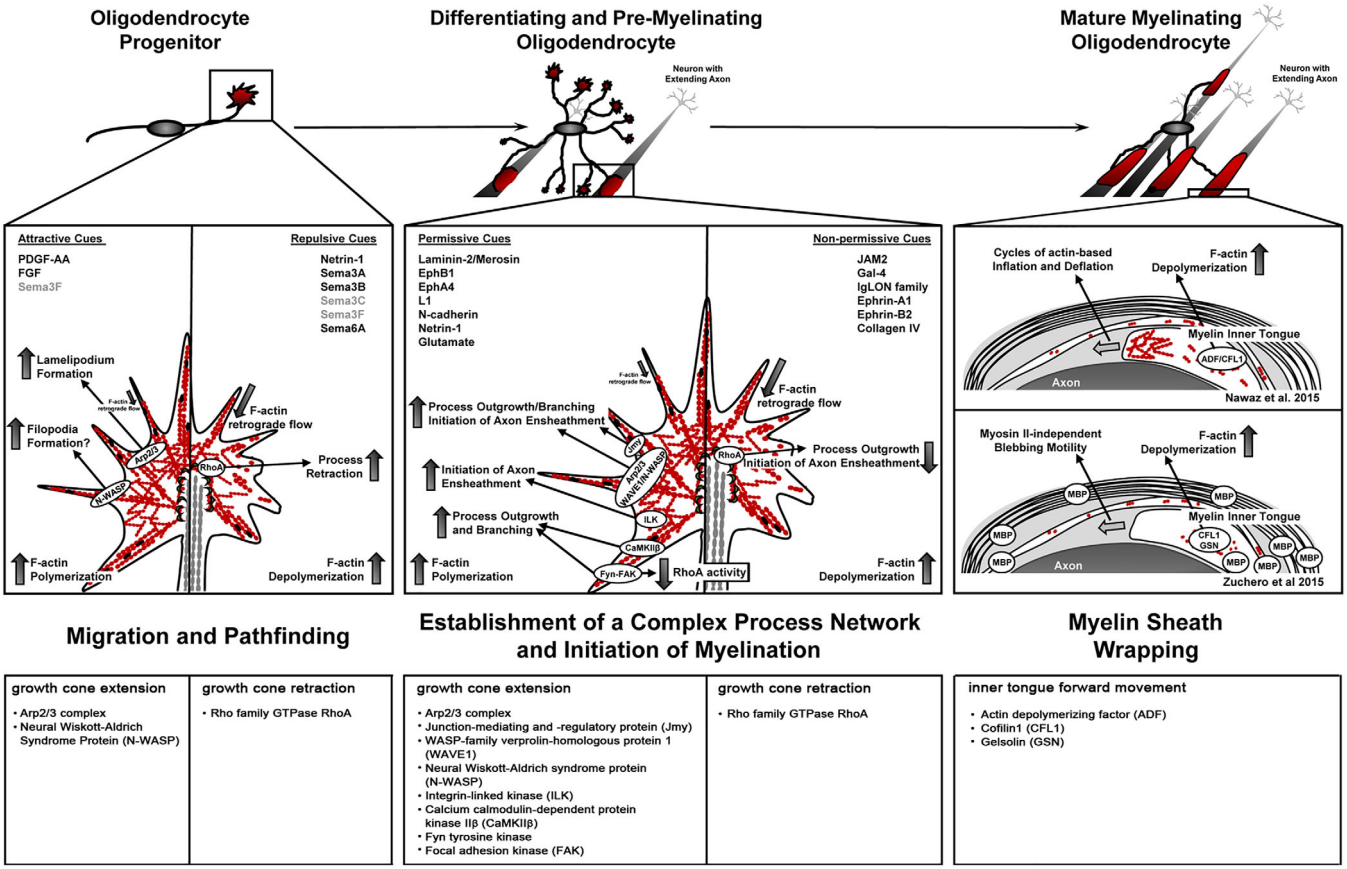

FIGURE 4 Summary of growth cone-driven actin cytoskeletal changes in cells of the oligodendrocyte (OLG) lineage. Cells of the OLG lineage undergo extensive changes in morphology when differentiating from a bipolar migratory OLG progenitor cell (OPC) first into a differentiating and premyelinating OLG that extends a large process network in search of axonal segments to be myelinated, and then into a mature OLG that generates and maintains a fully functional myelin sheath. At the progenitor stage (left), highly dynamic actin cytoskeletal mechanisms regulate growth cone behavior and, thereby, guide OPC migration along trajectories within the CNS in response to both attractive and repulsive extracellular cues. These motile behaviors are characterized by process extension events requiring F-actin polymerization, process retraction events driven by F-actin depolymerization, and process turning events that are mediated by an asymmetrical distribution of F-actin. Actin-binding proteins and key intracellular mediators implicated in OPC growth cone extension and retraction are depicted in the growth cone model (top) and listed in the bottom table. Differentiation into the differentiating OLG (middle) is associated with extensive process outgrowth and branching. In this process, F-actin polymerization and the actin regulatory proteins Arp2/3, Fyn, and focal adhesion kinase (FAK) play key roles in orchestrating actin cytoskeletal dynamics and motile behaviors (see growth cone model (top) and bottom table). Additional actin regulatory proteins, that is, integrin-linked kinase (ILK), calcium calmodulin-dependent protein kinase IIβ (CaMKIIβ), and junction-mediating and junction-regulatory protein (Jmy), have been implicated in this process. However, the interactions, physical and/or functional, between all the potential players involved are currently not well understood. At the premyelinating stages, OLG processes respond to extracellular cues, which can be permissive as well as nonpermissive, in an individual fashion. Growth cone responses at this stage are thought to be similar to the ones observed at the progenitor stage, and they are the determining factors regulating the initiation of myelination. The transition to the myelinating stage is associated with the loss of process extension events, as myelin wrapping is mediated largely by F-actin disassembly. F-actin severing proteins shown to be involved in this process are depicted in the model (top) and listed in the bottom table. Despite the consensus of F-actin disassembly as the major driver, there is still some controversy as to whether the force driving the myelin's inner tongue is generated by cycles of actin-based inflation and deflation or by MBP-dependent, myosin II-independent blebbing motility

associated with apparent changes in the expression of the cell surface marker O1 and the myelin proteins myelin-associated glycoprotein (MAG) and MBP (Osterhout et al., 1999). Similarly, the OLG process outgrowth regulatory role of Mayven, a kelch-related actin-binding protein shown to interact with Fyn, was found to be unrelated to a control of myelin gene expression when analyzed in primary cultures of differentiating OLGs (Jiang et al., 2005; S. K. Williams et al., 2005). Comparable observations were made when assessing myelin protein levels both in vivo and in vitro in the context of FAK-mediated process outgrowth and membrane extension in the presence of laminin-2/merosin (Buttery & ffrench-Constant, 1999; Camara et al., 2009; Lafrenaye & Fuss, 2011) and in primary cultures of differentiating OLGs upon netrin-1 stimulated process outgrowth (Rajasekharan et al., 2009). It is of note that changes in myelin gene expression seen in certain knockout mice, such as those for Fyn, are complicated to interpret due to the multifunctional character of the protein under

investigation and potential functional roles in OPCs (Kramer-Albers & White, 2011; White & Kramer-Albers, 2014). A similar scenario may account for the changes seen in MBP protein levels upon knockdown of the actin nucleation factor Jmy in primary cultures of differentiating OLGs (Azevedo et al., 2018), since Jmy can also function as a transcriptional co-activator (Zuchero et al., 2009). Nevertheless, the above data strongly suggest that at the premyelinating stages, morphological maturation of OLGs can be regulated by the key actin cytoskeleton regulators Arp2/3, Fyn and FAK by mechanisms that apparently function independently from those regulating transcriptional myelin gene expression.

Additional evidence for a regulation of OLG morphology by mechanisms that appear to function independently from those controlling myelin gene expression comes from our own studies, in which the role of sodium-dependent glutamate transporters was investigated in differentiating OLGs (Martinez-Lozada et al., 2014). In these initial studies, cells were analyzed by immunocytochemistry 6 hr post-treatment. In order to confirm that mRNA levels for myelin genes remain unchanged even under conditions that allow sufficient time for potential downstream signaling events, we developed a treatment paradigm as indicated in Figure 3 and analyzed cells at 24 hr after the initial treatment. For these experiments, we used the naturally occurring amino acid D-Aspartic acid (D-Asp), since previous studies demonstrated that D-Asp stimulates OLG process outgrowth in a manner similar to glutamate (Martinez-Lozada et al., 2014). In addition, D-Asp comes with the advantages of not activating non-NMDA ionotropic or metabotropic glutamate receptors and of not being metabolized by glutamine synthetase (Martinez-Lozada et al., 2014). We also chose a multiple application paradigm since the effect of D-Asp treatment on the downstream target CaMKIIβ was found to last for no more than 6 hr. Using this extended paradigm, we observed an increase in process outgrowth and branching that was similar under both conditions, that is, when analyzed at 8 hr post one-time D-Asp application (56 hr) and at 24 hr post three-time D-Asp applications (72 hr; Figure 3). Importantly, no changes in mRNA levels were seen at 72 hr (Figure 3). These findings provide further evidence for the existence of molecular pathways that can regulate the morphological maturation of premyelinating OLGs without significantly affecting transcriptional myelin gene expression.

The above discussion highlights that changes in process outgrowth mediated in differentiating OLGs by mechanisms of actin cytoskeletal dynamics can occur independently from major changes in transcriptional myelin gene expression. It is interesting to note that cellular mobile behaviors have been proposed to require a tight temporal link between actin cytoskeletal dynamics and transcriptional activity at gene loci encoding actin and actin regulatory proteins (Olson & Nordheim, 2010). Thus, it is tempting to speculate that in premyelinating OLGs, progress outgrowth-related maturation events are controlled by a morphology regulatory program that functions independently from the myelin gene expression regulatory program.

5 | CONCLUSION

The highly dynamic actin cytoskeleton of growth cones found at the tips of OPC and OLG processes emerges as a main driver for the motile behaviors and morphological changes that are associated with OPC guidance and migration, OLG process outgrowth and branching, and the initiation of myelination (Figure 4). The actin cytoskeletal mechanisms underlying these aspects of OPC/OLG biology are characterized by varying stoichiometries of F-actin polymerizing and depolymerizing events. At the transition from myelination initiation to myelin wrapping, however, a remarkable conceptual switch occurs as morphological changes are now mediated by predominantly F-actin depolymerization and disassembly (Figure 4).

The synchronized changes in morphology and transcriptional expression of OLG differentiation genes appear, at the early stages of the lineage, to be regulated by mechanisms that may be directly coupled to each other. At the premyelinating stages, on the other hand, evidence accumulates that morphological maturation may be controlled by a regulatory program that functions independently from the one targeting the transcriptional control of myelin gene expression. Interestingly, in the CNS of patients with Multiple Sclerosis (MS), the main demyelinating disease in human, OLGs have been detected that express an apparent full repertoire of myelin genes but fail to successfully initiate and/or complete myelination (Chang, Tourtellotte, Rudick, & Trapp, 2002). This finding could be taken as further evidence for regulatory programs that independently control either myelin gene expression or actin-driven morphology, since under the above pathological conditions the transcriptional myelin gene expression program appears mostly unaffected while the OLG morphology regulatory program seems to be largely dysfunctional. With this interpretation in mind, further defining the mechanisms that regulate, particularly at the premyelinating stages, the morphological aspects of OLG maturation is likely to provide important clues on how to achieve myelin repair under pathological conditions as they are seen in MS.

Overall, the findings presented in this review highlight the still under-developed understanding of the OLG growth cone, its actin cytoskeleton and its functions in cells of the OLG lineage. Future studies will clearly be crucial to gaining a better understanding of the roles of these players during developmental myelination as well as their potential contributions to pathological conditions in which OLGs and/or the myelin sheath are affected.

ACKNOWLEDGMENTS

The authors would like to express their regret to any authors whose work could not be cited due to space limitations. Support for the authors was provided by grants from the National Institute of Health (B.F.), the National Multiple Sclerosis Society (B.F.), Virginia's Commonwealth Health Research Board (B.F.) and the Upstate Foundation (DJO).

ORCID

Babette Fuss https://orcid.org/0000-0002-0356-2135

REFERENCES

Aggarwal, S., Snaidero, N., Pahler, G., Frey, S., Sanchez, P., Zweckstetter, M., … Simons, M. (2013). Myelin membrane assembly is driven by a phase transition of myelin basic proteins into a cohesive protein meshwork. *PLoS Biology*, *11*(6), e1001577. https://doi.org/10.1371/journal.pbio.1001577

Alkam, D., Feldman, E. Z., Singh, A., & Kiaei, M. (2017). Profilin1 biology and its mutation, actin(g) in disease. *Cellular and Molecular Life Sciences*, *74*(6), 967–981. https://doi.org/10.1007/s00018-016-2372-1

Almeida, R. G. (2018). The rules of attraction in central nervous system myelination. *Frontiers in Cellular Neuroscience*, *12*, 367. https://doi.org/10.3389/fncel.2018.00367

Asou, H., Hamada, K., & Sakota, T. (1995). Visualization of a single myelination process of an oligodendrocyte in culture by video microscopy. *Cell Structure and Function*, *20*(1), 59–70.

Azevedo, M. M., Domingues, H. S., Cordelieres, F. P., Sampaio, P., Seixas, A. I., & Relvas, J. B. (2018). Jmy regulates oligodendrocyte differentiation via modulation of actin cytoskeleton dynamics. *Glia*, *66*(9), 1826–1844. https://doi.org/10.1002/glia.23342

Bacon, C., Lakics, V., Machesky, L., & Rumsby, M. (2007). N-WASP regulates extension of filopodia and processes by oligodendrocyte progenitors, oligodendrocytes, and Schwann cells-implications for axon ensheathment at myelination. *Glia*, *55*(8), 844–858.

Bailly, M., Ichetovkin, I., Grant, W., Zebda, N., Machesky, L. M., Segall, J. E., & Condeelis, J. (2001). The F-actin side binding activity of the Arp2/3 complex is essential for actin nucleation and lamellipod extension. *Current Biology*, *11*(8), 620–625.

Banisadr, G., Frederick, T. J., Freitag, C., Ren, D., Jung, H., Miller, S. D., & Miller, R. J. (2011). The role of CXCR4 signaling in the migration of transplanted oligodendrocyte progenitors into the cerebral white matter. *Neurobiology of Disease*, *44*(1), 19–27. https://doi.org/10.1016/j.nbd.2011.05.019

Baraban, M., Koudelka, S., & Lyons, D. A. (2018). Ca (2+) activity signatures of myelin sheath formation and growth in vivo. *Nature Neuroscience*, *21*(1), 19–23. https://doi.org/10.1038/s41593-017-0040-x

Bauer, N. G., Richter-Landsberg, C., & Ffrench-Constant, C. (2009). Role of the oligodendroglial cytoskeleton in differentiation and myelination. *Glia*, *57*(16), 1691–1705.

Bechler, M. E., Byrne, L., & Ffrench-Constant, C. (2015). CNS myelin sheath lengths are an intrinsic property of oligodendrocytes. *Current Biology*, *25*(18), 2411–2416. https://doi.org/10.1016/j.cub.2015.07.056

Bechler, M. E., Swire, M., & Ffrench-Constant, C. (2018). Intrinsic and adaptive myelination—A sequential mechanism for smart wiring in the brain. *Developmental Neurobiology*, *78*(2), 68–79. https://doi.org/10.1002/dneu.22518

Borisoff, J. F., Chan, C. C., Hiebert, G. W., Oschipok, L., Robertson, G. S., Zamboni, R., … Tetzlaff, W. (2003). Suppression of Rho-kinase activity promotes axonal growth on inhibitory CNS substrates. *Molecular and Cellular Neurosciences*, *22*(3), 405–416.

Boyd, A., Zhang, H., & Williams, A. (2013). Insufficient OPC migration into demyelinated lesions is a cause of poor remyelination in MS and mouse models. *Acta Neuropathologica*, *125*(6), 841–859. https://doi.org/10.1007/s00401-013-1112-y

Breitsprecher, D., & Goode, B. L. (2013). Formins at a glance. *Journal of Cell Science*, *126*(Pt 1), 1–7. https://doi.org/10.1242/jcs.107250

Brockschnieder, D., Sabanay, H., Riethmacher, D., & Peles, E. (2006). Ermin, a myelinating oligodendrocyte-specific protein that regulates cell morphology. *The Journal of Neuroscience*, *26*(3), 757–762.

Brown, T. L., & Macklin, W. B. (2019). The actin cytoskeleton in myelinating cells. *Neurochemical Research*. https://doi.org/10.1007/s11064-019-02753-0. [Epub ahead of print].

Butt, A. M., Ibrahim, M., & Berry, M. (1997). The relationship between developing oligodendrocyte units and maturing axons during myelinogenesis in the anterior medullary velum of neonatal rats. *Journal of Neurocytology*, *26*(5), 327–338.

Buttery, P. C., & ffrench-Constant, C. (1999). Laminin-2/integrin interactions enhance myelin membrane formation by oligodendrocytes. *Molecular and Cellular Neurosciences*, *14*(3), 199–212.

Cahoy, J. D., Emery, B., Kaushal, A., Foo, L. C., Zamanian, J. L., Christopherson, K. S., … Barres, B. A. (2008). A transcriptome database for astrocytes, neurons, and oligodendrocytes: A new resource for understanding brain development and function. *The Journal of Neuroscience*, *28*(1), 264–278. https://doi.org/10.1523/JNEUROSCI.4178-07.2008

Camara, J., Wang, Z., Nunes-Fonseca, C., Friedman, H. C., Grove, M., Sherman, D. L., … ffrench-Constant, C. (2009). Integrin-mediated axoglial interactions initiate myelination in the central nervous system. *The Journal of Cell Biology*, *185*(4), 699–712. https://doi.org/10.1083/jcb.200807010

Cammarata, G. M., Bearce, E. A., & Lowery, L. A. (2016). Cytoskeletal social networking in the growth cone: How +TIPs mediate microtubule-actin cross-linking to drive axon outgrowth and guidance. *Cytoskeleton (Hoboken)*, *73*(9), 461–476. https://doi.org/10.1002/cm.21272

Carlier, M. F., & Shekhar, S. (2017). Global treadmilling coordinates actin turnover and controls the size of actin networks. *Nature Reviews. Molecular Cell Biology*, *18*(6), 389–401. https://doi.org/10.1038/nrm.2016.172

Chang, A., Tourtellotte, W. W., Rudick, R., & Trapp, B. D. (2002). Premyelinating oligodendrocytes in chronic lesions of multiple sclerosis. *The New England Journal of Medicine*, *346*(3), 165–173.

Chen, M., Xu, Y., Huang, R., Huang, Y., Ge, S., & Hu, B. (2017). N-cadherin is involved in neuronal activity-dependent regulation of myelinating capacity of zebrafish individual oligodendrocytes in vivo. *Molecular Neurobiology*, *54*(9), 6917–6930. https://doi.org/10.1007/s12035-016-0233-4

Chun, S. J., Rasband, M. N., Sidman, R. L., Habib, A. A., & Vartanian, T. (2003). Integrin-linked kinase is required for laminin-2-induced oligodendrocyte cell spreading and CNS myelination. *The Journal of Cell Biology*, *163*(2), 397–408.

Cohen, R. I. (2005). Exploring oligodendrocyte guidance: 'To boldly go where no cell has gone before'. *Cellular and Molecular Life Sciences*, *62*(5), 505–510.

Cohen, R. I., Rottkamp, D. M., Maric, D., Barker, J. L., & Hudson, L. D. (2003). A role for semaphorins and neuropilins in oligodendrocyte guidance. *Journal of Neurochemistry*, *85*(5), 1262–1278.

Colognato, H., Baron, W., Avellana-Adalid, V., Relvas, J. B., Baron-Van Evercooren, A., Georges-Labouesse, E., & ffrench-Constant, C. (2002). CNS integrins switch growth factor signalling to promote target-dependent survival. *Nature Cell Biology*, *4*(11), 833–841. https://doi.org/10.1038/ncb865

Courtemanche, N. (2018). Mechanisms of formin-mediated actin assembly and dynamics. *Biophysical Reviews*, *10*(6), 1553–1569. https://doi.org/10.1007/s12551-018-0468-6

de Faria, O., Jr., Pama, E. A. C., Evans, K., Luzhynskaya, A., & Karadottir, R. T. (2018). Neuroglial interactions underpinning myelin plasticity. *Developmental Neurobiology*, *78*(2), 93–107. https://doi.org/10.1002/dneu.22539

Dent, E. W., Gupton, S. L., & Gertler, F. B. (2011). The growth cone cytoskeleton in axon outgrowth and guidance. *Cold Spring Harbor Perspectives in Biology*, *3*(3), a001800. https://doi.org/10.1101/cshperspect.a001800

Diez-Revuelta, N., Higuero, A. M., Velasco, S., Penas-de-la-Iglesia, M., Gabius, H. J., & Abad-Rodriguez, J. (2017). Neurons define non-myelinated axon segments by the regulation of galectin-4-containing axon membrane domains. *Scientific Reports*, *7*(1), 12246. https://doi.org/10.1038/s41598-017-12295-6

Dimou, L., & Simons, M. (2017). Diversity of oligodendrocytes and their progenitors. *Current Opinion in Neurobiology*, *47*, 73–79. https://doi.org/10.1016/j.conb.2017.09.015

Domingues, H. S., Cruz, A., Chan, J. R., Relvas, J. B., Rubinstein, B., & Pinto, I. M. (2018). Mechanical plasticity during oligodendrocyte differentiation and myelination. *Glia*, *66*(1), 5–14. https://doi.org/10.1002/glia.23206

Dziembowska, M., Tham, T. N., Lau, P., Vitry, S., Lazarini, F., & Dubois-Dalcq, M. (2005). A role for CXCR4 signaling in survival and migration of neural and oligodendrocyte precursors. *Glia*, *50*(3), 258–269. https://doi.org/10.1002/glia.20170

Elazar, N., Vainshtein, A., Golan, N., Vijayaragavan, B., Schaeren-Wiemers, N., Eshed-Eisenbach, Y., & Peles, E. (2019). Axoglial adhesion by Cadm4 regulates CNS myelination. *Neuron*, *101*(2), 224–231.e225. https://doi.org/10.1016/j.neuron.2018.11.032

Elbaz, B., & Popko, B. (2019). Molecular control of oligodendrocyte development. *Trends in Neurosciences*, *42*(4), 263–277. https://doi.org/10.1016/j.tins.2019.01.002

Emery, B., & Lu, Q. R. (2015). Transcriptional and epigenetic regulation of oligodendrocyte development and myelination in the central nervous system. *Cold Spring Harbor Perspectives in Biology*, *7*(9), a020461. https://doi.org/10.1101/cshperspect.a020461

Espinosa-Hoyos, D., Jagielska, A., Homan, K. A., Du, H., Busbee, T., Anderson, D. G., … Van Vliet, K. J. (2018). Engineered 3D-printed artificial axons. *Scientific Reports*, *8*(1), 478. https://doi.org/10.1038/s41598-017-18744-6

Eyermann, C., Czaplinski, K., & Colognato, H. (2012). Dystroglycan promotes filopodial formation and process branching in differentiating oligodendroglia. *Journal of Neurochemistry*, *120*(6), 928–947. https://doi.org/10.1111/j.1471-4159.2011.07600.x

Fernandez-Gamba, A., Leal, M. C., Maarouf, C. L., Richter-Landsberg, C., Wu, T., Morelli, L., … Castano, E. M. (2012). Collapsin response mediator protein-2 phosphorylation promotes the reversible retraction of oligodendrocyte processes in response to non-lethal oxidative stress. *Journal of Neurochemistry*, *121*(6), 985–995.

Foerster, S., Hill, M. F. E., & Franklin, R. J. M. (2019). Diversity in the oligodendrocyte lineage: Plasticity or heterogeneity? *Glia*, *67*(10), 1797–1805. https://doi.org/10.1002/glia.23607

Forrest, A. D., Beggs, H. E., Reichardt, L. F., Dupree, J. L., Colello, R. J., & Fuss, B. (2009). Focal adhesion kinase (FAK): A regulator of CNS myelination. *Journal of Neuroscience Research*, *87*(15), 3456–3464.

Foster, A. Y., Bujalka, H., & Emery, B. (2019). Axoglial interactions in myelin plasticity: Evaluating the relationship between neuronal activity and oligodendrocyte dynamics. *Glia*, *67*(11), 2038–2049. https://doi.org/10.1002/glia.23629

Fox, M. A., Afshari, F. S., Alexander, J. K., Colello, R. J., & Fuss, B. (2006). Growth conelike sensorimotor structures are characteristic features of postmigratory, premyelinating oligodendrocytes. *Glia*, *53*(5), 563–566.

Frost, E., Kiernan, B. W., Faissner, A., & ffrench-Constant, C. (1996). Regulation of oligodendrocyte precursor migration by extracellular matrix: Evidence for substrate-specific inhibition of migration by tenascin-C. *Developmental Neuroscience*, *18*(4), 266–273. https://doi.org/10.1159/000111416

Fujiwara, I., Takeda, S., Oda, T., Honda, H., Narita, A., & Maeda, Y. (2018). Polymerization and depolymerization of actin with nucleotide states at filament ends. *Biophysical Reviews*, *10*(6), 1513–1519. https://doi.org/10.1007/s12551-018-0483-7

Gallo, G. (2006). RhoA-kinase coordinates F-actin organization and myosin II activity during semaphorin-3A-induced axon retraction. *Journal of Cell Science*, *119*(Pt 16), 3413–3423. https://doi.org/10.1242/jcs.03084

Gallo, G., & Letourneau, P. C. (2004). Regulation of growth cone actin filaments by guidance cues. *Journal of Neurobiology*, *58*(1), 92–102.

Garcion, E., Faissner, A., & ffrench-Constant, C. (2001). Knockout mice reveal a contribution of the extracellular matrix molecule tenascin-C to neural precursor proliferation and migration. *Development*, *128*(13), 2485–2496.

Gasperini, R. J., Pavez, M., Thompson, A. C., Mitchell, C. B., Hardy, H., Young, K. M., … Foa, L. (2017). How does calcium interact with the cytoskeleton to regulate growth cone motility during axon pathfinding? *Molecular and Cellular Neurosciences*, *84*, 29–35. https://doi.org/10.1016/j.mcn.2017.07.006

Gibson, E. M., Geraghty, A. C., & Monje, M. (2018). Bad wrap: Myelin and myelin plasticity in health and disease. *Developmental Neurobiology*, *78*(2), 123–135. https://doi.org/10.1002/dneu.22541

Gomez, T. M., & Letourneau, P. C. (2014). Actin dynamics in growth cone motility and navigation. *Journal of Neurochemistry*, *129*(2), 221–234. https://doi.org/10.1111/jnc.12506

Goodman, C. S. (1996). Mechanisms and molecules that control growth cone guidance. *Annual Review of Neuroscience*, *19*, 341–377. https://doi.org/10.1146/annurev.ne.19.030196.002013

Goshima, Y., Nakamura, F., Strittmatter, P., & Strittmatter, S. M. (1995). Collapsin-induced growth cone collapse mediated by an intracellular protein related to UNC-33. *Nature*, *376*(6540), 509–514. https://doi.org/10.1038/376509a0

Gregath, A., & Lu, Q. R. (2018). Epigenetic modifications-insight into oligodendrocyte lineage progression, regeneration, and disease. *FEBS Letters*, *592*(7), 1063–1078. https://doi.org/10.1002/1873-3468.12999

Hall, A., & Lalli, G. (2010). Rho and Ras GTPases in axon growth, guidance, and branching. *Cold Spring Harbor Perspectives in Biology*, *2*(2), a001818. https://doi.org/10.1101/cshperspect.a001818

Harboe, M., Torvund-Jensen, J., Kjaer-Sorensen, K., & Laursen, L. S. (2018). Ephrin-A1-EphA4 signaling negatively regulates myelination in the central nervous system. *Glia*, *66*(5), 934–950. https://doi.org/10.1002/glia.23293

Hardy, R. J., & Friedrich, V. L., Jr. (1996). Progressive remodeling of the oligodendrocyte process arbor during myelinogenesis. *Developmental Neuroscience*, *18*(4), 243–254.

He, X., Takahashi, S., Suzuki, H., Hashikawa, T., Kulkarni, A. B., Mikoshiba, K., & Ohshima, T. (2011). Hypomyelination phenotype caused by impaired differentiation of oligodendrocytes in Emx1-cre mediated Cdk5 conditional knockout mice. *Neurochemical Research*, *36*(7), 1293–1303. https://doi.org/10.1007/s11064-010-0391-0

Hernandez, M., Patzig, J., Mayoral, S. R., Costa, K. D., Chan, J. R., & Casaccia, P. (2016). Mechanostimulation promotes nuclear and epigenetic changes in oligodendrocytes. *The Journal of Neuroscience*, *36*(3), 806–813. https://doi.org/10.1523/jneurosci.2873-15.2016

Hines, J. H., Ravanelli, A. M., Schwindt, R., Scott, E. K., & Appel, B. (2015). Neuronal activity biases axon selection for myelination in vivo. *Nature Neuroscience*, *18*(5), 683–689. https://doi.org/10.1038/nn.3992

Holmes, K. C., Popp, D., Gebhard, W., & Kabsch, W. (1990). Atomic model of the actin filament. *Nature*, *347*(6288), 44–49. https://doi.org/10.1038/347044a0

Hoshina, N., Tezuka, T., Yokoyama, K., Kozuka-Hata, H., Oyama, M., & Yamamoto, T. (2007). Focal adhesion kinase regulates laminin-induced oligodendroglial process outgrowth. *Genes to Cells*, *12*(11), 1245–1254. https://doi.org/10.1111/j.1365-2443.2007.01130.x

Hughes, E. G., Kang, S. H., Fukaya, M., & Bergles, D. E. (2013). Oligodendrocyte progenitors balance growth with self-repulsion to achieve homeostasis in the adult brain. *Nature Neuroscience*, *16*(6), 668–676. https://doi.org/10.1038/nn.3390

Jalink, K., van Corven, E. J., Hengeveld, T., Morii, N., Narumiya, S., & Moolenaar, W. H. (1994). Inhibition of lysophosphatidate- and thrombin-induced neurite retraction and neuronal cell rounding by ADP ribosylation of the small GTP-binding protein Rho. *The Journal of Cell Biology*, *126*(3), 801–810. https://doi.org/10.1083/jcb.126.3.801

Jarjour, A. A., & Kennedy, T. E. (2004). Oligodendrocyte precursors on the move: Mechanisms directing migration. *The Neuroscientist*, *10*(2), 99–105.

Jarjour, A. A., Manitt, C., Moore, S. W., Thompson, K. M., Yuh, S. J., & Kennedy, T. E. (2003). Netrin-1 is a chemorepellent for oligodendrocyte precursor cells in the embryonic spinal cord. *The Journal of Neuroscience*, *23*(9), 3735–3744.

Jiang, S., Avraham, H. K., Park, S. Y., Kim, T. A., Bu, X., Seng, S., & Avraham, S. (2005). Process elongation of oligodendrocytes is promoted by the Kelch-related actin-binding protein Mayven. *Journal of Neurochemistry*, *92*(5), 1191–1203.

Kachar, B., Behar, T., & Dubois-Dalcq, M. (1986). Cell shape and motility of oligodendrocytes cultured without neurons. *Cell and Tissue Research*, *244*(1), 27–38.

Kahn, O. I., & Baas, P. W. (2016). Microtubules and growth cones: Motors drive the turn. *Trends in Neurosciences*, *39*(7), 433–440. https://doi.org/10.1016/j.tins.2016.04.009

Kanellos, G., & Frame, M. C. (2016). Cellular functions of the ADF/cofilin family at a glance. *Journal of Cell Science*, *129*(17), 3211–3218. https://doi.org/10.1242/jcs.187849

Kanellos, G., Zhou, J., Patel, H., Ridgway, R. A., Huels, D., Gurniak, C. B., … Frame, M. C. (2015). ADF and Cofilin1 control Actin stress fibers, nuclear integrity, and cell survival. *Cell Reports*, *13*(9), 1949–1964. https://doi.org/10.1016/j.celrep.2015.10.056

Kang, F., Purich, D. L., & Southwick, F. S. (1999). Profilin promotes barbed-end actin filament assembly without lowering the critical concentration. *The Journal of Biological Chemistry*, *274*(52), 36963–36972.

Kiernan, B. W., Gotz, B., Faissner, A., & ffrench-Constant, C. (1996). Tenascin-C inhibits oligodendrocyte precursor cell migration by both adhesion-dependent and adhesion-independent mechanisms. *Molecular and Cellular Neurosciences*, *7*(4), 322–335. https://doi.org/10.1006/mcne.1996.0024

Kim, H. J., DiBernardo, A. B., Sloane, J. A., Rasband, M. N., Solomon, D., Kosaras, B., … Vartanian, T. K. (2006). WAVE1 is required for oligodendrocyte morphogenesis and normal CNS myelination. *The Journal of Neuroscience*, *26*(21), 5849–5859.

Kirby, B. B., Takada, N., Latimer, A. J., Shin, J., Carney, T. J., Kelsh, R. N., & Appel, B. (2006). In vivo time-lapse imaging shows dynamic oligodendrocyte progenitor behavior during zebrafish development. *Nature Neuroscience*, *9*(12), 1506–1511. https://doi.org/10.1038/nn1803

Klages-Mundt, N. L., Kumar, A., Zhang, Y., Kapoor, P., & Shen, X. (2018). The nature of actin-family proteins in chromatin-modifying complexes. *Frontiers in Genetics*, *9*, 398. https://doi.org/10.3389/fgene.2018.00398

Kopp, M. A., Liebscher, T., Niedeggen, A., Laufer, S., Brommer, B., Jungehulsing, G. J., … Schwab, J. M. (2012). Small-molecule-induced Rho-inhibition: NSAIDs after spinal cord injury. *Cell and Tissue Research*, *349*(1), 119–132. https://doi.org/10.1007/s00441-012-1334-7

Korobova, F., & Svitkina, T. (2008). Arp2/3 complex is important for filopodia formation, growth cone motility, and neuritogenesis in neuronal cells. *Molecular Biology of the Cell*, *19*(4), 1561–1574. https://doi.org/10.1091/mbc.E07-09-0964

Koudelka, S., Voas, M. G., Almeida, R. G., Baraban, M., Soetaert, J., Meyer, M. P., … Lyons, D. A. (2016). Individual neuronal subtypes exhibit diversity in CNS myelination mediated by synaptic vesicle release. *Current Biology*, *26*(11), 1447–1455. https://doi.org/10.1016/j.cub.2016.03.070

Kramer-Albers, E. M., & White, R. (2011). From axon-glial signalling to myelination: The integrating role of oligodendroglial Fyn kinase. *Cellular and Molecular Life Sciences*, *68*(12), 2003–2012. https://doi.org/10.1007/s00018-010-0616-z

Krasnow, A. M., Ford, M. C., Valdivia, L. E., Wilson, S. W., & Attwell, D. (2018). Regulation of developing myelin sheath elongation by oligodendrocyte calcium transients in vivo. *Nature Neuroscience*, *21*(1), 24–28. https://doi.org/10.1038/s41593-017-0031-y

Kuhn, T. B., Meberg, P. J., Brown, M. D., Bernstein, B. W., Minamide, L. S., Jensen, J. R., … Bamburg, J. R. (2000). Regulating actin dynamics in neuronal growth cones by ADF/cofilin and rho family GTPases. *Journal of Neurobiology*, *44*(2), 126–144.

Kurisu, S., & Takenawa, T. (2009). The WASP and WAVE family proteins. *Genome Biology*, *10*(6), 226. https://doi.org/10.1186/gb-2009-10-6-226

Lafrenaye, A. D., & Fuss, B. (2011). Focal adhesion kinase can play unique and opposing roles in regulating the morphology of differentiating oligodendrocytes. *Journal of Neurochemistry*, *115*(1), 269–282.

Laursen, L. S., Chan, C. W., & ffrench-Constant, C. (2009). An integrin-contactin complex regulates CNS myelination by differential Fyn phosphorylation. *The Journal of Neuroscience*, *29*(29), 9174–9185. https://doi.org/10.1523/jneurosci.5942-08.2009

Lawson, C. D., & Ridley, A. J. (2018). Rho GTPase signaling complexes in cell migration and invasion. *The Journal of Cell Biology*, *217*(2), 447–457. https://doi.org/10.1083/jcb.201612069

Lee, S., Leach, M. K., Redmond, S. A., Chong, S. Y., Mellon, S. H., Tuck, S. J., … Chan, J. R. (2012). A culture system to study oligodendrocyte myelination processes using engineered nanofibers. *Nature Methods*, *9*(9), 917–922. https://doi.org/10.1038/nmeth.2105

Lena, J. Y., Legrand, C., Faivre-Sarrailh, C., Sarlieve, L. L., Ferraz, C., & Rabie, A. (1994). High gelsolin content of developing oligodendrocytes. *International Journal of Developmental Neuroscience*, *12*(5), 375–386.

Letourneau, P. C. (1981). Immunocytochemical evidence for colocalization in neurite growth cones of actin and myosin and their relationship to cell–substratum adhesions. *Developmental Biology*, *85*(1), 113–122. https://doi.org/10.1016/0012-1606(81)90240-2

Li, Y., Wang, P. S., Lucas, G., Li, R., & Yao, L. (2015). ARP2/3 complex is required for directional migration of neural stem cell-derived oligodendrocyte precursors in electric fields. *Stem Cell Research & Therapy*, *6*, 41–11. https://doi.org/10.1186/s13287-015-0042-0

Liang, X., Draghi, N. A., & Resh, M. D. (2004). Signaling from integrins to Fyn to Rho family GTPases regulates morphologic differentiation of oligodendrocytes. *The Journal of Neuroscience*, *24*(32), 7140–7149.

Lin, Y. C., & Redmond, L. (2009). Neuronal CaMKII acts as a structural kinase. *Communicative & Integrative Biology*, *2*(1), 40–41.

Linneberg, C., Harboe, M., & Laursen, L. S. (2015). Axo-glia interaction preceding CNS myelination is regulated by bidirectional Eph-Ephrin signaling. *ASN Neuro*. https://doi.org/10.1177/1759091415602859

Liu, A., Muggironi, M., Marin-Husstege, M., & Casaccia-Bonnefil, P. (2003). Oligodendrocyte process outgrowth in vitro is modulated by epigenetic regulation of cytoskeletal severing proteins. *Glia*, *44*(3), 264–274.

Liu, J., Magri, L., Zhang, F., Marsh, N. O., Albrecht, S., Huynh, J. L., … Casaccia, P. (2015). Chromatin landscape defined by repressive histone methylation during oligodendrocyte differentiation. *The Journal of Neuroscience*, *35*(1), 352–365. https://doi.org/10.1523/jneurosci.2606-14.2015

Liu, J., Moyon, S., Hernandez, M., & Casaccia, P. (2016). Epigenetic control of oligodendrocyte development: Adding new players to old keepers. *Current Opinion in Neurobiology*, *39*, 133–138. https://doi.org/10.1016/j.conb.2016.06.002

Lowery, L. A., & Van Vactor, D. (2009). The trip of the tip: Understanding the growth cone machinery. *Nature Reviews. Molecular Cell Biology*, *10*(5), 332–343. https://doi.org/10.1038/nrm2679

Lundgaard, I., Luzhynskaya, A., Stockley, J. H., Wang, Z., Evans, K. A., Swire, M., … Karadottir, R. T. (2013). Neuregulin and BDNF induce a switch to NMDA receptor-dependent myelination by oligodendrocytes. *PLoS Biology*, *11*(12), e1001743. https://doi.org/10.1371/journal.pbio.1001743

Luo, F., Zhang, J., Burke, K., Romito-DiGiacomo, R. R., Miller, R. H., & Yang, Y. (2018). Oligodendrocyte-specific loss of Cdk5 disrupts the architecture of nodes of Ranvier as well as learning and memory. *Experimental Neurology*, *306*, 92–104. https://doi.org/10.1016/j.expneurol.2018.05.001

Machesky, L. M., & Insall, R. H. (1998). Scar1 and the related Wiskott-Aldrich syndrome protein, WASP, regulate the actin cytoskeleton through the Arp2/3 complex. *Current Biology*, *8*(25), 1347–1356.

Marin, O., Valiente, M., Ge, X., & Tsai, L. H. (2010). Guiding neuronal cell migrations. *Cold Spring Harbor Perspectives in Biology*, *2*(2), a001834. https://doi.org/10.1101/cshperspect.a001834

Marques, S., Zeisel, A., Codeluppi, S., van Bruggen, D., Mendanha Falcao, A., Xiao, L., … Castelo-Branco, G. (2016). Oligodendrocyte heterogeneity in the mouse juvenile and adult central nervous system. *Science*, *352*(6291), 1326–1329. https://doi.org/10.1126/science.aaf6463

Martinez-Lozada, Z., Waggener, C. T., Kim, K., Zou, S., Knapp, P. E., Hayashi, Y., … Fuss, B. (2014). Activation of sodium-dependent glutamate transporters regulates the morphological aspects of oligodendrocyte maturation via signaling through calcium/calmodulin-dependent kinase IIbeta's actin-binding/-stabilizing domain. *Glia*, *62*(9), 1543–1558. https://doi.org/10.1002/glia.22699

Martinez-Munoz, L., Rodriguez-Frade, J. M., Barroso, R., Sorzano, C. O. S., Torreno-Pina, J. A., Santiago, C. A., … Mellado, M. (2018). Separating actin-dependent chemokine receptor nanoclustering from dimerization indicates a role for clustering in CXCR4 signaling and function. *Molecular Cell*, *70*(1), 106–119.e110. https://doi.org/10.1016/j.molcel.2018.02.034

Michalski, J. P., Cummings, S. E., O'Meara, R. W., & Kothary, R. (2016). Integrin-linked kinase regulates oligodendrocyte cytoskeleton, growth cone, and adhesion dynamics. *Journal of Neurochemistry*, *136*(3), 536–549. https://doi.org/10.1111/jnc.13446

Michalski, J. P., & Kothary, R. (2015). Oligodendrocytes in a nutshell. *Frontiers in Cellular Neuroscience*, *9*, 340. https://doi.org/10.3389/fncel.2015.00340

Miller, R. H. (2005). Dorsally derived oligodendrocytes come of age. *Neuron*, *45*(1), 1–3. https://doi.org/10.1016/j.neuron.2004.12.032

Miller, R. H., Payne, J., Milner, L., Zhang, H., & Orentas, D. M. (1997). Spinal cord oligodendrocytes develop from a limited number of migratory highly proliferative precursors. *Journal of Neuroscience Research*, *50*(2), 157–168. https://doi.org/10.1002/(sici)1097-4547(19971015)50:2<157::aid-jnr5>3.0.co;2-e

Mitew, S., Gobius, I., Fenlon, L. R., McDougall, S. J., Hawkes, D., Xing, Y. L., … Emery, B. (2018). Pharmacogenetic stimulation of neuronal activity increases myelination in an axon-specific manner. *Nature Communications*, *9*(1), 306. https://doi.org/10.1038/s41467-017-02719-2

Miyamoto, Y., Yamauchi, J., & Tanoue, A. (2008). Cdk5 phosphorylation of WAVE2 regulates oligodendrocyte precursor cell migration through nonreceptor tyrosine kinase Fyn. *The Journal of Neuroscience*, *28*(33), 8326–8337. https://doi.org/10.1523/jneurosci.1482-08.2008

Mullins, R. D., Bieling, P., & Fletcher, D. A. (2018). From solution to surface to filament: Actin flux into branched networks. *Biophysical Reviews*, *10*(6), 1537–1551. https://doi.org/10.1007/s12551-018-0469-5

Narita, A. (2011). Minimum requirements for the actin-like treadmilling motor system. *BioArchitecture*, *1*(5), 205–208. https://doi.org/10.4161/bioa.18115

Narumiya, S., & Thumkeo, D. (2018). Rho signaling research: History, current status and future directions. *FEBS Letters*, *592*(11), 1763–1776. https://doi.org/10.1002/1873-3468.13087

Naruse, M., Ishizaki, Y., Ikenaka, K., Tanaka, A., & Hitoshi, S. (2017). Origin of oligodendrocytes in mammalian forebrains: A revised perspective. *The Journal of Physiological Sciences*, *67*(1), 63–70. https://doi.org/10.1007/s12576-016-0479-7

Nawaz, S., Sanchez, P., Schmitt, S., Snaidero, N., Mitkovski, M., Velte, C., … Simons, M. (2015). Actin filament turnover drives leading edge growth during myelin sheath formation in the central nervous system. *Developmental Cell*, *34*(2), 139–151. https://doi.org/10.1016/j.devcel.2015.05.013

Neuhaus, J. M., Wanger, M., Keiser, T., & Wegner, A. (1983). Treadmilling of actin. *Journal of Muscle Research and Cell Motility*, *4*(5), 507–527.

O'Meara, R. W., Michalski, J. P., Anderson, C., Bhanot, K., Rippstein, P., & Kothary, R. (2013). Integrin-linked kinase regulates process extension in oligodendrocytes via control of Actin cytoskeletal dynamics. *The Journal of Neuroscience*, *33*(23), 9781–9793. https://doi.org/10.1523/jneurosci.5582-12.2013

Okabe, S., Fukuda, S., & Broxmeyer, H. E. (2002). Activation of Wiskott-Aldrich syndrome protein and its association with other proteins by stromal cell-derived factor-1alpha is associated with cell migration in a T-lymphocyte line. *Experimental Hematology*, *30*(7), 761–766.

Okada, A., Tominaga, M., Horiuchi, M., & Tomooka, Y. (2007). Plexin-A4 is expressed in oligodendrocyte precursor cells and acts as a mediator of semaphorin signals. *Biochemical and Biophysical Research Communications*, *352*(1), 158–163. https://doi.org/10.1016/j.bbrc.2006.10.176

Okada, A., & Tomooka, Y. (2012). Possible roles of Plexin-A4 in positioning of oligodendrocyte precursor cells in developing cerebral cortex. *Neuroscience Letters*, *516*(2), 259–264. https://doi.org/10.1016/j.neulet.2012.04.005

Okamoto, K., Bosch, M., & Hayashi, Y. (2009). The roles of CaMKII and F-actin in the structural plasticity of dendritic spines: A potential molecular identity of a synaptic tag? *Physiology (Bethesda, Md.)*, *24*, 357–366.

Olson, E. N., & Nordheim, A. (2010). Linking actin dynamics and gene transcription to drive cellular motile functions. *Nature Reviews. Molecular Cell Biology*, *11*(5), 353–365. https://doi.org/10.1038/nrm2890

Ono, K., Hirahara, Y., Gotoh, H., Nomura, T., Takebayashi, H., Yamada, H., & Ikenaka, K. (2018). Origin of oligodendrocytes in the vertebrate optic nerve: A review. *Neurochemical Research*, *43*(1), 3–11. https://doi.org/10.1007/s11064-017-2404-8

Ornelas, I. M., McLane, L. E., Saliu, A., Evangelou, A. V., Khandker, L., & Wood, T. L. (2016). Heterogeneity in oligodendroglia: Is it relevant to mouse models and human disease? *Journal of Neuroscience Research*, *94*(12), 1421–1433. https://doi.org/10.1002/jnr.23900

Ortega, M. C., Bribian, A., Peregrin, S., Gil, M. T., Marin, O., & de Castro, F. (2012). Neuregulin-1/ErbB4 signaling controls the migration of oligodendrocyte precursor cells during development. *Experimental Neurology*, *235*(2), 610–620. https://doi.org/10.1016/j.expneurol.2012.03.015

Osterhout, D. J., Wolven, A., Wolf, R. M., Resh, M. D., & Chao, M. V. (1999). Morphological differentiation of oligodendrocytes requires activation of Fyn tyrosine kinase. *The Journal of Cell Biology*, *145*(6), 1209–1218.

Paluch, E. K., & Raz, E. (2013). The role and regulation of blebs in cell migration. *Current Opinion in Cell Biology*, *25*(5), 582–590. https://doi.org/10.1016/j.ceb.2013.05.005

Pantaloni, D., Le Clainche, C., & Carlier, M. F. (2001). Mechanism of actin-based motility. *Science*, *292*(5521), 1502–1506. https://doi.org/10.1126/science.1059975

Park, J., Liu, B., Chen, T., Li, H., Hu, X., Gao, J., … Qiu, M. (2008). Disruption of Nectin-like 1 cell adhesion molecule leads to delayed axonal myelination in the CNS. *The Journal of Neuroscience*, *28*(48), 12815–12819. https://doi.org/10.1523/jneurosci.2665-08.2008

Pfeiffer, S. E., Warrington, A. E., & Bansal, R. (1993). The oligodendrocyte and its many cellular processes. *Trends in Cell Biology*, *3*, 191–197.

Piaton, G., Aigrot, M. S., Williams, A., Moyon, S., Tepavcevic, V., Moutkine, I., … Lubetzki, C. (2011). Class 3 semaphorins influence oligodendrocyte precursor recruitment and remyelination in adult central nervous system. *Brain*, *134*(Pt 4), 1156–1167. https://doi.org/10.1093/brain/awr022

Pizarro-Cerda, J., Chorev, D. S., Geiger, B., & Cossart, P. (2017). The diverse family of Arp2/3 complexes. *Trends in Cell Biology*, *27*(2), 93–100. https://doi.org/10.1016/j.tcb.2016.08.001

Pol, S. U., Polanco, J. J., Seidman, R. A., O'Bara, M. A., Shayya, H. J., Dietz, K. C., & Sim, F. J. (2017). Network-based genomic analysis of human oligodendrocyte progenitor differentiation. *Stem Cell Reports*, *9*(2), 710–723. https://doi.org/10.1016/j.stemcr.2017.07.007

Pollard, T. D. (2007). Regulation of Actin filament assembly by Arp2/3 complex and formins. *Annual Review of Biophysics and Biomolecular Structure*, *36*, 451–477.

Pollard, T. D., & Cooper, J. A. (2009). Actin, a central player in cell shape and movement. *Science*, *326*(5957), 1208–1212.

Rajasekharan, S., Baker, K. A., Horn, K. E., Jarjour, A. A., Antel, J. P., & Kennedy, T. E. (2009). Netrin 1 and Dcc regulate oligodendrocyte process branching and membrane extension via Fyn and RhoA. *Development*, *136*(3), 415–426. https://doi.org/10.1242/dev.018234

Rajasekharan, S., Bin, J. M., Antel, J. P., & Kennedy, T. E. (2010). A central role for RhoA during oligodendroglial maturation in the switch from netrin-1-mediated chemorepulsion to process elaboration. *Journal of Neurochemistry*, *113*(6), 1589–1597.

Ramón, Y., & Cajal, S. (1890a). Notas anatómicas I. Sobre la aparición de las expansiones celulares en la médula embrionaria. *Gaceta Sanitaria Barcelona*, *12*, 413–419.

Ramón, Y., & Cajal, S. (1890b). A quelle époque apparaissent les expansions des cellules nerveuses de la moelle épinière du poulet. *Anatomischer Anzeiger*, *5*, 609–613.

Redmond, S. A., Mei, F., Eshed-Eisenbach, Y., Osso, L. A., Leshkowitz, D., Shen, Y. A., … Chan, J. R. (2016). Somatodendritic expression of JAM2 inhibits oligodendrocyte myelination. *Neuron*, *91*(4), 824–836. https://doi.org/10.1016/j.neuron.2016.07.021

Ricard, D., Rogemond, V., Charrier, E., Aguera, M., Bagnard, D., Belin, M. F., … Honnorat, J. (2001). Isolation and expression pattern of human Unc-33-like phosphoprotein 6/collapsin response mediator protein 5 (Ulip6/CRMP5): Coexistence with Ulip2/CRMP2 in Sema3a-sensitive oligodendrocytes. *The Journal of Neuroscience*, *21*(18), 7203–7214.

Richardson, W. D., Kessaris, N., & Pringle, N. (2006). Oligodendrocyte wars. *Nature Reviews. Neuroscience*, *7*(1), 11–18.

Richter-Landsberg, C. (2001). Organization and functional roles of the cytoskeleton in oligodendrocytes. *Microscopy Research and Technique*, *52*(6), 628–636.

Richter-Landsberg, C. (2008). The cytoskeleton in oligodendrocytes. Microtubule dynamics in health and disease. *Journal of Molecular Neuroscience*, *35*(1), 55–63. https://doi.org/10.1007/s12031-007-9017-7

Richter-Landsberg, C. (2016). Protein aggregate formation in oligodendrocytes: Tau and the cytoskeleton at the intersection of neuroprotection and neurodegeneration. *Biological Chemistry*, *397*(3), 185–194. https://doi.org/10.1515/hsz-2015-0157

Ridley, A. J., & Hall, A. (1992). The small GTP-binding protein rho regulates the assembly of focal adhesions and actin stress fibers in response to growth factors. *Cell*, *70*(3), 389–399.

Rumsby, M., Afsari, F., Stark, M., & Hughson, E. (2003). Microfilament and microtubule organization and dynamics in process extension by central glia-4 oligodendrocytes: Evidence for a microtubule organizing center. *Glia*, *42*(2), 118–129.

Rusielewicz, T., Nam, J., Damanakis, E., John, G. R., Raine, C. S., & Melendez-Vasquez, C. V. (2014). Accelerated repair of demyelinated CNS lesions in the absence of non-muscle myosin IIB. *Glia*, *62*(4), 580–591. https://doi.org/10.1002/glia.22627

Schafer, I., Muller, C., Luhmann, H. J., & White, R. (2016). MOBP levels are regulated by Fyn kinase and affect the morphological differentiation of oligodendrocytes. *Journal of Cell Science*, *129*(5), 930–942. https://doi.org/10.1242/jcs.172148

Schmidt, C., Ohlemeyer, C., Labrakakis, C., Walter, T., Kettenmann, H., & Schnitzer, J. (1997). Analysis of motile oligodendrocyte precursor cells in vitro and in brain slices. *Glia*, *20*(4), 284–298.

Schnadelbach, O., Ozen, I., Blaschuk, O. W., Meyer, R. L., & Fawcett, J. W. (2001). N-cadherin is involved in axon-oligodendrocyte contact and myelination. *Molecular and Cellular Neurosciences*, *17*(6), 1084–1093. https://doi.org/10.1006/mcne.2001.0961

Seixas, A. I., Azevedo, M. M., Paes de Faria, J., Fernandes, D., Mendes Pinto, I., & Relvas, J. B. (2019). Evolvability of the actin cytoskeleton in oligodendrocytes during central nervous system development and aging. *Cellular and Molecular Life Sciences*, *76*(1), 1–11. https://doi.org/10.1007/s00018-018-2915-8

Sharma, K., Schmitt, S., Bergner, C. G., Tyanova, S., Kannaiyan, N., Manrique-Hoyos, N., … Simons, M. (2015). Cell type- and brain region-resolved mouse brain proteome. *Nature Neuroscience*, *18*(12), 1819–1831. https://doi.org/10.1038/nn.4160

Shekhar, S., Pernier, J., & Carlier, M. F. (2016). Regulators of actin filament barbed ends at a glance. *Journal of Cell Science*, *129*(6), 1085–1091. https://doi.org/10.1242/jcs.179994

Simpson, P. B., & Armstrong, R. C. (1999). Intracellular signals and cytoskeletal elements involved in oligodendrocyte progenitor migration. *Glia*, *26*(1), 22–35.

Sinha, B., Biswas, A., & Soni, G. V. (2018). Cellular and nuclear forces: An overview. *Methods in Molecular Biology*, *1805*, 1–29. https://doi.org/10.1007/978-1-4939-8556-2_1

Small, R. K., Riddle, P., & Noble, M. (1987). Evidence for migration of oligodendrocyte–type-2 astrocyte progenitor cells into the developing rat optic nerve. *Nature*, *328*(6126), 155–157. https://doi.org/10.1038/328155a0

Snaidero, N., Mobius, W., Czopka, T., Hekking, L. H., Mathisen, C., Verkleij, D., … Simons, M. (2014). Myelin membrane wrapping of CNS axons by PI(3,4,5)P3-dependent polarized growth at the inner tongue. *Cell*, *156*(1–2), 277–290. https://doi.org/10.1016/j.cell.2013.11.044

Snaidero, N., & Simons, M. (2014). Myelination at a glance. *Journal of Cell Science*, *127*(Pt 14), 2999–3004. https://doi.org/10.1242/jcs.151043

Snaidero, N., & Simons, M. (2017). The logistics of myelin biogenesis in the central nervous system. *Glia*, *65*(7), 1021–1031. https://doi.org/10.1002/glia.23116

Snaidero, N., Velte, C., Myllykoski, M., Raasakka, A., Ignatev, A., Werner, H. B., … Simons, M. (2017). Antagonistic functions of MBP and CNP establish cytosolic channels in CNS myelin. *Cell Reports*, *18*(2), 314–323. https://doi.org/10.1016/j.celrep.2016.12.053

Song, J., Goetz, B. D., Baas, P. W., & Duncan, I. D. (2001). Cytoskeletal reorganization during the formation of oligodendrocyte processes and branches. *Molecular and Cellular Neurosciences*, *17*(4), 624–636.

Spassky, N., de Castro, F., Le Bras, B., Heydon, K., Queraud-LeSaux, F., Bloch-Gallego, E., … Thomas, J. L. (2002). Directional guidance of oligodendroglial migration by class 3 semaphorins and netrin-1. *The Journal of Neuroscience*, *22*(14), 5992–6004.

Sperber, B. R., Boyle-Walsh, E. A., Engleka, M. J., Gadue, P., Peterson, A. C., Stein, P. L., … McMorris, F. A. (2001). A unique role for Fyn in CNS myelination. *The Journal of Neuroscience*, *21*(6), 2039–2047.

Spitzer, S. O., Sitnikov, S., Kamen, Y., Evans, K. A., Kronenberg-Versteeg, D., Dietmann, S., … Karadottir, R. T. (2019). Oligodendrocyte progenitor cells become regionally diverse and heterogeneous with age. *Neuron*, *101*(3), 459–471.e455. https://doi.org/10.1016/j.neuron.2018.12.020

Stadelmann, C., Timmler, S., Barrantes-Freer, A., & Simons, M. (2019). Myelin in the central nervous system: Structure, function, and pathology. *Physiological Reviews*, *99*(3), 1381–1431. https://doi.org/10.1152/physrev.00031.2018

Steffen, A., Faix, J., Resch, G. P., Linkner, J., Wehland, J., Small, J. V., … Stradal, T. E. (2006). Filopodia formation in the absence of functional WAVE- and Arp2/3-complexes. *Molecular Biology of the Cell*, *17*(6), 2581–2591. https://doi.org/10.1091/mbc.e05-11-1088

Strasser, G. A., Rahim, N. A., VanderWaal, K. E., Gertler, F. B., & Lanier, L. M. (2004). Arp2/3 is a negative regulator of growth cone translocation. *Neuron*, *43*(1), 81–94. https://doi.org/10.1016/j.neuron.2004.05.015

Suarez-Pozos, E., Thomason, E. J., & Fuss, B. (2019). Glutamate transporters: Expression and function in oligodendrocytes. *Neurochemical Research*. https://doi.org/10.1007/s11064-018-02708-x. [Epub ahead of print].

Sugimoto, Y., Taniguchi, M., Yagi, T., Akagi, Y., Nojyo, Y., & Tamamaki, N. (2001). Guidance of glial precursor cell migration by secreted cues in the developing optic nerve. *Development*, *128*(17), 3321–3330.

Takenawa, T., & Suetsugu, S. (2007). The WASP-WAVE protein network: Connecting the membrane to the cytoskeleton. *Nature Reviews. Molecular Cell Biology*, *8*(1), 37–48. https://doi.org/10.1038/nrm2069

Tamariz, E., & Varela-Echavarria, A. (2015). The discovery of the growth cone and its influence on the study of axon guidance. *Frontiers in Neuroanatomy*, *9*, 51. https://doi.org/10.3389/fnana.2015.00051

Tan, M., Cha, C., Ye, Y., Zhang, J., Li, S., Wu, F., … Guo, G. (2015). CRMP4 and CRMP2 interact to coordinate cytoskeleton dynamics, regulating growth cone development and axon elongation. *Neural Plasticity*, *2015*, 947423. https://doi.org/10.1155/2015/947423

Tepavcevic, V., Kerninon, C., Aigrot, M. S., Meppiel, E., Mozafari, S., Arnould-Laurent, R., … Lubetzki, C. (2014). Early netrin-1 expression impairs central nervous system remyelination. *Annals of Neurology*, *76*(2), 252–268. https://doi.org/10.1002/ana.24201

Tessier-Lavigne, M., & Goodman, C. S. (1996). The molecular biology of axon guidance. *Science*, *274*(5290), 1123–1133. https://doi.org/10.1126/science.274.5290.1123

Thurnherr, T., Benninger, Y., Wu, X., Chrostek, A., Krause, S. M., Nave, K. A., … Relvas, J. B. (2006). Cdc42 and Rac1 signaling are both required for and act synergistically in the correct formation of myelin sheaths in the CNS. *The Journal of Neuroscience*, *26*(40), 10110–10119.

Tian, Y., Yin, H., Deng, X., Tang, B., Ren, X., & Jiang, T. (2018). CXCL12 induces migration of oligodendrocyte precursor cells through the CXCR4activated MEK/ERK and PI3K/AKT pathways. *Molecular Medicine Reports*, *18*(5), 4374–4380. https://doi.org/10.3892/mmr.2018.9444

Trotter, J., & Mittmann, T. (2019). Diversity in the oligodendrocyte lineage: Current evidence. *Neuron*, *101*(3), 356–357. https://doi.org/10.1016/j.neuron.2019.01.032

Tsai, E., & Casaccia, P. (2019). Mechano-modulation of nuclear events regulating oligodendrocyte progenitor gene expression. *Glia*, *67*(7), 1229–1239. https://doi.org/10.1002/glia.23595

Tsai, H. H., Macklin, W. B., & Miller, R. H. (2006). Netrin-1 is required for the normal development of spinal cord oligodendrocytes. *The Journal of Neuroscience*, *26*(7), 1913–1922.

Tsai, H. H., & Miller, R. H. (2002). Glial cell migration directed by axon guidance cues. *Trends in Neurosciences*, *25*(4), 173–175 discussion 175–176.

Tsai, H. H., Niu, J., Munji, R., Davalos, D., Chang, J., Zhang, H., … Fancy, S. P. (2016). Oligodendrocyte precursors migrate along vasculature in the developing nervous system. *Science*, *351*(6271), 379–384. https://doi.org/10.1126/science.aad3839

Tsai, H. H., Tessier-Lavigne, M., & Miller, R. H. (2003). Netrin 1 mediates spinal cord oligodendrocyte precursor dispersal. *Development*, *130*(10), 2095–2105.

Umemori, H., Sato, S., Yagi, T., Aizawa, S., & Yamamoto, T. (1994). Initial events of myelination involve Fyn tyrosine kinase signalling. *Nature*, *367*(6463), 572–576. https://doi.org/10.1038/367572a0

van Bruggen, D., Agirre, E., & Castelo-Branco, G. (2017). Single-cell transcriptomic analysis of oligodendrocyte lineage cells. *Current Opinion in Neurobiology*, *47*, 168–175. https://doi.org/10.1016/j.conb.2017.10.005

Van Troys, M., Huyck, L., Leyman, S., Dhaese, S., Vandekerkhove, J., & Ampe, C. (2008). Ins and outs of ADF/cofilin activity and regulation. *European Journal of Cell Biology*, *87*(8–9), 649–667. https://doi.org/10.1016/j.ejcb.2008.04.001

Varland, S., Vandekerckhove, J., & Drazic, A. (2019). Actin post-translational modifications: The Cinderella of cytoskeletal control. *Trends in Biochemical Sciences*, *44*(6), 502-516. https://doi.org/10.1016/j.tibs.2018.11.010

Viita, T., & Vartiainen, M. K. (2017). From cytoskeleton to gene expression: Actin in the nucleus. *Handbook of Experimental Pharmacology*, *235*, 311–329. https://doi.org/10.1007/164_2016_27

Virtanen, J. A., & Vartiainen, M. K. (2017). Diverse functions for different forms of nuclear actin. *Current Opinion in Cell Biology*, *46*, 33–38. https://doi.org/10.1016/j.ceb.2016.12.004

Vitriol, E. A., & Zheng, J. Q. (2012). Growth cone travel in space and time: The cellular ensemble of cytoskeleton, adhesion, and membrane. *Neuron*, *73*(6), 1068–1081. https://doi.org/10.1016/j.neuron.2012.03.005

Waggener, C. T., Dupree, J. L., Elgersma, Y., & Fuss, B. (2013). CaMKIIbeta regulates oligodendrocyte maturation and CNS myelination. *The Journal of Neuroscience*, *33*(25), 10453–10458. https://doi.org/10.1523/jneurosci.5875-12.2013

Wang, H., Rusielewicz, T., Tewari, A., Leitman, E. M., Einheber, S., & Melendez-Vasquez, C. V. (2012). Myosin II is a negative regulator of oligodendrocyte morphological differentiation. *Journal of Neuroscience Research*, *90*(8), 1547–1556.

Wang, H., Tewari, A., Einheber, S., Salzer, J. L., & Melendez-Vasquez, C. V. (2008). Myosin II has distinct functions in PNS and CNS myelin sheath formation. *The Journal of Cell Biology*, *182*(6), 1171–1184.

Wegner, A. (1976). Head to tail polymerization of actin. *Journal of Molecular Biology*, *108*(1), 139–150. https://doi.org/10.1016/s0022-2836(76)80100-3

Wheeler, N. A., & Fuss, B. (2016). Extracellular cues influencing oligodendrocyte differentiation and (re)myelination. *Experimental Neurology*, *283*(Pt B), 512–530. https://doi.org/10.1016/j.expneurol.2016.03.019

White, R., & Kramer-Albers, E. M. (2014). Axon-glia interaction and membrane traffic in myelin formation. *Frontiers in Cellular Neuroscience*, *7*, 284. https://doi.org/10.3389/fncel.2013.00284

Wiggan, O., Schroder, B., Krapf, D., Bamburg, J. R., & DeLuca, J. G. (2017). Cofilin regulates nuclear architecture through a myosin-II dependent mechanotransduction module. *Scientific Reports*, *7*, 40953. https://doi.org/10.1038/srep40953

Williams, A., Piaton, G., Aigrot, M. S., Belhadi, A., Theaudin, M., Petermann, F., … Lubetzki, C. (2007). Semaphorin 3A and 3F: Key players in myelin repair in multiple sclerosis? *Brain*, *130*(Pt 10), 2554–2565. https://doi.org/10.1093/brain/awm202

Williams, S. K., Spence, H. J., Rodgers, R. R., Ozanne, B. W., Fitzgerald, U., & Barnett, S. C. (2005). Role of Mayven, a kelch-related protein in oligodendrocyte process formation. *Journal of Neuroscience Research*, *81*(5), 622–631.

Wilson, R., & Brophy, P. J. (1989). Role for the oligodendrocyte cytoskeleton in myelination. *Journal of Neuroscience Research*, *22*(4), 439–448.

Winder, S. J., & Ayscough, K. R. (2005). Actin-binding proteins. *Journal of Cell Science*, *118*(Pt 4), 651–654. https://doi.org/10.1242/jcs.01670

Wolf, R. M., Wilkes, J. J., Chao, M. V., & Resh, M. D. (2001). Tyrosine phosphorylation of p190 RhoGAP by Fyn regulates oligodendrocyte differentiation. *Journal of Neurobiology*, *49*(1), 62–78.

Xiang, X., Zhang, X., & Huang, Q. L. (2012). Plexin A3 is involved in semaphorin 3F-mediated oligodendrocyte precursor cell migration. *Neuroscience Letters*, *530*(2), 127–132. https://doi.org/10.1016/j.neulet.2012.09.058

Yang, C., & Svitkina, T. (2011). Filopodia initiation: Focus on the Arp2/3 complex and formins. *Cell Adhesion & Migration*, *5*(5), 402–408. https://doi.org/10.4161/cam.5.5.16971

Young, L. E., Heimsath, E. G., & Higgs, H. N. (2015). Cell type-dependent mechanisms for formin-mediated assembly of filopodia. *Molecular Biology of the Cell*, *26*(25), 4646–4659. https://doi.org/10.1091/mbc.E15-09-0626

Zhang, X. F., Schaefer, A. W., Burnette, D. T., Schoonderwoert, V. T., & Forscher, P. (2003). Rho-dependent contractile responses in the neuronal growth cone are independent of classical peripheral retrograde actin flow. *Neuron*, *40*(5), 931–944. https://doi.org/10.1016/s0896-6273(03)00754-2

Zhang, Y., Chen, K., Sloan, S. A., Bennett, M. L., Scholze, A. R., O'Keeffe, S., … Wu, J. Q. (2014). An RNA-sequencing transcriptome and splicing database of glia, neurons, and vascular cells of the cerebral cortex. *The Journal of Neuroscience*, *34*(36), 11929–11947. https://doi.org/10.1523/jneurosci.1860-14.2014

Zheng, J. Q. (2000). Turning of nerve growth cones induced by localized increases in intracellular calcium ions. *Nature*, *403*(6765), 89–93. https://doi.org/10.1038/47501

Zuchero, J. B., Coutts, A. S., Quinlan, M. E., Thangue, N. B., & Mullins, R. D. (2009). p53-cofactor JMY is a multifunctional actin nucleation factor. *Nature Cell Biology*, *11*(4), 451–459. https://doi.org/10.1038/ncb1852

Zuchero, J. B., Fu, M. M., Sloan, S. A., Ibrahim, A., Olson, A., Zaremba, A., … Barres, B. A. (2015). CNS myelin wrapping is driven by actin disassembly. *Developmental Cell*, *34*(2), 152–167. https://doi.org/10.1016/j.devcel.2015.06.011

How to cite this article: Thomason EJ, Escalante M, Osterhout DJ, Fuss B. The oligodendrocyte growth cone and its actin cytoskeleton: A fundamental element for progenitor cell migration and CNS myelination. *Glia*. 2019;1–18. https://doi.org/10.1002/glia.23735

Neurochemical Research
https://doi.org/10.1007/s11064-019-02848-8

ORIGINAL PAPER

GLAST Activity is Modified by Acute Manganese Exposure in Bergmann Glial Cells

Miguel Escalante[1] · Jazmín Soto-Verdugo[1] · Luisa C. Hernández-Kelly[1] · Dinorah Hernández-Melchor[1] · Esther López-Bayghen[1] · Tatiana N. Olivares-Bañuelos[2] · Arturo Ortega[1]

Received: 24 April 2019 / Revised: 22 July 2019 / Accepted: 25 July 2019

Abstract
Glutamate is the major excitatory amino acid neurotransmitter in the vertebrate brain. It exerts its actions through the activation of specific plasma membrane receptors expressed in neurons and glial cells. Overactivation of glutamate receptors results in neuronal death, known as excitotoxicity. A family of sodium-dependent glutamate transporters enriched in glial cells are responsible of the vast majority of the removal of this amino acid form the synaptic cleft. Therefore, a precise and exquisite regulation of these proteins is required not only for a proper glutamatergic transmission but also for the prevention of an excitotoxic insult. Manganese is a trace element essential as a cofactor for several enzymatic systems, although in high concentrations is involved in the disruption of brain glutamate homeostasis. The molecular mechanisms associated to manganese neurotoxicity have been focused on mitochondrial function, although energy depletion severely compromises the glutamate uptake process. In this context, in this contribution we analyze the effect of manganese exposure in glial glutamate transporters function. To this end, we used the well-established model of chick cerebellar Bergmann glia cultures. A time and dose dependent modulation of [^{3}H]-D-aspartate uptake was found. An increase in the transporter catalytic efficiency, most probably linked to a discrete increase in the affinity of the transporter was detected upon manganese exposure. Interestingly, glucose uptake was reduced by this metal. These results favor the notion of a direct effect of manganese on glial cells, this in turn alters their coupling with neurons and might lead to changes in glutamatergic transmission.

Keywords GLAST · Bergmann glia · Glutamate · Manganese · Neurotoxicity

Introduction

Glutamate is the major excitatory amino acid transmitter in the vertebrate brain. It exerts its actions through the activation of specific membrane receptors that have been subdivided in terms of their molecular structure and signaling properties in ionotropic (iGluRs) and metabotropic (mGluRs) glutamate receptors [1, 2]. Neurons and glial cells express both subtypes of receptors, several membrane to nucleus signaling cascades have been described to be activated by glutamate in both cell types [3].

Overstimulation of glutamate receptors is linked to neuronal death, and most of the time it is related to a deficient removal of this amino acid transmitter from the synaptic cleft [4]. A family of sodium-dependent plasma membrane glutamate transporters, known as excitatory amino acid transporters (EAATs), are responsible for the glutamate uptake mainly into glial cells, albeit these proteins are also present in neurons. Of the five EAATs subtypes described thus far, EAAT1 also known as glutamate/aspartate transporter (GLAST) and EAAT2 first named as glutamate transporter 1 (Glt-1) are regarded as glial glutamate transporters, although Glt-1 has been also found in neurons [5]. In any event, the density of glial glutamate transporters exceeds that of their neuronal counterparts and therefore the vast majority of the brain glutamate uptake activity takes place in glial cells [6].

Special issue in honor of Prof In honor of Professor Michael Robinson.

✉ Arturo Ortega
arortega@cinvestav.mx

[1] Departamento de Toxicología, Centro de Investigación Y de Estudios Avanzados del IPN, Apartado Postal 14-740, 07360 Ciudad de Mexico, Mexico

[2] Instituto de Investigaciones Oceanológicas, Universidad Autónoma de Baja California, 22860 Ensenada, Baja California, Mexico

Published online: 30 July 2019

Once internalized into the glial compartment, a fraction of glutamate is metabolized to glutamine via the glia-enriched enzyme glutamine synthetase. The associated Na^+ influx reverses the direction of the neutral amino acid transporter (SNAT3/5) resulting in the astrocytic release of glutamine in the vicinity of the presynaptic terminal, which takes it up presumably by means of SNAT2 [7, 8]. Glutamine is then converted back to glutamate by the enzyme glutaminase and packed into synaptic vesicles completing the recycling of this neurotransmitter in what has been known as the *Glutamate/Glutamine* shuttle [9]. An exquisite and precise coupling between glutamate uptake and glutamine release is achieved through an activity-dependent interaction of glial glutamate and glutamine transporters [10, 11].

Manganese (Mn) is a trace element widely found in the environment and for which defined roles as enzyme cofactor have been acknowledged [12]. Nevertheless, occupational exposure as the one present in workers of the mining industry has been linked to symptoms that resemble Parkinson's disease: tremors, bradykinesia, facial spasms [13]. An accumulation of this metal in the *globus pallidus* has been reported in post-mortem samples of exposed population [14]. In fact, the dopaminergic neurons of the *substantia nigra pars compacta* have been identified as a target of manganese accumulation [15].

A significant amount of work has been reported in recent years regarding the biological basis of Mn neurotoxicity and its parallelism to Parkinson's disease. Upon sustained Mn exposure, a disruption of Ca^{2+} homeostasis is present resulting in the activation of proteases such as calpains, that damages the soluble NSF attachment protein receptor (SNARE) complex halting neurotransmitter release [16]. Concomitantly, an increase in α-synuclein expression that leads to endoplasmic reticulum (ER) stress is also present after exposure to this metal both in neurons and astrocytes [17].

All of the cellular responses described above, lead to an energy deficit that most probably distort the highly ATP-consuming glutamate uptake. Pioneer work from the groups of Aschner and Lee have described that long term Mn exposure affects glutamate turnover using cortical astrocytes [18, 19]. In this contribution, we decided to evaluate the effect of short term Mn exposure in the well-established model of chick cerebellar cultured Bergmann glial cells (BGC), as a proven model system of radial glia that totally enwrap glutamatergic synapses: the ones established between the parallel fibers and the Purkinje cells in the molecular layer of the cerebellum [20]. Moreover, we also decided to explore a plausible interaction of Mn with the glutamate transporter expressed in these cells: GLAST/EAAT1. Our results strongly suggest that Mn modulates the transporter function by slightly increasing its catalytic efficiency to uptake glutamate. Surprisingly, also a robust decrease in glucose uptake was found.

Methods

Animals

Chicken embryos (Avimex, Mexico City, Mexico) were kept at 37 °C until usage. All experiments were performed according to the International Guidelines on the Ethical Use of Animals in Research and approved by the Cinvestav Animal Ethics Committee. Every effort was made to reduce the number of embryos used and their suffering.

Bergmann Glia Cells Cultures

Bergmann glia primary cultures were prepared according to a previously established protocol [21]. BGC were isolated from chicken embryos (14-day-old). Cerebella were dissected out, cut into small pieces and incubated for 15 min at 37 °C in Puck's medium containing trypsin (0.25 mg/mL) and DNase (0.08 mg/mL) to dissociate the tissue. The media was removed and substituted with Opti-MEM containing 2.5% fetal bovine serum (FBS), 2 mM glutamine, and gentamicin (50 µg/mL) for mechanical dissociation. BGC were then recovered by the repeated removal of dissociated cells and diluted to 1×10^6 cells/mL. The cultures were maintained at 37ºC and 95% air/5% CO_2 in a humidified incubator. All experiments were performed 4–7 days post-isolation.

Cell Viability Assay

Cell viability was measured by the 3-(4,5-dimethylthiazol-2-yl)-2,5-diphenyltetrazolium bromide (MTT) assay. BGC were seeded in 96-well plates (1×10^5 cells/well) and maintained as mentioned above. Subsequently, the cultures were treated with $MnCl_2$ or vehicle in DMEM reduced serum medium (0.5% FBS) for the indicated time. After treatment, 20 µL of MTT solution (5 mg/mL) were added to each well and plates were incubated for 3 h at 37 °C. Next, media were discarded and 50 µL of dimethyl sulfoxide (DMSO) (Sigma-Aldrich, MO, USA) were added to each well to dissolve the crystals formed by MTT reagent (Sigma-Aldrich, MO, USA). Absorbance was measured with a microplate reader (BioTek Instruments, VT, USA) at 570 nm. Experiments were performed in quadruplicates in three independent cultures.

[^{3}H]-D-Aspartate Uptake

D-Aspartate uptake studies were carried out as previously described [22]. BGC were seeded in 24-well plates

(5×10^5 cells/well) and maintained as described above. On the day of the experiment, culture media were washed and replaced with uptake buffer (pre-warmed HEPES-buffered solution containing 25 mM HEPES, 130 mM NaCl, 5.4 mM KCl, 1.8 mM $CaCl_2$, 0.8 mM $MgCl_2$, 33.3 mM glucose, and 1 mM NaH_2PO_4, pH 7.4). Next, cultures were treated with $MnCl_2$ (indicated concentrations) or vehicle for the indicated time periods. After treatment, cultures were incubated with pre-warmed uptake buffer containing 0.4 µCi/mL [^{3}H]-D-aspartate ([^{3}H]-D-Asp) (specific activity: 16.5 Ci/mmol, Perkin Elmer, MA, USA). D-Asp (glutamate analogue) was used as it has the advantage of being nonmetabolizable while still using the same transporter system as glutamate. Uptake was terminated after 12 min of incubation with ice-cold uptake buffer, and cells were lysed by incubation with 0.1 N NaOH for 2 h at room temperature**.** An aliquot of the lysate was transferred to a scintillation vial, liquid scintillation cocktail and 50 µL of glacial acetic acid (to quench chemiluminescence) were added, and radioactivity was measured in a scintillation analyzer (PerkinElmer, MA, USA). The remainder of the lysate was used for protein determination by the Bradford protein assay (Bio-Rad, CA, USA). Radioactivity counts were corrected for protein levels and calculated as [^{3}H]-D-Asp pmol/(mg protein min^{-1}). Experiments were performed in quadruplicates in three–four independent cultures.

For the determination of the kinetic constants K_m and V_{max}, cultures were treated with 200 µM $MnCl_2$ or vehicle for 30 min. After treatment, cultures were incubated with pre-warmed uptake buffer containing 0.4 µCi/mL [^{3}H]-D-Asp (24.2 nM) + D-Asp (unlabeled D-aspartate concentrations of 0–250 µM) (Sigma-Aldrich, MO, USA). Uptake was terminated after 12 min of incubation by three washes with ice-cold uptake buffer, and cells were lysed by incubation with 0.1 N NaOH for 2 h at room temperature**.** Sample aliquots were then measured for incorporated radioactivity and protein content as described above. A robust nonlinear regression was used to fit a model to the experimental data and estimate the parameters of Michaelis–Menten equation (GraphPad Prism Software, La Jolla California USA). Experiments were performed in quadruplicates in three independent cultures.

Some experiments were performed just by adding $MnCl_2$ (final concentration of 200 µM) or vehicle to the uptake buffer (containing 0.4 µCi/mL [^{3}H]-D-Asp), and the incorporated radioactivity as a function of time was evaluated. These experiments were terminated after the indicated incubation time points by three washes with ice-cold uptake buffer. Next, cells were lysed and measured for incorporated radioactivity and protein content as previously described. A robust nonlinear regression was used to fit a model to the experimental data (GraphPad Prism Software, La Jolla California USA). Experiments were performed in quadruplicates in three independent cultures.

[^{3}H]-2-Deoxy-D-Glucose Uptake

Glucose uptake studies were carried out as previously described [23]. BGC were seeded in 24-well plates (5×10^5 cells/well) and maintained as above mention. On the day of the experiment, culture media were washed and replaced with uptake buffer (pre-warmed HEPES-buffered solution containing 25 mM HEPES, 130 mM NaCl, 5.4 mM KCl, 1.8 mM $CaCl_2$, 0.8 mM $MgCl_2$, 5 mM glucose, and 1 mM NaH_2PO_4, pH 7.4). Next, cultures were treated with 200 µM $MnCl_2$ or vehicle for 30 min. After treatment, cultures were incubated with pre-warmed uptake buffer (without glucose) containing 0.8 µCi/mL [^{3}H]-2-deoxy-D-glucose ([^{3}H]-2DOG) (specific activity: 32.5 Ci/mmol, Perkin Elmer, MA, USA) + 2DOG (unlabeled 2-deoxy-D-glucose concentrations of 0–5 mM) (Sigma-Aldrich, MO, USA). Uptake was terminated after 30 min of incubation by three washes with ice-cold uptake buffer (without glucose), and cells were lysed by incubation with 0.1 N NaOH for 2 h at room temperature**.** An aliquot of the lysate was transferred to a scintillation vial, liquid scintillation cocktail and 50 µL of glacial acetic acid (to quench chemiluminescence) were added, and radioactivity was measured in a scintillation analyzer (PerkinElmer, MA, USA). The remainder of the lysate was used for protein determination by the Bradford protein assay (Bio-Rad, CA, USA). Radioactivity counts were corrected for protein levels and calculated as [^{3}H]-2DOG pmol/(mg protein min^{-1}). A robust nonlinear regression was used to fit a model to the experimental data and estimate the parameters of Michaelis–Menten equation. Experiments were performed in quadruplicates in three independent cultures.

Real-Time PCR

Confluent monolayers were treated with 150 µM D-Asp in DMEM reduced serum medium (0.5% FBS) for the indicated time periods. After treatment, cells were harvested with TRIzol Reagent (Sigma-Aldrich, MO, USA) and total RNA was isolated using the Direct-zol RNA MiniPrep kit (Zymo Research, CA USA). Real-time PCR was performed for the amplification of glutamate/aspartate transporter (GLAST) with a cycler real-time PCR detection system (Applied Biosystem, CA, USA). The real-time PCR reactions were carried out in a total volume of 10 µL, containing a 20 ng RNA template of each sample, 200 nM of the appropriate primers (Table 1) and the KAPA SYBR FAST One-Step qRT-PCR Master Mix (1X KAPA SYBR FAST qPCR Master Mix Universal, 10 nM dNTP, 1X KAPA RT

Table 1 Sequences of primers for RT-PCR reactions

cDNA	Primers
GLAST	Forward: GGCTGCGGGCATTCCTC Reverse: CGGAGACGATCCAAGAACCA
S17	Forward: CCGCTGGATGCGCTTCATCAG Reverse: TACACCCGTCTGGGCAAC

GLAST glutamate/aspartate transporter, *S17* ribosomal protein S17

Mix and/or 1X ROX dye) (Kapa Biosystems, MA, USA). The PCR protocol was carried out as follows: 5 min at 42 °C for cDNA synthesis followed by 5 min at 95 °C for inactivation. Next, 3 s denaturation at 95 °C and 30 s at the specific annealing temperature (Ta) for 40 cycles. Fluorescence was detected at the end of each elongation step. Each sample was normalized with the relative amplification of the ribosomal protein S17. Relative quantification of mRNA in the samples was calculated by the $2^{-\Delta\Delta C_T}$ method. Experiments were performed in duplicates in four independent cultures.

Statistical Analysis

Results are expressed as the mean ± SEM from a minimum of three independent cultures. Statistical analysis was carried out with one-way analysis of variance (ANOVA) followed by Dunnett's multiple comparison test. Multiple t tests (one unpaired t test per condition) were used for statistical analysis of transport kinetic experiments. A probability of 0.05 or less was considered statistically significant. All analyses were performed with GraphPad Prism Software (La Jolla California USA).

Results

Effect of Mn on Bergmann Glia Viability

Several studies had established the susceptibility of various cell types to Mn-induced neurotoxicity, astrocytes being more resistant compared to neurons [24–27]. The basal ganglia represent the main target for Mn neurotoxicity, but Mn is also well known to accumulate in other brain regions including the cerebellum [28, 29], thus providing a rationale for examining cells derived from this region. Cell viability of BGC was assessed by the MTT assay. As shown in Fig. 1, there was no apparent cell death in cultured Bergmann glia exposed to different time periods (0.5, 12 and 24 h, panel A, B, and C respectively), and Mn concentrations (100, 200, 300, 500 and 1000 µM). These results allowed us to move forward and evaluate the activity of the glutamate/aspartate transporter (GLAST) upon exposure to Mn in the absence of direct cell death.

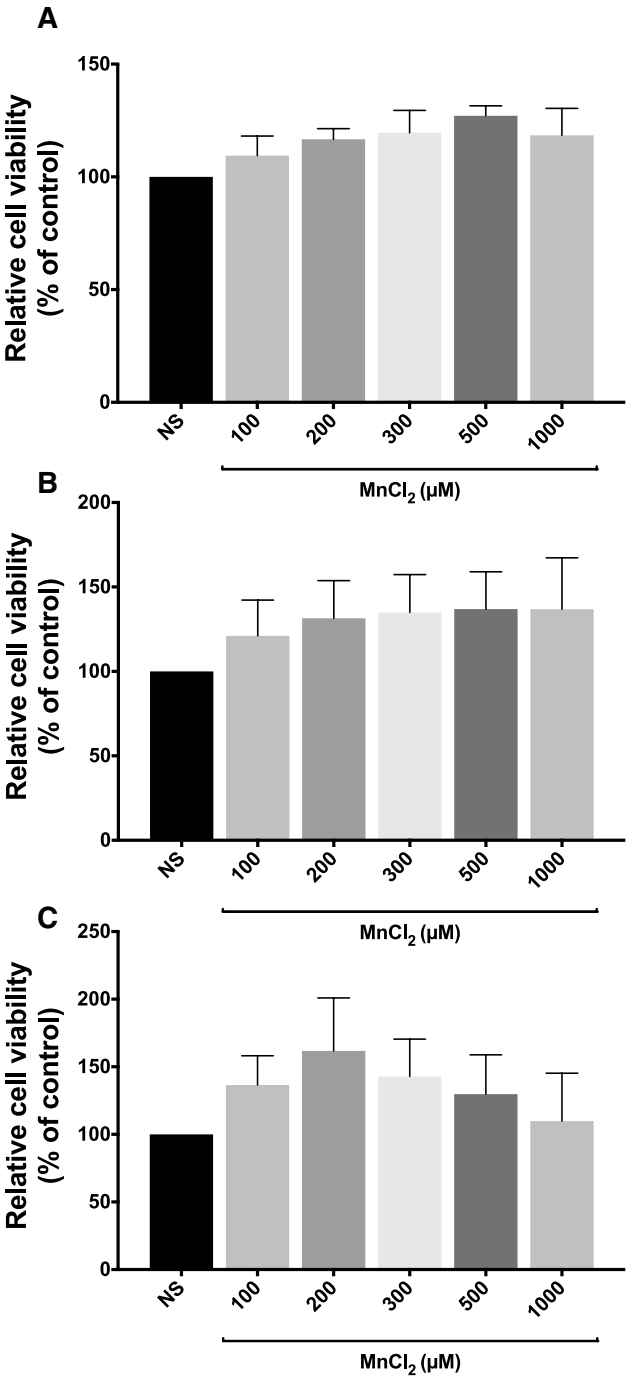

Fig. 1 Mn does not affect cell viability of Bergmann glial cells. Total formazan was measured in control (*NS,* non-stimulated) and $MnCl_2$ (100, 200, 300, 500 or 1000 µM) treated primary cultures of BGC for 0.5 h (**a**), 12 h (**b**) or 24 h (**c**). Data represent the mean ± SEM from three independent sets of cultures, each performed in quadruplicate (one-way ANOVA followed by Dunnett's multiple comparison test)

Mn Exposure Modifies [^{3}H] D-Aspartate Uptake

An increasing body of evidence have showed that Mn decreases GLAST/GLT-1 expression and function in

astrocyte cultures, possibly leading to excitotoxic neuronal injury [30, 31]. Although these studies have advanced our understanding on the mechanisms by which Mn represses these transporters, little is known about Mn-acute exposure consequences over their function. In order to gain insight into a plausible effect of Mn on GLAST activity we performed [^{3}H]-D-Asp uptake assays with a fixed radioligand concentration (24.2 nM). BGC exposed to Mn (30 min), either to 200 or 300 µM, results in a significant increase in the amount of [^{3}H]-D-Asp incorporated into the cells. As shown in Fig. 2, this effect is the same whether or not Mn is present in the uptake buffer. Although, when Mn is present in the uptake buffer a marginally reduction on GLAST activity increase is observed. Previous work from our lab has demonstrated that exposure to D-Asp (1 mM) reduces BGC uptake activity and leads to the activation of many signal transduction pathways [32, 33]. The fact that the Mn-induced GLAST activity increment is overturned by co-treatment with 1 mM D-Asp suggest that D-Asp and Mn trigger different mechanisms that affects GLAST function.

Next, we performed time and dose course studies to try to establish a direct correlation between the previously observed effect and Mn exposure. As depicted in Fig. 3, Mn-induced GLAST activity increase is dose (A) and time-dependent (B). Moreover, we can also observe that this effect reaches its maximum after 5 min of incubation.

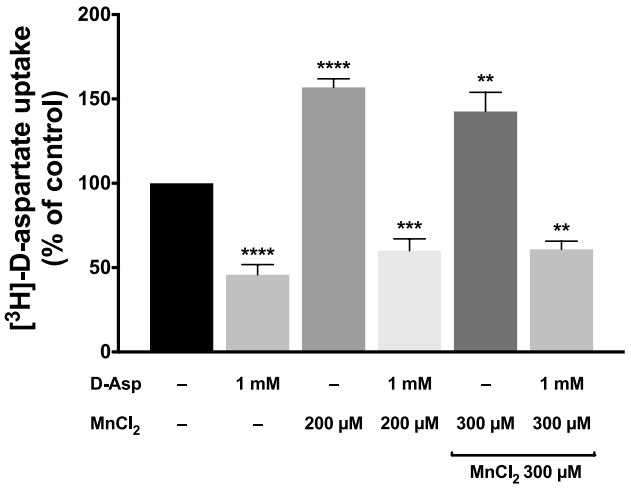

Fig. 2 Mn exposure augments GLAST activity. Total [^{3}H]-D-Asp (0.4 µCi/mL, specific activity: 16.5 Ci/mmol) uptake was measured in control (NS, non-stimulated) and $MnCl_2$ (200 or 300 µM) treated primary cultures of BGC for 0.5 h. $MnCl_2$ (300 µM) was added to the uptake buffer when indicated. Statistically significant differences between the controls and experimental groups are indicated by **p < 0.01, ***p < 0.001, ****p < 0.0001 versus NS. Data represent the mean ± SEM from four independent sets of cultures, each performed in quadruplicate (one-way ANOVA followed by Dunnett's multiple comparison test)

From our perspective, two possible hypotheses were worth in-deep investigation. Either exposure to Mn increases plasma membrane glutamate transporters, or it affect the transporter's kinetic parameters. Our first approach was to perform [^{3}H]-D-Asp uptake assays after a 24 h pre-incubation with 150 µM D-Asp. We know from unpublish work of our lab that a long-term incubation with D-Asp, at a concentration where V_0 tends to equal V_{max} (150 µM D-Asp), significative lessens the total amount of GLAST mRNA (Fig. 4, box). Under these circumstances, the effect of Mn

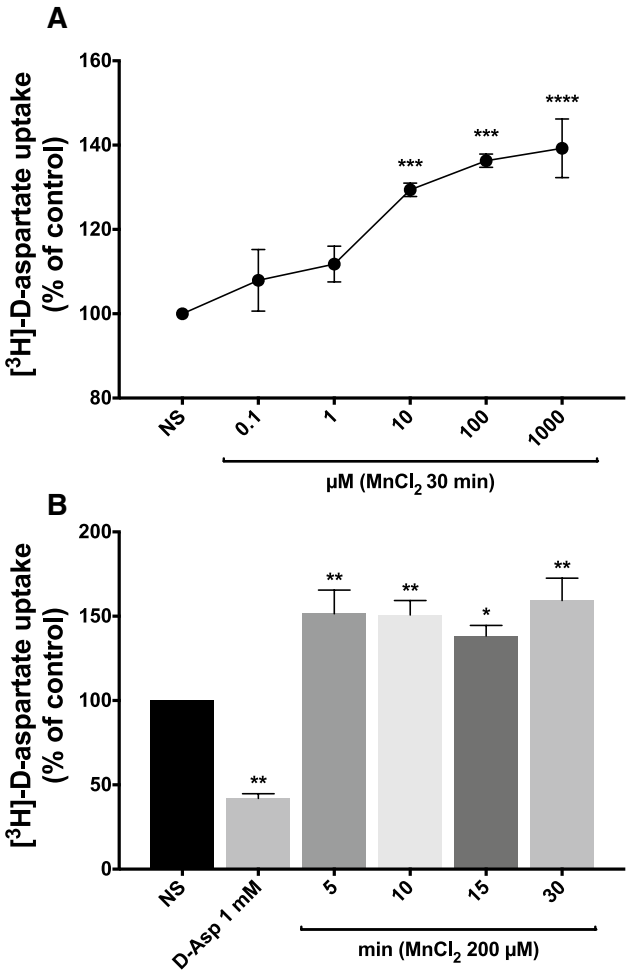

Fig. 3 Mn-induced GLAST activity increase is dose- and time-dependent. **a** Total [^{3}H]-D-Asp (0.4 µCi/mL, specific activity: 16.5 Ci/mmol) uptake was measured in control (NS, non-stimulated) and $MnCl_2$ (0.1, 1, 10, 100, or 1000 µM) treated primary cultures of BGC for 0.5 h. **b** Total [^{3}H]-D-Asp (0.4 µCi/mL, specific activity: 16.5 Ci/mmol) uptake was measured in control (NS, non-stimulated) and $MnCl_2$ (200 µM) treated primary cultures of BGC for 5, 10, 15 or 30 min. Statistically significant differences between the controls and experimental groups are indicated by *p < 0.05, **p < 0.01, ***p < 0.001, ****p < 0.0001 versus NS. Data represent the mean ± SEM from three independent sets of cultures, each performed in quadruplicate (one-way ANOVA followed by Dunnett's multiple comparison test)

over GLAST activity remains as a discrete but significative augmentation that is also overturned by co-treatment with D-Asp (Fig. 4). This result suggests that the total amount of transporters at the plasma membrane may not be affected by Mn exposure.

In order to gain an insight of the mechanism by which Mn exposure increases GLAST activity, we decided to determine the kinetic parameters of the transporter in treated (200 µM for 30 min) and non-treated cells. As shown in panel A from Fig. 5, no apparent change in V_{max} was detected. Furthermore, even there was a slightly reduction in the K_m, more importantly there was a considerable change in the catalytic efficiency (V_{max}/K_m) of the transporter in Mn-treated cells. V_{max}/K_m is the rate constant for the coming together of substrate and product into a productive complex, which at concentrations much smaller than K_m becomes the limiting factor of the catalyzed reaction [34]. This change in the catalytic efficiency of GLAST could account for the increased amount of [^{3}H]-D-Asp incorporated without altering the Michaelis–Menten parameters. In addition, we

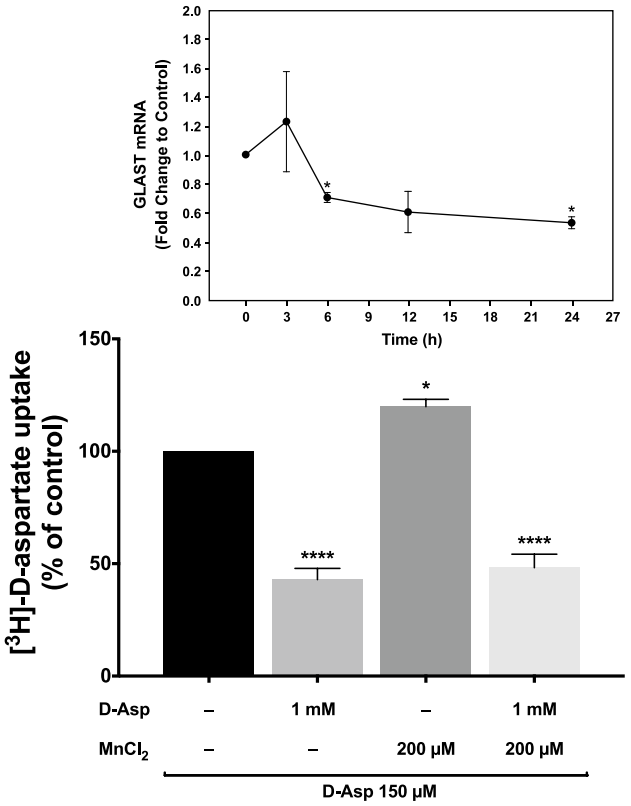

Fig. 4 Mn effect on GLAST activity after a decrease in GLAST expression. Total [^{3}H]-D-Asp (0.4 µCi/mL, specific activity: 16.5 Ci/mmol) uptake was measured in control (NS, non-stimulated) and $MnCl_2$ (200 µM) treated primary cultures of BGC for 0.5 h after a pre-incubation with 150 µM D-Asp for 24 h. An incubation with 150 µM D-Asp for 24 h reduces the relative amount of GLAST mRNA in BGC (Box: Relative GLAST mRNA was quantify in control (NS) and D-Asp (150 µM) treated primary cultures of BGC for 3, 6, 12 or 24 h). Statistically significant differences between the controls and experimental groups are indicated by *p < 0.05, ****p < 0.0001 versus NS. Data represent the mean ± SEM from three independent sets of cultures, each performed in quadruplicate (one-way ANOVA followed by Dunnett's multiple comparison test)

A

	Saturable Transport		
	V_{max} (pmol/mg·min)	K_m (µmol/L)	V_{max}/K_m (pmol/mg·min/(µmol/L))
NS	469.0	21.21	22.112
$MnCl_2$	437.0	16.46	26.549

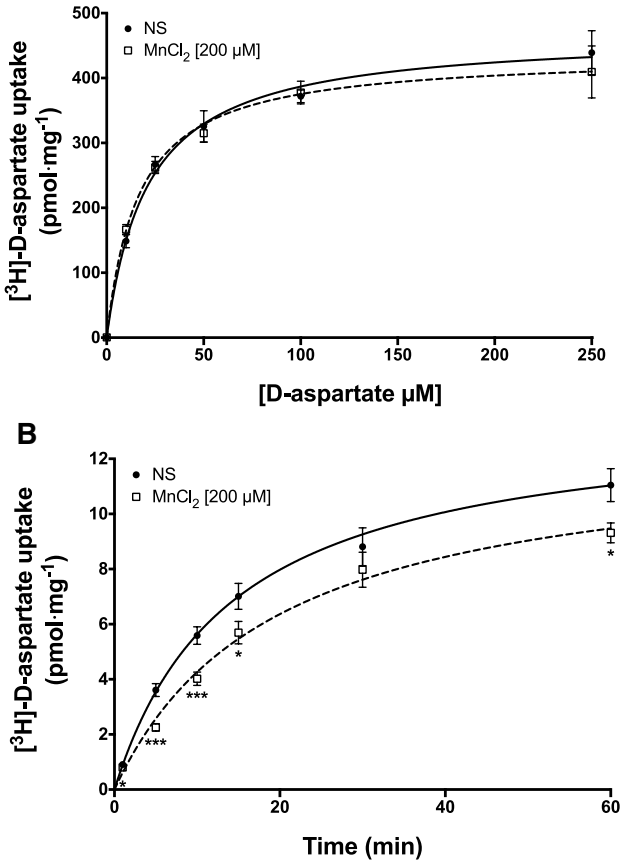

Fig. 5 Impact of Mn exposure on GLAST kinetic parameters. **a** Total [^{3}H]-D-Asp (0.4 µCi/mL, specific activity: 16.5 Ci/mmol) uptake was measured in control (NS, non-stimulated) and $MnCl_2$ (200 µM) treated primary cultures of BGC for 0.5 h. Varying concentrations of D-Asp (ranging from 0 to 250 µM) + [^{3}H]-D-Asp (24.2 nM) were added to the uptake buffer and uptake was measured over a 12 min period of time in order to determine the kinetic parameters of the transporter. **b** Total [^{3}H]-D-Asp (0.4 µCi/mL, specific activity: 16.5 Ci/mmol) uptake was measured in the presence (200 µM $MnCl_2$) or absence (NS) of Mn in the uptake buffer for 1, 5, 10, 15, 30 or 60 min. Statistically significant differences between the controls and experimental groups are indicated by *p < 0.05, ***p < 0.001 versus NS. Data represent the mean ± SEM from three independent sets of cultures, each performed in quadruplicate (Multiple t tests). A robust nonlinear regression was used to fit a model to our data and estimate the kinetic parameters

decided to examine if the merely presence of Mn (200 µM) in the uptake buffer could have an effect on the function of the transporter. Panel B from Fig. 5 shows that there is a significant reduction on the incorporation of [^{3}H]-D-Asp as a function of time when Mn is added to the uptake buffer. These results support the notion of a direct interaction of Mn with GLAST.

Mn Affects Glucose Transport Activity

An increase in glutamate uptake in glial cells has been regarded as a signal to an augmented glucose uptake, in a metabolic coupling known as the *astrocyte/neuronal lactate shuttle* [35]. Glial metabolism is mainly glycolytic, and the accumulation of lactate leads to its release to the extracellular space via the monocarboxylate transporter 1 (MCT-1) [36]. Neurons take up this lactate via MCT-4 and metabolize it through the tricarboxylic acid cycle. In BGC cultures, we have previously reported an aspartate-dependent increase in [^{3}H]-2-DOG influx [23]. To our surprise, a clear reduction in glucose uptake was found in Mn-treated cells (Fig. 6). This diminished transport is related to a significant decrease in V_{max}, suggesting a reduced amount of glucose transporters in the plasma membrane. Further experiments, beyond the scope of this communication, will address this non-expected finding.

	Saturable Transport		
	V_{max} (pmol/mg·min)	K_m (mmol/L)	V_{max}/K_m (pmol/mg·min/(mmol/L))
NS	2317	3.360	689.583
$MnCl_2$	1908	4.018	474.863

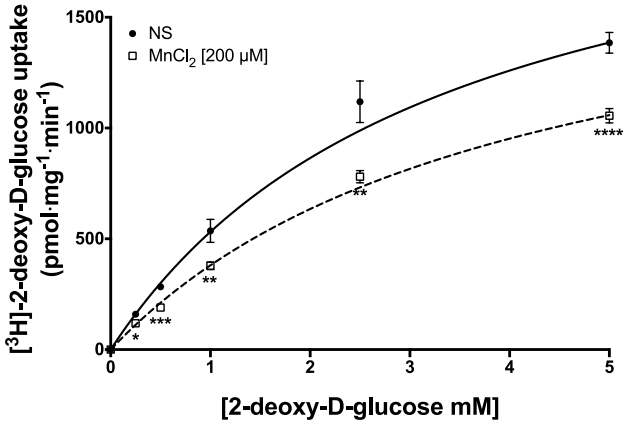

Fig. 6 Mn decreases BGC glucose transport capacity. Total [^{3}H]-2DOG (0.8 µCi/mL, specific activity: 32.5 Ci/mmol) uptake was measured in control (NS, non-stimulated) and $MnCl_2$ (200 µM) treated primary cultures of BGC for 0.5 h. Varying concentrations of 2DOG (ranging from 0 to 5 mM) + [^{3}H]-2DOG (24.6 nM) were added to the uptake buffer and uptake was measured over a 30 min period of time in order to determine the kinetic parameters of the transporter. Statistically significant differences between the controls and experimental groups are indicated by *$p < 0.05$, **$p < 0.01$, ***$p < 0.001$, ****$p < 0.0001$ versus NS. Data represent the mean ± SEM from three independent sets of cultures, each performed in quadruplicate (Multiple t tests). A robust nonlinear regression was used to fit a model to our data and estimate the kinetic parameters

Discussion

The molecular mechanisms associated to Mn toxicity in the central nervous system have been focused on the deleterious action of this metal to the mitochondria of dopaminergic neurons and related model systems such as pheochromocytoma cells (PC-12) or induced pluripotent stem cells (iPSC)-derived human dopaminergic neurons [18, 37]. Nevertheless, the clear association between peripheral manganese levels and attention-deficit/hyperactivity disorder, calls for glutamatergic synapses as targets of this metal [38]. In fact, pioneer work from Aschner and his colleagues has demonstrated that one of the mechanisms of Mn neurotoxicity is associated with the disruption of the glutamate and glutamine transport systems in cortical glial cells [39, 40]. Despite of these well-documented reports, a closer look into the effects of acute Mn exposure of radial glial cells, that in the one hand completely enwrap glutamatergic synapses [41], and in the other hand do not undergo the so-called astrocytic conversion [42] is lacking. One could argue that this is not a major issue, but it is clear that GLAST regulation is different in radial glia such as Bergmann and Müller cells compared to cortical astrocytes [43–45]. While in radial glia glutamate down-regulates GLAST expression and function, the opposite effect takes place in cortical astrocytes. Therefore, in this contribution, we addressed the effect of short-term (min) manganese exposure of chick cerebellar BGC cultures, a model system that has proven useful in the characterization of the involvement of glial cells in glutamatergic glia/neuron coupling (reviewed in [46]).

After the corroboration that Mn at micromolar concentrations does not compromise cell viability, we explored the effect of the treatment of confluent BGC monolayers with this metal on GLAST activity. The high abundance of this protein allows us to measure the uptake activity at a low concentration of the radioactive tracer ([^{3}H]-D-Asp). We were able to reproduce a 1.5-fold increase in GLAST activity due to the treatment of the cells with different Mn concentrations (Fig. 3, panel a). The effect is dose-dependent and reaches its maximal effect after 5 min. In order to gain an insight into the kinetic parameters affected by this metal, we performed Michaelis–Menten saturation curves. Although at first sight we expected an increase in V_{max} that could be related to an augmentation of GLAST molecules

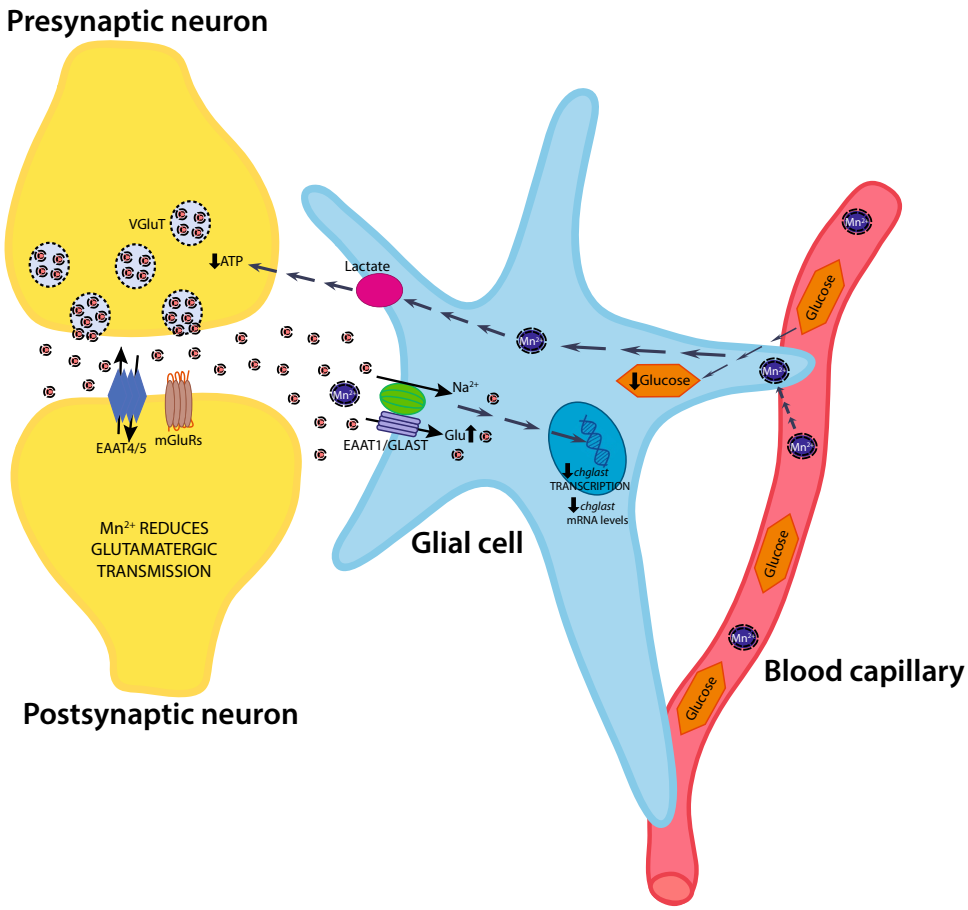

Fig. 7 Proposed model for the effects of acute Mn exposure on GLAST activity in BGC. See text for details

in the plasma membrane, we could only detect a discrete augmentation of the affinity of the transporter triggered by Mn. Interestingly, the ratio between V_{max} and K_m, a parameter known as the catalytic efficiency [47], presented an increase after incubation with Mn. It is tempting to speculate that this metal interacts with the glutamate transporters present at the plasma membrane leading to a change in their conformation that is reflected in an increased uptake efficiency. To better understand this direct possible interaction, we performed a time course of [^{3}H] D-Asp uptake in the presence of 200 µM $MnCl_2$. A discrete reduction in the uptake was obtained and although the identity of the metal molecular target(s) is unknown, a direct interaction of Mn with the transporter cannot be ruled out. Still, we are unable to explain the increase in the uptake at low aspartate concentrations when the cells are preincubated with Mn. We expected either an increase in V_{max} or a clear-cut change in the affinity of the transporter. This is not the case; we only detected an augmentation in the transporter catalytic efficiency that in fact reflects the increase in GLAST activity upon $MnCl_2$ exposure.

What could be the relevance of this small change in glutamate transport in the context of Bergmann glia function? To shed some light into this issue, we decided to evaluate the uptake of [^{3}H]-2-DOG. Glutamate uptake has been linked to glucose entrance in various glial systems, including cultured Bergmann glia. Again, an unexpected result was detected. A clear reduction in glucose uptake is present after a 30 min incubation with 200 µM $MnCl_2$. It is an unexpected finding taking into consideration that upon Mn exposure only a small increase in aspartate transport is present, one would expect either no effect in glucose uptake or a small increase. At this stage, it is clear that the exposure to environmental relevant concentrations of Mn has a complex action in cultured Bergmann glia that it is quite possible to interfere with glutamatergic transmission in the cerebellar cortex in vivo [48]. A graphical summary of our findings and their plausible impact in glutamatergic neurons is presented in Fig. 7. It is tempting to speculate that Mn neurotoxicity is at least in part, glia-mediated: the recorded decrease in D-Asp incorporation as a function of time when Mn is present could lead to a sustained increase in extra synaptic glutamate, that in turn could over-stimulate neuronal glutamate receptors resulting in an excitotoxic insult. Moreover, the decrease in glucose uptake after Mn exposure could interrupt the astrocyte/neuronal/lactate shuttle reducing the lactate supplied to neurons, with a consequent decrease in the repolarization process and thus hampering glutamatergic transmission. Work actually

in progress in our group is aimed to characterize the effect Mn exposure in glia metabolism.

Acknowledgements ME and JSV were supported by Conacyt-Mexico PhD scholarships. This work was funded by Conacyt-Mexico (255087) Grant to AO.

References

1. Maj C, Minelli A, Giacopuzzi E et al (2016) The role of metabotropic glutamate receptor genes in schizophrenia. Curr Neuropharmacol 14:540–550
2. Mayer ML (2011) Structure and mechanism of glutamate receptor ion channel assembly, activation and modulation. Curr Opin Neurobiol 21:283–290. https://doi.org/10.1016/j.conb.2011.02.001
3. Borroto-Escuela DO, Tarakanov AO, Brito I, Fuxe K (2018) Glutamate heteroreceptor complexes in the brain. Pharmacol Rep 70:936–950. https://doi.org/10.1016/j.pharep.2018.04.002
4. Ambrogini P, Torquato P, Bartolini D et al (2019) Excitotoxicity, neuroinflammation and oxidant stress as molecular bases of epileptogenesis and epilepsy-derived neurodegeneration: the role of vitamin E. Biochim Biophys Acta Mol Basis Dis. https://doi.org/10.1016/j.bbadis.2019.01.026
5. Danbolt NC, Furness DN, Zhou Y (2016) Neuronal vs glial glutamate uptake: resolving the conundrum. Neurochem Int 98:29–45. https://doi.org/10.1016/j.neuint.2016.05.009
6. Danbolt NC (2001) Glutamate uptake. Prog Neurobiol 65:1–105
7. Chaudhry FA, Schmitz D, Reimer RJ et al (2002) Glutamine uptake by neurons: interaction of protons with system a transporters. J Neurosci 22:62–72
8. Billups D, Marx M-C, Mela I, Billups B (2013) Inducible presynaptic glutamine transport supports glutamatergic transmission at the calyx of Held synapse. J Neurosci 33:17429–17434. https://doi.org/10.1523/JNEUROSCI.1466-13.2013
9. Shank RP, Campbell GL (1984) Glutamine, glutamate, and other possible regulators of alpha-ketoglutarate and malate uptake by synaptic terminals. J Neurochem 42:1162–1169
10. Martínez-Lozada Z, Guillem AM, Flores-Méndez M et al (2013) GLAST/EAAT1-induced Glutamine release via SNAT3 in Bergmann glial cells: evidence of a functional and physical coupling. J Neurochem 125:545–554. https://doi.org/10.1111/jnc.12211
11. Marx M-C, Billups D, Billups B (2015) Maintaining the presynaptic glutamate supply for excitatory neurotransmission. J Neurosci Res 93:1031–1044. https://doi.org/10.1002/jnr.23561
12. Takeda A (2003) Manganese action in brain function. Brain Res Brain Res Rev 41:79–87
13. Kwakye G, Paoliello M, Mukhopadhyay S et al (2015) Manganese-induced parkinsonism and Parkinson's disease: shared and distinguishable features. Int J Environ Res Public Health 12:7519–7540. https://doi.org/10.3390/ijerph120707519
14. Reaney SH, Bench G, Smith DR (2006) Brain accumulation and toxicity of Mn(II) and Mn(III) exposures. Toxicol Sci 93:114–124. https://doi.org/10.1093/toxsci/kfl028
15. Robison G, Sullivan B, Cannon JR, Pushkar Y (2015) Identification of dopaminergic neurons of the substantia nigra pars compacta as a target of manganese accumulation. Metallomics 7:748–755. https://doi.org/10.1039/c5mt00023h
16. Wang C, Ma Z, Yan D-Y et al (2018) Alpha-synuclein and calpains disrupt SNARE-mediated synaptic vesicle fusion during manganese exposure in SH-SY5Y cells. Cells 7:258. https://doi.org/10.3390/cells7120258
17. Liu C, Yan D-Y, Tan X et al (2018) Effect of the cross-talk between autophagy and endoplasmic reticulum stress on Mn-induced alpha-synuclein oligomerization. Environ Toxicol 33:315–324. https://doi.org/10.1002/tox.22518
18. Chen P, Bornhorst J, Aschner M (2018) Manganese metabolism in humans. Front Biosci (Landmark Ed 23:1655–1679.
19. Lee E, Karki P, Johnson JJ et al (2017) Manganese control of glutamate transporters' gene expression. Adv Neurobiol 16:1–12. https://doi.org/10.1007/978-3-319-55769-4_1
20. Somogyi P, Takagi H, Richards JG, Mohler H (1989) Subcellular localization of benzodiazepine/GABAA receptors in the cerebellum of rat, cat, and monkey using monoclonal antibodies. J Neurosci 9:2197–2209
21. Ortega A, Eshhar N, Teichberg VI (1991) Properties of kainate receptor/channels on cultured Bergmann glia. Neuroscience 41:335–349
22. Ruiz M, Ortega A (1995) Characterization of an Na(+)-dependent glutamate/aspartate transporter from cultured Bergmann glia. NeuroReport 6:2041–2044
23. Mendez-Flores OG, Hernández-Kelly LC, Suárez-Pozos E et al (2016) Coupling of glutamate and glucose uptake in cultured Bergmann glial cells. Neurochem Int 98:72–81. https://doi.org/10.1016/j.neuint.2016.05.001
24. Lee E-SY, Yin Z, Milatovic D et al (2009) Estrogen and tamoxifen protect against Mn-induced toxicity in rat cortical primary cultures of neurons and astrocytes. Toxicol Sci 110:156–167. https://doi.org/10.1093/toxsci/kfp081
25. Malthankar GV, White BK, Bhushan A et al (2004) Differential lowering by manganese treatment of activities of glycolytic and tricarboxylic acid (TCA) cycle enzymes investigated in neuroblastoma and astrocytoma cells is associated with manganese-induced cell death. Neurochem Res 29:709–717
26. Kim J, Pajarillo E, Rizor A et al (2019) LRRK2 kinase plays a critical role in manganese-induced inflammation and apoptosis in microglia. PLoS ONE 14:e0210248. https://doi.org/10.1371/journal.pone.0210248
27. Gandhi D, Sivanesan S, Kannan K (2018) Manganese-induced neurotoxicity and alterations in gene expression in human neuroblastoma SH-SY5Y cells. Biol Trace Elem Res 183:245–253. https://doi.org/10.1007/s12011-017-1153-5
28. Sepúlveda MR, Dresselaers T, Vangheluwe P, Everaerts W (2012) Evaluation of manganese uptake and toxicity in mouse brain during continuous MnCl2 administration using osmotic pumps. Contrast Media Mol Imaging 7(4):426–434. https://doi.org/10.1002/cmmi.1469
29. Ye Q, Kim J (2015) Effect of olfactory manganese exposure on anxiety-related behavior in a mouse model of iron overload hemochromatosis. Environ Toxicol Pharmacol 40:333–341. https://doi.org/10.1016/j.etap.2015.06.016
30. Karki P, Smith K, Johnson J et al (2014) Role of transcription factor yin yang 1 in manganese-induced reduction of astrocytic glutamate transporters: putative mechanism for manganese-induced neurotoxicity. Neurochem Int 88:53–59. https://doi.org/10.1016/j.neuint.2014.08.002
31. Karki P, Webb A, Smith K et al (2014) Yin Yang 1 is a repressor of glutamate transporter EAAT2, and it mediates manganese-induced decrease of EAAT2 expression in astrocytes. Mol Cell Biol 34:1280–1289. https://doi.org/10.1128/MCB.01176-13
32. Martínez-Lozada Z, Hernández-Kelly LC, Aguilera J et al (2011) Signaling through EAAT-1/GLAST in cultured Bergmann glia cells. Neurochem Int 59:871–879. https://doi.org/10.1016/j.neuint.2011.07.015
33. Martinez D, Garcia L, Aguilera J, Ortega A (2014) An acute glutamate exposure induces long-term down regulation of GLAST/EAAT1 uptake activity in cultured Bergmann glia cells. Neurochem Res 39:142–149. https://doi.org/10.1007/s11064-013-1198-6

34. Northrop DB (1998) On the Meaning of Km and V/K in Enzyme Kinetics. J Chem Educ 75:1153. https://doi.org/10.1021/ed075p1153
35. Pellerin L, Magistretti PJ (2012) Sweet sixteen for ANLS. J Cereb Blood Flow Metab 32:1152–1166. https://doi.org/10.1038/jcbfm.2011.149
36. Broer S, Rahman B, Pellegri G et al (1997) Comparison of lactate transport in astroglial cells and monocarboxylate transporter 1 (MCT 1) expressing Xenopus laevis oocytes. Expression of two different monocarboxylate transporters in astroglial cells and neurons. J Biol Chem 272:30096–30102
37. Neely MD, Davison CA, Aschner M, Bowman AB (2017) Manganese and rotenone-induced oxidative stress signatures differ in iPSC-derived human dopamine neurons. Toxicol Sci 159:366–379. https://doi.org/10.1093/toxsci/kfx145
38. Shih J-H, Zeng B-Y, Lin P-Y et al (2018) Association between peripheral manganese levels and attention-deficit/hyperactivity disorder: a preliminary meta-analysis. Neuropsychiatr Dis Treat 14:1831–1842. https://doi.org/10.2147/NDT.S165378
39. Sidoryk-Wegrzynowicz M, Aschner M (2013) Manganese toxicity in the central nervous system: the glutamine/glutamate-gamma-aminobutyric acid cycle. J Intern Med 273:466–477. https://doi.org/10.1111/joim.12040
40. Johnson J, Pajarillo EAB, Taka E et al (2018) Valproate and sodium butyrate attenuate manganese-decreased locomotor activity and astrocytic glutamate transporters expression in mice. Neurotoxicology 64:230–239. https://doi.org/10.1016/j.neuro.2017.06.007
41. Somogyi P, Tamás G, Lujan R, Buhl EH (1998) Salient features of synaptic organisation in the cerebral cortex. Brain Res Brain Res Rev 26:113–135
42. Buffo A, Rossi F (2013) Origin, lineage and function of cerebellar glia. Prog Neurobiol 109:42–63. https://doi.org/10.1016/j.pneurobio.2013.08.001
43. Gegelashvili G, Civenni G, Racagni G et al (1996) Glutamate receptor agonists up-regulate glutamate transporter GLAST in astrocytes. NeuroReport 8:261–265
44. Bernabe A, Mendez JA, Hernandez-Kelly LCR, Ortega A (2003) Regulation of the Na^+-dependent glutamate/aspartate transporter in rodent cerebellar astrocytes. Neurochem Res 28:1843–1849
45. Ramirez-Sotelo G, Lopez-Bayghen E, Hernandez-Kelly LCR et al (2007) Regulation of the mouse Na^+-dependent glutamate/aspartate transporter GLAST: putative role of an AP-1 DNA binding site. Neurochem Res 32:73–80. https://doi.org/10.1007/s11064-006-9227-3
46. Martinez-Lozada Z, Ortega A (2015) Glutamatergic transmission: a matter of three. Neural Plast 2015:787396. https://doi.org/10.1155/2015/787396
47. Koshland DE (2002) The application and usefulness of the ratio kcat/KM. Bioorg Chem 30:211–213. https://doi.org/10.1006/BIOO.2002.1246
48. Miyazaki T, Yamasaki M, Hashimoto K et al (2017) Glutamate transporter GLAST controls synaptic wrapping by Bergmann glia and ensures proper wiring of Purkinje cells. Proc Natl Acad Sci USA 114:7438–7443. https://doi.org/10.1073/pnas.1617330114

Mol Neurobiol
DOI 10.1007/s12035-017-0756-3

Glutamate-Dependent Translational Control of Glutamine Synthetase in Bergmann Glia Cells

Reynaldo Tiburcio-Félix[1] · Miguel Escalante-López[2] · Bruno López-Bayghen[2] · Daniel Martínez[1] · Luisa C. Hernández-Kelly[2] · Samuel Zinker[1] · Dinorah Hernández-Melchor[2] · Esther López-Bayghen[2] · Tatiana N. Olivares-Bañuelos[3] · Arturo Ortega[2]

Received: 3 April 2017 / Accepted: 24 August 2017

Abstract Glutamate is the major excitatory transmitter of the vertebrate brain. It exerts its actions through the activation of specific plasma membrane receptors expressed both in neurons and in glial cells. Recent evidence has shown that glutamate uptake systems, particularly enriched in glia cells, trigger biochemical cascades in a similar fashion as receptors. A tight regulation of glutamate extracellular levels prevents neuronal overstimulation and cell death, and it is critically involved in glutamate turnover. Glial glutamate transporters are responsible of the majority of the brain glutamate uptake activity. Once internalized, this excitatory amino acid is rapidly metabolized to glutamine via the astrocyte-enriched enzyme glutamine synthetase. A coupling between glutamate uptake and glutamine synthesis and release has been commonly known as the glutamate/glutamine shuttle. Taking advantage of the established model of cultured Bergmann glia cells, in this contribution, we explored the gene expression regulation of glutamine synthetase. A time- and dose-dependent regulation of glutamine synthetase protein and activity levels was found. Moreover, glutamate exposure resulted in the transient shift of glutamine synthetase mRNA from the monosomal to the polysomal fraction. These results demonstrate a novel mode of glutamate-dependent glutamine synthetase regulation and strengthen the notion of an exquisite glia neuronal interaction in glutamatergic synapses.

Keywords Glutamine synthetase · Bergmann glia · Glutamate/glutamine shuttle · Translational control · Polysomal fraction

✉ Arturo Ortega
arortega@cinvestav.mx

[1] Departamento de Genética y Biología Molecular, Centro de Investigación y de Estudios Avanzados del IPN, Apartado Postal 14-740, 07360 Ciudad de México, Mexico

[2] Departamento de Toxicología, Centro de Investigación y de Estudios Avanzados del IPN, Apartado Postal 14-740, 07360 Ciudad de México, Mexico

[3] Instituto de Investigaciones Oceanológicas, Universidad Autónoma de Baja California, 22860 Ensenada, Mexico

Introduction

Glutamate (Glu) is the major excitatory amino acid in the vertebrate brain. It exerts its actions through specific membrane receptors present both in neurons and in glia cells. Ligand-gated ion channels as well as G protein-coupled receptors (GPCR) are activated by this amino acid. The former are known as ionotropic Glu receptors and were first subdivided in terms of their pharmacological properties in *N*-methyl-D-aspartate receptors (GRIN), α-amino-3-hydroxy-5-methyl-4-isoxazole propionic acid receptors (GRIA), and kainate receptors (GRIK). These protein complexes are composed of four homo or hetero subunits of the corresponding subtype. The vast diversity of the molecular composition of these receptors, together with the diverse post-transcriptional modifications of their corresponding messenger RNAs (mRNAs) and the differential subunit assembly at the plasma membrane, has hampered the development of specific ligands [1]. Metabotropic Glu receptors (GRM) are members of class C of G protein-coupled receptors (GPCR) and have been divided in terms of their primary structure in class I, II, and III [2]. Overstimulation of both types of Glu receptors is linked to an uncontrolled neuronal death, a phenomena known as excitotoxicity [3].

Published online: 05 September 2017

A family of Glu membrane transporters of the solute carrier gene family, known as excitatory amino acid transporters (EAATs), provides the proper regulation of Glu extracellular levels. Although these transporters are expressed both in neurons and in glia cells, the bulk of Glu uptake activity in the brain depends on glial Glu transporters (EAAT1/GLAST, EAAT2/GLT1). Once Glu is internalized into glial cells it is metabolized via glutamine synthetase (GS) (EC 6.3.1.2) to glutamine (Gln) and released to the vicinity of the presynaptic neuron through the reverse function of type N of sodium-dependent neutral amino acid transporters (SNAT 3, 5). Gln is taken up by the presynaptic neurons by an unidentified Gln transporter and de-aminated back to Glu by glutaminase (EC 3.5.1.2) and packed into synaptic vesicles through vesicular Glu transporters (VGLUTs) completing the *so-called* Glu/Gln shuttle, a metabolic cascade critically involved in Glu turnover and neuronal availability [4]. Such a metabolic interplay between neurons and glia requires the coordinated involvement of numerous proteins [5].

Focusing only in the glia compartment, an activity-dependent recruitment of GLAST/SNAT3/cysteine/Glu antiporter has been characterized recently [6]. In fact, the increase in $[Na^+]_i$ associated to the Glu uptake provides the driving force for the reversed function of SNAT 3/5 that results in Gln release [7, 8]. Another component of the transporter complex is the $Na^{+/}K^+$ ATPase [9], explaining the necessity of an increase in glucose uptake [10] and the reported overall decrease in protein synthesis linked to Glu exposure of glia cells. It has been established that in periods of depressed protein synthesis, a selected group of proteins are synthetized [11].

Among the proteins needed to support intense periods of glutamatergic activity, GS is an attractive candidate. Inhibition of GS activity blocks Glu-mediated neurotransmission [12]. In this context, using the established model of cultured Bergmann glia, we present herein evidence for a Glu-dependent translational control of GS synthesis and activity, supporting the notion of an exquisite biochemical coordination of Glu uptake and Gln release as the framework of a tripartite synapse.

Materials and Methods

Materials

Tissue culture reagents were obtained from GE Healthcare (Carlsbad, CA, USA). D-aspartate (Asp) and L-glutamate (Glu) were obtained from Tocris Cookson (St. Louis, MO USA). Polyclonal anti-phospho-ribosomal protein S6 (rpS6, Ser 235/236) and anti-rpS6 were purchased from Cell Signaling Technology (Danvers, MA), whereas anti-GS polyclonal antibodies were from Santa Cruz Biotechnology (Dallas, TX). Anti-rabbit antibodies and the enhanced chemiluminescence reagent (ECL) were obtained from GE Healthcare Life Sciences (Mexico). All other chemicals were purchased from Sigma (St. Louis, MO, USA).

Cell Culture and Stimulation Protocol

Primary cultures of cerebellar Bergmann glia cells (BGC) were prepared from 14-day-old chick embryos as previously described by Ortega et al. [13]. All efforts were made to reduce the number of embryos used and their suffering according to International Guidelines on the Ethical Use of Animals. Cells were plated at a density of 0.5 × 106/mL in 60 mm diameter six-well plastic culture dishes in Dulbecco's modified Eagle's medium (DMEM) containing 10% fetal bovine serum, 2 mM glutamine, and gentamicin (50 μg/mL) and used on the fourth to seventh day after culture. Before any treatment, confluent monolayers were switched to non-serum DMEM media containing 0.5% bovine serum albumin (BSA) for 30 min and treated with Glu or Asp added to culture medium for the indicated time periods.

Cell Immunostaining

BGC were seeded on coverslips and fixed by exposure to ice-cold acetone for 10 min and air dried for 1 h. Cells were rinsed with phosphate-buffered saline (PBS) twice and fixed for 10 min in 4% paraformaldehyde. Coverslips were rinsed again twice with Tris-buffered saline (TBS) and one more time with TBS/Tween 20 (0.05%). Non-specific binding was prevented by incubation with 1% BSA in TBS (BSA/TBS) for 1 h. Cells were exposed to a 1:100 dilution of the primary antibody anti-GS, in BSA/TBS overnight at 4 °C, followed by the incubation with the respective fluorescein-labeled goat anti-rabbit anti-sera in BSA/TBS (1:500) for 2 h at room temperature. Preparations were mounted with Fluoroshield/DAPI. Cell preparations were examined under a fluorescence microscopy (Zeiss Axioskop 40 immunofluorescence microscope and the AxioVision software; Carl Zeiss, Inc., Thornwood, NY).

Ribosomal Profiles

Confluent BGC monolayers were exposed to a 1 mM concentration of Glu or Asp for 0, 15, or 30 min. The cells were harvested and washed with PBS supplemented with 100 μg/mL cycloheximide and centrifuged at 16,000×*g* for 7 min at 4 °C in a Beckman SW28 rotor and suspended into 200 μL of lysis buffer (10 mM Tris–HCl pH 7.4, 100 mM KCl, 10 mM $MgCl_2$, 1% Triton X-100, 2 mM dithiothreitol, and 100 μg/mL cycloheximide) containing phosphatase inhibitors (10 mM NaF, 1 mM Na_2MoO_4, and 1 mM Na_3VO_4) and a cocktail of protease inhibitors. Glass beads were added, and cells were mixed five times 30 s each. Cells were centrifuged for 10 min at 14,000×*g*. The supernatant was layered on top of

a 15–50% sucrose gradient and centrifuged at 141,000×*g* for 5:30 h. All gradients were scanned at 254 nm from the top with an ISCO gradient collector. Each fraction was precipitated with ethanol and centrifuged at 16,000×*g* for 30 min.

Numerical Analysis

The area under the ribosomal profile curves was calculated using Wolfram Mathematica 11 (Champaign, IL, USA). A cubic Hermite polynomial was used to interpolate the coordinates, obtained by mapping, from each ribosomal profile. And then, the definite integral of the Hermite polynomials within the domain corresponding to the polysome fraction was calculated.

SDS-PAGE and Western Blots

Whole protein extracts or pellets from ribosomal profile were homogenized in RIPA buffer (50 mM Tris–HCl, 1 mM EDTA, 150 mM NaCl, 1 mM phenylmethylsulfonyl fluoride, 1 mg/mL aprotinin, 1 mg/mL leupeptin, 1% NP-40, 0.25% sodium deoxycholate, 10 mM NaF, 1 mM Na_2MoO_4, and 1 mM Na_3VO_4pH 7.4). Samples were denaturized in Laemmli sample buffer, and equal amount of proteins (50 μg as determined by the Bradford method) were resolved through SDS-PAGE slab gels and then electroblotted to nitrocellulose membranes. Blots were stained with Ponceau S stain to confirm that protein content was equal in all lanes. Membranes were soaked in PBS to remove the Ponceau S and incubated in TBS containing 3% dried skimmed milk and 0.1% Tween 20 for 30 min to block the excess of non-specific protein binding sites. Membranes were then incubated overnight at 4 °C with the proper primary antibodies followed by secondary antibodies. Immunoreactive polypeptides were detected by chemiluminescence with a MicroChemi (DNR Bio-Imaging System). Densitometry analyses were performed with the ImageJ software [14].

RNA Extraction and qRT-PCR

Total RNA was isolated from confluent Bergmann glial cell cultures (treated, non-treated) and extracted using the TRIZOL Reagent (Sigma). Every treatment condition per experiment was analyzed as technical duplicates. PCR was performed in a reaction volume of 10 μL. Quantitative real-time reverse transcription-PCR (qRT-PCR) was performed by a one-step method with 20 ng of total RNA using KAPA SYBR FAST One-Step qRT-PCR system (Kapa Biosystems). Samples were subjected to quantitative PCR (qPCR) using Step One Plus Real-time PCR System (Applied Biosystems). The qPCR profile consisted of an initial cDNA synthesis by M-MuLV Reverse Transcriptase at 42 °C for 5 min, an inactivation of the reverse transcriptase at 95 °C for 5 min, followed by 40 cycles of 95 °C for 3 s, 60 °C 30 s. A melt curve stage was added. To quantify GS mRNA levels, we used previously designed and reported oligonucleotides: GS Forward 5′-ATGGAGGTCTCAAG CACATC-3′ and GS Reverse 5′-GTTTCGTTGAGGAG ACACGTA-3′. As an endogenous control we amplified ribosomal protein S17 mRNA with the following primers: S17 Forward 5′-CCGCTGGATGCGCTTCATCAG-3′ and S17 Reverse 5′-TACACCCGTCTGGGCAAC-3′. The relative abundance of GS mRNA is expressed as sample versus a control normalized to S17 chick ribosomal mRNA levels and was calculated as $2^{-\Delta\Delta CT}$. Data are presented as mean values ± SDs and analyzed by the online resource BootstRatio [15]; $p < 0.05$ was considered statistically significant.

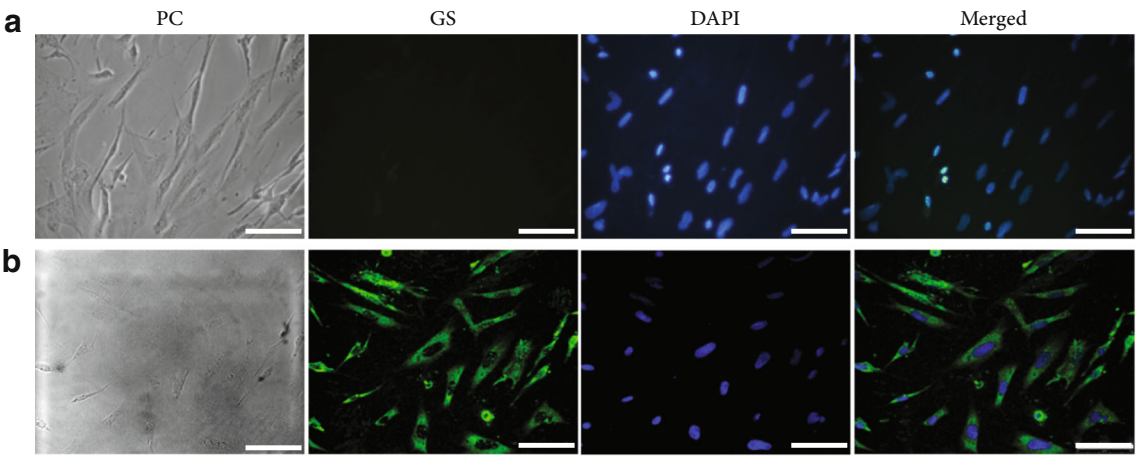

Fig. 1 Cellular localization of glutamine synthetase in BGC cultures. Primary cultures of Bergmann glial cells (BGC) were incubated with an anti-glutamine synthetase (GS) antibody in a dilution 1:100. A negative control (no primary antibody) is shown (**a**), and a cell staining with anti-GS antibodies (green) is shown (**b**). Phase contrast (PC) microphotograph of BGC morphology, DAPI counter-stained nucleus (blue), and merged images are also shown. Scale bar 50 μm

GS Activity

The GS activity was determined as described by Haghighat [16]. The GS-catalyzed c-glutamyl transferase assay was established in a 12-well format for BGC cultures. The cells were treated and rinsed with PBS and 130 μL of 50 mM imidazole at pH 6.8. The culture dish was frozen at − 80° C for 30 min and then incubated for 15 min at room temperature. Thirty microliters were separated to quantify the protein concentration by the Bradford method. Thereafter, 100 μL of an assay solution was added to each well (50 mM imidazole, 20 mM Na_2HSO_4 0.16 mM ADP, 50 mM Gln, 25 mM hydroxylamine, 2 $MnCl_2$) and incubated for 45 min at 37 °C. The reaction was stopped with 400 μL of stopping solution (2.42% ferric chloride, 1.45% TCA, and 1.82% HCl). The absorption was read at 540 nm using a SpectraFluor Plus (Tecan) plate reader. The specific activity is expressed as nanomoles of γ-glutamyl hydroxamate per milligram of protein/45 min.

Results

GS Localization in Cultured BGC

Given the central role of GS in the Glu/Gln shuttle, we first explored the expression and subcellular distribution of GS in our culture system. To this end, an immunocytochemical approach was chosen and results are depicted in Fig. 1. As described for mouse Bergmann glia, in cultured chick BGC, GS is localized in the cytoplasm of the cells (Fig. 1b). It should be mentioned that the labeling efficiencies of the chosen antibodies were proved, supporting the few existing studies about the cellular distribution of GS [17]. These glia cells are likely to play a specific role in the Glu/Gln shuttle, and GS expression in BGC is consistent with their plausible importance in glutamatergic transmission.

Glu-Dependent GS Expression Regulation in Cultured BGC

In order to shed some light into a plausible Glu-dependent GS expression regulation, BGC were exposed to 1 mM Glu. The Western blot analysis shown in Fig. 2a reveals a rather fast increase in GS protein levels with a maximal effect after 30 min, suggesting a posttranscriptional effect that might be explained in terms of increased *gs* mRNA translation or a diminished GS degradation. A drastic decrease in GS protein is also observed after 60 and 120 min of Glu. Pharmacological characterization of the Glu response demonstrated that the effect on GS expression is mediated by GLAST/EAAT1, since it is completely prevented by the EAAT blocker DL-*threo*-β-Benzyloxyaspartic acid (TBOA) at a 100 μM concentration (Fig. 2b). It also has to be noted that a GRIA antagonist like

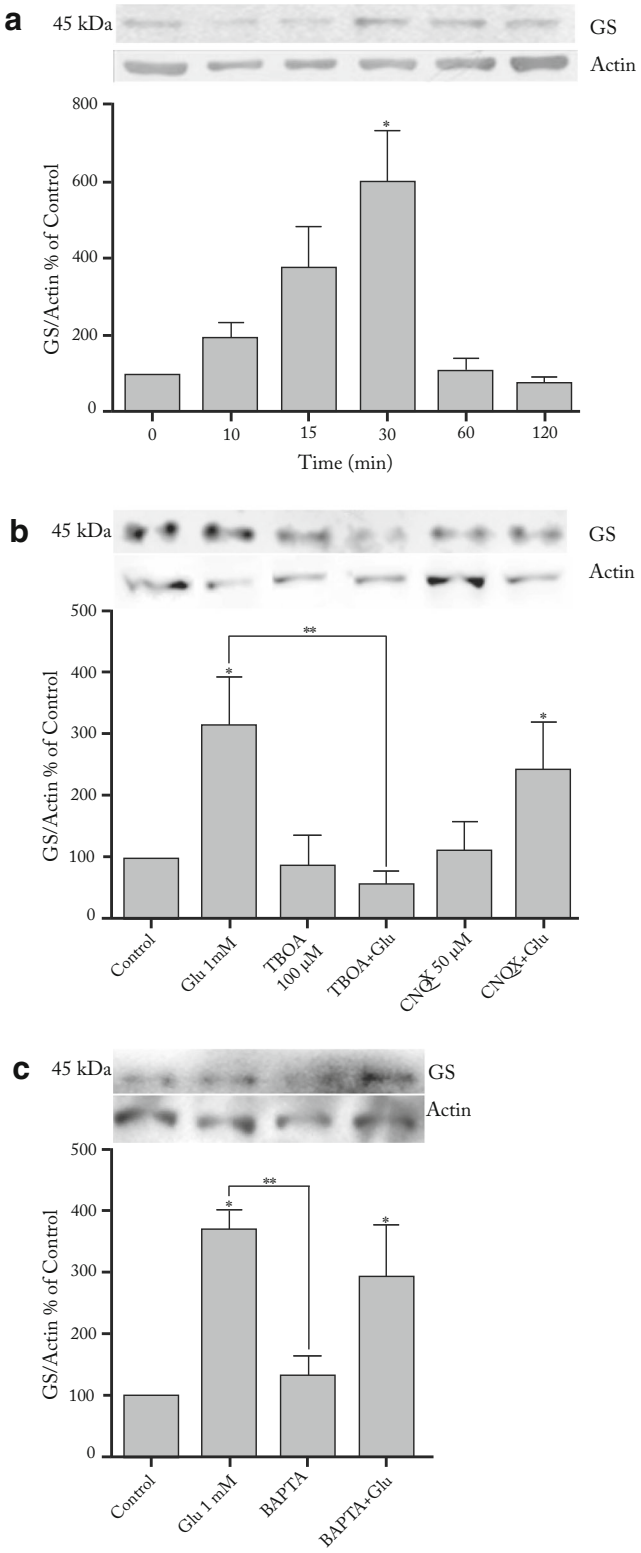

6-cyano-7-nitroquinoxaline-2,3-dione (CNQX) is not capable to reduce the Glu response (Fig. 2b). Therefore, one can be confident that GS augmentation is a GLAST/EAAT1-mediated effect, since in our system, this is the only EAAT expressed [18].

◀ **Fig. 2** Glutamate induces glutamine synthetase protein levels in Bergmann glial cells. **a** BGC monolayers were exposed to 1 mM glutamate (Glu) over a period of 120 min. Time zero represents Glu unexposed BGC. **b** BGC were pretreated with the EAAT blocker DL-*threo*-β-Benzyloxyaspartic acid (TBOA, 100 μM) and GRIA antagonist 6-cyano-7-nitroquinoxaline-2,3-dione (CNQX, 50 μM) prior to treatment with 1 mM Glu (30 min). **c** BGC were pretreated with the Ca^{2+} chelator BAPTA-AM (25 μM) min prior to treatment with 1 mM Glu (30 min). At the indicated experimental conditions, total extracts were immunoblotted with anti-GS and then analyzed. Anti-actin Western blots were used as loading controls. A representative blot is presented on top of each graph. Three independent experiments ± SD are graphed for each data point as GS/Actin (% of control). Statistical analysis was performed using a one-way ANOVA, with the GraphPad Prism software. *$p < 0.05$

To establish a biochemical mechanism of this effect, experiments were carried out in the presence of the protein translation inhibitor cycloheximide (CHX) (Fig. 3). Data show that the described increase in GS protein expression in Glu-treated cells is inhibited by CHX. It should be noted a tendency to an augmentation in GS protein levels after 60 and 120 min Glu treatment in the presence of CHX, suggesting that the protease that cleaves GS is also regulated at the translational level.

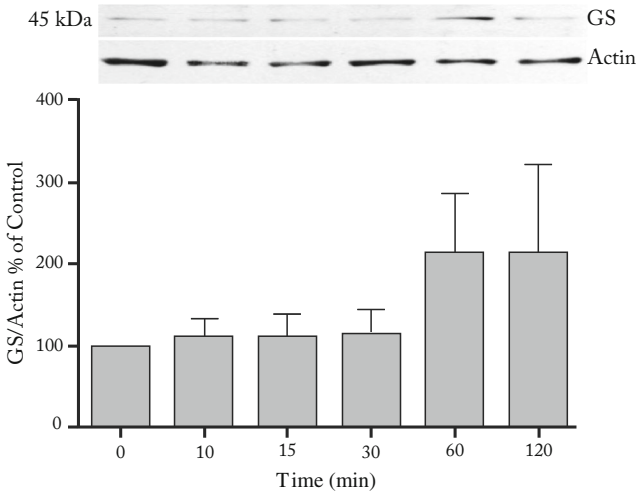

Fig. 3 Cycloheximide inhibits glutamine synthetase protein levels in Bergmann glial cells. BGC monolayers were exposed to 1 mM glutamate (Glu) in the presence of the protein translation inhibitor cycloheximide, 100 μg/mL over a period of 120 min. Time zero represents Glu unexposed BGC. At the indicated time point, total extracts were prepared and immunoblotted with anti-GS. Anti-actin Western blot was used as loading control. A representative blot is presented on top of the graph. Three independent experiments ± SD are graphed for each data point as GS/Actin % of control. Statistical analysis was performed using a one-way ANOVA, with the GraphPad Prism software

GS Activity in Glu-Treated Cells

The described increase in GS protein as a result of Glu exposure would only be of relevance to the Glu/Gln shuttle if it is accompanied by an augmentation of GS enzymatic activity. To this end, we measured the accumulation of γ-glutamyl hydroxamate as an index of GS activity [16]. An unambiguous increment in GS activity that matches with the augmented levels of GS is obtained (Fig. 4).

Glu-Dependent Increase in *gs* mRNA in the Polysomal Fraction

The fast and significant increase in GS synthesis in Glu-treated cells suggested that its mRNA could probably be associated to the polysomal fraction, as has been described for other stimuli [19]. To this end, ribosomal profiles were prepared from Glu-treated cells for the indicated time periods (Fig. 5). An increase in the area under the curve of the polysomal fraction is evident after a 30-min treatment, suggesting a plausible Glu-induced shift in the cellular translational profile (Fig. 5a). Moreover, we were able to detect a modulation of polysomal associated ribosomal s6 phosphorylation (rpS6) under Glu (Fig. 5b). At this stage, we decided to quantify *gs* mRNA in the polysomal fraction of Glu-treated cells. The results showed an approximately threefold enrichment of *gs* mRNA is present after 15 min, demonstrating a dynamic control of GS production under Glu (Fig. 6). It is important to mention that a 100 μM Glu concentration is also capable to modify the ribosomal profile, as depicted in panel C of Fig. 6.

Taking together these results demonstrate that in cultured BGC, GS protein expression is activated by Glu in a time-dependent fashion and that its production is controlled at the translational level by a recruitment of *gs* mRNA to the polysomal fraction.

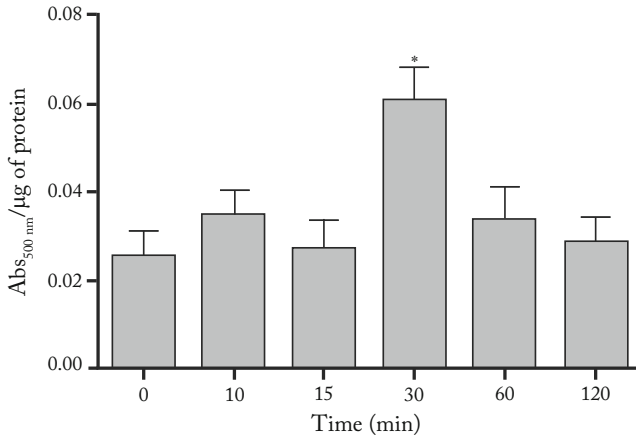

Fig. 4 Glutamine synthetase enzymatic activity in Bergmann glial cells increases in response to glutamate stimulation. GS enzymatic activity was measured by the accumulation of γ-glutamyl hydroxamate as an index of GS activity. BGC monolayers exposed to 1 mM Glu were measured by spectrophotometry at 500 nm, at minutes 10–120. Time zero represents Glu unexposed BGC. Three independent experiments ± SD are graphed for each data point as Abs/μg of protein. *$p < 0.05$

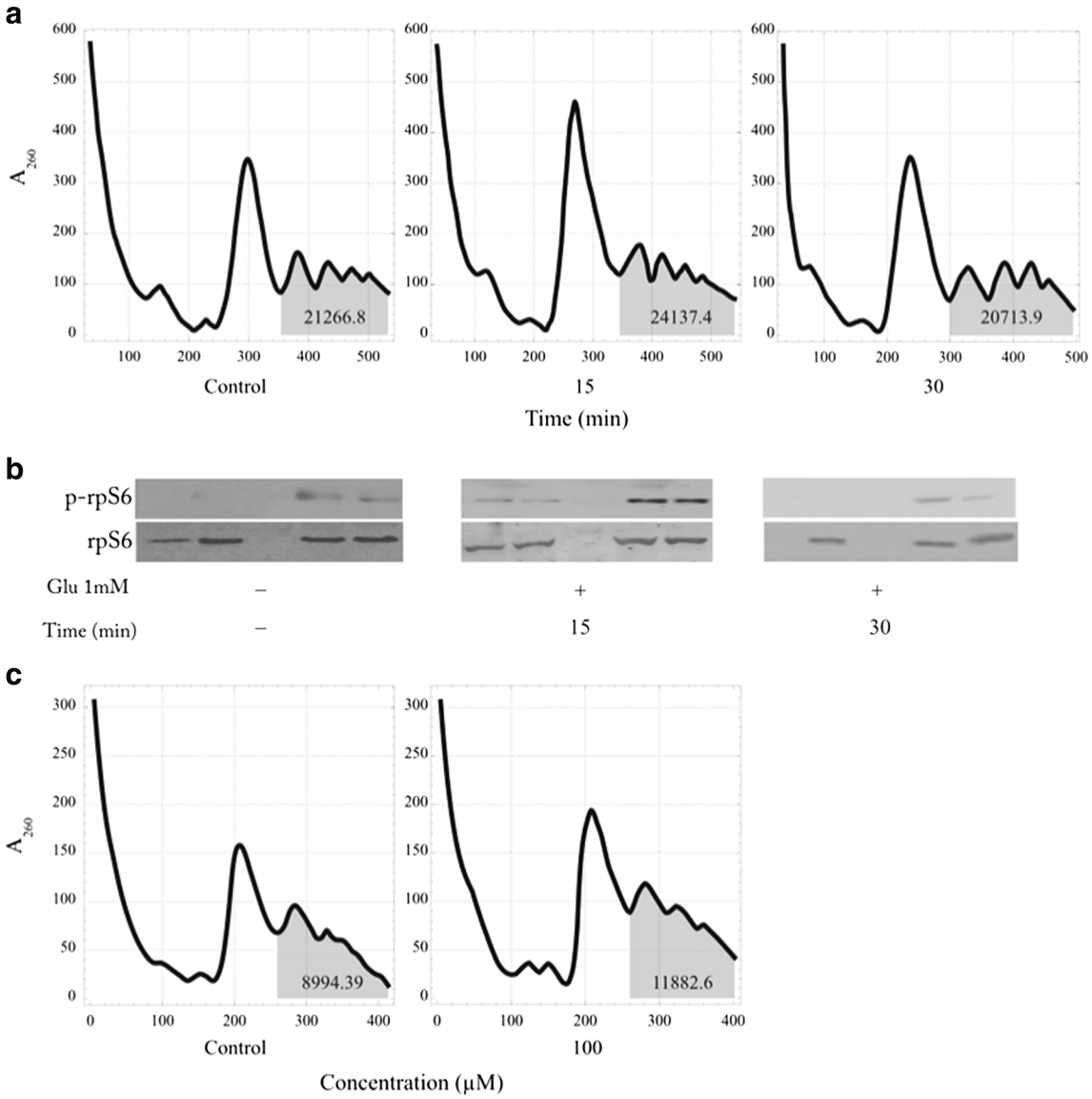

Fig. 5 Glutamate induces changes in ribosomal profiles in Bergmann glial cells. Ribosomal subunit profiles were analyzed by sucrose gradient centrifugation. BGC were exposed for 15 or 30 min to 1 mM Glu (**a**) and for 30 min to 100 μM Glu concentration (**c**). The area under the curve was calculated with MATLAB. Western blot analysis of *p*-rpS6 phosphorylation using anti-rpS6 and anti-phospho-rpS6 antibodies is presented (**b**). Control profiles represent Glu unexposed BGC. A typical profile and Western blot of three independent experiments with similar results is shown

Discussion

Glutamatergic transmission, besides of the fact that represents the most abundant excitatory system in the vertebrate brain, is a good example of the critical involvement of glia cells in synaptic transactions. This interpretation is supported by the fact that most of the Glu uptake activity takes place in the glial compartment and is driven by the mostly enriched glial transporters namely EAAT1/GLAST and EAAT2/GLT-1 [20]. Although the functionality and even the existence of the Glu/Gln shuttle have been debated over the years (see for example, McKenna et al. [21]), the results described in this contribution favor the importance of this biochemical cascade for the proper recycling of this excitatory neurotransmitter. Regardless of the ratio of Glu taken up to Gln released and the unambiguous importance of Glu oxidation [22], in the past years, key findings support an efficient coupling of Glu uptake, GS activity, and Gln release in astrocytes that surround glutamatergic synapses such as the retina, auditory brainstem, the calyx of the Held synapse, and the cerebellar cortex [5, 7, 8, 23, 24], pointing out that much of the debate about the contribution of glial EAATs to the production and release of Gln results from data obtained from heterogeneous preparations of glia cells that hardly represent those astrocytes adjacent to glutamatergic synapses.

It is the use of an appropriate system, like cultured BGC, that we and others have been able to demonstrate a coupling

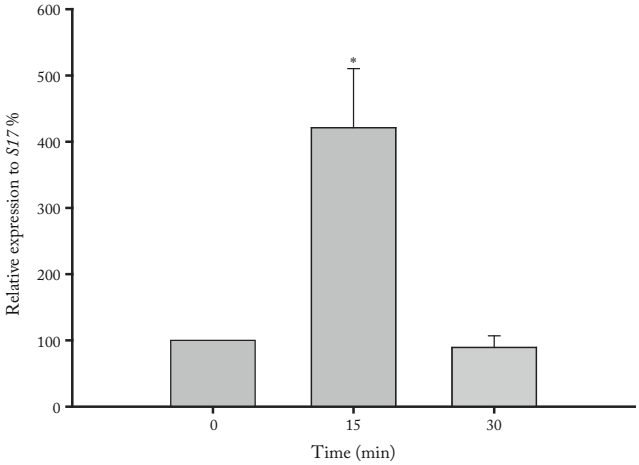

Fig. 6 Glutamate regulates the amount of *gs* mRNA in the polysomal fraction of BGC exposed to 1 mM Glu for 0, 15 or 30 min. The results are expressed as the percentage of *gs* mRNA of control BGC. The relative expression of *gs* gene was examined by qPCR and normalized to the expression of *S17* chick ribosomal mRNA. Data were analyzed by the BootstRatio online resource ($n = 3$, $*p < 0.05$)

between EAAT activity and GS release. Moreover, an increase in glucose uptake has also been documented as a consequence of EAAT1/GLAST activity [25]. All these data prompted us to study the regulation of GS by Glu. To our surprise, a significant increase in GS activity and protein levels was present after 15 to 30 min of treatment with the excitatory amino acid. The rapid increase in the protein levels suggested either an increase in translation or a stabilization of the protein. Taking into consideration that we had previously reported that Glu regulates protein synthesis in BGC and that after 15 min of exposure, translation is stocked at the elongation phase of protein synthesis due to the phosphorylation of eukaryotic elongation factor 2 (eEF2) [26, 27], we focused on the subset of mRNAs with complex 5′untranslated regions (5′-UTR) that normally are poorly translated, but in an scenario in which an accumulation of eukaryotic initiation factors (eIFs), occurs are translated, such as GS [28].

As depicted in Fig. 3, this is indeed the case, a CHX-sensitive increase in GS levels is present under Glu exposure. It is relevant to mention that the decrease in the amount of GS after 60 min with the amino acid is relevant (Fig. 3). Moreover in the experiments in which the protein synthesis inhibitor CHX is present, an increase is recorded after 60 and 120 min suggesting that a de novo protease is responsible for GS breakdown, the characterization of this phenomena is beyond the scope of this communication, but we have started its characterization.

The ribosomal protein S6 (rpS6) was the first ribosomal protein shown to undergo a stimulus-dependent phosphorylation that is believed to be crucial for mRNA binding to the ribosome, suggesting its involvement in translation efficacy [29]. Therefore, once we could demonstrate that Glu modulates the ribosomal profiles, we explored the phosphorylation status of rpS6 in the ribosomal fractions, interestingly enough, after 15 min of Glu treatment, rpS6 associated to the polysomal fraction is phosphorylated, possibly enhancing *gs* mRNA binding to the polysomes. If indeed, that would be the case; then, we should be able to detect this specific mRNA via a qRT-PCR in the polysomes, results shown in Fig. 6. It is important to mention that the enrichment of *gs* mRNA in the polysomal fraction is present before the maximal level of GS is detected, and this differential kinetics might be explained in terms of higher sensitivity of PCR versus Western blot and/or the lag between binding of *gs* mRNA and release of the finished polypeptide.

At this stage, it is tempting to speculate that in the cerebellar cortex, Glu released from the parallel fibers is taken up by BGC through EAAT1/GLAST. A fraction of this Glu is metabolized to Gln by a de novo translated *gs* mRNA in the polysomal fraction. Accumulated Gln is then released via

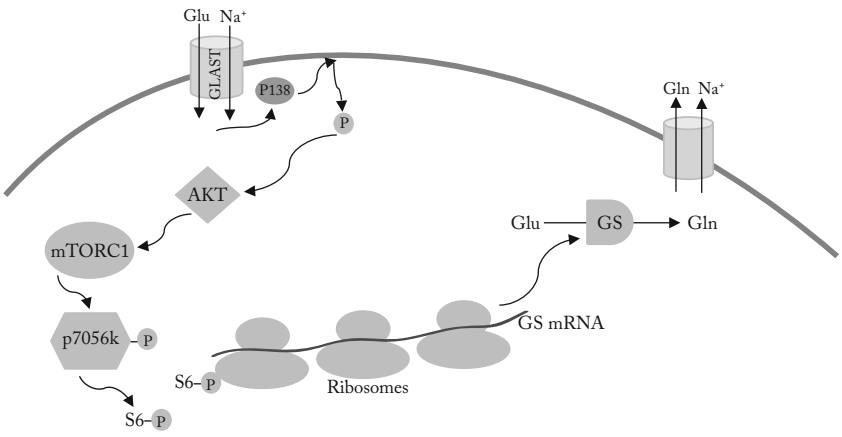

Fig. 7 Schematic representation of Glu-dependent GS translational control. Glu response is Ca^{2+} independent, and results in PKB phosphorylation followed by mTORC1 activation that induces rpS6 phosphorylation via p70S6K [25, 26, 31]. Phospho-rpS6 favors *gs* mRNA binding to the polysomes increasing GS translation, protein levels, and activity, that in coordination with GLAST activity results in the accumulation of Gln and its release via SNAT3 [7]

SNAT3 [7]. Translation of *gs* mRNA is linked to a decrease in the elongation rate, also triggered by Glu, as described previously [30]. It is important to mention that in BGC, Glu exerts its actions through the activation of glial GRI, GRM, and also via the signaling properties of the EAAT1/GLAST. Through the use of Glu transporters blocker, TBOA, we were able to show that the increase in GS levels is a transporter-mediated effect.

The precise and coordinated function of plasma membrane Glu binding proteins and the recruitment of Glu, Gln, and glucose transporters is probably the biochemical framework of this process.

In summary, we present here biochemical evidence of a EAAT1/GLAST-mediated Glu-dependent translational control of GS. This coupling, that might prove to be relevant for Glu turnover in glutamategic synapses. Work currently in progress in our lab is aimed at the characterization of the signaling cascades involved in a Glu-dependent GS synthesis. A summary of our findings is depicted in Fig. 7.

Acknowledgements RTF and DM are supported by CONACyT Mexico scholarships. This work was funded by CONACyT, Mexico (255087), and *Soluciones para un México Verde, S.A. de C.V.* grants to AO.

Compliance with Ethical Standards All efforts were made to reduce the number of embryos used and their suffering according to International Guidelines on the Ethical Use of Animals.

References

1. Mayer ML (2011) Emerging models of glutamate receptor ion channel structure and function. Structure 19:1370–1380
2. Sengmany K, Gregory KJ (2016) Metabotropic glutamate receptor subtype 5: molecular pharmacology, allosteric modulation and stimulus bias. Br J Pharmacol 173:3001–3017
3. Zhou Y, Danbolt NC (2014) Glutamate as a neurotransmitter in the healthy brain. J Neural Transm 121:799–817
4. Hertz L, Rothman D (2017) Glutamine-glutamate cycle flux is similar in cultured astrocytes and brain and both glutamate production and oxidation are mainly catalyzed by aspartate aminotransferase. Biology (Basel) 6:17
5. Martínez-Lozada Z, Ortega A (2015) Glutamatergic transmission: a matter of three. Neural Plast 2015:1–11
6. Suárez-Pozos E, Martínez-Lozada Z, Mendez-Flores O et al (2017) Characterization of the cystine/glutamate antiporter in cultured Bergmann glia cells. Neurochem. Int 52:52–59
7. Martínez-Lozada Z, Guillem AM, Flores-Méndez M et al (2013) GLAST/EAAT1-induced glutamine release via SNAT3 in Bergmann glial cells: evidence of a functional and physical coupling. J Neurochem 125:545–554
8. Todd AC, Marx M-C, Hulme SR, et al (2017) SNAT3-mediated glutamine transport in perisynaptic astrocytes in situ is regulated by intracellular sodium. Glia 65:900–916
9. Rose EM, Koo JCP, Antflick JE et al (2009) Glutamate transporter coupling to Na,K-ATPase. J Neurosci 29:8143–8155
10. Pellerin L, Bonvento G, Chatton P et al (2002) Role of neuron-glia interaction in the regulation of brain glucose utilization. Diabetes Nutr Metab 15:268–273
11. González-Mejia ME, Morales M, Hernández-Kelly LC et al (2006) Glutamate-dependent translational regulation in cultured Bergmann glia cells: involvement of p70S6K. Neuroscience 141:1389–1398
12. Bröer A, Deitmer JW, Bröer S (2004) Astroglial glutamine transport by system N is upregulated by glutamate. Glia 48:298–310
13. Ortega A, Eshhar N, Teichberg VI (1991) Properties of kainate receptor/channels on cultured Bergmann glia. Neuroscience 41: 335–349
14. Schneider CA, Rasband WS, Eliceiri KW (2012) NIH Image to ImageJ: 25 years of image analysis. Nat Methods 9:671
15. Clèries R, Galvez J, Espino M et al (2012) BootstRatio: a web-based statistical analysis of fold-change in qPCR and RT-qPCR data using resampling methods. Comput Biol Med 42:438–445
16. Haghighat N (2005) Estrogen (17-beta-Estradiol) enhances glutamine synthetase activity in C6-glioma cells. Neurochem Res 30: 661–667
17. Anlauf E, Derouiche A (2013) Glutamine synthetase as an astrocytic marker: Its cell type and vesicle localization. Front Endocrinol (Lausanne) 4:144
18. Ruiz M, Ortega A (1995) Characterization of an Na+-dependent glutamate/aspartate transporter from cultured Bergmann glia. Neuroreport 6:2041–2044. https://doi.org/10.1097/00001756-199510010-00021
19. Biever A, Boubaker-vitre J, Cutando L et al (2017) Repeated exposure to D-amphetamine decreases global protein synthesis and regulates the translation of a subset of mRNAs in the striatum. Front Mol Neurosci 9:1–11
20. Danbolt NC, Furness DN, Zhou Y (2016) Neuronal vs glial glutamate uptake: resolving the conundrum. Neurochem Int 98:29–45
21. McKenna MC, Stridh MH, McNair LF et al (2016) Glutamate oxidation in astrocytes: roles of glutamate dehydrogenase and aminotransferases. J Neurosci Res 94:1561–1571
22. McKenna MC (2013) Glutamate pays its own way in astrocytes. Front Endocrinol (Lausanne) 4:191
23. López-Colomé AM, López E, Mendez-Flores OG, Ortega A (2016) Glutamate receptor stimulation up-regulates glutamate uptake in human Müller glia cells. Neurochem Res 41:1797–1805
24. Uwechue NM, Marx M-C, Chevy Q, Billups B (2012) Activation of glutamate transport evokes rapid glutamine release from perisynaptic astrocytes. J Physiol 590:2317–2331
25. Mendez-Flores OG, Hernández-Kelly LC, Suárez-Pozos E et al (2016) Coupling of glutamate and glucose uptake in cultured Bergmann glial cells. Neurochem Int 98:72–81
26. Gonzalez-Mejia ME, Morales M, Hernandez-Kelly LCR et al (2006) Glutamate-dependent translational regulation in cultured Bergmann glia cells: involvement of p70S6K. Neuroscience 141: 1389–1398
27. Barrera I, Flores-Méndez M, Hernández-Kelly LC et al (2010) Glutamate regulates eEF1A phosphorylation and ribosomal transit time in Bergmann glial cells. Neurochem Int 57:795–803
28. Shin D, Park C (2004) N-terminal extension of canine glutamine synthetase created by splicing alters its enzymatic property. J Biol Chem 279:1184–1190
29. Ruvinsky I, Meyuhas O (2006) Ribosomal protein S6 phosphorylation: from protein synthesis to cell size. Trends Biochem Sci 31: 342–348
30. Barrera I, Hernández-Kelly LC, Castelán F, Ortega A (2008) Glutamate-dependent elongation factor-2 phosphorylation in Bergmann glial cells. Neurochem Int 52:1167–1175
31. Zepeda RC, Barrera I, Castelán F et al (2008) Glutamate-dependent transcriptional regulation in Bergmann glia cells: involvement of p38 MAP kinase. Neurochem Res 33:1277–1285